Mitchell Auditorium & Atrium

5th UHMWPE International Meeting

September 22-23 2011

Drexel UNIVERSITY

Honorary President: Luigi Costa, Ph.D.

President: Steven M. Kurtz, Ph.D.

Sponsored by:

Ticona

Performance Driven Solutions™

5th UHMWPE International Meeting

Dear Participant,

The purpose of this meeting is to bring together engineers, scientists, and clinicians from academia and industry to present leading-edge research on the development and applications of medical grade UHMWPE. The focus of the present meeting is on clinical, radiographical, and retrieval studies of highly crosslinked UHMWPE, with a special emphasis on the performance of knee arthroplasty; advances in Vitamin E and antioxidant technologies for UHMWPE; structural composites and woven fiber applications of medical grade UHMWPE; as well as advances in biological aspects of UHMWPE wear debris.

Abstracts were evaluated by the Scientific Committee for inclusion in the program, either as a podium presentation or a poster.

Scientific Committee:

Honorary President:
Luigi Costa, Ph.D.

President:
Steven M. Kurtz, Ph.D.

Enrique Gòmez Barrena, M.D.
Elena Brach del Prever, M.D.
Pierangiola Bracco, Ph.D.
Jeremy Gilbert, Ph.D.
Yrjo Konttinen, M.D., Ph.D.
Amanda Marshall, M.D.
Orhun Muratoglu, Ph.D.
Javad Parvizi, M.D.
Lisa Pruitt, Ph.D.
Jose Antonio Puertolas, Ph.D.
Clare Rimnac, Ph.D.
Joanne Tipper, Ph.D.

5th UHMWPE International Meeting – AGENDA: THURSDAY, SEPTEMBER 22, 2011

7.00 a.m.	On-Site Registration Opens	
8:00 a.m.	Welcome, Opening Remarks	*Steven Kurtz*
Session I:	**Wear and Mechanical Behavior of HXLPE** Session Co-Moderators: *Clare Rimnac, Ph.D. and José Antonio Puertolas, Ph.D.*	
8:15 a.m.	**Invited Talk 1:** Tradeoffs in Crosslinked UHMWPE Used in Total Joint Arthroplasty	*Lisa Pruitt*
8:35 a.m.	**Podium Talk 1:** Wear Measurement of Highly Cross-Linked UHMWPE Using a 7Be Tracer Implantation Technique	*Markus Wimmer*
8:50 a.m.	**Podium Talk 2:** Characterization of Network Parameters for UHMWPE Using Plane Strain Compression	*Anuj Bellare*
9:05 a.m.	**Podium Talk 3:** Peak Stress Intensity Factor Governs Crack Propagation Velocity in Crosslinked UHMWPE	*P. Sirimamilla*
9:20 a.m.	**Podium Talk 4:** Polyether Ether Ketone as an Orthopaedic Bearing Surface Against UHMWPE	*Aiguo Wang*
9:35 a.m.	**Podium Talk 5:** In Vivo Oxidative Stability and Clinical Performance for 1st- and 2nd-Generation Highly Crosslinked Polyethylenes	*Steven M. Kurtz*
9:50 a.m.	Round Table Q/A and Discussion of Session 1	
10:05 a.m.	Morning Coffee Break	
Session II:	**Vitamin E in UHMWPE** Session Co-Moderators: *Pierangiola Bracco, Ph.D. and Jeremy Gilbert, Ph.D.*	
10:30 a.m.	**Invited Talk 2:** Can Incorporation Of Vitamin E be an Alternative to Remelting of Radiation Cross-linked UHMWPE?	*Luigi Costa*
10:50 a.m.	**Podium Talk 6:** Development and Validation of Vitamin E Containing Ultra-High Molecular Weight Polyethylene Grades	*Rainer Walkenhorst*
11:05 a.m.	**Podium Talk 7:** Homogeneity and Grafting of Small and Large Quantities of Vitamin E in Ultra High Molecular Weight Polyethylene	*Reto Lerf*
11:20 a.m.	**Podium Talk 8:** A Risk Assessment of the Biocompatibility of Vitamin E Blended UHMWPE	*Angelina Duggan*
11:35 a.m.	**Podium Talk 9:** Crosslinked Vitamin E Blends with Improved Grafting and Wear Resistance	*Orhun Muratoglu*
11:50 a.m.	Round Table Q/A and Discussion of Session 2	
12:20 p.m.	Boxed Lunch and POSTER SESSION	

5th UHMWPE International Meeting – AGENDA: THURSDAY, SEPTEMBER 22, 2011

Session III:	**Additives and Modifications of UHMWPE** Session Co-Moderators: *Lisa Pruitt, Ph.D. and Enrique Gòmez Barrena, M.D.*	
2:00 p.m.	**Invited Talk 3:** FDA Keynote	*Michael Kasser*
2:20 p.m.	**Podium Talk 10:** Cytotoxic Effects of Anti-Oxidant Compounds on Primary Human Peripheral Blood Mononuclear Cells	*Joanne Tipper*
2:35 p.m.	**Podium Talk 11:** MWNT´s Acting Like Radical Scavenger in Gamma Irradiated UHMWPE/Multiwall Carbon Nanotubes Nanocomposites	*Maria Martínez-Morlanes*
2:50 p.m.	**Podium Talk 12:** The Impact of Aging Environment on the Oxidation of Stabilized and Unstabilized Crosslinked Polyethylenes	*J. Berlin*
3:05 p.m.	**Podium Talk 13:** Mechanical Properties, Fatigue and Wear Resistance of an Easily Crosslinkable Polyethylene with a Mw of 500 kg/mol	*Harold Smelt*
3:20 p.m.	Round Table Q/A and Discussion of Session 3	
3:35 p.m.	Afternoon Coffee Break	
Session IV:	**Oxidation** Session Co-Moderators: *Luigi Costa, Ph.D. and Orhun Muratoglu, Ph.D.*	
4:00 p.m.	**Podium Talk 14:** Oxidation Initiated by Cyclic Loading in the Presence of Lipids	*Keith Wannomae*
4:15 p.m.	**Podium Talk 15:** Evaluation of Oxidation in Virgin UHMWPE Hip and Knee Components After Retrieval and Shelf Aging	*M. Morrison*
4:30 p.m.	**Podium Talk 16:** Comparison of One-step and Sequentially Irradiated Ultra-High Molecular Weight Polyethylene for Total Joint Replacements	*M. Slouf*
4:45 p.m.	**Podium Talk 17:** Relationship Between In Vivo Stresses and Oxidation of UHMWPE in Hip Joint Replacement	*Marco Regis*
5:00 p.m.	Round Table Q/A and Discussion of Session 4	
5:15 p.m.	Day 1 Meeting Adjourns	
6:00 p.m.	Drexel Transportation – Transition to Penn Museum **Reception and Dinner Begins at Museum** Drexel Transportation – Transition from Museum to Bossone and Center City	

7.30 a.m.	On-Site Registration Opens	
Session V:	**Wear Debris** Session Co-Moderators: *Jay Parvizi, M.D. and Joanne Tipper, Ph.D.*	
8:00 a.m.	**Invited Talk 4:** The Macrophage	*Yrjö T. Konttinen*
8:20 a.m.	**Podium Talk 18:** Decreased Functional Biological Activity of Polyethylene Wear Debris from Revised HXLPE Liners	*Marla Steinbeck*
8:35 a.m.	**Podium Talk 19:** The Anti-inflammatory Properties of Vitamin E Significantly Reduce TNF-α Release from Primary Human Monocytes After Stimulation with UHMWPE Wear Particles	*C. Bladen*
8:50 a.m.	**Podium Talk 20:** Dendritic Cell Activation by Ultra High Molecular Weight Polyethylene	*B. Scharf*
9:05 a.m.	**Podium Talk 21:** Effect of UHMWPE Particles on Mesenchymal Stem Cell Replication	*Amanda Marshall*
9:20 a.m.	**Podium Talk 22:** Imaging Intra-cellular Polyethylene Wear Debris with Coherent Anti-Stokes Raman Scattering Spectroscopy	*Martin Lee*
9:35 a.m.	Round Table Q/A and Discussion of Session 1	
9:50 a.m.	Morning Coffee Break	
Session VI:	**Retrieval Analysis** Session Co-Moderators: *Amanda Marshall, M.D. and Steven M. Kurtz, Ph.D.*	
10:30 a.m.	**Invited Talk 5:** The Role of Retrieval Analysis in Validation of New Polyethylenes	*Clare Rimnac*
10:50 a.m.	**Podium Talk 23:** Surface Damage, In Vivo Oxidation, and Reasons of Revision for Highly Crosslinked Tibial Inserts for TKA	*Dan MacDonald*
11:05 a.m.	**Podium Talk 24:** Oxidation of Highly Cross-linked Tibial Inserts	*Barbara Currier*
11:20 a.m.	**Podium Talk 25:** In Vivo Performance of Highly Cross-linked UHMWPE	*S. Rowell*
11:35 a.m.	**Podium Talk 26:** Autonomous Mathematical Reconstruction of Polyethylene Tibial Inserts to Measure Low Wear Volumes	*C. Knowlton*
11:50 a.m.	**Podium Talk 27:** Bacterial Adherence in Infected Arthroplasties: Material Differences	*Enrique Gòmez Barrena*
12:05 p.m.	Round Table Q/A and Discussion of Session 6	
12:20 p.m.	Meeting Adjourns	

5th UHMWPE International Meeting – POSTER PRESENTATIONS

Poster No. 1	Using Oxidative Induction Time to Determine Antioxidant Concentration in UHMWPE	*E.G. Heuer*
Poster No. 2	The Influence of Antioxidants and Crosslinking on the Absorption of a Model Physiological Fluid	*J.B. Berlin*
Poster No. 3	Oxidation Leads to an Increase in Wear Rate for Irradiated/Melted UHMWPE	*A. L. Neil*
Poster No. 4	Oxidation of Wear Tested and Shelf-aged UHMWPE Acetabular Liners	*Askim Senyurt*
Poster No. 5	Structural Differences of UHMWPE Induced by High Dose Gamma Irradiation	*Kerstin Von Der Ehe*
Poster No. 6	Anisotrophy of Ram Extruded NIST 1050 Reference UHMWPE	*H.L. Kluk*
Poster No. 7	In Vivo Crosslink Density Changes in Highly Crosslinked UHMWPE Bearings	*S.D. Reinitz*
Poster No. 8	Resistance of Crosslinked, Vitamin E Blended UHMWPE to Oxidation	*John C. Knight*
Poster No. 9	Resistance of Crosslinked, Vitamin E Blended UHMWPE to Fatigue Crack Propagation	*John C. Knight*
Poster No. 10	Chronic Impingement of Lumbar Disc Arthroplasty Increases the Functional Biological Activity of Polyethylene Wear Debris	*Ryan Baxter*
Poster No. 11	The Novel Use of UHMWPE as a Spinal Implant	*Oded Loebl*
Poster No. 12	Introduction of a Novel Modified UHMWPE Prosthetic Material; Test Results	*Gabriella Zsoldos*
Poster No. 13	Effects of Resin Type and Remelting on Crack Propagation in Crosslinked UHMWPE	Nathan D. Webb
Poster No. 14	Diamond-Like-Carbon Coatings for UHMWPE: A Way to Minimize Wear and Bacterial Adherence	*Gema del Prado*
Poster No. 15	HALS (Hindered Amine Light Stabilizers) as Alternative Stabilizer for Medical Implants	*Leon Stijkel*
Poster No. 16	Wear of Vitamin E UHMWPEs Under Ideal and Adverse Conditions	*Joanne Tipper*
Poster No. 17	Do Drugs Administered During Total Joint Replacement Surgery Affect the Wear of UHMWPE?	*Joanne Tipper*
Poster No. 18	The Mechanical Wear Properties and Surface Characteristics of the UHMWPE Material Used on Wear Couple Systems	*Geriel Ettienne-Modest*
Poster No. 19	Effect of Thermal Treatment on the Wear of Radiation Crosslinked UHMWPE With and Without Vitamin E	*Aiguo Wang*
Poster No. 20	Systematic Review of Highly Crosslinked Polyethylene Wear Rates and Patient Factors	*J.D. Patel*
Poster No. 21	Wear Evaluation of Simpirica's LimiFlex™ Flexion-Limiting Device Containing UHMWPE	*Ryan Siskey*
Poster No. 22	Wear Analysis of Fixed and Mobile Bearing Knee Systems	*L.A. Korduba*
Poster No. 23	High Oxidation and Wear resistances of Polyethylene Arisen by Vitamin E-blending and Poly (MPC) Grafting	*Masayuki Kyomoto*
Poster No. 24	Oxidation in UHMWPE Powder Containing Vitamin E: Combined TSL, ESR, and FTIR Analyses	*Dereje Abdi*
Poster No. 25	Detection of Oriented Allyl Radicals at Room Temperature in Gamma-Irradiated UHMWPE	*Jahan M.Shah*
Poster No. 26	Comparison of Damage in Design Matched Mobile and Fixed Bearing Total Knee Arthroplasty Prostheses	*Kirsten E.Stoner*
Poster No. 27	Retrieval Analysis of Tibial Post Wear Damage and Implant Design in Four Contemporary Designs of Constrained Condylar Knee	*Xiaonan Wang*
Poster No. 28	Effect of Non-uniform De-cohesion on Crack Initiation from Notches in Crosslinked UHMWPE	*P. Sirimamilla*

Poster No. 29	A New Highly Crystalline UHMWPE: A Comparative Study Against Conventional Resins	*F. J. Medel*
Poster No. 30	Toughness in Highly Crosslinked UHMWPEs by Essential Work of Fracture	*F.J. Pascual*
Poster No. 31	Detection of Vitamin E in UHMWPE by Colorimetry and Water Contact Angle Techniques	*A. Terriza*

5th UHMWPE International Meeting

With Special Thanks To:

Drexel UNIVERSITY

Ticona
Performance Driven Solutions™

GUR® UHMW-PE

Ticona
Performance Driven Solutions™

Orthopedic Implant Material-of-Choice.

GUR® UHMW-PE

Ultra-High Molecular Weight Polyethylene

As the leader in UHMW-PE, and with almost 50 years' of application experience, Ticona helps meet the needs of orthopedic surgeons with proven long-term materials performance in joint replacements.

Outstanding properties profile

- Low wear
- Excellent lubricity
- Biocompatibility
- Abrasion resistance
- High energy absorption
- Exceptional impact strength
- Vitamin E filled premium grades
- High purity
- Conforms to ASTM F648, ISO 5834-1

GUR UHMW-PE for:

- Hip, knee and shoulder arthroplasty
- Other joint replacements
- Spine applications

TICONA 50 YEARS OF POLYMER INNOVATION

To learn more visit
www.ticona.com/products/uhmw-pe
or call 1.800.833.4882

Ticona Engineering Polymers
8040 Dixie Highway, Florence, KY, USA 41042

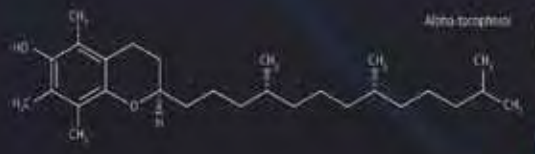

Tradeoffs in Crosslinked UHMWPE used in Total Joint Arthroplasty

Lisa A. Pruitt
Department of Mechanical Engineering, UC Berkeley, Berkeley, CA 94720

Introduction: Ultra high molecular weight polyethylene (UHMWPE) wear is a common cause of late failure in total joint arthroplasty (TJA). Highly crosslinked UHMWPE resins have demonstrated reduced wear in total hip arthroplasty (THA) and total knee arthroplasty (TKA), although occasional fractures have occurred *in vivo* [1,2]. More recently, there has been an interest in the use of highly crosslinked UHMWPE for use in total shoulder arthroplasty (TSA) [3]. Since the contact stresses are higher in TKA and TSA than THA, use of highly crosslinked UHMWPE's in TKA or TSA may result in mechanical failure of the tibial or glenoid insert. In order to maintain the wear resistance of highly crosslinked UHMWPE and retain high strength as well as providing fatigue or fracture resisitance particularly for use in TKA or TSA, modified or "second generation" highly crosslinked UHMWPE resins have been developed. However, it is not clear how the various manufacturing methods will affect *in vivo* performance. The purpose of this work is to evaluate the wear, fatigue, and oxidation behavior of a large number of clinically-relevant first and second generation ultra-high formulations which may have application in TJA.

Materials and Methods: Nine distinct clinically-relevant formulations of UHMWPE were evaluated, including two untreated controls. The materials were subjected to gamma irradiation in one or multiple doses (0 to 10 Mrad) followed by heat treatments either above or below the melting temperature (130^{o}C or 147^{o}C). All resins were either compression molded GUR 1020 or ram extruded GUR 1050. Multidirectional wear tests were performed on a custom pin-on-disc tribotester (20-30 MPa, bovine serum, 500,000 cycles) using a previously-validated protocol [4]. Fatigue crack propagation (FCP) tests were conducted on compact tension specimens using a standard fracture mechanics protocol [5]. Oxidation was measured using FTIR spectroscopy following artificial aging using a previously-validated environment [6].

Results: Wear tests showed that first and second generation cross-linked ultra-high had substantially lower wear rates than untreated control materials, which depended primarily on radiation dose and secondarily on heat treatment and resin (Figure 1). FCP tests showed that highly cross-linked and re-melted materials demonstrated the worst FCP resistance, untreated controls had the best FCP resistance and sub-melt annealed or moderately cross-linked materials had intermediate FCP resistance (Figure 2). Artificial aging showed that sub-melt annealed materials have the potential to oxidize while re-melted materials were oxidatively stable (Figure 3).

Conclusions: There is a trade-off amongst wear rate, resistance to fatigue crack propagation, and oxidative stability in clinically-relevant cross-linked formulations of UHMWPE. Moderately cross-linking re-melted materials produces good fatigue and oxidation resistance but fair wear resistance; sub-melt annealing highly cross-linked materials produces good wear and fatigue properties but leaves the material susceptible to oxidation.

References:

[1] Furmanski et al., Biomaterials (2009); [2] Patten et al., J. Bone.Joint. Surg, (2010); [3] Kurtz, S., *UHMWPE Handbook* (2009); [4] Zhou et al. *ASME J Tribol,* (2005) ; [5] Baker et al. *J Biomed Mat Res A,* (2003); [6] Van Citters et al. *J Tribology,* (2004).

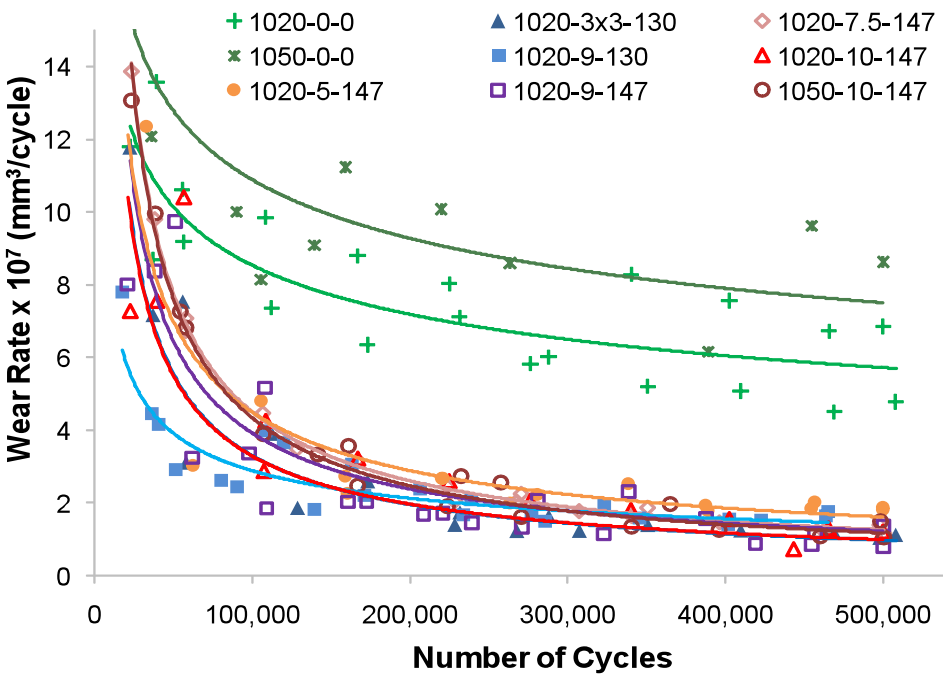

Figure 1. Wear data showing wear rates were substantially lower for both first and second generation cross-linked ultra-high compared to untreated (n=2 tests). Steady-state wear rate depended primarily on radiation dose, and secondarily on heat treatment and resin. Nine different highly crosslinked UHMWPE resins were tested. The key at the top of the graph indicates the resin type, irradiation dose, and annealing temperature (resin type-irradiation dose-annealing temperature)

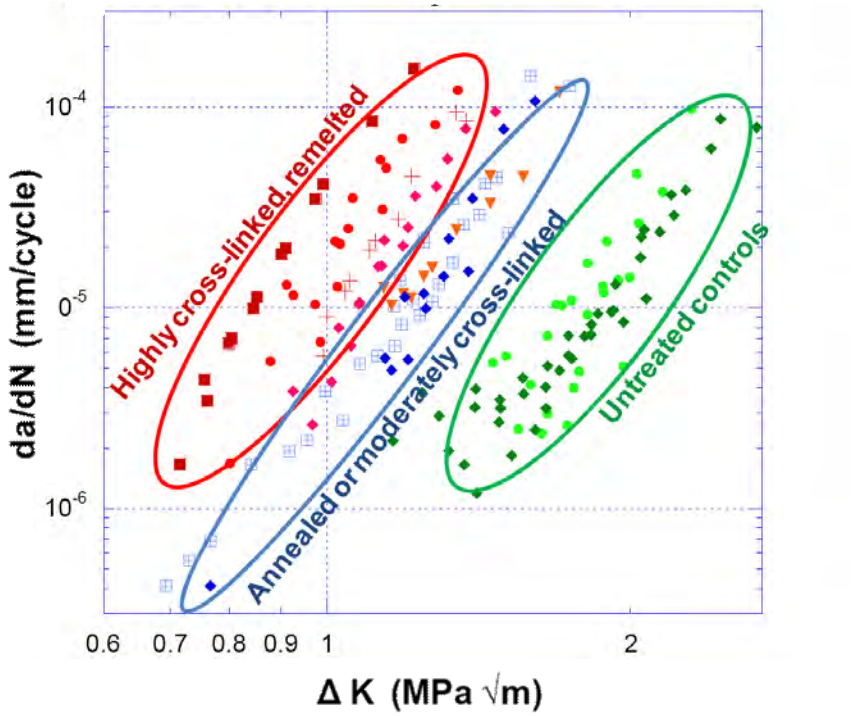

Figure 2. Fatigue crack propagation (FCP) data showing that sub-melt annealing and moderate cross-linking preserved FCP resistance better than re-melting. The key indicates the resin type, irradiation dose, and annealing temperature.

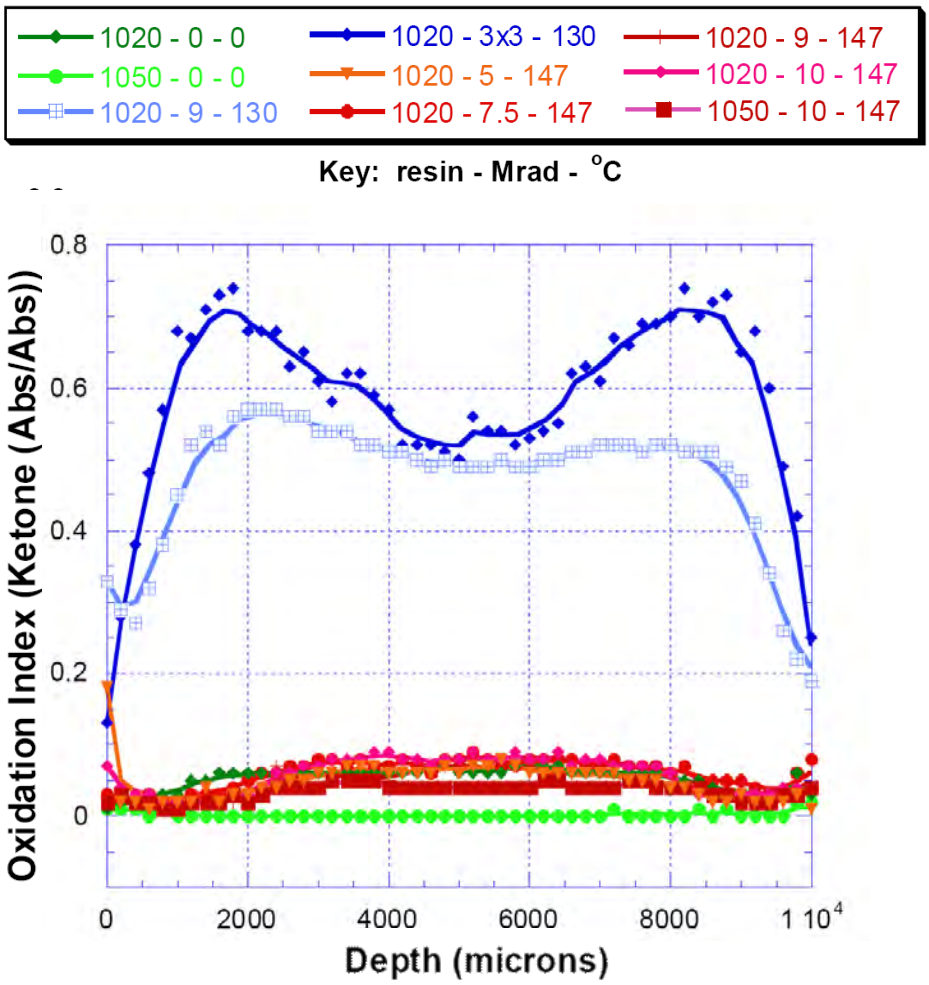

Figure 3. Artificial aging data demonstrating that annealed materials oxidized while re-melted materials remained chemically unchanged. The key indicates the resin type, irradiation dose, and annealing temperature.

1020 - 0 - 0
1020 - 3x3 - 130
1020 - 9 - 147
1050 - 0 - 0
1020 - 5 - 147
1020 - 10 - 147
1020 - 9 - 130
1020 - 7.5 - 147
1050 - 10 - 147
Key: resin - Mrad - °C

Wear Measurement of Highly Cross-Linked UHMWPE Using a 7Be Tracer Implantation Technique

Wimmer M[1], Dwiwedi Y[1], Laurent M[1], Chipps K[2], Blackmon J[3], Kozub R[4], Bardayan D[5], Gross C[5], Stracener D[5], Smith M[5], Nesaraya C[5], Erikson L[6], Patel N[6], Rehm E[7], Ahmed I[7], Greene J[7], Greife U[6]

[1]Rush University Medical Center, Chicago, Illinois 60612, [2]Rutgers University, Piscataway, NJ 08854, [3]Louisiana State University, Baton Rouge, LA 7080, [4]Tennessee Technological University, Cookeville, TN 38505, [5]Oak Ridge National Laboratory, Oak Ridge, TN 37831, [6]Colorado School of Mines, Golden, CO 80401, [7]Argonne National Laboratory, Argonne, Illinois L 60439

Statement of Purpose: The very low wear rates achieved with the current highly cross-linked ultrahigh molecular weight polyethylenes (UHMWPE) used in hip and knee prostheses have proven to be difficult to measure accurately. The method of choice has been gravimetry, but its accuracy and precision are limited by polymer fluid absorption and static charging. Not only can the correction for fluid absorption *significantly exceed* the wear value, its accuracy is limited because fluid absorption in a wear specimen cannot be reproduced exactly in the soak or load-soak controls used to effect the correction. Undercorrection sometimes leads to negative "wear" values that are obviously incorrect. Efforts have therefore been made to circumvent these limitations with tracer methods using radioactive nuclei [1, 2] and rare earth tracers [3, 4]. The purpose of this study was to effect a proof-of-concept on the use of the radioactive tracer beryllium-7 (^{7}Be) to determine wear in a highly cross-linked orthopedic UHMWPE.

Methods: The radioactive ^{7}Be source for the experiment was produced in the ATOMKI cyclotron institute in Debrecen, Hungary, via the ^{7}Li(p,n)7Be reaction. After chemical extraction from the ^{7}Li matrix, the ^{7}Be was transferred to a sputter cathode for injection in a tandem accelerator at the Oak Ridge National Laboratory, TN. The activity available resulted in ^{7}Be beam currents of 10^{5}-10^{6} ions/sec at the sample location. A new implantation setup consisting of a wheel with 20 foils of increasing thickness and additional energy "smearing" foils was installed at the beam line. This setup assured a homogenous distribution of implanted nuclei up to 8.5 um below the surface. Three cross-linked (100 kGy e-beam, WIAM - warm-irradiated, adiabatic-melted) and four conventional UHMWPE pins, 9.3 mm in diameter, all compression-molded from GUR 1050, were thus activated with 10^{9} to 10^{10} nuclei.

A six-station pin-on-flat apparatus (OrthoPOD™, AMTI, Inc., Boston, MA) was used to wear test the activated pins, along with non-activated control pins. In this test, the flat face of the pin slid against a polished wrought cobalt-chromium disk; each pin was immersed in 15 g of lubricant (bovine newborn calf serum) at 37°C and subjected to a constant nominal contact pressure of 3 MPa along a 5 x 5 mm path. A 20% Germanium gamma detector was employed to determine activity loss of the UHMWPE pins. Wear of each pin was calculated taking into account the natural decay of ^{7}Be.

In addition, we checked for any oxidative material degradation stemming from high energy implantation. A UHMWPE pin was irradiated with a "cold" ^{7}Li beam at 10^{11} ions/sec and another pin at 10^{13} ions/sec, both values exceeding the maximum intended beam currents for ^{7}Be implantation. An oxidation index versus depth profile was then acquired by Fourier transform infrared spectroscopy on thin films obtained by microtoming the pins along their axis. The oxidation index was defined as the carbonyl peak (1740 cm^{-1}) absorbance normalized to the vinylene group (1360 cm^{-1}) absorbance [5]. These oxidation profiles were compared with those for untreated and artificially aged [6]control pins.

Results: The fraction of radioactivity lost, corrected for natural decay , versus wear cycles was much lower for the three highly cross-lined pins than for the four conventional pins, as shown in Fig. 1. Indeed, for the conventional UHMPWE, the wear was high enough to remove the homogeneous radioactive layer, leading to a tapering-off of lost activity starting at approximately 2 million cycles.

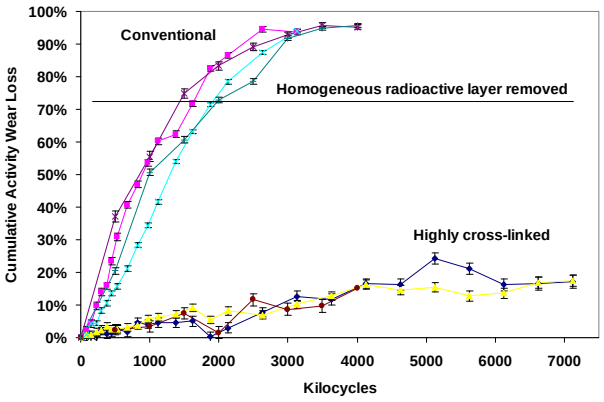

Fig. 1. Activity loss versus wear cycles for the cross-linked and conventional UHMWPEs.

The conventional-to-cross-linked ratio of the activity loss (equivalent to the wear rate) was 13.1 ± 0.8, in the expected range for these materials [7-9]. The average activity loss, linear wear, mass wear rates per million cycles are given in Table 1 for the two polyethylenes. A wear rate of 0.26 μm/million cycles, corresponding to 17 μg/million cycles, was detected for the cross-linked UHMWPE in this experiment, with an estimated detection limit of 50 to 100 nm/million cycles.

Table 1. Activity loss and estimated wear rates for the conventional and cross-lined UHMWPEs.

	Conventional UHMWPE	Cross-Linked UHMWPE
% Activity Wear/1 Million Cycles	40.6 ± 1.1	3.1 ± 0.1
Linear Wear μm/1 Million Cycles*	3.4 ± 0.4	0.26 ± 0.04
Mass Wear μg/1 Million Cycles	230 ± 27	17 ± 3
Mass Wear per Area $\mu g/cm^2$/1 Million Cycles	320 ± 40	24 ± 4

*assumes 10% error in SRIM range

The effect of ion fluence during implantation on the wear rate could be examined given that the ion fluence used varied from pin to pin. The wear rates as a function of ion fluence for the seven pins are shown in Fig. 2. There appears to be a slight trend of wear rate decrease with ion fluence increase, perhaps associated with a slight amount of cross-linking.

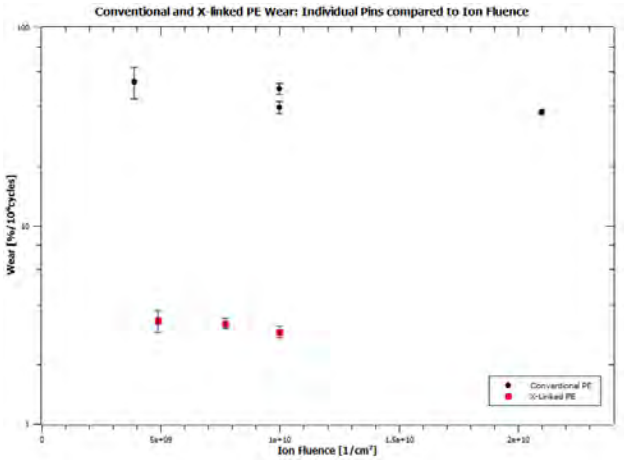

Fig. 2. Wear rate versus ion fluence for the four conventional and three cross-linked UHMWPE pins tested.

For the oxidative degradation study, the average oxidation index was 0.040 ± 0.010 for the pin subjected to 10^{11} ions/sec and 0.112 ± 0.026 for the pin subjected to 10^{13} ions/sec, versus 0.044 ± 0.006 for the nonimplanted control and 0.393 ± 0.001 for the accelerated aged nonimplanted control. Thus, the lower ion implantation rate did not have a detectable effect on the oxidative degradation of the UHMWPE. The higher implantation rate had an effect, but the oxidation index was still well below that for the aged sample.

Conclusions: This study demonstrated the feasibility of using ^{7}Be as a radioactive tracer to measure very low wear rates in UHMWPE, and to our knowledge this constitutes the first such measurement on a highly cross-linked UHMWPE. The 13-fold higher wear rate for the conventional material relative to the cross-linked material was in the expected range and agreed well previously reported values. The detection limit was estimated to be of 50 to 100 nm of linear wear per million cycles for the 9.3 mm diameter pins used here. By optimizing conditions, such as increasing the dose of activating nuclei and by improving the reproducibility of gamma measurements, additional sensitivity to measure wear rates should be achievable. Ion implantation at the rates used in the study were not found to have a significant effect on oxidative degradation. The observed trend toward a decrease in the wear rate with increased ion fluence requires further study.

Future applications of this tracer technology may include the analysis of location-specific wear, such as loss of material in the post or backside of a tibial insert. It may also be suitable for continuous wear measurements while applying various loading profiles, thus allowing a quicker and more sophisticated assessment of input variables on UHMWPE wear. The technique may also be applicable to other wear resistant orthopedic materials such as ceramics.

References: (1) Sauvage T. Nucl Instrum Meth B. 1998;143: 397-402. (2) Wall CM. Wear. 2005;259:964-971. (3) Kunze J. J ASTM International. 2006;3: AI100253. (4) Ngai V. Wear. 2009;267:679-682. (5) ASTM Standard Fxxx. (6) ASTM Standard F2003-2. (7) Muratoglu OK. Biomaterials. 1999;20:1463-1470. (8) McKellop H. J Orthop Res. 1999;17:157-167. (9) Laurent MP. J Arthroplasty. 2008;23:751-761.

Characterization of Network Parameters for UHMWPE using Plane Strain Compression

[1]Bellare, A; [1]Patel-Wilson, T; [1]Abreu, EL
[1]Department of Orthopedic Surgery, Brigham and Women's Hospital, Harvard Medical School, Boston, MA

Statement of Purpose: Currently ultra-high molecular weight polyethylene (PE) is irradiated using ionizing radiation to a dose of 50-100kGy which converts the linear, highly entangled PE macromolecules into a crosslinked and entangled network. Laboratory wear test and clinical wear studies on highly entangled and crosslinked PEs have shown them to be more resistant to particulate wear in total joint replacement prostheses, which has been of major factor limiting their lifetime [1-3]. The irradiated PEs are usually thermally stabilized to decrease free radicals created by the radiation since they can otherwise lead to long term oxidative degradation. The density of crosslinks in these PEs are then measured using equilibrium swelling techniques or by measurement of gel content, which involve the use of solvents in which PE macromolecules unravel and disentangle in the solvent. The swell ratio and gel content are thereby governed by the crosslinks and the entanglements trapped between crosslinks since these macromolecular segments cannot unravel. While these techniques provide a relatively reliable measure of crosslink density in PE, it is more important to measure the effective crosslinks, which is the sum of entanglements acting as physical crosslinks and chemical crosslink associated with radiation, which is a true measure of crosslinks in irradiated PE. In this study, we compared two constitutive models governing the large strain deformation of polymers to describe the plane strain compression of unirradiated (control) and irradiated PE, and extracted molecular level parameters such as effective crosslink density and molecular weight between crosslinks. This study demonstrates that this characterization technique is an effective alternate method to characterize the network parameters of orthopedic grade PE.

Methods: Ram extruded rod stock of GUR 1050 (Ticona GmbH, Oberhausen, Germany) was obtained from Meditech Medical Polymers (Fort Wayne, IN). The stock was γ-irradiated (Steris, Northborough, MA) to a dose of 0kGy (PE-0), 50kGy (PE-50), 100kGy (PE-100) and 200kGy (PE-200), then heated to 170ºC for 4 hours and slow cooled to room temperature. The unirradiated and crosslinked PE stock was machined into 4.1mm x 4.1mm x 4.7mm blocks that snugly fit into a custom-built channel-die equipped with cartridge heaters and a temperature controller. Each sample (n=6) was preheated to 150ºC and then compressed in the die using a universal tensile tester (Admet Inc, Norwood, MA) operating at a crosshead speed of 0.25 mm/min until the samples fractured. The true stress-true strain behavior was then modeled in a strain range of 0.1-0.35 using the eight-chain model developed by Arruda and Boyce [4] or Gaussian chain statistics [5]. The eight-chain model for plane strain compression takes the form [6]: $\sigma = Y + \sigma_R$, where Y is the plastic flow stress and

$$\boldsymbol{\sigma_R = \frac{G_N}{3} n^{1/2} \left(\frac{1}{\lambda_{chain}}\right) L^{-1} \left(\frac{\lambda_{chain}}{n^{1/2}}\right) (\lambda^2 - \lambda^{-2})}$$

σ_R is the rubberlike stress generated by the entangled molecular network; G_N is the initial strain hardening modulus of the network (defined as $N_e kT$, where N_e is the effective crosslink density, k is the Boltzmann constant, and T is the absolute temperature); n is the number of rigid links between crosslinks; and

$$\boldsymbol{\lambda_{chain} = \sqrt{\frac{(\lambda^2 + 1 - \lambda^{-2})}{3}}}$$

where λ is the compression ratio, and $L^{-1}(x)$ is the inverse Langevin function, $L(x)=\coth(x)-1/x$. The molecular weight between crosslinks, M_e, was calculated using the following equation:

$$\boldsymbol{N_e = \rho \frac{N_A}{M_e}\left(1 - \frac{2M_e}{M_n}\right)}$$

where ρ is the density of the amorphous phase of PE (=0.855g/cc), N_A is Avogadro's number and M_n is the number average molecular weight of PE, reported to be 4.1×10^5 g/mole [7]. For the Gaussian equation [6],

$$\boldsymbol{\sigma_R = G_N(\lambda^2 - \lambda^{-2})}$$

Statistical differences were assessed by ANOVA with Bonferroni *post-hoc* test and Student's t-test, considering p-values less than 0.05 to be significant.

Results: The true stress true strain behavior of PE was significantly affected by γ-irradiation, as shown by representative stress-strain curves in Figure 1. PE-0 and PE-50 failed at substantially higher applied stress and strain compared to PE-100 and PE-200. Higher levels of irradiation caused a larger impact, with PE-100 and PE-200 failing at applied pressures between 5-10 MPa and at lower strains than PE-0 and PE-50.

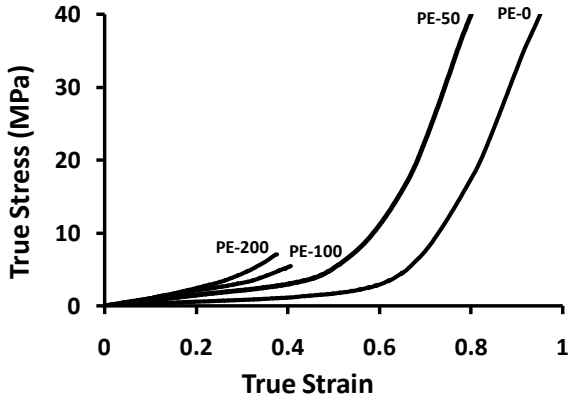

Figure 1. Representative true stress-strain plots of PE-0, PE-50, PE-100, and PE-200. PE-0 and PE-50 failed at 58 and 47 MPa, respectively, the scale is reduced for clarity.

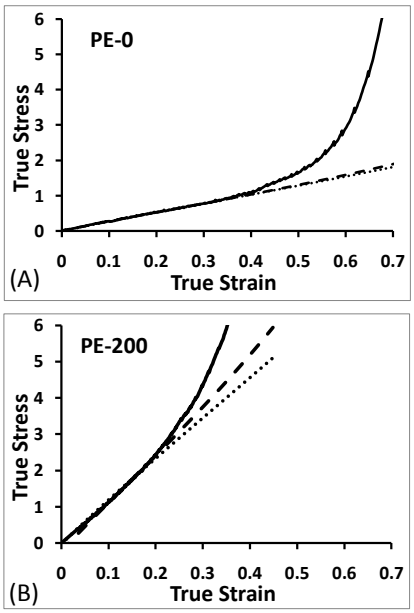

Figure 2. True stress-strain curves of PE samples: (A) unirradiated and (B) γ-irradiated to 200kGy. The graphs show the respective experimental curves (continuous lines), and plots obtained using the eight-chain model (dashed lines) and gaussian model (dotted lines).

The strain hardening modulus (G_N) and the effective crosslink density (N_e) increased with increasing radiation dose while the molecular weight between crosslinks (M_e) decreased regardless of the models used, as shown on Table 1. The differences in values of G_N and N_e between groups were significant ($p \leq 0.06$). Both models also showed a monotonic decrease in effective molecular weight between crosslinks (M_e) ($p \leq 0.02$).

Eight-Chain Model			
Sample	G_N (MPa)	$N_e \times 10^{-26}$ (m^{-3})	M_e (g/mole)
PE-0	0.480 ± 0.182	0.81 ± 0.31	7117 ± 2708
PE-50	1.617 ± 0.112	2.77 ± 0.19	1868 ± 130
PE-100	2.086 ± 0.222	3.57 ± 0.38	1455 ± 146
PE-200	2.432 ± 0.125	4.16 ± 0.21	1240 ± 65
Gaussian Approximation			
Sample	G_N (MPa)	$N_e \times 10^{-26}$ (m^{-3})	M_e (g/mole)
PE-0	0.565 ± 0.213	0.97 ± 0.37	5997 ± 2255
PE-50	2.072 ± 0.087	3.55 ± 0.15	1454 ± 61
PE-100	3.053 ± 0.260	5.23 ± 0.45	991 ± 80
PE-200	3.538 ± 0.190	6.06 ± 0.33	852 ± 48

Table 1. Unirradiated and γ-irradiated PE: Strain hardening modulus (G_N), effective crosslink density (N_e) and effective molecular weight between crosslinks (M_e) calculated using the eight-chain and Gaussian models.

The strain hardening moduli obtained using the eight-chain and Gaussian models were significantly different from each other only for the crosslinked PEs ($p<0.01$).

Discussion: In this study, the plane strain compression behavior of PE was modeled using the eight-chain model developed by Arruda and Boyce [4] and Gaussian chain statistics [5] to extract network parameters. Unlike solvent based characterization techniques, which provide a measure of crosslink density and molecular weight between chemical crosslinks alone, this technique provides the "effective" crosslink density and includes both chemical crosslinks induced by radiation as well as the entanglements which act as "effective" physical crosslinks since it does not utilize solvents which disentangle the macromolecules. The effective crosslink density and the molecular weight between the effective crosslinks are more appropriate parameters since the large strain behavior of crosslinked PE originates from stretching of the molecular network of crosslinked chains as well as entangled chains. The effective crosslink density is also expected to more accurately govern the wear behavior of crosslinked PE than solely the density of chemical crosslinks associated with irradiation since entanglements of PE also contribute to wear resistance, evident from the fact that less entangled (i.e., lower molecular weights) PE have a lower resistance to wear. The values of N_e obtained from application of the eight chain model are in general agreement with a previous study [6]. It should however be pointed out that the deformation in that study was conducted in the solid state where lamellar deformation mechanisms contributed to strain in addition to the extension of the rubber-like entanglement network. The entanglement density of PE-0 was much higher than the equilibrium entanglement density (maximum possible entanglement density) of PE, reported to be 1240 g/mole [8]. The higher value obtained from this model is partly due to the fact that the PE was not maintained in the melt state long enough for the equilibrium entanglement density to be attained prior to experimentation and probably also due to several underlying assumptions of the model, such as strain rate effects and molecular relaxation during deformation, which were neglected. Yet, this model has the advantage of taking into account the contributions of entanglements as physical crosslinks, which other solvent-based techniques are unable to take into account. In addition, this model can also be applied to solid state deformation conducted at room temperature, thereby measuring effective crosslink density without any unraveling or re-entanglement that can occur upon melting or dissolving PE. In summary, constitutive modeling of the deformation of PE can be effective in characterizing the network parameters of PE, which has a strong effect on its mechanical and tribological behavior that are important for its long-term performance in total joint replacement prostheses.

References: [1]Muratoglu O. Biomat 1999; 29: 1463-70.
[2]McKellop H. J Orthop Res 1999;17(2):157-67.
[3] Kurtz, SM, Clin Orthop Rel Res 2011 Epub
[4]Arruda E. J Mech Phys Solid 1993;41:389-412.
[5]Haward RN. Marcomol 1993 ;26:5860-5869.
[6]Bartczak Z. Macromol 2005 ;38:7702-13.
[7]Spiegelberg, SH. Trans Soc Biomat 1999, 216.
[8]Pearson DL. Macromol 1994 ;27 :711-19.

Peak Stress Intensity Factor Governs Crack Propagation Velocity in Crosslinked UHMWPE

P. Abhiram Sirimamilla[1], Jevan Furmanski[2], Clare Rimnac[1]
1. Case Western Reserve University, Cleveland, Ohio, 2. Los Alamos National Laboratory, Los Alamos, New Mexico.

Introduction: Ultra high molecular weight polyethylene (UHMWPE) joint replacement components experience physiological loading which is comprised of both cyclic and quasi-static components [1]. The traditional fracture mechanics approach uses the Paris relationship [2] to estimate fatigue crack propagation (FCP) resistance as a function of the rate of crack growth per cycle (da/dN) and the applied stress intensity factor range (ΔK). The Paris relationship estimates the FCP resistance of the material but recent studies suggest that a static mode mechanism governs fatigue crack propagation in UHMWPE [3, 4]. The hypothesis of this study is that fatigue crack propagation velocity in crosslinked UHMWPE is driven by the peak stress intensity, Kmax, during cyclic loading, rather than the stress intensity factor range, ΔK.

Methods: Round compact tension specimens of remelted 65 kGy and 100 kGy gamma-irradiated UHMWPE were machined according to ASTM 1820-01 in the transverse direction with: notch depth, a=18mm; specimen length, w=40mm; thickness, b=18mm; and, side groove depth of 2 mm on each side. The notch was razor sharpened an additional 1.6 mm at a rate of 0.16mm/min beyond the notch making the total crack length 19.6 mm. Three test conditions were evaluated (waveform/frequency/load ratio) with two specimens tested per condition (n=2):

1) Square wave/1 Hz/R=0.1 (P_{min}/P_{max})
2) Sine wave/0.1 Hz/R=0.1
3) Sine wave/3 Hz/R = 0.5

Testing was conducted under ambient laboratory conditions on an Instron 8511 servohydraulic load frame. A travelling microscope was used to measure crack growth. The load and position data from the testing frame were sampled at 500 Hz throughout the test. From the data measured, crack growth rates (da/dt, da/dN), applied stress intensity factor range (ΔK), and maximum stress intensity range (K_{max}) were calculated. A velocity normalizing factor Q, which describes the theoretical altered average crack velocity under non-sinusoidal load waveforms compared to a sine wave with the same peak stress, was calculated from the load data.

Results: Both crosslinked materials tested showed Kmax dominated crack growth. For each material, the crack propagation behavior was distinctly different for each of the three testing conditions when plotted using the Paris relationship (da/dN vs. ΔK; Figs 1a and 2a). However the data collapsed to a single stable propagation power-law relationship when average velocity was correlated to Kmax (da/dt vs Kmax; Figs 1b and 2b). The remelted 100 kGy material was less resistant to fatigue crack growth than the remelted 65 kGy material (Table 1). As expected, for each material, the rate of crack propagation for the square waveform was higher than for the sine waveform, and the difference agreed well with the velocity normalizing factor Q. The normalizing factor estimated for the remelted 65 kGy and 100 kGy materials were Q=2.8 and Q=2.1, respectively.

Discussion: This work supports earlier work reported for non-crosslinked UHMWPE material where it was found that crack growth was dependent on K_{max} [3, 4] and is governed by quasi-static driving forces [4]. Static mode fracture holds that even a static load will drive crack propagation in UHMWPE without the application of any cyclic loading [5]. The results suggest that, although crosslinked UHMWPE is a ductile polymer, the fracture mechanisms governing crack propagation are primarily static mode in nature, which is characteristic of brittle materials [4]. The findings of this study may be useful in designing UHMWPE joint replacements by considering K_{max} as the driving force for fatigue crack propagation.

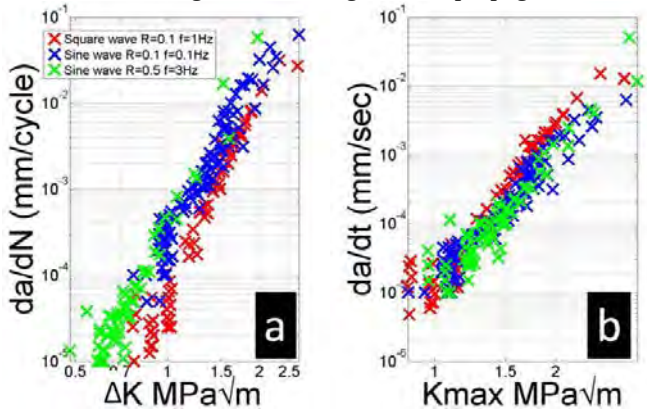

Figure 1: FCP behavior for remelted 65 kGy material showing the peak stress dependence of the crack propagation rate: (a) FCP behavior appear distinct when plotted as da/dN vs ΔK (Paris relationship); (b) FCP behavior collapses to a single relationship when plotted as da/dt vs Kmax. The factor to normalize da/dt for the square wave data in (b) was Q=2.8.

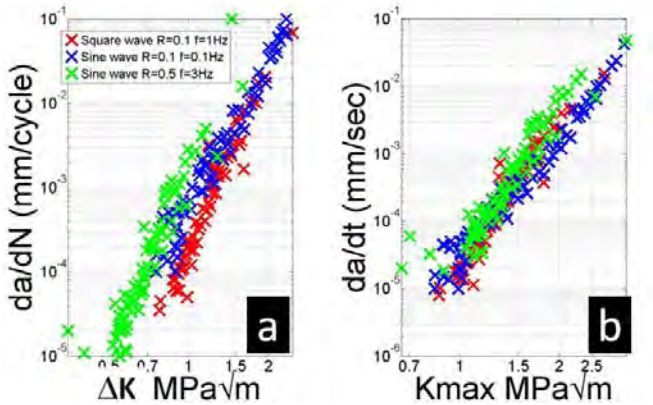

Figure 2: FCP behavior for remelted 100 kGy material showing the peak stress dependence of the crack propagation rate: (a) FCP behavior appear distinct when plotted as da/dN vs ΔK (Paris relationship); (b) FCP behavior collapses to a single relationship when plotted as da/dt vs Kmax. The factor to normalize da/dt for the square wave data in (b) was Q=2.1.

Table 1: Average velocity vs K_{max} relationship constants

Testing Condition	Remelted 65 kGy		Remelted 100 kGy	
	m	**C**	**m**	**C**
Square wave f=1Hz, R = 0.1	7.64	3.1e-5	6.81	5.7e-5
Sine wave f=0.1Hz, R = 0.1	5.95	1.6e-5	5.44	3.8e-5
Sine wave f=3Hz, R = 0.5	5.70	1.9e-5	6.80	4.2e-5

*C is in mm/sec$(MPa\sqrt{m})^m$.

References: [1] Douglas et al., J Biomechanics; 1997; 30 (9)959-965; [2] Anderson TL ISBN 0-8493-4277-5; [3] Furmanski et al, Polymer 48 (2007) 3512-3519. [4] Furmanski and Rimnac CORR 2010 Dec 3, Epub ahead of print. [5] Trans 57th ORS 2010; Poster 0333.

Acknowledgements: NIH/NIAMS T32 AR00750, NIH/NIAMS R01AR047192, Orthoplastics, Wilbert J Austin Chair.

Polyether Ether Ketone as an Orthopaedic Bearing Surface against UHMWPE

Wang, A., Lawrynowicz, D., Zhang, Z., Korduba, LA., Herrera, L.
Stryker Orthopaedics, Mahwah, NJ

Statement of Purpose: Soft-on-soft bearings for orthopaedic joint replacements have the potential to be beneficial in comparison to traditional metal-on-polyethylene couples. There have been laboratory and clinical studies in the past to study soft-on-soft couples in both the hip and knee. Moore et al studied a soft-on-soft knee couple (polyacetal on UHMWPE) in 63 knees and found no failures as a result of fracture or wear of the femoral component [1]. McKellop et al conducted a hip simulator test and found 23% less wear with polyacetal heads on an UHMWPE cups compared to a standard metal heads on UHMWPE cups [2]. The purpose of these tests was to assess the tribological viability of another soft-on-soft bearing couple, polyether ether ketone (PEEK) against UHMWPE, as a bearing couple for orthopaedic applications (US Patent Application #20100312348).

Methods: Two knee tests and a hip simulator test were conducted. The knee testing was conducted on a 6-station knee simulator (MTS, Eden Prairie, MN). All motion and loading was computer controlled and followed ISO 14243-3 [3]. The components consisted of cobalt-chrome (CoCr) femoral components, femoral components machined from industrial grade PEEK, and femoral components injection molded with medical grade PEEK. All components were tested against inserts manufactured from GUR 1020 UHMWPE that were vacuum/flush packaged and sterilized in nitrogen (N2\Vac®, Stryker Orthopaedics, Mahwah, NJ). Both tests were conducted for a total of three million cycles.

The hip simulator test was conducted on a multi-station hip joint simulator (MTS, Eden Prairie, MN). The femoral heads were either cobalt-chrome or machined from industrial grade PEEK. The heads articulated against GUR 1020 UHMWPE that was sequentially annealed and irradiated three times and then gas plasma sterilized (X3®, Stryker Orthopaedics, Mahwah, NJ). Testing was run at 1Hz with cyclic Paul curve physiologic loading applied axially, at a maximum of 2450 N [4]. Testing was conducted for a total of five million cycles.

The lubricant used for all testing was Alpha Calf Fraction (Hyclone Labs, Logan, UT) diluted to 50% with a pH-balanced 20-mMole solution of deionized water and EDTA [5]. Standard test protocols were used for cleaning, weighing and assessing the wear loss of the inserts [6]. Statistical analysis was performed using the Student's t-test.

Results: The results of knee testing are shown in Figure 1. There is a significant reduction of 36% when comparing the wear of the tibial inserts running against machined PEEK components to those against CoCr components ($p = 0.048$). The second test also produced a large reduction (41%) in wear rate when comparing molded PEEK to CoCr. However, this difference was not significantly different ($p= 0.08$).

Figure 2 shows the results of the hip test. There is a significant reduction in wear rate when using PEEK as a bearing surface ($p = 0.019$). Wear of the highly crosslinked polyethylene cups against PEEK heads was not measurable despite the use of soak control specimens.

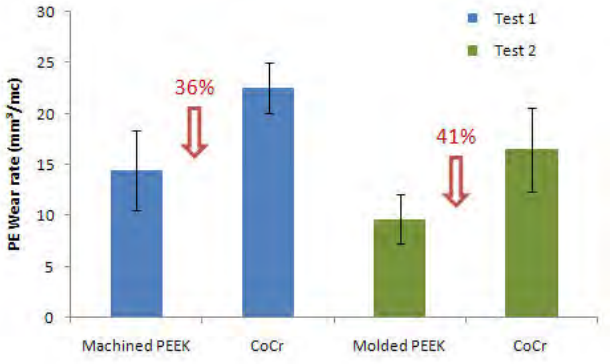

Figure 1: Wear rates of conventional UHMWPE tibial inserts (N2\Vac®) for knee simulator testing after 3 million cycles.

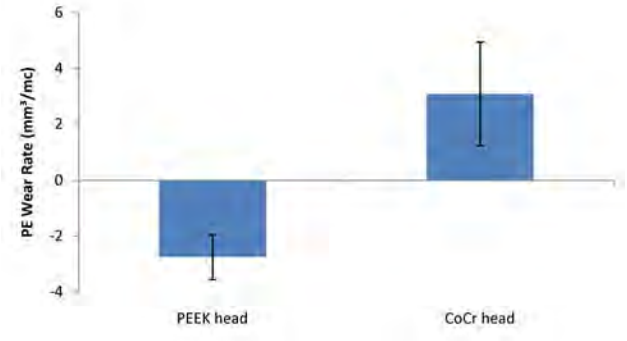

Figure 2: Wear rates for highly crosslinked UHMWPE cups (X3®) for hip simulator testing after 5 million cycles.

Conclusions: The PEEK-on-polyethylene bearing couples used in this testing show promise as a potential alternative to the standard metal-on-polyethylene. Besides the benefit of lower wear, as demonstrated by the current testing, the soft-on-soft coupling also has the advantages of lower stiffness, no release of metal ions, and potentially lower manufacturing costs.

References: [1] Moore DJ, Freeman MAR, Revell PA, Bradley GW, Tuke M. J Arthroplasty, 1998; 13(4): 388-395. [2] McKellop HA, Bradley GW, Freeman MAR, Tuke MA. Clin Mater, 1993; 14(2): 127-132. [3] ISO/DIS 14243-3 [4] Paul JP, Proc Inst Mech Engrs, 1966; 181 (3J): 8-15. [5] Wang A, Essner A, Schmidig G, J. Biomed. Mater. Res. Part B: Appl Biomater, 2004; 68B: 45-52. [6] ASTM F2025

In Vivo Oxidative Stability and Clinical Performance for 1st- and 2nd-Generation Highly Crosslinked Polyethylenes

[1,2]Kurtz, SM; [1]MacDonald, D; [1]Gawel, H; [3]Parvizi J; [4]Klein, G; [4]Hartzband, M; [5]Garino, J; [6]Marshall, A; [7]Mont M; [4]Levine, H; [8]Kraay, M; [9]Stulberg, S; [8]Rimnac, C

[1]Drexel University, Philadelphia, PA; [2]Exponent, Philadelphia, PA; [3]Rothman Institute, Philadelphia, PA; [4]Hartzband Center for Hip & Knee Replacement, Paramus, NJ; [5]Penn Presbyterian Medical Center, Philadelphia, PA; [6]University of Texas Health Science Center at San Antonio, San Antonio, TX; [7]Sinai Hospital of Baltimore, Baltimore, MD; [8]Case Western Reserve University and University Hospitals Case Medical Center, Cleveland, OH; [9]Cleveland Clinic at Lutheran Hospital, Cleveland, OH

skurtz@drexel.edu

Introduction: Highly crosslinked polyethylenes (HXLPEs) have been in use in total hip replacement for more than a decade [1]. There is consensus in the literature that these materials show improved wear in vivo and significantly reduce osteolysis [2]. However, questions remain regarding the long-term oxidative stability of HXLPEs and the influence of mechanical behavior on THA clinical performance. Starting in 2005, 2nd generation HXLPEs were developed to improve the clinical performance of HXLPE. Examples of 2nd generation HXLPEs include sequentially annealed [3] and vitamin E diffused HXLPEs [4].

The purpose of this multicenter study was to assess the oxidative stability, mechanical behavior, wear and reasons for revision of 2nd generation HXLPEs and compare them to our ongoing retrieval collection of 1st generation annealed and remelted HXLPEs [5, 6]. We hypothesized the sequentially annealed components would exhibit wear rates similar to 1st generation HXLPEs. We also hypothesized that 2nd generation HXLPEs would be more oxidatively stable than 1st generation HXLPEs.

Methods: 376 hip liners were consecutively retrieved during revision surgeries at 7 surgical centers and continuously analyzed over the past 10 years in a prospective, multicenter study of THA revision outcomes and retrieval analysis. 25 liners were sterilized using non-ionizing methods (Gas Sterilized; Implanted 8.1±3.5 years), 45 liners were sterilized in an inert environment (Gamma Inert; Implanted 6.1±3.8 years), 177 were highly crosslinked and remelted (Longevity, Durasul, Marathon, XLPE: Remelted; Implanted 1.8±2.1 years), 84 were highly crosslinked and annealed (Crossfire: Annealed 1; Implanted 3.6±2.7 years), and 44 were highly crosslinked and annealed in 3 sequential steps (X3: Annealed 2; Implanted 1.2±0.9 years).

The analytical methods have been described previously [5, 6], but are summarized below. Oxidation was characterized in accordance with ASTM 2102 using transmission FTIR performed on thin sections (~200μm) from the superior/inferior axis. Lipids were extracted from the HXLPEs prior to analysis by 6 hours in boiling hexane. Sections were then exposed to NO for 16 hours and rescanned using an FTIR spectrometer to assess hydroperoxide content, a metric of oxidation potential.

Mechanical behavior was assessed via the small punch test (ASTM 2183). Small cylindrical samples were taken from the superior and inferior regions of the inserts both at the surface and below the surface. Liner penetration was assessed directly using a calibrated micrometer.

Results: The predominant reasons for revision were loosening, instability, and infection (Fig. 1). Thus far one Vitamin E-diffused has been revised in the study after 1 year for instability (Fig. 2).

Oxidation and oxidation potential were higher in the Gamma Inert and both annealed groups than the Remelted and Gas Sterilization groups ($p<0.001$; Kruskal-Wallis Test), particularly at the rim (Figs. 3-4). This pattern was also observed when excluding implants over 3 years (the longest implanted Annealed 2 liner) (Figs. 3B&4B). Oxidation significantly correlated with implantation time only at the rim of the Annealed 1 liners (Rho=0.689; $p<0.001$) and the bearing surface of the Remelted (Rho=0.210; $p=0.008$) and Annealed 2 liners (Rho=0.432; $p=0.011$). The oxidation index was low and uniform in the Vitamin E-diffused liner (Average Max Oxidation Index = 0.14), as was the oxidation potential (Average Maximum Hydroperoxide Index = 0.13).

At the superior bearing surface, the ultimate load negatively correlated with implantation time in the Annealed 1 liners (Rho=-0.238; $p=0.036$), but not with any other cohort ($p>0.05$). The Annealed groups had the highest ultimate load at the bearing surface (Kruskal-Wallis Test; $p<0.001$). The Gas Sterilized liners had the lowest superior surface ultimate load ($p<0.020$).

Gas Sterilized and Gamma Inert liners had significantly higher wear rates than all of the HXLPE cohorts ($p\leq0.01$). No differences were detected in wear rates among the HXLPE liners ($p>0.576$).

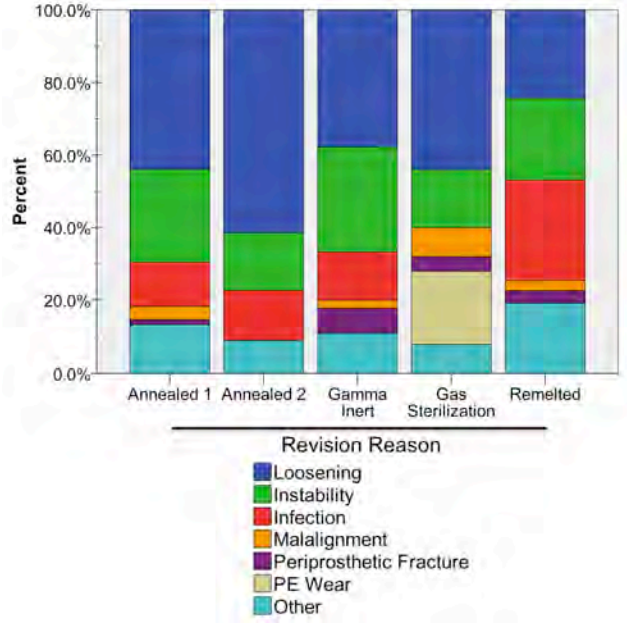

Fig. 1: Revision Reasons for the 375 retrieved liners.

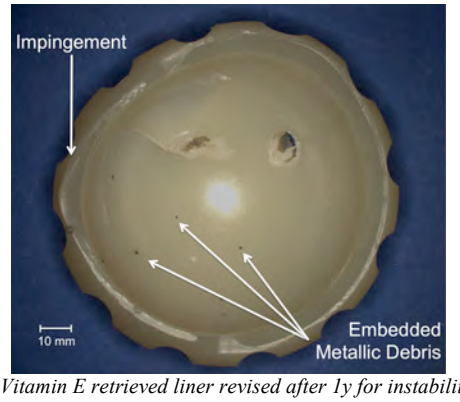

Fig. 2: Vitamin E retrieved liner revised after 1y for instability, with notable evidence of chronic rim impingement.

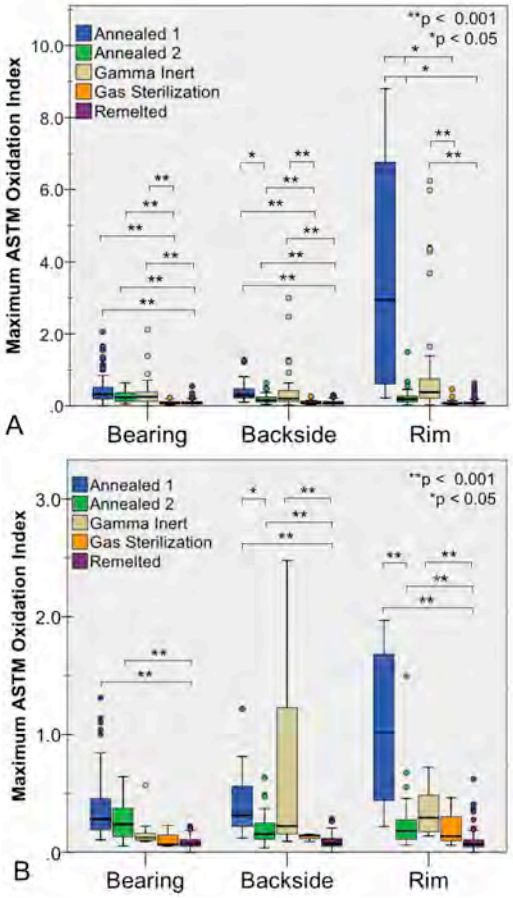

Figure 3: Regional oxidation of all the liners (A) and the subset of liners in vivo ≤3 years (B).

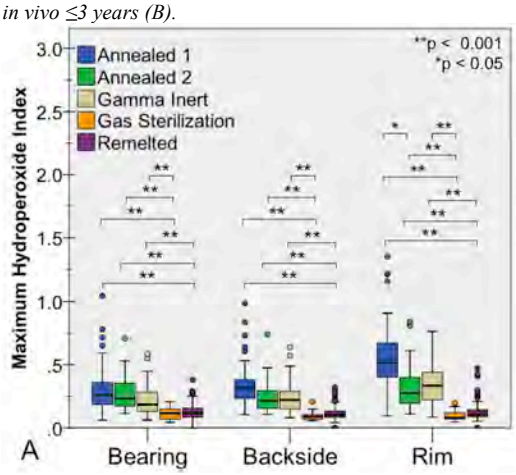

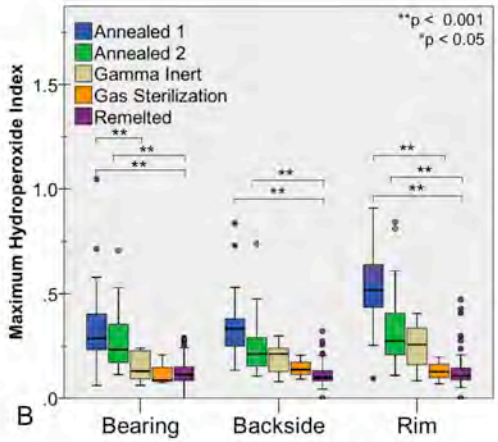

Figure 4: Regional hydroperoxide content of all the liners (A) and the subset of liners in vivo ≤3 years (B).

Conclusions: This ongoing study continues to evaluate the polyethylene properties and reasons for revision among clinically relevant HXLPEs used in total hip replacement, including 2nd generation HXLPEs. All of the HXLPEs materials in this study have thus far proven effective at reducing wear rates compared to the Gamma Inert and Gas Sterilized controls. The oxidative stability and mechanical behavior of these materials, however, is formulation dependent. With respect to oxidation, it is clear that sequential annealing reduced oxidation when compared with first-generation annealing. Additional Vitamin E retrievals are needed to compare with the existing collection of thermally stabilized HXLPEs that have been characterized thus far.

Acknowledgements: This study was supported by NIH R01 AR47904. Institutional support has been received from Stryker Orthopedics, Zimmer Inc., and Stelkast.

References:

[1] Kurtz SM. The UHMWPE Biomaterials Handbook (2nd Edition). Burlington, MA: Academic Press; 2009.

[2] Kurtz SM, Gawel HA, Patel JD. History and systematic review of wear and osteolysis outcomes for first-generation highly crosslinked polyethylene. Clin Orthop Relat Res. 2011.

[3] Dumbleton JH, D'Antonio JA, Manley MT, Capello WN, Wang A. The basis for a second-generation highly cross-linked UHMWPE. Clin Orthop Relat Res. 2006;453:265-71.

[4] Oral E, Wannomae KK, Hawkins N, Harris WH, Muratoglu OK. Alpha-tocopherol-doped irradiated UHMWPE for high fatigue resistance and low wear. Biomaterials. 2004;25:5515-22.

[5] Macdonald D, Sakona A, Ianuzzi A, Rimnac CM, Kurtz SM. Do first-generation highly crosslinked polyethylenes oxidize in vivo? Clin Orthop Relat Res. 2010.

[6] Kurtz SM, Medel FJ, MacDonald DW, Parvizi J, Kraay MJ, Rimnac CM. Reasons for revision of first-generation highly cross-linked polyethylenes. J Arthroplasty. 2010;25:67-74.

Can incorporation of vitamin E be an alternative to remelting of radiation cross-linked UHMWPE?

L. Costa*, P. Bracco*, S. Zanetti*, P. Dalla Pria**, D. Masoni**
*) Dipartimento di chimica IFM, Via Giuria 7, 10125 Torino
**) SAMO SpA, via Matteotti 37, 40057 Cadriano Granarolo Emilia, Bologna

Introduction Although UHMWPE has been successfully used in total joint replacement for more than 30 years now, its lifetime is often limited due to oxidative degradation induced by radiation sterilization with high energy radiation in air. Alkyl macroradicals formed upon irradiation can react with oxygen dissolved in the polymer matrix, triggering an oxidative cascade that reduces UHMWPE molecular mass with consequent worsening of mechanical properties, embrittlement, and decrease of the abrasive wear resistance and increase of wear debris [1,2]. Radiation cross-linking and subsequent melting of UHMWPE has been successfully used to decrease wear. However, postirradiation melting also reduces crystallinity and mechanical properties of the irradiated polymer [3].

The incorporation of the antioxidant vitamin E has been proposed recently as an alternative to postirradiation melting to avoid oxidation and simultaneously preserve the mechanical properties of crosslinked UHMWPE [4].

Blending of vitamin E to the powder prior to consolidation was originally proposed to stabilize UHMWPE against oxidation caused by irradiation in air. Once consolidated, the blend can be crosslinked with the use of ionizing radiation. The presence of vitamin E in UHMWPE during irradiation protects the polymer from oxidation but partially hinders the cross-linking reaction, while the vitamin E itself is reacted. Nevertheless, the degradation products of vitamin E have been shown to retain a stabilizing activity [5].

Many recent studies have focused on the optimization of the vitamin E concentration and the subsequent radiation dose to obtain a simultaneously wear- and oxidation-resistant UHMWPE [6]. We postulate that 0.1%wt of vitamin E can provide adequate oxidation stability, without detrimentally affect the wear resistance. The aim of this study was to investigate the effect of radiation dose on cross-linking efficiency, oxidative stability and mechanical properties of blends of UHMWPE with 0.1%wt of vitamin E.

Materials and Methods: GUR 1020 UHMWPE plates, blended with vitamin E (0.1wt %) have been γ irradiated to a nominal dose of 25, 50, 75 and 100 kGy and tested without any further thermal treatment. The materials have been microtomed to 160μm thick films and characterized before and after accelerated aging for 14 days (ASTM F2003-02). Oxidation indexes were determined by FTIR (Perkin Elmer Spectrum 100) according to ASTM F 2102. A Perkin Elmer Pyris differential scanning calorimeter (DSC) was used to measure crystallinity: the samples were heated at a heating rate of 10°C/min from 30 to 180°C and the degree of crystallinity was determined using a heat of fusion, ΔH_f, of 293 J/g. Crosslink density was measured by swelling cylinders (Ø 5mm, h 3mm) in xylene pre-heated to 130°C for 2 hours. The crosslink density was then calculated according to ASTM F2214. Mechanical testing was performed in accordance with ASTM D882-02. The free radical content was investigated by Electron Paramagnetic Resonance (EPR). The measurements were performed at room temperature with a Bruker EMX X-band spectrometer at a microwave power of 0.1 mW.

Results and discussion:

The nominal radiation doses reported above were based on the manufacturer's certification. We investigated the accuracy of the real absorbed doses with FTIR, using a well established internal protocol which involves the determination of trans-vinylene species. The "experimental" doses calculated by this method are reported in table 1.The cross-link density of the irradiated, unaged blends are reported in table 1. Cross-link density increases steadily with radiation dose. Wear resistance has not been investigated in this study, but since cross-link density has been shown to be directly related to wear, it can be used as an indicator of wear resistance. The cross-link density measured for the 100 kGy irradiated 0.1%wt vitamin E blended UHMWPE is lower than that registered on a 100 kGy irradiated virgin UHMWPE [7], but it is comparable to that of a 75 kGy irradiated UHMWPE, which has often been regarded as the optimum compromise between wear and fatigue resistance.

Nominal radiation dose (kGy)	Experimental radiation dose (kGy)	MW between cross-links [g/mol]
25	37	16000
50	59	9100
75	78	7800
100	88	6700

Table 1 Cross-link density of 0.1 wt% vitamin E-blended, irradiated UHMWPE

Alkyl radicals in irradiated polyethylene are detectable only in the first 24h after irradiation, after which only stable radicals (allyl, tertiary) trapped in the amorphous-crystalline interphase can be revealed. The total concentration of residual free radicals measured over 24h after irradiation on the irradiated vitamin E blends was maximum in the 100kGy irradiated sample, but did not exceed 0.15 mmol/kg.

The maximum oxidation index measured before ageing was ≤0.05 on all samples. After ageing, the maximum OI was measured in the sample irradiated to the highest dose, but even there it did not exceed the value of 0.14.

Figure 1 shows, as an example, the FTIR spectra obtained from a 100 kGy irradiated, 0.1wt% vitamin E-blended UHMWPE before and after accelerated ageing, indicating a substantially constant oxidation level.

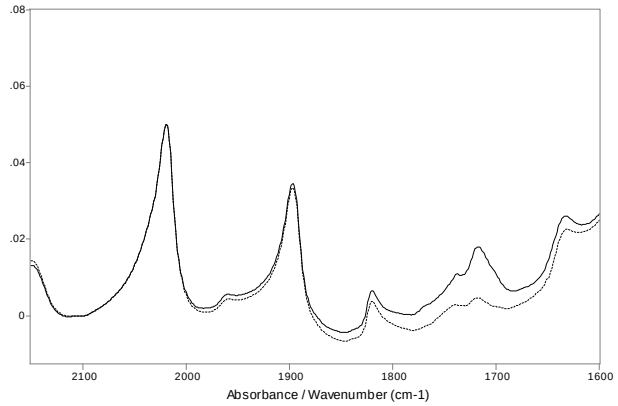

Figure 1 FTIR spectra of 100 kGy irradiated, 0.1wt% vitamin E-blended UHMWPE before (—) and after (---) accelerated ageing

Percent crystallinity of the irradiated blends increases slightly with the radiation dose, as a result of "tie" chain scission, due to irradiation, and rearrangement of those chains into the crystalline structure. Crystallinity does not vary significantly after ageing, confirming that no significant structural changes occur to the polymer.

		% Crystallinity	
Nominal radiation dose (kGy)	**Experimental radiation dose (kGy)**	**Before ageing**	**After ageing**
25	37	58	57
50	59	57	57
75	78	59	61
100	88	59	60

Table 2 Percent crystallinity of 0.1 wt% vitamin E-blended, irradiated UHMWPE

The mechanical properties of irradiated vitamin E blended UHMWPE do not differ from that of unaged irradiated virgin UHMWPE [7]. While the mechanical performances of irradiated UHMWPE are well known to deteriorate rapidly, the tensile tests performed on the irradiated blends before and after accelerated ageing show little differences: US decreases slightly, while YS increases and EB decreases. These small changes can be presumably attributed to a slight increase of the cross-linking degree induced by the prolonged stay at 70°C that favor partial melting of small crystalline domains and/or rearrangement of the crystalline-amorphous interphase, allowing reaction of some trapped radicals.

	Yield strength (MPa)		Elongation at break (%)		Ultimate strength (MPa)	
Radiation dose (kGy) Experimental (Nominal)	**Before ageing**	**After ageing**	**Before ageing**	**After ageing**	**Before ageing**	**After ageing**
37 (25)	20	23	490	360	62	62
59 (50)	22	24	440	324	68	62
78 (75)	22	24	400	272	65	60
88 (100)	22	24	350	260	64	60

Table 3 Mechanical properties of 0.1wt% vitamin E-blended, irradiated UHMWPE

Conclusions:

Vitamin E is known to be a very active antioxidant for polyolefines. We have shown that UHMWPE blended with 0.1%wt of vitamin E exhibit a high oxidation resistance, even after irradiation to 100kGy in air and subsequent accelerated ageing in a highly oxidizing environment. This observation suggests that cross-linking of vitamin E blended UHMWPE can be performed simply by irradiation without any following thermal treatment, nor even the "homogenization" step at 120°C required for vitamin E-doped UHWMPE, thus avoiding the loss of crystallinity which is responsible for undesirable changes in mechanical properties and fatigue resistance. The efficiency of cross-linking is decreased in the presence of vitamin E, but an additive concentration of 0.1%wt still allows to modulate the cross-link density to the desired level.

References:

[1] Costa L et al. Biomaterials. 1998;19:659–668
[2] Costa L et al. In: Kurtz SM, ed. The UHMWPE Biomaterials Handbook. Burlington, MA: Elsevier Academic Press; 2009:309–323
[3] Oral E et al. Biomaterials. 2006;27:917–925.
[4] Bracco P et al Clin Orthop Relat Res. 2011; in press
[5] Bracco P et al Polym Degrad Stab 2007;92:2155–62
[6] Kurtz SM et al. J Biomed Mater Res A 2009;90:549–563.
[7] Oral E et al. Biomaterials 2005;26:6657–63

For submission: Convert to PDF and email abstract with contact information to skurtz@exponent.com

Development and Validation of Vitamin E Containing Ultra-High Molecular Weight Polyethylene Grades

Julia Hufen, Rainer Walkenhorst.
Ticona GmbH, Oberhausen Germany

Introduction: UHMW-PE has been used in the field of orthopedic implants for about 50 years, now. But a lot of things have changed since the early days of Sir John Charnley [1]. Especially, crosslinking has brought the wear resistance of UHMW-PE to a different level. The next big step in the material development for total joint replacements was introducing antioxidants to increase the longevity of the implant with regards to shelf life and in-vivo oxidation. The idea of using vitamin E as a biocompatible antioxidant was brought up more a decade ago e.g. [2] and has been the subject of intensive scientific discussions since then. Ticona has finally developed, validated and commercialized two new UHMW-PE grades based on the existing, commercially available Type 1 and Type 2 UHMW-PE grades [3]. Right from the beginning, the governing idea of the development was to offer a material that can be processed in the same way as the existing grades GUR 1020 and GUR 1050 and offers identical mechanical properties but with an improved oxidation resistance. These new grades are called GUR 1020-E and GUR 1050-E. It has been published before that only trace amounts of vitamin E like less than 500 ppm are sufficient for an effective oxidation resistance [4], so that the described grades with 1000 ppm offer some additional safety. As is shown here, the mechanical properties of the grades are still identical to the existing GUR grades without vitamin E.

Methods: In the present paper, we focus on the quality control and the performance properties of GUR 1020-E and 1050-E. These grades are being produced by a blending process that ensures the desired concentration (1000 ppm) of the vitamin E in a homogeneous distribution throughout the whole lot.

Mechanical testing of the consolidated material has been performed with and without vitamin E in addition to quality control testing such as concentration determination. Extensive biocompatibility testing as well as ageing tests have also been performed.

Results: One of the first challenges in the development process was the homogeneous distribution of the Vitamin E and to check the concentration of vitamin E in the powder. A new extraction/HPLC test method was developed [5] that showed reliable results and proved itself superior to the analysis by other methods like FT-IR. The concentration determination by extraction/HPLC was validated and shows excellent correlation and reproducibility [5].

The mechanical properties of the new materials also had to be verified to ensure, that the Vitamin E added samples do not show a significant change in key properties. Selected results are shown in Table 1.

In order to prove the feasibility of the new vitamin E containing grades for implant applications, a series of biocompatibility tests was performed: USP Clas VI (ISO 10993-6; -10; -11), physicochemical test (USP <661>), genotoxicity (ISO 10993-3), Hemolysis (ISO 10993-4) and cytotoxicity (ISO 10993-5).The result reports are included in the Drug Master File (DMF) 10904 and the Device Master File (MAF) 588.

	GUR 1020	GUR 1020-E	GUR 1050	GUR 1050-E
Density [g/ml]	0,929	0,929	0,926	0,926
Charpy Imp. [kJ/m2]	240	230	160	170
Abrasion (SandSlurry)	99	98	85	85
Tensile strength at 50 % elongation [MPa]	20	19	19	19
Ultimate Tensile strength [MPa]	46	46	45	41
Elongation at break [%]	503	505	425	390
E-Modulus [MPa]	676	620	604	582

Table 1: Key mechanical properties

As the material is sold in powder form and might be stored for several weeks and due to the fact that vitamin E is known to be temperature sensitive, ageing studies were performed to ensure that the vitamin E concentration stays on an acceptable level during storage.

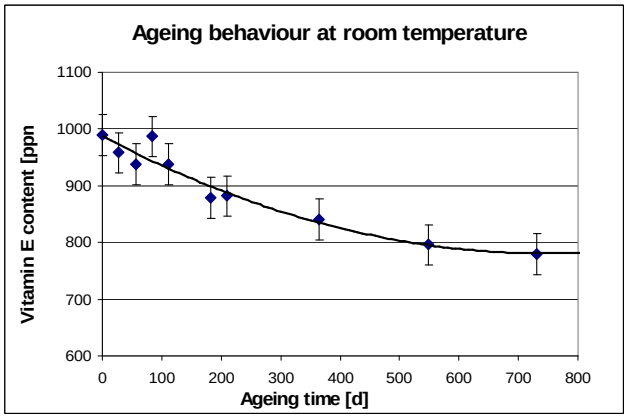

Figure 1: Ageing behavior of GUR1020-E

Conclusions: GUR 1020-E and 1050-E have been proven to be feasible for medical applications in terms of biocompatibility. Also, it has been shown that these grades may be viewed as oxidation resistant UHMW-PE grade, equivalent in mechanical properties to the unblended materials GUR 1020 and 1050. Finally, a satisfactory long term stability of the material has been shown.

References:

[1] UHMWPE Biomaterials Handbook, Ed.: Kurtz SM, Second Edition, 2009, Elsevier Inc;
[2] Tomita N, Kitakura T, et.al., J. Biomedical Material Res.48, 474 (1999)
[3] ASTM F648 and ISO 5834-1
[4] Kurtz SM, Dumbleton J, Siskey RS, Wang A, Manley M, J Biomed Mater Res A 2008, published online
[5] Hufen J, Walkenhorst R, Stein H, Keil N., Poster presentation ORS 2009.

Homogeneity and Grafting of Small and Large Quantities of Vitamin E in Ultra High Molecular Weight Polyethylene

Reto Lerf[1], Daniel Zurbrügg[2], Daniel Delfosse[1].
[1]Mathys Ltd. Bettlach, Switzerland; [2] Niutec AG Winterthur, Switzerland.

Statement of Purpose: The further improvement of UHMWPE for joint replacement application is topical. The reduction of the wear rate may be achieved by cross-linking and by an increase in the oxidative stability trough the addition of vitamin E (Kurtz SM, 2009). Although the stabilising effect of vitamin E is undisputed, the physical and chemical state of vitamin E in cross-linked UHMWPE is still under investigation. On the one hand, it was found that migration of vitamin E out of the polymer is unlikely (Oral E, 2006). On the other hand, grafting of vitamin E molecules to the polyethylene backbone was postulated (Wolf C, 2011). The purpose of the current investigation is to quantify the amount of grafting of vitamin E in UHMWPE in concentrations, 0.1 % and 1.0% blended and an E-Poly® product by Biomet.

Methods: UHMWPE powder GUR 1020 and two different concentrations of vitamin E (0.1 wt % and 1.0 wt%) were mixed and sintered. The samples with vitamin E addition of 0.1 % correspond to the pre-forms of vitamys® hip cups by Mathys Ltd Bettlach, i.e. hemispheres of diameter 68 mm. The experimental 1.0 % vitamin E samples were discs (Ø: 110 mm, H: 22 mm). Cross-linking was done at a gamma dose of 96.5 kGy. To be sure that the amount of grafting was not influenced by an inhomogeneous distribution of vitamin E, profiles in the as sintered condition were analysed by Fourier transform infrared spectroscopy (FTIR) before sampling the cross-linked specimens. Two profiles were analysed in each sample. 0.3 mm sections were cut in two directions perpendicular to each other by a microtom HM 350 (Microm GmbH, Germany). From the E-Poly sample by Biomet (E-Poly liner Ringloc-X by Biomet, size 66/36), a vitamin E profile in the pole region and another one close to the rim were established. The spectra of all sections were recorded by a Bio-Rad FTS-45 (Bio-Rad Laboratories, United Kingdom) in transmission with an aperture size of 1x1 cm at a resolution of 4 cm-1. The vitamin E index (VEI) was calculated as the ratio of the area of a characteristic vitamin E peak (1275 -1245 cm-1) to the polyethylene reference peak at 1985-1850 cm-1. The relative vitamin E index (RVEI) was calculated by subtracting the background of a pure UHMWPE.
To assess the extent of vitamin E grafting, three 0.3 mm sections were cut from the centre of both, the non-irradiated and the cross-linked 0.1 % and 1.0 % experimental samples. From the E-Poly implant, such sections were taken from the middle of the liner wall. VEI was determined as described above. Then the sections were extracted for 48 h in heptane at 98 °C and finally dried at room temperature. Again, FTIR was used to calculate VEI as described above.

Results: The control of the homogeneity of the vitamin E distribution in the as sintered condition yielded a very uniform and equal VEI over both perpendicular profiles in the samples of both vitamin E concentrations, of 0.1 % and 1.0 %. The mean relative vitamin E index (RVEI) of all sections analysed by FTIR was 0.0227 ± 0.0006 in the 0.1 % material. In the 1.0 % vitamin E sample, RVEI was 0.2786 ± 0.0067. Figure 1 illustrates these vitamin E profiles for both concentrations, for the 0.1 % vitamys® pre-form material and for experimental 1.0 %, respectively. The vitamin E content in the E-Poly liner exhibits a gradient. Minimum RVEI analysed by FTIR is 0.082 at the articulation surface at the pole and the maximum value RVEI 0.208 at the outer surface on the rim. The mean relative vitamin E index (RVEI) of the pole profile is 0.137 and 0.159 in the rim profile, respectively. Figure 2 depicts the two vitamin E profiles, pole and rim, as relative vitamin E index in the E-Poly product by Biomet.

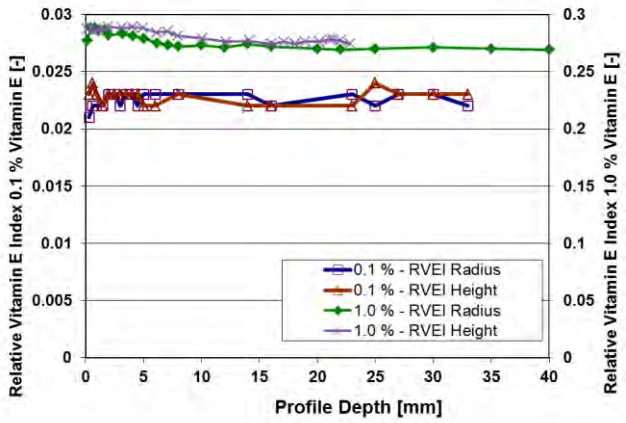

Figure 1. Concentration profiles trough the 0.1 % vitamin E sample (left scale) and the 1.0 % sample (right scale)

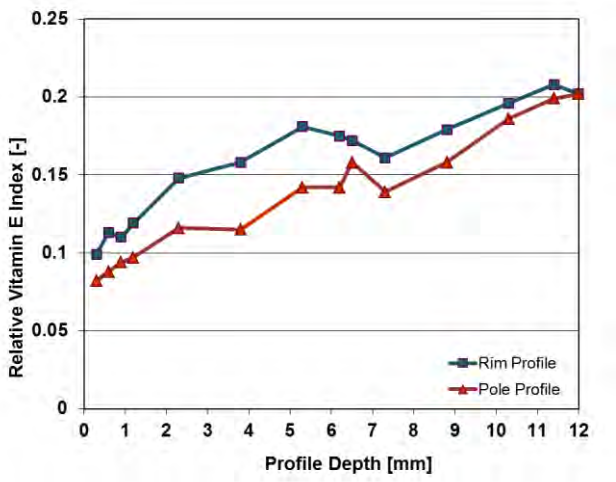

Figure 2: Concentration of vitamin E as pole profile and rim profile trough the E-Poly liner by Biomet.

There is a marked disparity in the amount of vitamin E extracted in the as sintered and the cross-linked state.

Vitamin E of the non-irradiated samples is completely extracted. After extraction, RVEI of both samples is below the detection limit of 0.001. Besides cross-linking, an effect of irradiation is the (at least partial) bonding of vitamin E to the polymer. These grafted molecules of anti-oxidant can no longer be extracted. The extracted amount of vitamin E is 23 % for the 0.1 % vitamys® sample and reaches 87 % in the experimental 1.0 % material. From the E-Poly liner, 95 % could be extracted. Hence, bonding of vitamin E is not proportional to the vitamin E concentration. At low concentrations, the majority of the vitamin E remains in the polymer, whereas at high concentration the majority can be extracted. However, at high and low concentrations a certain amount of vitamin E remains in the polymer, most likely grafted to the polymer chains. Figure 3 depicts RVEI before and after extraction and lists the percentages of vitamin E extracted.

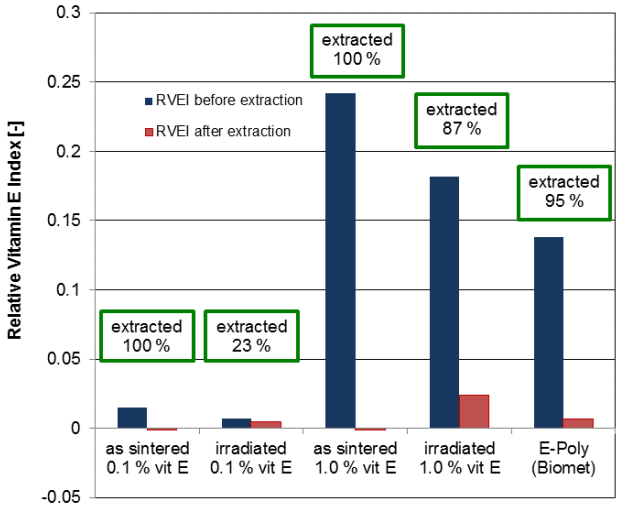

Figure 3. RVEI before and after extraction. The percentage of decrease in RVEI is indicated for each sample.

Conclusions: The production route of mixing vitamin E to UHMWPE powder results in a homogenous distribution of this anti-oxidant in the whole consolidated PE body. Therefore, artefacts in gauging the vitamin E concentration by FTIR due to inhomogeneity can be excluded. Irradiation of UHMWPE blended with vitamin E induces grafting of the α-tocopherole to the polymer macromolecules. The amount of vitamin E remaining in the polymer is not proportional to the initial concentration. It seems rather that there is a saturation of the absolute amount of vitamin E grafted for a given dose of irradiation. A dependence of the percentage grafted on the irradiation dose is reported by Wolf et al. (Wolf C, 2011). The grafting of the anti-oxidant has shown to reduce the amount of vitamin E which can be leached out. Therefore, protection of the UHMWPE against oxidation remains high (Lerf R, 2010). However, more experimental data with variable concentrations of vitamin E and different irradiation doses are required to understand the phenomenon of vitamin E grafting in irradiated UHMWPE.

References:

Kurtz SM et al, in: Kurtz SM, editor. UHMWPE biomaterials handbook 2nd ed. Amsterdam: Elsevier; 2009 p. 237–46
Oral E et al., Biomaterials 2006;27: 2434-2439
Wolf C et al., ORS 2011 Annual Meeting, poster 1178
Lerf R et al., Biomaterials 2010;31: 3643–3648

A Risk Assessment of the Biocompatibility of Vitamin E Blended UHMWPE

Angelina Duggan, Ph.D.[1], Ryan Siskey, M.S.[1,2], Steven Kurtz, Ph.D.[1,2]
[1]Exponent, Philadelphia PA; [2]Drexel University, Philadelphia PA
rsiskey@exponent.com

Statement of Purpose:
The elution of vitamin E and its degradation products from highly crosslinked UHMWPE (HXLPE) is not completely understood, and is hypothesized to depend on the formulation of the HXLPE, and whether the material is blended prior to irradiation or doped afterwards. The objective of this study was to evaluate the vitamin E blended UHMWPE used in StelKast's EXp™ acetabular liner to determine if the vitamin E pre-blended in UHMWPE matrix was susceptible to elution after radiation crosslinking. Secondly, if vitamin E could be eluted from the UHMWPE, the extract was analyzed to determine if any vitamin E degradation products were present. In parallel, a series of ISO 10993 protocols were conducted to assess the biocompatibility of the material.

Methods:
A series of polar and non-polar extractions were carried out on ethylene oxide-sterilized EXp™ GUR 1020-E acetabular liners (StelKast, McMurray, Pa) in hexane and isopropanol (IPA), respectively. For comparison, gamma inert sterilized ProAR™ GUR 1050 acetabular liners and a raw vitamin E sample provided by the resin manufacturer (Ticona, Oberhausen, Germany) served as controls, and were also extracted per the polar and non-polar protocol as the EXp™ liners. Four liners were provided of each material in as-packaged and sterilized condition.

Hexane extractions occurred between 74°C and 78°C for 72 hours and the IPA extractions occurred at room temperature for 18 hours. The materials were analyzed for changes in mass as a result of the extraction and the resultant extracts were analyzed using gas chromatography-mass spectrometry (GC-MS) and liquid chromatography-mass spectroscopy (LC-MS). The study groups have been summarized as Table 1 below. All GC-MS analyses of the hexane extracts were repeated in triplicate. The LC-MS of the hexane and IPA extracts were conducted on a single sample. Similarly, the GC-MS of the IPA extract was conducted on a single sample. The preparation of the extracts and the GC-MS and LC-MS analyses were conducted according to standard laboratory operating procedures.

Table 1. Summary of extractions and subsequent analyses

Sample	Solvent	Analytical Techniques
EXp™ 1020-E Acetabular Liners	Hexane	GC-MS, LC-MS
EXp™ 1020-E Acetabular Liners	IPA	GC-MS, LC-MS
ProAR™ 1050 Acetabular Liners	Hexane	GC-MS
Vitamin E (Ticona)	Hexane	GC-MS

To assess the biocompatibility of the acetabular liner material, ISO 10993 was used to assess genotoxicity, cytotoxicity, irritation and sensitization.

Results:
For all study groups, the mass change resulting from the extractions were less than 0.5% of the mass of the material subjected to the solvents and bordered on the measurement resolution of the microbalance used. Phthalates and aliphatic hydrocarbons were detected using GC-MS in all liner groups extracted using hexane (Figure 1). For the same hexane extracted liners, LC-MS showed no vitamin E or vitamin E degradation products. Lastly, the IPA extracted GUR 1020-E liners showed no detectable vitamin E or vitamin E degradation products using either GC-MS or LC-MS.

The presence of the phthalates in the extracts from both the GUR 1020-E groups and GUR 1050 groups mitigate the phthalate as a transformation or degradation product of vitamin E. Further, the

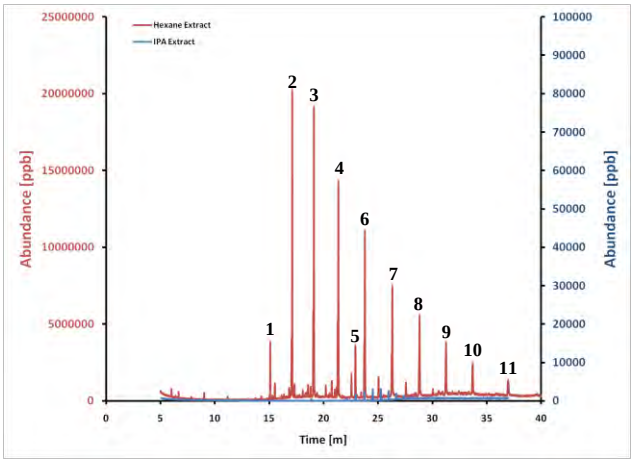

Figure 1. Chromatograms for the extracts of the EXp 1020-E liners using IPA (blue) and hexane (red) for comparison. Peaks 1-4 and 6-11 were confirmed as hydrocarbons and peak 5 was confirmed as diethylhexyl phthalate. The blue trace shows the presence of trace quantities of hydrocarbons.

phthalates identified in the GUR 1020-E group were diethylhexyl phthalate which is the diethylhexyl esterified derivative of phthalic acid. The phthalate identified in the GUR 1050 group was mono (diethyl hexyl phthalate), which is a mono diethylhexyl ester of phthalic acid. It is not uncommon for di-esterfied acids to hydrolyze back to their half (single) esters. The phthalates likely originated from the packaging of both liners and therefore the detected compounds are actually one compound, diethylhexyl phthalate (the di-ester) which, under the conditions of sample extraction and analysis, likely hydrolyzed (trace acid or base would have done this) to generate the mono (single or half) ester, mono-diethylhexyl phthalate. Regardless of these compounds, vitamin E was not detected in the extracts from any of the test groups, as confirmed by raw material provided by Ticona.

Gene-level and chromosomal mutagenicity testing was conducted per ISO 10993-3 and the EXp™ liners tested in their as packaged as sterilized condition were found non-mutagenic. Irritation and sensitization testing was conducted per ISO 10993-10 and the EXp™ liners were found to meet all reactivity requirements and did not elicit a sensitization response. Cytotoxicity testing was conducted per ISO 10993-5 and the EXp™ liners were found non-cytotoxic. The results of this test, the results of the extraction studies provided above, and the

results of the other ISO 10993 compliant testing provided above suggest the EXp™ liner to be non-carcinogenetic as well.

Conclusions:

The GUR 1020-E vitamin E blended UHMWPE used in StelKast's EXp™ acetabular liner was found to be stable when extracted using both polar and non-polar solvents. Specifically, neither solvent was found to cause the elution of vitamin E or vitamin E related degradation products or impurities from the HXLPE matrix. The presence of phthalates in the extracts from the 1020-E liners were mitigated by the presence of a similar species of phthalate in the conventional GUR 1050 liners. The phthalates are likely of the same origin and are attributed to residue from the packaging used for the liners.

Wolf et al, was the first to address the issue of biocompatibility of consolidated and irradiated UHMWPE containing transformation products of vitamin E. It has been shown that consolidation and crosslinking dose generate transformation products. However, the results of the current study suggest that no degradation products could be extracted from the radiation crosslinked GUR 1020-E material. If there are vitamin E transformation products present in the material, they appear to either be trapped within the polyethylene matrix or chemically bonded to the polyethylene backbone. Further, Oral et.al., reported that a small but measureable amount of vitamin E could be extracted from vitamin E doped UHMWPE. However, the results of the current study suggest that for blended vitamin E, the vitamin E may also be trapped within the matrix.

Lastly, the biocompatibility of the GUR 1020-E acetabular liner material was assessed for genotoxicity, cytotoxicity, irritation and sensitization. For all tests the EXp™ material was found to be biocompatible and without adverse effects that could pose a potential human health risk.

In conclusion, the results of this study strongly support the hypothesis that the elution of antioxidants and their degradation products from HXLPEs is formulation dependent. In Wolf's studies, vitamin E and degradation products could be extracted from GUR 1020 that was preblended with 8,000 ppm of vitamin E but only crosslinked with 25 kGy of gamma radiation. Although we found no vitamin E or degradation products from elution testing of the EXp™ material, these findings should not be generalized to other formulations of HXLPEs containing antioxidants.

References:

Lehninger, A.L. 1975. *Biochemistry*, 2nd Edition. New York: Worth Publishing, p. 680.

Nelson, D. L. & Cox, M. M. 2005. *Lehninger Principles of Biochemistry*, 4th Edition. New York: W. H. Freeman and Company, pp. 648-649.

Oral, E., K. K. Wannomae, et al. (2006). "Migration stability of alpha-tocopherol in irradiated UHMWPE." Biomaterials 27(11): 2434-2439.

Rontani, J-F, Nassiry, M., Mouzadahir, 2007. Free radical oxidation (autooxidation) of α-tocopherol (vitamin E): A potential source of 4,8,12,16-tetramethylheptadecan-4-olide in the environment. Organic Geochemistry 38:37-47.

Wolf, G. (2006). "How an increased intake of alpha-tocopherol can suppress the bioavailability of gamma-tocopherol." Nutr Rev 64(6): 295-299.

Wolf, G. (2007). "Estimation of the human daily requirement of vitamin E by turnover kinetics of labeled RRR-alpha-tocopherol." Nutr Rev 65(1): 46-48.

Crosslinked Vitamin E Blends with Improved Grafting and Wear Resistance

+[1,2]Oral, E; [1]Neils, A; [1]Rowell, SL; [1,2]Muratoglu OK
+[1]Harris Orthopaedic Laboratory, Massachusetts General Hospital, Boston, MA; [2]Department of Orthopaedic Surgery, Harvard Medical School
eoral@partners.org

Statement of Purpose

Vitamin E-stabilization of irradiated UHMWPE for oxidation resistant total joint implants can be done by blending vitamin E into UHMWPE powder, consolidation of the mixture, and irradiation [1]. This method avoids post-irradiation melting, which decreases the fatigue strength of irradiated UHMWPE [2].

Table 1. The radiation doses used to crosslink vitamin E blended UHMWPE.

Vitamin E concentration (wt%)	Radiation Dose (kGy)
-	100
0.05	120
0.1	125
0.2	160
1	198

Free radicals formed on the polymer during irradiation recombine to form cross-links, which impart increased wear resistance [3]. When vitamin E is present in UHMWPE during irradiation, it reacts with the free radicals, decreasing crosslinking compared to virgin UHMWPE at the same radiation dose [4]. At the same time, it is possible that some of the vitamin E gets grafted onto the polymer as previously shown with other antioxidants [5]. This is beneficial as it would localize some of the antioxidant and prevent elution.

In this study, we determined the amount of grafting in vitamin E-blended and irradiated UHMWPE. We hypothesized that increasing irradiation temperature would increase crosslinking despite decreasing vitamin E potency due to degradation at the higher temperature. To test our hypothesis, we determined the vitamin E content, vitamin E grafting, crosslink density and wear properties of vitamin E-blended UHMWPE irradiated at room temperature and at 120°C.

Materials and Methods

Medical grade GUR1050 UHMWPE (Orthoplastics, UK) was blended with 1 wt% vitamin E and consolidated. One group was irradiated using e-beam (2.5 MeV, MIT, MA) to 25, 50, 75, 100, 125 and 150 kGy at room temperature (RT). Another group was pre-heated at 120°C for 2 hours and then irradiated to the same doses (Warm). Thin sections (150 μm-thick) were microtomed from the irradiated blocks. Fourier transform infrared spectroscopy (FTIR) was used to determine a vitamin E index (1245-1275 cm^{-1} normalized to 1850-1985 cm^{-1}) before and after extraction with boiling hexane for 16 hours. Graft percentage was calculated by the ratio of the post-extraction vitamin E index to that before extraction.

Crosslink density was measured by swelling 3 mm cubes in xylene pre-heated to130°C for 2 hours. The gravimetric swell ratio was converted to a volumetric swell ratio using the density of polyethylene as 0.94 g/cc and the density of xylene at 130°C as 0.75 g/cc. The crosslink density was further calculated as previously described [7].

Cylindrical pins (dia. 9 mm, height 13 mm) were machined from virgin UHMWPE and blends of UHMWPE containing 0.05, 0.1, 0.2 and 1 wt% vitamin E. These pins were irradiated as described in Table 1. Pin-on-disc (POD) wear testing was performed as previously described [8] at 2 Hz for 1.2 million-cycles (MC). Wear was determined gravimetrically every ~0.16 MC and the wear rate was determined by the weight change from 0.5 to 1.2 MC.

Results

The goal of this study was to determine the extent of grafting in vitamin E-blended, irradiated UHMWPE. We used 1 wt% vitamin E blends because at this concentration, we could detect vitamin E by FTIR even after irradiation. However, we know from previous studies on the crosslinking of UHMWPE in the presence of vitamin E that radiation behavior as a function of concentration may not be linear; this remains a limitation of our study.

We showed previously that vitamin E decreased crosslinking in UHMWPE, thus at 1 wt% vitamin E, crosslink density is lower than at vitamin E concentrations typically considered for implants, e.g. 0.1 or 0.2 wt% at the equivalent radiation dose [5]. During irradiation used for crosslinking UHMWPE, vitamin E interferes with the free radicals on the polymer chains, which also results in the transformation of vitamin E into other products. Thus, vitamin E concentration decreased with increasing radiation dose (Fig 1). Increasing irradiation temperature resulted in higher vitamin E concentrations after irradiation (Fig 1), suggesting longer post-irradiation oxidative stability.

We also showed that vitamin E was grafted in UHMWPE by irradiation (Fig 2). Grafting may suggest longer term in vivo oxidative stability without elution.

Figure 1. Vitamin E index as a function of radiation dose and temperature.

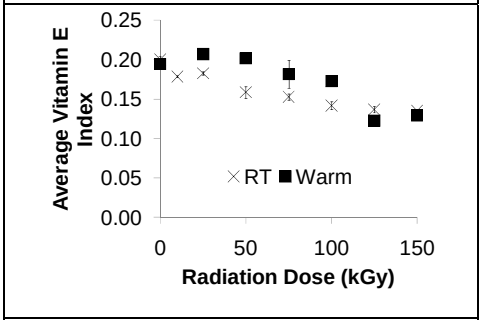

Warm irradiation was likely to cause more thermal degradation of vitamin E and the free radical scavenging of vitamin E was likely faster at higher temperature. It was unexpected not only that vitamin E content was better preserved after warm irradiation but also that increasing

irradiation temperature increased grafting (Fig 2). The implication of this result is that by controlling irradiation temperature, grafting of antioxidants can be maximized for optimal oxidation resistance.

Figure 2. The extent of vitamin E grafting on UHMWPE as a function of radiation dose and temperature.

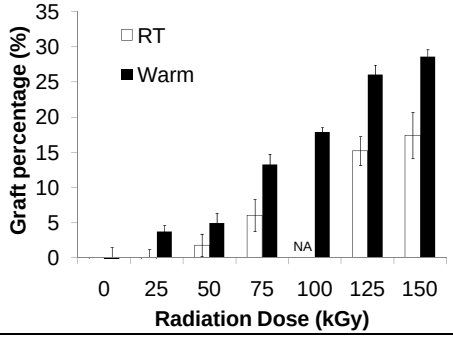

Figure 3. Cross-link density of vitamin E-blended, irradiated UHMWPE as a function of radiation dose and temperature.

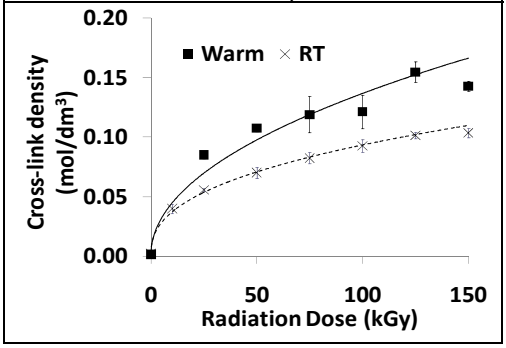

The crosslink density of vitamin E-blended, irradiated UHMWPE was higher than that irradiated at RT (Fig 3), again suggesting that the free radical scavenging activity of vitamin E was less at higher temperature. Since the wear of UHMWPE decreases with increasing crosslinking [4], this suggests that warm irradiation leads to lower wear rate.

This was corroborated by wear testing, where warm irradiation of UHMWPE resulted in lower wear rate than irradiation at room temperature for irradiated vitamin E blends of UHMWPE (Fig 4). The blends were irradiated to different doses to obtain similar crosslink density.

Figure 4. Wear rates of irradiated blends.

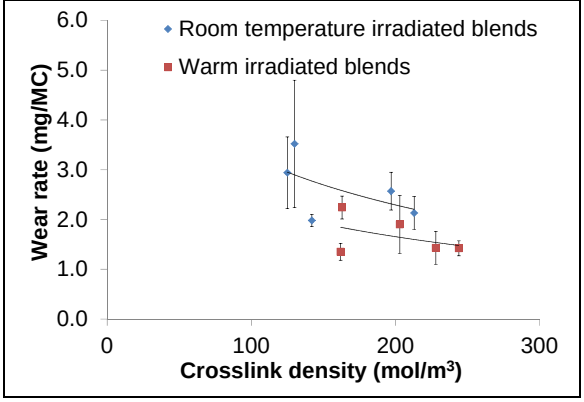

Conclusions

While radiation crosslinking of vitamin E-blended UHMWPE decreases crosslinking compared to virgin UHMWPE and also decreases the vitamin E in UHMWPE for long-term oxidative stability, it also results in increased grafting of the antioxidant on the polymer, presumably resulting in longer-term stability. Moreover, warm irradiation allowed for increased preservation of the antioxidant, increased grafting, increased cross-linking and decreased wear. This result is significant for the wear and oxidation stability of stabilized UHMWPE joint implants.

Acknowledgements

This study was funded by laboratory funds.

References

[1] Kurtz et al. JBMR 90A:549-563 (2009); [2] Oral et al. Biomaterials 27(6):917-925 (2006); [3]Muratoglu et al. Biomaterials 24(8): 1527-1537 (2003); [4]Oral et al. Biomaterials 29(26): 3557-3560 (2008); [5]Allen et al. Radiat. Phys. Chem.. 38(5): 461-465 (1991); [6] Oral et al. Biomaterials 31:7051-7060 (2010); [7] Bragdon et al. JOA 16(5): 658-665 (2001).

Cytotoxic Effects of Anti-Oxidant Compounds on Primary Human Peripheral Blood Mononuclear Cells

Joanne L Tipper, Julie Liu, Catherine L Bladen.
Institute of Medical & Biological Engineering, University of Leeds, Leeds, LS2 9JT, UK.

Statement of Purpose: Sterilisation of UHMWPE joint replacement components by gamma irradiation causes the release of free radicals, which if not dealt with by post irradiation processing, can lead to oxidative damage within the polymer [1]. Oxidation of the UHMWPE components has been shown to lead to altered mechanical properties and increased wear [2]. The addition of anti-oxidant compounds, in particular Vitamin E, has been gaining popularity over recent years and UHMWPE containing 1000 ppm Vitamin E (VE) is now now offered as an alternative bearing material in the clinic. A number of other anti-oxidant compounds are being added to UHMWPE such as hindered phenols [3], anthocyanins, lanthanides and nitroxides. The emphasis in these studies has been on studying the effects of these compounds on the mechanical properties of the polymer and/or on wear resistance, with little regard for the biological consequences. The aim of this study was to investigate the effects of these anti-oxidant compounds on the cell viability of a human histiocytic cell line and peripheral blood mononuclear cells (PBMNCs) *in vitro*.

Methods: The cytotoxicity of several anti-oxidant compounds was investigated and compared to vitamin E. These included HPA01, a hindered phenol; TEMPO, a nitroxide; and the lanthanides Europium (II) and Europium (III). U937 human histiocytes or PBMNCs from healthy volunteers (ethical approval granted by University of Leeds ethics committee) were seeded at 2 x 10^4 per well and incubated in RPMI 1640 medium with antioxidant compounds at concentrations between 1µm and 5 mM in an atmosphere of 5% (v/v) CO_2 in air (n = 4). Glutathione (100 µm), a naturally occurring anti-oxidant, and cells only were included as negative controls and 75 µm Menadione, a known inducer of oxidative stress, was included as positive control. Cell viability was measured using the ATP-Lite assay after 24h. Data was fitted to a sigmoidal dose response curve by log transforming the X column values then normalizing the Y column values. A non-linear regression was then performed.

Results The dose response curve for vitamin E in PBMNCs is shown in Figure 1. Vitamin E was well tolerated by the cells, only becoming toxic at high concentrations (≥4 mM). All other anti-oxidant compounds were toxic to the cells at micro molar concentrations. The dose response curve for the hindered phenol HPA01 in PBMNCs is shown in Figure 2, which is representative of the response to both nitroxide and lanthanide anti-oxidants. In general the primary cells were less sensitive to the anti-oxidant compounds, indicated by the higher concentrations required to exert an adverse effect on cell viability. Interestingly, the HPA01 and TEMPO antioxidants conferred protection against the toxic effects of solvents (DMSO and ethanol) in both the cell line U937 and in primary cells, suggesting that these compounds are functioning as antioxidants.

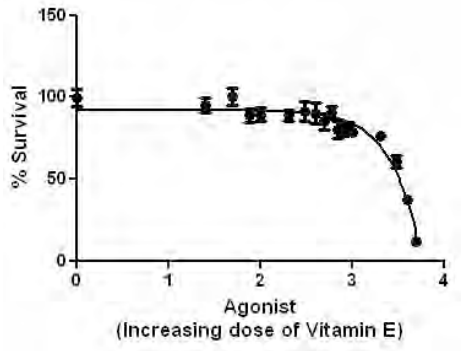

Figure 1. Dose response curve for vitamin E in PBMNCs

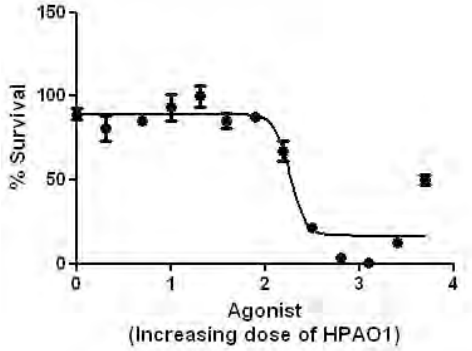

Figure 2. Dose response curve for HPAO1 in PBMNCs

Conclusions: Concerns about residual free radicals in UHMWPE and the resultant oxidative damage to the polymer has lead to the inclusion of a number of different anti-oxidant compounds in UHMWPE, however the biological consequences of these compounds have not been considered. This study has revealed that the majority of these compounds are toxic to human monocytic cells at relatively low doses, however, it is not known whether these compounds will leach from the polymer *in vivo* and therefore pose a cytotoxic risk. Previous studies on HPA01 have indicated that the compound is not lost from the bulk material [4], however it is not known whether the compounds will be lost from particulate wear debris, which has a comparatively large surface area. In addition, at low concentrations the HPA01 and TEMPO antioxidants had a protective effect against the solvents, and this requires further investigation. The concentration of antioxidants included in TJR components has been determined based on oxidative index, however, important the biological effects of these compounds should also be considered, in terms of cytotoxicity, resistance to oxidative stress and osteolytic cytokine release from macrophages.

References

[1] Oral et al 2004 Biomaterials 25, 5515-22. [2] Muratoglu et al 1999 Biomaterials 20, 1463-70. [3] Narayan et al 2010 Trans 56th ORS p2317. [4] King & Sharp 2010 Trans 56th ORS p2286.

Detection of vitamin E in ultra high molecular weight polyethylene by colorimetry and water contact angle techniques

A. Terriza[1], M.J. Martínez-Morlanes[2], F. Yubero[1], J.A. Puértolas[2,3]
[1]Instituto de Ciencias de Materiales de Sevilla, (CSIC-U. Sevilla), Spain
[2]Instituto de Ciencia de Materiales de Aragón, Universidad de Zaragoza-CSIC, Spain
[3]Instituto de Investigaciones en Ingeniería de Aragón, Universidad de Zaragoza, Zaragoza, Spain

INTRODUCTION:

The incorporation of vitamin E in medical grade polyethylenes intended for surgical implant has well recognize benefits due to its anti-oxidant effect keeping the wear performance of highly crosslinked ultra high molecular weight polyethylene (UHMWPE) [1]. Vitamin E is usually quantified by FTIR using a vitamin E index defined as the area ratio between the absorption peak at 1262 cm^{-1}, which correspond to the C-O stretching of the phenol group, and a reference absorption peak at 1895 cm^{-1} corresponding to the polyethylene skeleton. However, this method has a 0.2 wt% detection limit. UV absorbance is also used to detect vitamin E, by means of the absorption at 290 nm corresponding to the aromatic chromophone in vitamin E [2]. In this case, the detection limit is about 0.01 wt%. However, these two methods are destructive and not free of some controversial. So there is still a challenge to identify more robust non destructive methods to quantify more reliable vitamin E index in medical grade polyethylenes. In this work we assess the influence of the vitamin E, introduced by diffusion in the UHMWPE, on the color and the water contact angle.

METHODS:

The raw materials used in this study were GUR 1050 UHMWPE. Vitamin E was incorporated into the foregoing materials by diffusion. The discs were soak in a bath of vitamin E at 120ºC in a N_2 atmosphere during different periods. At the end of the diffusion process, the discs were taken out of the bath, cleaned and homogenized at 120ºC during 24 hours in N_2. Thus, specimens with concentrations of α-tocopherol of 0.3-3.0 % were prepared. The vitamin E concentration was also evaluated by UV spectroscopy. Water contact angle (WCA) measurements were performed with deionized water. Colorimetric analysis of the samples was also evaluated.

RESULTS:

Figure 1 shows the correlation between WCA and percentage of vitamin E in the discs. It is observed a smooth increase of WCA from 102º to 117º as the amount of vitamin E incorporated in the polyethylene increases from 0.0 % to 3.0 %. Unfortunately the R-squared of the linear regression is very low (0.26) due to the high uncertainty in the determination of WCA (in general about a 4% of the actual measured value) compared with the small increase of WCA with vitamin E doping. Therefore, this characterization cannot be used alone to quantify the amount of vitamin E incorporated in the polyethylenes.

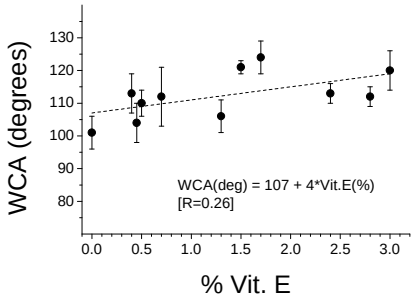

Figure 1. Correlation between WCA and percentage of vitamin E in UHMWPE discs.

Figure 2 shows the variation in color difference ΔE (in CIELAB color space) between vitamin E doped and undoped UHMWPE. It is observed a linear increase of ΔE between 6 to 20 as the amount of vitamin E incorporated in the polyethylene increases between 0.3 and 3.0 %. Other set of vitamin E doped UHMWPE samples, previously irradiated with 90 kGy, show color differences 3 units larger than the non-irradiated for the same level of vitamin E doping. In both cases, the R-squared of the linear regressions is about 0.95, suggesting that this procedure might be used for quantification purposes.

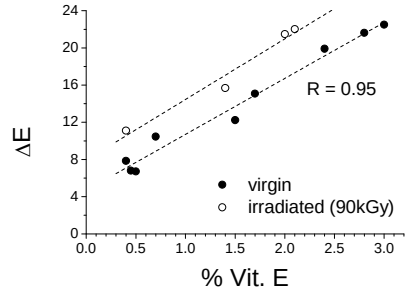

Figure 2. Correlation between color difference ΔE and vitamin E content in UHMWPE disks

CONCLUSIONS:

It is observed an increase of WCA as the vitamin E doping in UHMWPE increases. However, only a very rough estimation of vitamin E content of polyethylene sample with an unknown vitamin E doping level could be assessed by this procedure. On the other hand, a linear correlation between the color difference and percentage of vitamin E incorporated in UHMWPE has been found. In this former case, the statistics of the analysis was more favorable, suggesting that this procedure might be used for quantification purposes.

REFERENCES
[1] Puértolas JA et al. J. Appl. Polym. Sci. 2011; 120: 2282.
[2] Bracco P et al. Clin Orthop Relat Res 2010

ACKNOWLEDGEMENTS:
This study was financed by Consolider FUNCOAT-CSD2008-00023, which is a project of the Spanish Ministerio de Ciencia y Tecnología.

The impact of aging environment on the oxidation of stabilized and unstabilized crosslinked polyethylenes

[1]Berlin, J.A.; [1]Braithwaite, G.J.C.; [2]Knight, J.; [2]Pletcher, D.; [2]Rufner, A.
[1]Cambridge Polymer Group, 56 Roland Street, Suite 310, Boston, MA, [3]Zimmer, Inc., 1800 West Center Street, Warsaw, IN 46580

Statement of Purpose: Although Vitamin E (VE) stabilized materials have been accelerated aged in conventional environments before [1-3], their clinical oxidation performance is as yet unknown. Two standard accelerated aging tests for polyethylene medical devices are found in ASTM F1980 (80 °C convection oven) and ASTM F2003 (70 °C 5 atm oxygen bomb), respectively. While these environments model some shelf aging of UHMWPE materials appropriately, there is no directly relevant *in vivo* aging model to predict long-term clinical outcomes. It is thus of interest to determine the long-term response of VE doped materials in a more clinically relevant environment. We have investigated a new VE blended, highly crosslinked UHMWPE material in both standard accelerated environments ASTM F1980 [4] and ASTM F2003 [5], and in an accelerated bovine synovial fluid (BSF) environment at 60 °C under 5 atm O_2. Aging results for 200 kGy 0.27% VE UHMWPE ("VE-PE") have shown improved stability compared to earlier generation materials. BSF provides an interesting aggressive accelerated aging environment that creates a different oxidation profile in conventional materials as compared to the standard aging environments. In BSF, conventional material oxidized over time mainly in the bulk rather than at the surface.

Methods: Consolidated GUR 1050 was either gamma sterilized to 25-37 kGy (UHMWPE), e-beam irradiated to 100 kGy and post-melted (HXPE), or stabilized with 0.27 % VE by powder blending and e-beam irradiated to 200 kGy (VE-PE). Samples were packaged in vacuum-sealed bags and stored frozen to minimize unintended degradation or aging between tests. Five to seven 10-mm cubes of each material were aged according to ASTM F1980 and ASTM F2003, respectively. Additionally, seven cubes of each material were aged in BSF at 60 ºC 5 atm O_2. Care was taken to make sure that all cube surfaces were exposed to the aging environment. One cube of each material was removed at 1, 2, 3, 5, 6, 8, and 24 weeks. ASTM F1980 samples were run for 6 weeks. Two-hundred micron slices were microtomed from the center of each cube for oxidation induction time (OIT) and oxidation index (OI) analysis. OI was measured according to ASTM F2102 through the full thickness of the samples at intervals of 200 µm. Surface oxidation index (SOI) was measured as the average oxidation index from the surface to 3 mm subsurface. Bulk oxidation index (BOI) was measured as the average oxidation index through the central 0.5 mm of the sample. Two samples were cored from the FT-IR slices post-analysis using a 6-mm punch for OIT analysis. OIT was measured according to ASTM D3895 using a new analysis method equivalent to the tangent method, but insensitive to misleading/atypical features present in the oxidative exotherm. The FT-IR sample of UHMWPE aged in BSF for 2 months was reflux extracted in hexanes for three days and re-analyzed.

Results: Table 1 shows the SOI and BOI for the materials in each environment by time point. Figure 1 shows the OIT of VE-PE samples in each environment over time. OI and OIT analysis of VE-PE post-aging up to 6 weeks in ASTM F1980 and up to 6 months in ASTM F2003 and in 60 ºC BSF at 5 atm O_2 indicated no detectable oxidative degradation. HXPE showed measurable oxidation by OI analysis after 5 weeks in the ASTM F2003 environment. By 6 months, OI analysis could not be performed on HXPE. Extreme degradation of UHMWPE occurred at 6 weeks in ASTM F2003 and 6 months in BSF, preventing OI analysis. The oxidation profile of UHMWPE was unique in BSF. Rather than subsurface oxidation peaks, the UHMWPE oxidized more in the bulk. There was also an increase in alcohol group content in the bulk in addition to the usual increase in ketones. This oxidation profile may be the result of exposing the UHMWPE to both high partial pressure of oxygen and a physiological solution known to contain absorbable and adsorbable chemical species. Hexanes extraction of the conventional material aged in BSF for 2 months did not change the oxidation profile, suggesting that both the ketone and alcohol peaks are not due to absorbed species.

Table 1: SOI and BOI of accelerated aged UHMWPE samples over 24 weeks. ASTM F1980 was run only for 6 weeks. Starred (*) samples were not measurable. [1]

		0w	1w	2w	3w	5w	6w	8w	24w
VE-PE									
SOI	ASTM F1980	-0.08	-0.07	-0.06	-0.04	-0.07	-0.05	-	-
	ASTM F2003	-0.08	-0.06	-0.05	0.00	-0.01	-0.05	0.00	0.02
	BSF	-0.08	-0.01	0.01	0.07	-0.02	0.04	0.07	0.00
BOI	ASTM F1980	-0.09	0.09	-0.08	-0.07	-0.07	-0.06	-	-
	ASTM F2003	-0.09	-0.05	-0.05	-0.04	-0.07	-0.03	-0.02	0.00
	BSF	-0.09	-0.02	0.00	0.04	0.01	0.03	0.05	-0.03
HXPE									
SOI	ASTM F1980	-0.07	-0.08	-0.06	-0.05	0.13	0.05	-	-
	ASTM F2003	-0.07	-0.06	-0.05	0.04	0.62	1.59	4.15	*
	BSF	-0.07	-0.06	0.00	-0.07	-0.06	-0.05	-0.06	-0.05
BOI	ASTM F1980	-0.06	-0.07	-0.06	-0.05	0.03	0.19	-	-
	ASTM F2003	-0.06	-0.06	-0.04	0.07	0.78	1.84	4.26	*
	BSF	-0.06	-0.05	0.00	-0.08	-0.06	-0.05	-0.05	-0.04
UHMWPE									
SOI	ASTM F1980	-0.03	-0.02	0.09	0.02	0.22	0.33	-	-
	ASTM F2003	-0.03	0.03	0.04	0.61	3.85	*	*	*
	BSF	-0.03	0.02	0.06	0.08	0.14	0.10	0.53	*
	BSF extracted	-	-	-	-	-	-	0.62	*
BOI	ASTM F1980	-0.03	-0.04	-0.02	0.01	0.03	0.05	-	-
	ASTM F2003	-0.03	0.02	0.20	0.72	2.53	*	*	*
	BSF	-0.03	0.01	0.07	0.12	0.31	0.42	1.27	*
	BSF extracted	-	-	-	-	-	-	1.40	*

Conclusions: VE-PE exhibits excellent long-term oxidative stability even in extreme aging conditions up to 6 months. Results show improvement in oxidative stability as compared to HXPE materials. OIT provides a measure of oxidative degradation distinctively different from OI, but both data sets imply enhanced stability with VE-PE. BSF does not appear to increase oxidation in VE-

[1] The detection limit of the FT-IR is below 0.05. Any OI values below this value imply negligible oxidation.

PE, but does oxidize UHMWPE with a unique OI profile with maximum oxidation through the bulk of the material. *In vivo* retrieval data yields an oxidation profile inconsistent with the oxidation profile observed here in BSF. The discrepancy may be due to mechanical deformations *in vivo* that are not considered in this study or to the state of the BSF, which may affect the ability of the synovial fluid to protect the UHMWPE implant from oxidation. It may be that BSF components are stabilizing the UHMWPE surface by preferentially degrading, as has been noted elsewhere [6], but it is unclear what is causing the bulk oxidation effect. Further studies to understand the effects of BSF on oxygen and radical exposure of UHMWPE will be necessary to determine if BSF may be used to create a more clinically relevant accelerated aging environment.

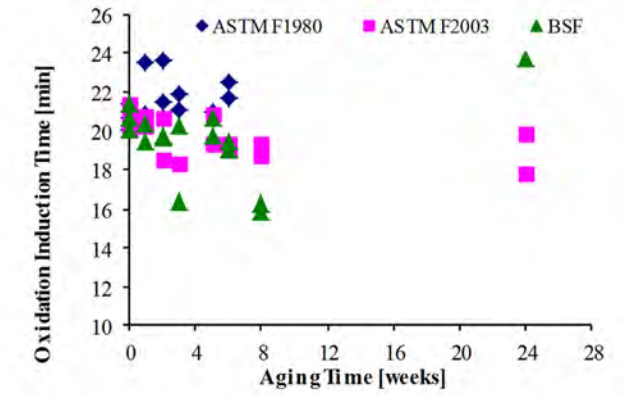

Figure 1: OIT of VE-PE at aging time points up to 24 weeks in accelerated aging environments.

References:

[1]S.M. Kurtz, et al. J Biomed Mater Res A. (2009)
[2] E. Oral et al. Biomaterials (2006)
[3] C. Wolf et al. J Mater Sci-Mater M. (2006)
[4] ASTM F 1980-99, "Test Method: Standard Guide for Accelerated Aging of Sterile Medical Device Packages"
[5] ASTM F 2003-02, "Test Method for Accelerated Aging of Ultra-High Molecular Weight Polyethylene after Gamma Irradiation in Air"
[6] P. Puig-Parellada, J.M. Planas. Biochem Pharmacol (1978)

Acknowledgements: Materials provided by Zimmer, Inc. Funding was provided by Zimmer, Inc.

Oxidation Initiated by Cyclic Loading in the Presence of Lipids

*Wannomae, KK; *Konsin, ZB; +*Muratoglu, OK
* Harris Orthopaedic Laboratory, Massachusetts General Hospital, Boston, MA 617-726-3869

Introduction

Radiation crosslinking greatly improves the wear resistance of ultra high molecular weight polyethylene (UHMWPE) formulations used in total joint arthroplasty, but it also generates residual free radicals – precursors of oxidative embrittlement. In order to stabilize irradiated UHMWPE against oxidation, two common methods include post-irradiation melting to eradicate all detectable free radicals, and incorporating an anti-oxidant, such as vitamin E. In previous studies, vitamin E diffused, irradiated UHMWPE (E-PE) remained oxidatively stable during cyclic loading when conventional UHMWPE gamma sterilized in inert components oxidized [1]. However, *in vivo* cyclic loading occurs in the presence of lipids that can also accelerate oxidation [2]. Therefore a more aggressive challenge is proposed: cyclic loading of lipid-doped components. Both E-PE and irradiated and melted UHMWPE (CISM-100) were tested under these adverse conditions

Materials and Methods

CISM-100 was manufactured by irradiating GUR1050 to 100 kGy as a bar stock, which was subsequently melted then machined into test specimens. E-PE was manufactured by irradiating GUR1050 to 100 kGy as a preform. The irradiated material was diffused with vitamin E and homogenized, machined into test specimens, and terminally gamma sterilized. All samples in this study were modeled after Type A flexural fatigue samples of 6.5 mm thickness, as described in ASTM D671.

Testing was performed on three sample groups: Lipid-Doped E-PE, Lipid-Doped CISM-100, and Non-Doped CISM-100. The lipid chosen was squalene, which has been found to absorb into UHMWPE components in vivo [3]. Lipid-doping was performed by immersing the samples in pure squalene at 55°C until the desired squalene content of 18 mg was achieved.

All sample groups were tested in air at 80°C, in an environmental chamber. Each loaded specimen (n=4) was clamped at the base while load applicators deflected the samples according to a sinusoidal waveform about the zero line. The actuator was programmed to deflect the samples at a frequency of 0.5 Hz, to a peak alternating stress of 10MPa. Unloaded controls (n=3) were placed in proximity to the loaded samples but not subjected to load.

Specimen failure was defined as the complete fracture of the head of the component of the base. When a specimen failed, it was removed from the environmental chamber and immediately analyzed. Samples that did not fail were removed and analyzed after 1.5 million cycles of testing. Unloaded controls were always removed and analyzed at the same time as the loaded specimens.

Microtomed thin films (~150 μm) from all samples were boiled in hexane for 16 hours to remove any absorbed species and subsequently analyzed by FTIR (Varian FTS2000, Palo Alto, CA) to quantify oxidation, per ASTM F2102.

Results

The average number of cycles until failure (N_f) and the average ASTM Maximum Oxidation Index (MOI) are given for each sample group in Table 1. Representative oxidation profiles of the loaded samples and unloaded controls for each group are shown in Fig 1 and Fig 2, respectively.

Table 1: Average number of cycles until failure and average MOI for all groups.

Sample	N_f (cycles)	MOI Loaded Samples (A.U.)	MOI Unloaded Controls (A.U.)
Lipid-Doped, E-PE	N/A*	0.01 ± 0.00	0.01 ± 0.00
Lipid-Doped CISM-100	760,000 ± 90,000	0.74 ± 0.15	0.25 ± 0.11
Non-Doped CISM-100	1,390,000**	0.50 ± 0.47	0.04 ± 0.03

*All Lipid-Doped E-PE specimens completed 1.5 million cycles without failure
** Only 2 of 4 Non-Doped CISM-100 samples failed – standard deviation was omitted

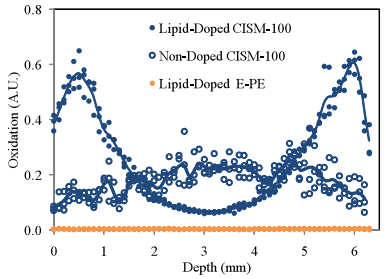

Fig 1: Representative oxidation profiles of the loaded samples in each group after testing. Actual data is represented by individual data points; the solid line is their splined average.

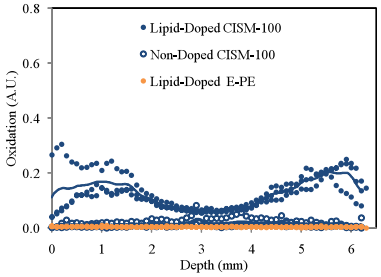

Fig 2: Oxidation profiles of unloaded controls corresponding to the representative loaded samples shown in Fig 1. Actual data is represented by individual data points; the solid line is their splined average.

Discussion

In both CISM-100 groups, loaded samples oxidized to a much greater degree than their corresponding unloaded controls, indicating that cyclic loading can diminish the oxidative stability of this material. Furthermore, Lipid-Doped CISM-100 oxidized far more than Non-Doped CISM-100 – squalene further challenges the oxidative stability of CISM-100 under cyclic loading. However, Lipid-Doped E-PE showed no detectable signs of oxidation and completed 1.5 million cycles of testing without failure. Vitamin E must have actively protected E-PE from oxidation induced by cyclic loading following exposure to squalene.

Acknowledgement

This study was funded by a research grant from Biomet, Inc.

References

[1]Wannomae KK, et al. EFORT 2008: F265; [2] Oral, et al. ORS 2009: 2283.; [3]Costa L, et al. Biomaterials 2001; 22 (4): 307-315.

Oxidation Initiated by Cyclic Loading in the Presence of Lipids

*Wannomae, KK, *Konsin, ZB, *Muratoglu, OK
* Harris Orthopaedic Laboratory, Massachusetts General Hospital, Boston, MA 617-726-3869

Statement of Purpose: Radiation crosslinking greatly decreases the wear of ultra high molecular weight polyethylenes (UHMWPEs) used in total joint arthroplasties, but it also generates residual free radicals – precursors of oxidative embrittlement. Subsequent melting eradicates all detectable free radicals; an example of this material is Longevity UHMWPE (Zimmer, Inc., Warsaw IN). Stabilization with the infusion of vitamin E also yields an oxidatively stable material; an example of this material is E1 UHMWPE (Biomet, Inc., Warsaw, IN). However, traditional accelerated aging methods did not consider the effect of mechanical loading or lipid absorption – both of which occur *in vivo* – on the oxidative behavior of UHMWPE. By coupling the adverse effects of thermal aging with mechanical stress and lipid initiated oxidation, we sought to investigate if either irradiated and melted PE or vitamin E stabilized PE was prone to environmental stress cracking (ESC). We hypothesize that the active protection of vitamin E is necessary to protect highly crosslinked PEs under such unfavorable conditions.

Methods: The irradiated and melted samples (CISM-100) were manufactured by e-beam irradiating UHMWPE stock to 100 kGy and subsequently melting it and machining samples. CISM-100 manufactured from GUR1020 and GUR1050 were tested.

The vitamin E stabilized samples (VitE-PE) were manufactured by doping UHMWPE preforms with vitamin E by immersing in pure vitamin E at 120°C and subsequently homogenizing to ensure a uniform vitamin E profile. The preforms were then machined down to the final sample size, vacuum packaged and terminally gamma sterilized. VitE-PE manufactured from GUR1020 and GUR1050 were tested.

The lipid squalene was chosen for the aging experiments as it was found to absorb into UHMWPE implants *in vivo* [1]. To be sure that all sample groups contained the same amount of squalene, initial tests were done on 1 cm cubes to determine how each material absorbed squalene. The cubes were immersed in squalene at 55°C and weighed after varying amounts of time.

The ESC tests were performed on samples modeled after ASTM D671, Type A, specimens. These ESC samples were doped with squalene at 55°C and placed in an insulated chamber maintained at 80°C on an MTS hydraulic system (Eden Prairie MN). The body of the specimen was immobilized and the head was impinged upon by load applicators at a frequency of 0.5 Hz, creating a reciprocating mechanical stress of 10 MPa in the triangular neck region. When a crack was observed or when the sample fractured, it was classified as failed and removed from the chamber along with its control samples, which sat in the same chamber but were not cyclically loaded. Upon failure or at the conclusion of five weeks of testing, samples were analyzed by FTIR to quantify oxidation in the neck region, per ASTM F2102.

Results: CISM-100 absorbed squalene significantly faster than the VitE-PE components, but there was no noticeable difference between GUR1020 and GUR1050 in either material. Table 1 shows the doping times and squalene contents for the ESC samples in all sample groups.

Table 1: Doping times and squalene contents for ESC samples.

Material	CISM-100 (1020)	CISM-100 (1050)	VitE-PE (1020)	VitE-PE (1050)
Doping Time	4 hrs	4 hrs	7.7 hrs	7.7 hrs
Sq. Content	15 ± 1 mg	16 ± 1 mg	20 ± 5 mg	19 ± 1 mg

All squalene doped CISM-100 samples (both GUR1020 and GUR1050) failed prior to reaching 5 weeks of testing (Figs 1-2).

Figure 1. Oxidation profiles CISM-100 (GUR 1020) after lipid doping and ESC testing. The cyclically loaded samples are shown in solid colors with solid lines representing their splined averages; the controls for the loaded samples are shown in the same color with empty data points and dashed lines for their splined averages. The number of cycles to failure for each sample is noted.

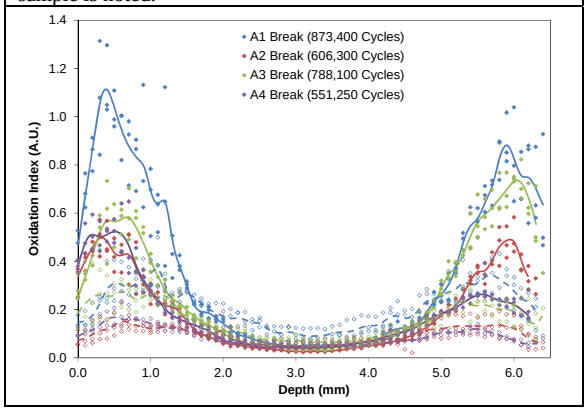

Figure 2. Oxidation profiles of CISM-100 (GUR 1050) after lipid doping and ESC testing. The cyclically loaded samples are shown in solid colors with solid lines representing their splined averages; the controls for the loaded samples are shown in the same color with empty data points and dashed lines for their splined averages. The number of cycles to failure for each sample is noted.

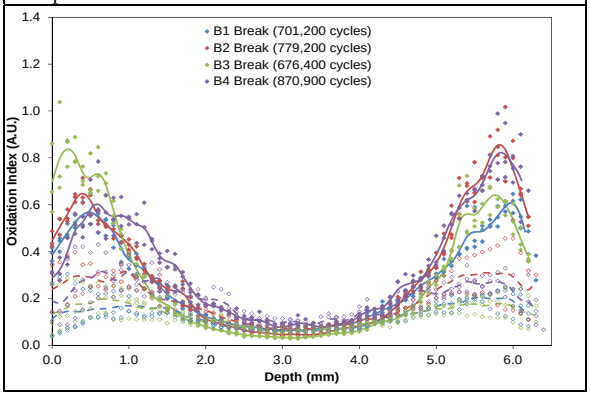

All squalene doped VitE-PE samples (both GUR1020 and GUR1050) survived 5 weeks of cyclic loading (approximately 1.5×10^6 cycles). Furthermore, FTIR revealed no detectable oxidation in either the control samples or the cyclically loaded VitE-PE samples (Figs 3-4).

Figure 3. Oxidation profiles of VitE-PE (GUR1020) after lipid doping and ESC testing. The cyclically loaded samples are shown in solid colors with solid lines representing their splined averages; the controls for the loaded samples are shown in empty black points with a dashed line for its splined average.

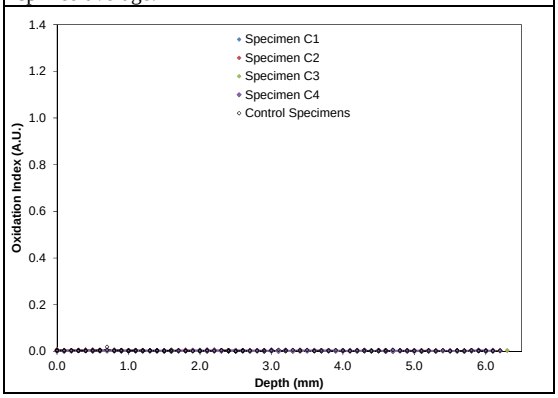

Figure 4. Oxidation profiles of VitE-PE (GUR1050) after lipid doping and ESC testing. The cyclically loaded samples are shown in solid colors with solid lines representing their splined averages; the controls for the loaded samples are shown in empty black points with a dashed line for its splined average.

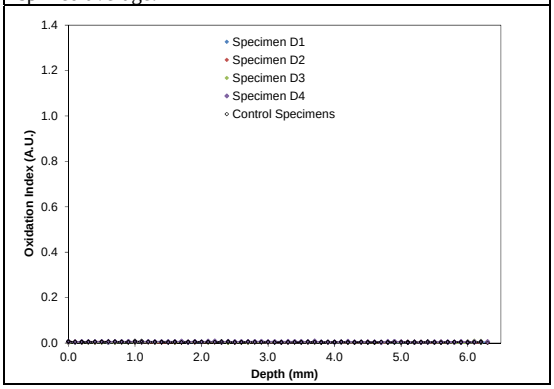

Conclusion: Oxidation initiated by cyclic loading and by the presence of an unstable lipid can cause a loss of stability, even in materials containing no residual free radicals such as CISM-100. The active protection granted by antioxidants such as vitamin E may be necessary to combat oxidation in the long term *in vivo*.

Acknowledgement: This study was funded by a research grant from Biomet, Inc.

References:

1. Costa L. Biomaterials. 2001; 22(4): 307-15.

Evaluation of Oxidation in Virgin UHMWPE Knee Components after Retrieval and Shelf Aging

M.L. Morrison
Smith & Nephew Orthopaedics, Memphis, TN 38116

Statement of Purpose: Recent studies have reported measurable oxidation in highly crosslinked, re-melted UHMWPE components after retrieval [1-3]. While it is debatable as to when the oxidation occurred, the susceptibility to oxidation was unexpected due to the lack of measurable free radicals and the proven in-vitro oxidation resistance of these materials under aggressive aging conditions [4]. Virgin UHMWPE components sterilized with ethylene oxide (EtO) gas uniquely represent another type of orthopaedic implant with no measurable free radicals and proven in-vitro oxidation resistance [5].

The primary purpose of this study was to determine if retrieved, virgin UHMWPE knee components are susceptible to either in-vivo or ex-vivo oxidation. Additional goals in this study included evaluations of (a) the distributions and qualitative amounts of lipids within the retrieved components, and (b) the relationship between the peak-height and peak-area oxidation indices.

Methods: All of the retrieved components evaluated were fabricated from virgin UHMWPE that was subsequently sterilized with EtO (i.e., no exposure to radiation). Twelve Genesis II™ tibial inserts (Smith & Nephew, Memphis, TN) were evaluated after a mean (± SD) in-vivo time of 18.9 ± 19.9 months (Range = 0.6 – 66) and a mean (± SD) ex-vivo, shelf-aging time of 75.6 ± 42.9 months (Range = 37 – 168). Seven of these inserts were fabricated from ram-extruded GUR1050, and five were fabricated from compression-molded GUR1020. For each knee component, samples were removed from (a) the visible wear scar in the bearing region and (b) the central spine of the tibial insert (i.e., non-bearing region). A microtome was used to produce one through-thickness, thin film (~200 μm thick) from each of these samples from each component. Three, through-thickness oxidation profiles were measured per film in the shelf-aged condition (i.e., no extraction) by FTIR spectroscopy. This analysis protocol was performed again with the same films after extraction. Extraction of the absorbed esterified fatty acids (EFAs) was conducted by refluxing the thin films in boiling hexanes for 16 hours [6]. One sample was selected for extraction for a total of 32 hours to evaluate the efficacy of extraction after 16 hours. The same FTIR analysis protocol was then conducted again to evaluate changes in the spectra and the derived metrics.

The standard peak-area oxidation index (PA-OI) was calculated as the ratio of the area under the peak near 1718 cm^{-1} to the area under the methylene peak at 1368 cm^{-1}, as delineated in ASTM F2102-06. A peak-height oxidation index (PH-OI) was calculated as the ratio of the height of the peak at 1718 cm^{-1} to the height of the peak at 1368 cm^{-1}. Finally, indices were calculated to evaluate the presence and distribution of EFA. An ester index (EI) was calculated as the ratio of the height of the predominate peak between 1738 and 1748 cm^{-1} to the height of the peak at 1368 cm^{-1}. For all of these indices, the baseline and integration limits for the numerator were adjusted depending upon the width of the resultant peak. The baseline and integration limits for the denominator always remained constant at 1330 and 1396 cm^{-1}. Measurable indices were defined as those greater than 0.05 in this study.

Correlation between variables was evaluated with the non-parametric Spearman's rank correlation coefficient (ρ). Comparisons of the metrics derived from the FTIR spectra after extraction for various times was evaluated with the nonparametric Mann-Whitney test and the parametric t-test with a 0.05 level of significance (α).

Results: EFAs were present at all of the surfaces evaluated prior to extraction. In the bearing regions, the penetration depths of the EFAs ranged from 100 to 1900 μm on the proximal surfaces and from 100 to 700 μm on the distal surfaces (Figure 1). The EI profiles typically exhibited asymmetry with higher EIs on the proximal surfaces, and the penetration depths generally increased with longer in-vivo times as reported previously [7]. The mean (± standard deviation) EI_{max} in the bearing region was 0.45 ± 0.17 with a range from 0.10 to 0.70.

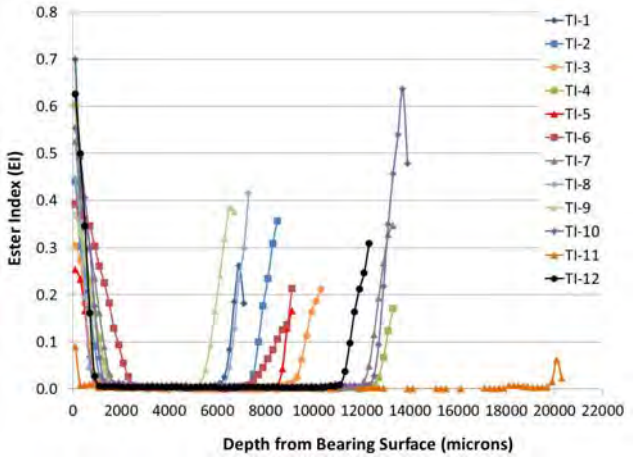

Figure 1: Ester-index profiles from the bearing regions before extraction.

In the non-bearing regions, the penetration depths were slightly lower and ranged from 100 to 1100 μm on the proximal surfaces and from 100 to 500 μm on the distal surfaces. The mean (± standard deviation) EI_{max} was 0.30 ± 0.12 with a range of 0.10 to 0.58. These maxima almost always occurred at the surfaces, and the EI_{max} were higher in the bearing regions than the non-bearing regions. Examination of the penetration of esters with time shows that the penetration depth was strongly associated with the in-vivo time.

After ex-vivo shelf aging and extraction, the ester indices were dramatically reduced by 43-97% in all of the samples. However, the EIs did not reduce to zero, and the ester peaks did not disappear from the spectra. In the non-bearing regions, all but one component (TI-1) exhibited

EIs below the detection limit after extraction. On the other hand, 9 out of 12 tibial inserts had measurable EIs and clearly defined peaks or shoulders between 1738 and 1748 cm^{-1} after extraction. In theory, these results could be due to incomplete ester extraction.

To better evaluate the effectiveness of the extraction protocol, a sample with an obvious ester peak after extraction (TI-4) was selected for an additional 16 hours of extraction. After a total extraction time of 32 hours, no significant changes were observed in the PA-OI_{max} (0.35 ± 0.04, p=0.2752), PH-OI_{max} (0.23 ± 0.01, p=0.2752) or EI_{max} (0.19 ± 0.03, p=0.3827) compared to the same films after extraction for 16 hours. Because no additional changes were observed in the spectra with increased extraction time, it was concluded that 16 hours of extraction was sufficient.

After extraction, measurable oxidation was observed in 10 of the 12 tibial inserts evaluated (Figure 2). In the bearing regions, the mean (± standard deviation) PA-OI_{max} was 0.28 ± 0.19 (Range = 0.02 – 0.56). The two inserts that did not exhibit any measurable oxidation (TI-10 and TI-11) were among the inserts that had experienced the shortest in-vivo and ex-vivo times in this study. Six of these inserts had peaks in the PA-OI profiles at the bearing surface, and four of the inserts exhibited sub-surface peaks at depths of 300 to 500 µm. Measurable oxidation was also observed on the distal surfaces of four of these components. The penetration depth of the measurable oxidation ranged from 500 to 2100 µm at the bearing surface (i.e., proximal side) and from 300 to 1100 µm on the distal side of the bearing region.

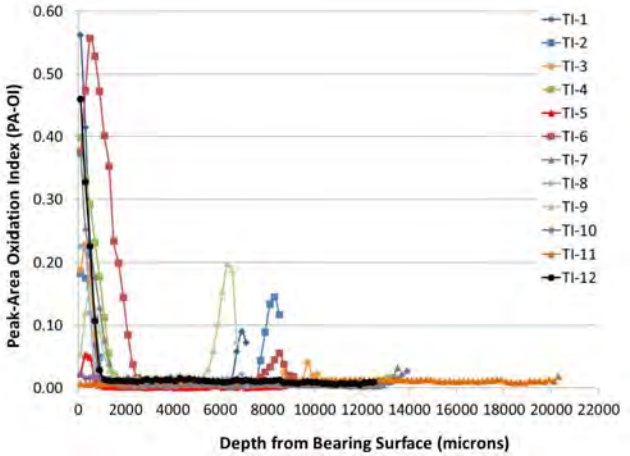

Figure 2: Peak-area oxidation index (PA-OI) profiles from the bearing regions after extraction.

In the non-bearing regions, measurable oxidation was observed in only one tibial insert (TI-1), which experienced one of the shortest in-vivo times, the longest ex-vivo time and exhibited one of the highest EI_{max}. The measurable oxidation occurred on the proximal side of the insert to a depth of about 300 µm with the peak occurring at the surface.

The correlation between the measured PH-OI_{max} before extraction and the true PA-OI_{max} measured after extraction was strong and statistically significant (ρ=0.94, p<0.001) for the measurements in the bearing regions. More than 96% of the variation in the measured PH-OI_{max} before extraction was accounted for by the true PA-OI_{max} measured after extraction.

Correlation analyses for the PA-OI_{max} in the bearing regions after extraction did not exhibit strong, statistically significant correlations with any of these variables. The best correlation was with the total time since implantation (ρ=0.51, p=0.09), followed by the shelf-aging time (ρ=0.24, p=0.46) and the in-vivo time (ρ=0.20, p=0.54).

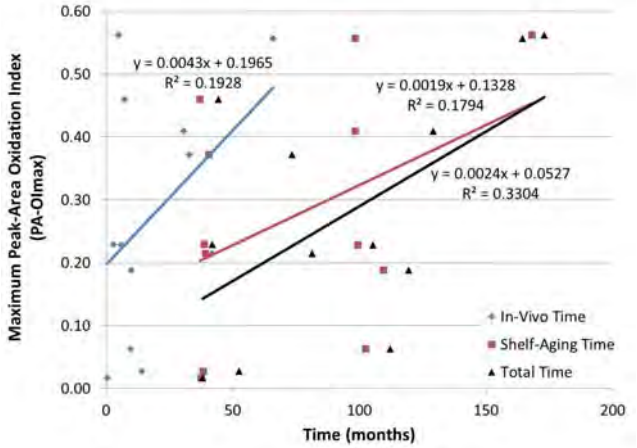

Figure 3: Maximum peak-area oxidation indices (PA-OI_{max}) in the bearing regions after extraction as a function of the in-vivo time, ex-vivo shelf-aging time, or total time since implantation.

Conclusions: Esterified fatty acids (EFAs) were found at all of the surfaces examined with concentrations and penetration depths that appeared to be related to both mechanical loading and the exposure to synovial fluid. Evaluation of hexane extraction for both 16 and 32 hours demonstrated that all of the extractable species were successfully removed after 16 hours of extraction.

There was a strong, statistically significant correlation between the pre-extraction peak-height oxidation indices and the post-extraction peak-area oxidation indices, which suggests that measuring the ketone-peak height without conducting extraction might be a viable alternative for the analysis of oxidation in retrievals in limited circumstances.

Finally, relatively low but measurable oxidation was observed in 10 of the 12 tibial inserts after extraction. Unfortunately, the data generated in this small study did not provide conclusive evidence as to *when* the measured oxidation occurred. Despite the absence of strong correlations with this small data set, the combination of this study with the two previous studies of similar materials that reported no measurable oxidation [7, 8] suggests that the oxidation occurred during shelf aging after retrieval.

References: [1] Rowell SL. ORS 2010:2304. [2] Rowell SL. ORS 2010:2345. [3] Currier BH. JBJS-A 2010;92 :2409. [4] Collier JP. CORR 2003;414:289. [5] Collier JP. CORR 1996;333:76. [6] Wannomae KK. J Arthop 2006;21:1005. [7] Costa L. Biomater 1998;19:1371. [8] Bracco P. JBJS-B 2009;91:274.

Comparison of one-step and sequentially irradiated ultra-high molecular weight polyethylene for total joint replacements

Miroslav Slouf[1], Jiri Kotek[1], Josef Baldrian[1], Jana Kovarova[1], Jaroslav Fencl[2], Tomas Bouda[3], Ivica Janigova[4]
[1]Institute of Macromolecular Chemistry AS CR, Heyrovskeho namesti 2, 16206 Praha 6, Czech Republic
[2]Beznoska Ltd., Delnicka 2727, 27201 Kladno, Czech Republic
[3]Czech Technical University, Faculty of Mechanical Engineering, Technicka 4, 16607 Praha 6, Czech Republic
[4]Polymer Institute SAS, Dubravska cesta 9, 84541 Bratislava 45, Slovakia

Statement of Purpose: Structure and properties of several single-step and sequentially irradiated ultra-high molecular weight polyethylenes (UHWMPE) with various thermal treatments were compared. In order to verify the results, the same characterization was carried out for commercially available UHMWPE liners made of sequentially-irradiated polymer (X3, Stryker, Mahwah, NJ) and one-step irradiated polymer (PE-IMC, Beznoska, Kladno, Czech Republic). The structure was studied by a number of spectroscopic, diffraction, thermal and microscopic methods. Mechanical properties were assessed by small-punch, microhardness and wear testing. Our results suggested that sequential irradiation followed by annealing did not lead to unusual structure at neither molecular nor supermolecular level. Consequently, the mechanical properties, including wear resistance, were comparable with one-step irradiated UHMWPEs.

Sample	IRR1	TT1	IRR2	TT2	IRR3	TT3
ID	[kGy]	[type]	[kGy]	[type]	[kGy]	[type]
M0	x	x	x	x	x	x
M1	75	RM	x	x	x	x
M2	75	AN	x	x	x	x
M3	37.5	AN	37.5	AN	x	x
M4	25	AN	25	AN	25	AN
M5	25	AN	25	AN	25	RM

Table 1. List of modified UHMWPEs; IRR: irradiation, TT: annealing (AN; 110 °C) or remelting (RM; 150 °C).

Methods: Modified UHMWPE samples (Table 1) were prepared by standard industrial procedures (MediTECH, Vreden, Germany; starting material Chirulen 1020; irradiation, annealing and/or remelting at low-oxygen atmosphere). Commercial UHMWPE liners (Table 2) were obtained from the Czech total joint replacement manufacturer Beznoska Ltd. (Kladno, Czech Republic). The methods of characterization of UHMWPE structure (IR, ESR, SWAXS, EM, DSC, TGA) and properties (SPT, microhardness, wear resistance) were described in our previous papers [1–4].

Sample	IR		ESR	SPT			MHv
ID	OI [ ]	VI [ ]	[mole/g]	PL [N]	UL [N]	UD[mm]	[MPa]
M0	0.00	0.000	0	59.1	57.3	4.6	47
M1	0.03	0.071	0	56.1	81.0	4.3	39
M2	0.15	0.074	1.5E-12	62.1	80.5	3.7	48
M3	0.23	0.076	1.5E-12	63.0	79.5	3.6	48
M4	0.16	0.077	1.6E-12	62.8	81.0	3.7	45
M5	0.00	0.076	0	57.5	83.9	4.2	38

Table 2. Characterization of irradiated samples; OI and VI are oxidation and trans-vinylene indexes; PL, UL, and UD are peak load, ultimate load and ultimate displacement, respectively; MHv is Vickers microhardness.

Results and discussion: The UHMWPE samples, which were all irradiated with the same dose (Table 1), indicated that the final properties were determined rather by the last thermal treatment (AN or RM) than by the number of irradiation cycles. According to their properties (Table 2), the samples could be divided into two groups: AN-samples (M2-M4; the last step: annealing) and RM-samples (the last step: remelting). All RM-samples exhibited lower oxidation damage (Table 2: IR/OI) and zero concentration of residual radicals (ESR) due to a complete removal of radicals after RM [1–4]. All AN-samples showed somewhat higher yield point (SPT/PL and MHv) and lower drawability (SPT/UL) in comparison with RM-samples, which could be attributed to higher crystallinity and thicker lamellae after AN as documented by SWAXS, EM and DSC (results not shown). Similar results were obtained for commercial UHMWPE liners (Table 3). Moreover, simple wear test indicated that sequential irradiation did not improve wear resistance significantly (Table 3: WR). The comparison with literature is ambiguous: the first studies suggested improved properties of sequentially-irradiated polymer [5, 6], while a later investigation [7] and this work did not show any apparent benefit in comparison with one-step irradiation.

Sample	IR		ESR	SPT			Wear
ID	OI [ ]	VI [ ]	[mole/g]	PL [N]	UL [N]	UD[mm]	WR [%]
PE-neat	0.00	0.000	0	64	60	4.5	100
PE-X3	0.24	0.080	~1e-10	75	101	3.6	39
PE-IMC	0.03	0.064	0	71	86	4.1	37

Table 3. Characterization of commercial UHMWPE liners; samples PE-neat (virgin Chirulen 1020), PE-X3 (sequential irradiation, annealed) and PE-IMC (one-step irradiation, remelted) were described above; WR is a relative wear rate from a multidirectional pin-on-disk.

Conclusions: In all investigated UHMWPE samples, the final structure and properties were determined by the last thermal treatment step and the difference between standard and sequential irradiation was negligible.

Acknowledgements: Project TA01011406.

References:

[1] Slouf M. J Biomed Mater Res B. 2008;85B:240–251.
[2] Lednicky F. J Macromol Sci B. 2007;46:521–531.
[3] Stara H. J Macromol Sci B. 2008;47:1148–1160.
[4] Slouf M. J Macromol Sci B. 2009;48:587–603.
[5] Dumbleton JH. Clin Orthop Relat R.2006;453:265-71.
[6] Wang A. J Phys D Appl Phys. 2006;39:3213–3219.
[7] Morrison ML. J Biomed Mater Res B. 2009;90B:87–100.

Relationship between in vivo stresses and oxidation of UHMWPE in hip joint replacement

M. Regis[(1)], P. Bracco[(2)], L. Giorgini[(1)], S. Fusi[(1)], L. Costa[(2)], C. Schmid[(3)].
[1]LimaCorporate SpA, Via Nazionale 52, 33038 Villanova di S.Daniele (UD), Italy.
[2]Dipartimento di Chimica IFM, Università degli Studi di Torino, Via P. Giuria 7, 10125 Torino, Italy.
[3]Dipartimento di Ingegneria Industriale e dell'Informazione, Ingegneria dei Materiali, Università degli Studi di Trieste, Via A.Valerio, 6A, 34127 Trieste, Italy.

Statement of Purpose: UHMWPE orthopaedic components show a limited period of life: wear and *in vivo* damage are the most limiting factors [1]. Research has been focused on the development of a wear-resistant UHMWPE, that reduces the production of debris and subsequently osteolysis [2], and on inhibiting oxidation in the material. Oxidation causes a reduction of the mechanical properties of UHMWPE, especially yield strength and fatigue resistance [3-5], affecting the *in vivo* behaviour of UHMWPE. Oxidation of UHMWPE components is affected by a number of process parameters: irradiation dose, dose rate, irradiation temperature, macro-radical elimination through post-irradiation thermal treatments [2]. Further, the hypothesis that also mechanical stress can induce oxidation has been advanced [3, 6-9]. In fact, even if annealing is widely used to avoid the presence of residual stresses in the UHMWPE, it is not possible to prevent the material from the action of the *in vivo* stress forces that act in the joint. Therefore, the evidence of this correlation has to be found by the means of an evaluation of retrieved components. The aim of this study is to demonstrate that stress induced by the *in vivo* joint forces on EtO sterilised UHMWPE components is responsible of an increased oxidation of the material.

Methods: The specimens at disposal for this study were four retrieved LimaCorporate (Villanova di S.Daniele, UD, Italy), LTO acetabular liners, produced from UHMWPE GUR 1120 Calcium Stearate-added sheets, EtO sterilised, implanted between 1985 and 1997, and a 50x50x60 mm virgin UHMWPE block, taken as reference. Since an evaluation of the liners cumulative weight loss was not possible, the liners circumferential thickness was measured, in order to estimate the total amount of *in vivo* wear of the component following the expression: $\Delta w = 2t^* - (T + t)$; where T is the maximum measured thickness, t is the minimum measured thickness and t* is the nominal thickness. Cross-sections thin films (~150 µm thickness) of the liners were microtomed (Reicher-Jung POLYCUT S, cutting speed 4 cm/s) for FTIR analysis. To evaluate and compare the oxidation level of the retrieved components with virgin UHMWPE and with Δw values, FTIR line scans of the samples were performed along the thickness of the worn cross section, together with IR maps of the whole cross section (Perkin-Elmer SPECTRUM SPOTLIGHT 300, transmission mode, 16 scans at 4 cm^{-1} resolution, autofocus every 10^{th} scan, spot dimensions from 100x100 µm to 25x25 µm). The results of FTIR analyses have been compared with the stress distribution of the *in vivo* forces obtained from a FE analysis (Ansys 10.0) that reproduced the normal loading conditions in the hip joint replacement [10], in order to find a relationship between stress and *in vivo* oxidation.

Results: Wear measurements established a specific correlation between *in vivo* lifetime and wear loss (Table A, Figure 1).

Sample	*Size*	*Δw [mm]*	*Years of implant*
E1	Ø28mm	4,348	16
E2	Ø28mm	0,600	4
E3	Ø32mm	1,663	12
E4	Ø32mm	0,949	9
Ref.	-	-	-

Table A. Δw and years of implant

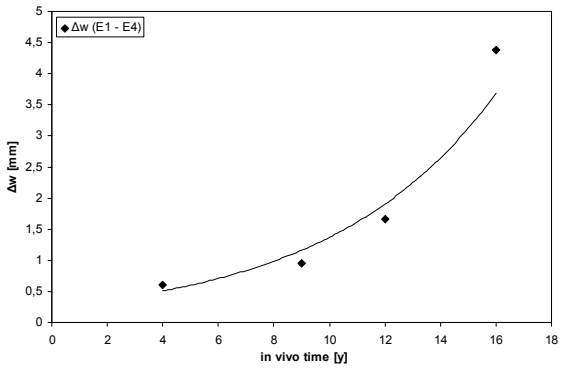

Figure 1. Δw versus *in vivo* time

Considering the differences between liners geometry and *in vivo* wear conditions, it is not possible to define a correlation law for Δw versus *in vivo* time, however, from Figure 1 it is possible to see that the higher *in vivo* lifetime, the higher Δw value is observed with an exponential trend. The FTIR quantitative analysis of the oxidation product along the cross section of the retrieved samples led to the determination of the oxidation profiles indicated in Figure 5. The highest amount of oxidation is found in the most worn liner, E1, which has also the highest *in vivo* lifetime among the analysed components.

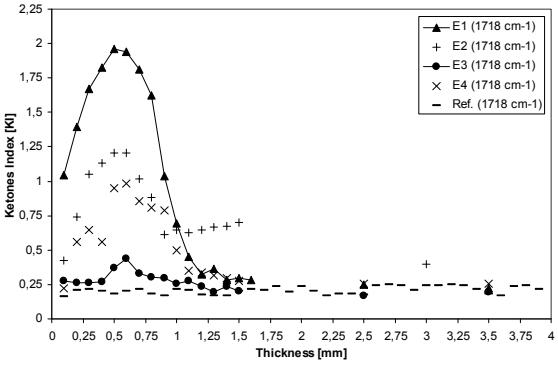

Figure 2. Ketones profiles

The Ketones distribution profile reveals that oxidation does not follow a diffusion-like pattern, and it is different

between different geometries. The highest oxidation value does not correspond to the internal, worn surface of the liner (0 mm distance), but it is found within the first 500 - 600 µm from the inner surface for both Ø28 mm and Ø32 mm liners. Oxidation reaches the minimum detected values in the bulk region of the liner section, where it is similar to the one observed in the reference control specimen (0,2-0,3). The same, minimum oxidation levels were observed in the backside surfaces. Despite the material removal due to wear mechanisms is different according to the respective liner geometry, the oxidation profile maintain the same trend. The IR maps examination revealed that the oxidised area is deeply localized, and it is completely asymmetric (Figure 3, left). In terms of spatial distribution, the oxidised regions correspond to the most worn areas, with a maximum in the first mm below the bearing surface. This confirms the indication given by the line scan measurements. The stress distribution obtained from the FEA was very similar (Figure 3, right).

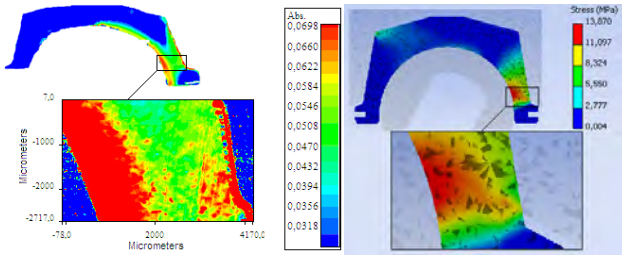

Figure 3. left, IR maps; right, FEA (E3 sample)

Even with different geometries, thus with different stresses distribution, the same similarities with the IR maps have been observed (Figure 4).

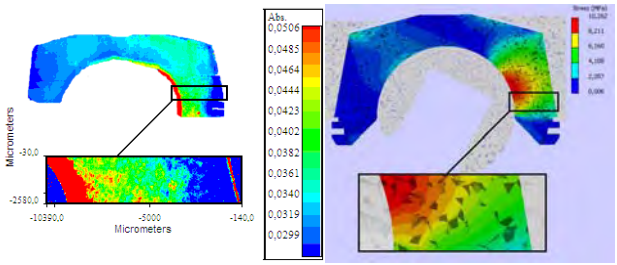

Figure 4. left, IR maps; right, FEA (E2 sample)

Conclusions: The experimental data collected in this study indicate that, as expected, there is a correlation between the observed global wear and *in vivo* time, although anatomic conditions, patient activity and retrieval motivations could seriously affect the reproducibility of the phenomenon in such a differentiated sample outline. Oxidation profiles maintain the same trend in all the analysed samples, with the highest peak at a 0,5 – 0,6 mm depth below the bearing surface. The reference unmachined and unloaded UHMWPE sample, on the contrary, did not show any oxidation appearance. The oxidation profiles shape indicates therefore a dependence of the *in vivo* material degradation on mechanisms not related to diffusion phenomena, as for example external contamination with lipids, oxygen or other molecules. Considering the fact that the analysed samples were EtO sterilized, therefore did not contain any free radical due to sterilization methods, the comparison between the results obtained from the IR maps and the FE analysis established a clear correspondence between *in vivo* stress and *in vivo* UHMWPE oxidation in qualitative terms: where the stress, there the oxidation. Even for different geometries, stress profiles and oxidation level match both in terms of peak values and area extension along the liners cross section. Moreover, liners oxidation is correlated to their *in vivo* lifetime, while it is not correlated to the global wear amount. This because the highest oxidation values were located below the bearing surface, and therefore no additional material removal due to oxidised UHMWPE could take part in the wear process, and also because the wear seems to be related simply to *in vivo* time, as for standard, non-crossliked UHMWPE. However, data achieved so far do not permit the identification of a direct correlation between stress level and oxidation products quantitative amount. For this reason, further studies have to be foreseen to confirm from a quantitative point of view what the evidences show in qualitative terms.

References: [1] H.G. Willert, H. Bertram, H.G. Buchhorn, 1990, Clin orthop, 258, 95-107; [2] L. Costa, M.P. Luda, L. Trossarelli, Polym degrad stab, 1997, 55, 329-338; [3] Oral E, Christensen SD, Malhi AS et al, J arthrop, 21, 580-591; [4] E.M. Brach Del Prever, L. Costa, M. Crova et al, Biomat, 1996, 17, 873-878; [5] L. Costa, K. Jacobson, P. Bracco, E.M. Brach Del Prever, Biomat, 2002, 23, 1613-1624; [6] S.M. Kurtz, O.K. Muratoglu, M. Evans, A.A. Edidin, Biomat 1999, 20, 1659-688; [7] S.M. Kurtz, 2004, Elsevier academic press ed.; [8] L. Costa, M.P. Luda, L. Trossarelli, Polym degrad stab, 1997, 58, 41-54; [9] L. Costa, P. Bracco, E.M. Brach del Prever et al, UHMWPE for arthroplasty: from synthesys to implant, Turin university, 2005; [10] G. Bergmann, G. Deuretzbacher, M. Heller et al, 2001, J Biomech 34, 859–871.

What is a macrophage?

Yrjö T. Konttinen[1,2,3], Jukka Pajarinen[1], Vesa-Petteri Kouri[1], Mari Ainola[1], Michiaki Takagi[4], Enrique Gomez-Barrena[5], Stuart B. Goodman[6], Jiri Gallo[7], Jami Mandelin[1]

[1]Institute of Clinical Medicine, Department of Medicine, Helsinki University Central Hospital, Helsinki, FI; [2]ORTON Orthopedic Hospital of the Invalid Foundation, Helsinki, FI; [3]COXA Hospital for Joint Replacement, Tampere, FI; [4]Yamagata School of Medicine, Yamagata, Japan; [5]Autonomic University of Madrid, Madrid, Spain; [6]Stanford University, Stanford, USA; [7]Olomouc University, Olomouc, Czech Republic

Statement of Purpose: In a metal-on-UHMWPE hip, at each step taken $>10^5$ polyethylene particles are released into periprosthetic tissues. In computer controlled hip simulations performed using Paul's gait curve the elderly patients are supposed to take a modest 10^6 steps per year and the implant prototypes are tested for 10 year life-in-service. This high particle load has been the main driving force to improve the wear resistance of UHMWPE by radiation-induced cross-linking, combined with treatments to minimize radical-induced material deterioration [1]. Somewhat paradoxically, aseptic loosening is not caused by wear particles *per se*, but by host response against the wear particles. In particle disease, macrophage takes the center stage [2,3]. Indeed, a potential alternative approach to prevent and treat particle disease is to prevent or moderate the host response against particles. The purpose of this presentation is to introduce the macrophage to a material scientist.

Macrophage maturation: Macrophages are large haematopoietic cells, able to phagocytose even immunologically non-opsonized particles, e.g. polyethylene, metal or polymethylmethacrylate. Hematopoietic stem cells mature along the monocyte-macrophage lineage for 2-3 d in bone marrow, circulate ~18 h as monocytes and migrate to tissues. With the help of a survival signal, macrophage-colony stimulating factor (M-CSF), and the local microenvironment [4] they differentiate to tissue-type M0-macrophages. 5×10^9 cells are formed daily, balanced by programmed cell death (apoptosis) of old, worn-out or damaged macrophages.

Macrophage activation: Low-dose interferon-γ (IFN-γ) primes the macrophage via Janus kinases and signal transducer and activator of transcription-1α (JAK1/2-STAT1) pathway. Such primed macralternate
ophages undergo classical or alternative activation by exposure to a second stimulus, e.g. tumor necrosis factor-α/TNF-α (lipopoly-saccharide, high-dose IFN-γ) or interleukin-4/IL-4 (IL-13), respectively [5].

Macrophage differentiation and function: M-CSF stimulated macrophages are called M0 macrophages. They are quiescent cells, normally responsible for cleaning of tissues. They take care of apoptotic cells rests in such a way that no inflammation is produced.

These M0 macrophages can be polarized into other types of macrophages by cytokines. This forms a corollary with Th0 helper cell differentiation: Th0 and M0 cells develop to Th1 cells and M1 macrophages, respectively, under the influence of IFN-γ and other above mentioned stimuli. M1 cells form M1 granulomas and are effective in phagocytosis of intracellular pathogens, e.g. *M. tuberculosis*, but also of phagocytosable wear particles, which they however cannot digest. Th0/M0 develop to Th2/M2 cells under the influence of IL-4 and above mentioned stimuli. M2 cells are effective in antigen capture and presentation, mast cell and eosinophil engagement and type 2 granuloma formation. They play a role in defense against parasites and other extracellular pathogens. We are at present working with a hitherto non-described and very pro-inflammatory macrophage produced by IL-23, known as M17 macrophage. It has been verified using gene ontogeny analysis (validated with quantitative real time-polymerase chain reaction) and xMAP suspension array (validated using enzyme-linked immunosorbent assay) in gene ontogeny and signalling pathway impact analysis.

Macrophages and osteolysis: Macrophage activation results in osteolysis [6]. Osteoclast precursors, with the help of receptor activator of nuclear factor kappa B (RANK), bind RANK-ligand (RANKL), which drives M0 macrophages to one more lineage, the multinuclear bone resorbing osteoclast. TNF-α and IL-1 potentiate this process, whereas a soluble RANKL neutralizer osteoprotegerin (OPG) inhibits it. Indeed, RANKL/OPG ratio is considered to regulate osteoclastogenesis [7] although *in vivo* the RANKL-RANK interaction may occur in a direct cell-cell contact, e.g. between mesenchymal stromal cell and osteoclast progenitor.

A few giant osteoclasts form the cutting cone in basic multicellular units (BMU) in osteons (compact bone) and hemiosteons (trabecular bone), which under a few weeks resorb bone. The resorption space (lacuna) is in helthy bone in a few months filled by the closing cone composed of osteoblasts. BMU units can undergo a few activation-resorption-formation (ARF) cycles.

Conclusions: Macrophage are formed in bone marrow and recruited from blood. In healthy connective tissue they form M0 macrophages to collect and handle cellular and matrix rests without causing inflammation. If more such work is to be performed, they differentiate to anti-inflammatory M2 macrophages, e.g. under the influence of IL-4 from mast cells. However, if the immunogenetic background, or pathogen-associated molecular patterns or alarmins (in short danger-associated molecular pattern), are encountered, they have a potential to develop into more aggressive M1 and M17 macrophages, multinuclear foreign body giant cells, osteoclasts and granulomas.

References: [1] Gomez-Barrena *et al.* Acta Orthop 2008;79:832-840; [2] Santavirta S *et al.* J Bone Joint Surg 1990;72-A:252-258; [3] Santavirta S *et al.* J Bone Joint Surg 1991;73-B:38-42; [4] Konttinen *et al.* Clin Orthop Rel Res 2005;430:28-38; [5] Ma G *et al.* Cell Mol Life Sci 2003;60:2334-2346; [6] Lassus *et al.* Clin Orthop Rel Res 1998;352:7-15; [7] Mandelin *et al.* JBJB 2003;85B:1196-1201

Decreased Functional Biological Activity of Polyethylene Wear Debris from Revised HXLPE Liners

Ryan M. Baxter, MS†, Steven M. Kurtz, PhD†, Marla J. Steinbeck PhD†
† Drexel University, Philadelphia, PA

Statement of Purpose: Despite the widespread implementation of highly crosslinked polyethylene (HXLPE) liners to reduce the incidence of osteolysis [**1**], it is not known if the improved wear resistance will outweigh the inflammatory potential of submicron HXLPE wear debris *in vivo*.

Thus, we sought to determine differences in the size, shape, number and biological activity of polyethylene wear debris obtained from primary THA revision surgery of CPE versus remelted or annealed HXLPE liners.

Methods: Pseudocapsular tissue samples were collected from 14 patients undergoing primary revision arthroplasty of uncemented, metal-on-polyethylene hip components.

For the CPE cohort (n=4), liners were revised after an average of 6.4 years (range 2.3-9.3) for wear, loosening and osteolysis. For the annealed HXLPE cohort (n=5), liners were revised after an average of 4.2 years (range 2.0-5.2) for loosening or malposition. For the remelted HXLPE cohort (n=5), liners were revised after an average of 3.3 years (ranges 1.7-6.6) for loosening or malposition. Implantation time was not significantly different between cohorts (p=0.333).

Polyethylene wear particles were isolated from pseudocapsular tissues using nitric acid and imaged using ESEM. Subsequently, particle size, shape, number were determined. Particle characteristics were used to calculate the biological activity of wear debris from each THA polyethylene cohort [**1**]. Statistical analysis (Wilcoxon) was performed using JMP 8.0.

Results: Tissues from both remelted and annealed HXLPE cohorts contained significantly smaller and rounder particles compared to the CPE cohort ($p<0.001$). Despite an increased percentage of submicron particles ($p=0.02$), the total number of particles/gram of tissue was decreased for both HXLPE cohorts ($p=0.01$) (**Fig. 1**).

For predetermined particle size ranges (0.1-1, 1-10, >10 μm), the distribution of particle volume as a percentage of the total volume (mm^3) was not significantly different between any of the cohorts. Based on these similarities, the specific biological activity per unit volume (SBA) was also comparable between all three cohorts.

On the contrary, the total particle volume (mm^3)/gram in HXLPE cohort tissues was decreased due to decreases in both size and number of HXLPE wear debris ($p=0.01$). Accordingly, when the SBA was normalized by the total particle volume to determine functional biological activity (FBA), FBA of the wear particles from both HXLPE cohorts was significantly reduced compared to the CPE cohort ($p=0.01$) (**Fig. 2**)

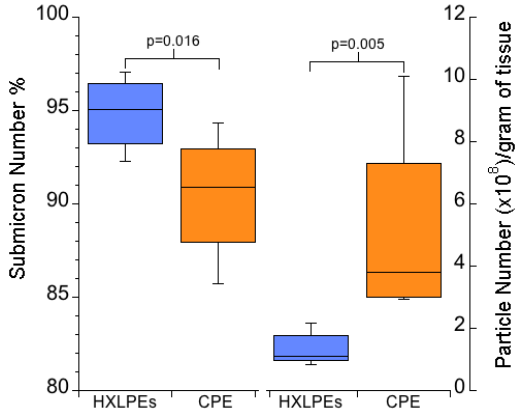

Figure 1. The percentage of submicron particles was increased for both HXLPE cohorts compared to the CPE cohort. On the contrary, the total number of particles/gram of tissue was decreased for both HXLPE cohorts. HXLPE, highly crosslinked; CPE, conventional.

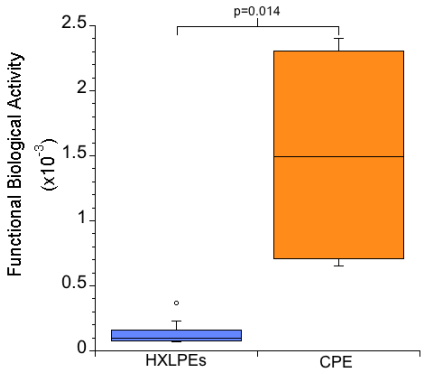

Figure 2. After normalizing specific biological activity by the total particle volume (mm^3)/gram of tissue, functional biological activity (FBA) was significantly lower for both HXLPE cohorts compared to the CPE cohort. HXLPE, highly crosslinked; CPE, conventional.

Conclusions: *In vitro* simulator studies have shown increased, similar or decreased numbers of HXLPE wear debris compared to CPE [**3, 4, 5**]. In this *in vivo* study, we report a significantly decreased HXLPE wear debris number. Overall, the predicted osteolytic potential of wear debris generated by HXLPE liners *in vivo* is significantly reduced by the improvements in polyethylene wear resistance.

References: [**1**] McKellop H. *JOR.*1999;17:157-67. [**2**] Fisher J. *Proc IME H*, 2001;215:127-32. [**3**] Scott M. *JBMR B,* 2005;73:325-37. [**4**] Yamamoto K. *JBMR A,* 2001;56:65-73. [**5**] Bowsher JG. *JBMR B.* 2008;86:253-63.

Acknowledgements: NIH (R01AR47904).

The anti-inflammatory properties of Vitamin E significantly reduce TNF-α release from primary human monocytes after stimulation with UHMWPE wear particles

+[1]Bladen, CL; [1]Fisher, J; [1]Ingham, E; [1]Tipper, JL
+[1]Institute of Medical and Biological Engineering, University of Leeds, UK
J.L.Tipper@leeds.ac.uk

STATEMENT OF PURPOSE:
Vitamin E (VE) has been added to Ultra High Molecular Weight Polyethylene (UHMWPE) acetabular cups and tibial trays to reduce oxidative damage to the polymer. Wear rates of VE polyethylene (PVE) have been shown to be reduced in the hip and the knee [1,2]. When the biological effect of VE-containing UHMWPE on macrophages was investigated, it was found that the biological response i.e. the production of osteolytic mediators (e.g.) TNF-α, was significantly reduced in peripheral blood mononuclear cells (PBMNCs) stimulated with UHMWPE + VE particles compared to virgin UHMWPE [3]. VE is known to have anti-inflammatory and anti-oxidant properties. The aim of this study was to stimulate TNF-α release in PBMNCs using lipopolysaccharide (LPS) or clinically relevant wear particles (UHMWPE or PVE) and investigate the effect of VE as an anti-inflammatory.

METHODS:
Particle Generation: Clinically relevant particles were generated aspetically by articulation using a single station multidirectional wear simulator according to an established protocol [4]. The load used was 160 N and the lubricant was RPMI 1640 medium supplemented with 25% FBS. UHMWPE refers to particles generated from GUR1050 polyethylene. PVE refers to particles generated from GUR1050 polyethlylene containing 1000 ppm vitamin E.
Vitamin E stock production: Vitamin E (VE) was provided as dl-α-tocopherol acetate at a concentration of 500 mg/ml. A 20 mM stock solution of VE was prepared in RPMI 1640 cell culture medium and serial dilutions were made to achieve working concentrations.
Co-culture of primary human monocytes with UHMWPE wear particles: Mononuclear cells (ethical approval granted by University of Leeds, Faculty of Biological Sciences ethics committee) were isolated from whole heparinised blood using lymphoprep™ gradients. Mononulear cells were seeded into 24 well tissue culture plates at a seeding density of $2x10^5$ cells per well in complete RPMI 1640 medium supplemented with 10% (v/v) foetal bovine serum and antibiotics. In the case of UHMWPE or UHMWPE containing VE (1000ppm), the particles were placed in 1.5% (w/v) low melting temperature agarose since the particles float in solution, prior to cell seeding. Where VE was added topically, a dose of 800 μM was used immediately after cell seeding. Cell viability assays (ATPlite™) and TNF-α production (ELISA) were measured at 24 hrs post cell seeding. In all experiments cells only (negative control) and LPS (positive control) were used. 4 replicates were used in each condition and each experiment was repeated with a minimum of three donors.

RESULTS:

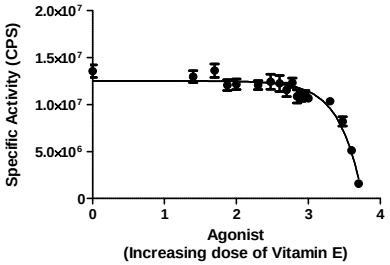

Figure 1. Vitamin E dose response.

Cytotoxicity of Vitamin E was assessed in PBMNCs by ATPlite™ assay and was only observed at relatively high doses (Fig 1. >3 mM). It was concluded that topically added Vitamin E at the doses used in experiments (800 μM) was not cytotoxic.

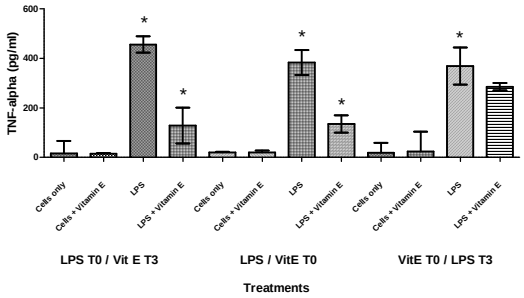

Figure 2. LPS induced stimulation of TNF-α production in PBMNCs +/- topically added VE (800 μM).
Topically added VE (800μM) modulated the response of LPS-stimulated monocytes to produce lower levels of TNF-α compared to control LPS-stimulated monocytes (Fig 2.). This modulation was significant when VE was added either at 3 hrs after initial LPS stimulation or at the same time as LPS addition. Addition of Vitamin E at 3 hrs prior to LPS stimulation did not significantly reduce the amount of TNF-α produced.

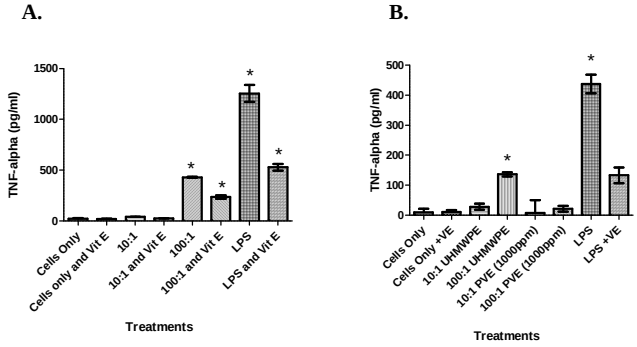

Figure 3. **(A)** The effect of clinically relevant GUR1050 UHMWPE wear particles on TNF-α production +/- topically added VE. **(B)** The effect of clinically relevant wear particles containing 1000ppm VE (PVE) on TNF-α production in PBMNCs.
Clinically relevant UHMWPE particles at a dose of 100 μm^3 significantly stimulated the production of TNF-α (Fig 3a). There was a significant reduction in TNF-α production in the presence of UHMWPE particles and 800 μM VE, added topically (Fig 3a).
Particles generated from clinically relevant polyethylene containing 1000ppm VE (PVE) significantly reduced the production of TNF-α from PBMNCs compared to GUR1050 UHMWPE wear particles or LPS controls (Fig 3b).

CONCLUSIONS:
Results shown confirmed that VE modulates the response of LPS-stimulated monocytes to produce lower levels of TNF-α compared to control LPS-stimulated monocytes. This trend is also observed when VE is added topically to UHMWPE stimulated PBMNCs. Wear particles generated from UHMWPE containing 1000ppm VE also produced lower levels of TNF-α. The exact mechanism of how VE affects the release of inflammatory mediators from particle-stimulated macrophages is not yet understood. It may involve anti-inflammatory and/or antioxidant effects, it may act at the posttranslational level or VE may affect the production of inflammatory mediators by reducing phagocytosis of the particles, this will form the basis of future studies.

REFERENCES:
[1] Oral et al., 2006. J Arthroplasty 21 (4), 580-591.
[2] Teramura et al., 2008. J Orthop Res **26**, 460-464.
[3] Teramura S, Russell S, Ingham E *et al*. (2009). Trans 55th ORS, Las Vegas, p2277.
[4] Ingram et al 2002. Biomed Mat Eng, 12 (2) 177-88

Dendritic Cell Activation by Ultra High Molecular Weight Polyethylene

Brian Scharf[1], Laura Santambrogio[1], and Neil Cobelli[2]

[1]Department of Pathology, Albert Einstein College of Medicine [2]Division of Orthopedic Surgery, Montefiore Medical Center

Statement of Purpose: Ultra high molecular weight polyethylene (PE) has been one of the most commonly utilized bearing surface materials in joint replacement arthroplasty for over four decades. Osteolysis is a chronic inflammatory process which all too commonly can lead to revision surgery. This process is the clinical outcome of immune recognition of PE particulate debris created by prosthetic wear. The purpose of this study is to determine whether Dendritic Cells (DCs), a type of antigen presenting cell that plays a major role in both the innate and adaptive immune responses, are involved in this immune response to PE. The analysis of the possible involvement of DCs at site of osteolysis will complement what is already known of macrophage involvement and indicate the full spectrum of the immune system involvement in PE recognition. This will be necessary in designing strategies to skew a disruptive immune response towards a tissue regenerating and more beneficial immune recognition.

Methods:**Gene chip assay:** Gene expression analysis was performed on control and PE treated DC. RNA was extracted using the Qiagen mRNA extraction kit. Five micrograms of total RNA were hybridized on the Human Toll-like Receptor Oligo GEarray (SuperArray Biosciences Corporation). Data are reported as average hybridization number for each gene subtracted for background.

Results: These results positively confirm that DCs can effectively recognize PE polymers and upon recognition initiate a TLR1/2 mediated inflammatory pathway. Previous data from our laboratory indicated that oxidized alkane polymers are capable of binding TLR1/2 and TLR2 receptors on DCs[1]. To determine whether PE binding to TLR1/2 and TLR2 was able to induce a pro-inflammatory expression program an RNA expression profile was performed on DCs exposed to oxidized PE particles. All data sets were corrected for background subtraction and normalized to housekeeping genes before being compared to each other (Figure 1). Genes that showed either up-regulation or down-regulation by 1.5 fold or more between control and PE treated samples were considered relevant. Up-regulation of the mRNA encoding for two of the adaptors involved in the early stages of TLR2 signaling (MYD88 and TIRAP) was observed in PE treated but not control cells. Likewise, MAP and RIP kinases involved in signal transduction (MAP2K3, MAP3K14 and RIPK2) were also up-regulated (Figure 1b and 1c). Finally, mRNA of transcription factors such as NFKB1, NFKB2, NFKB1A, RELB and IRF7 were up regulated in PE exposed cells but not in control cells. Altogether, this is an indication that the TLR2 signaling transduction pathway was engaged upon DC/PE interaction (Figure 1b and 1c). This signaling pathway ultimately lead to up-regulation of mRNA encoding for pro-inflammatory cytokines (IL-1, IL-6, IL-8, IL-12 and TNFα) as well as surface molecules (CD80, CD81, MHC class I) (Figure 1b and 1c).

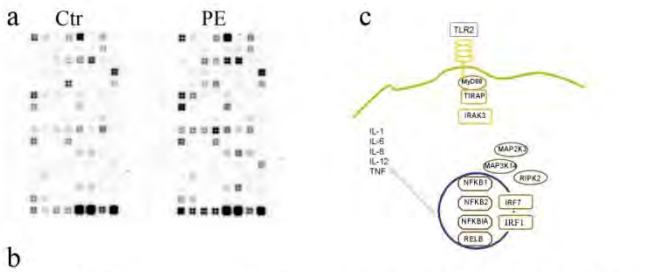

b

Adaptors		
MYD88	4485	7755
TIRAP	2071	3239
IRAK1	14851	11923
IRAK2	389	385
IRAK3	752	1742
IRAK4	428	387
IRF1	5459	8263
IRF3	16251	18607
IRF7	2771	10763
TRAF6	349	457

Kinases		
MAP2K3	9986	22530
MAP2K4	521	886
MAP2K6	359	337
MAP3K1	298	268
MAP3K14	5589	12393
MAP3K7IP1	634	861
MAP3K7IP2	550	598
MAP4K4	506	498
MAPK10	286	295
MAPK11	347	266
MAPK12	692	892
MAPK13	1372	2029
MAPK14	376	403
MAPK8	885	800
MAPK8IP3	3644	3832
MAPK9	1124	1290
MAP3K7	1630	1844
RIPK2	1773	5661

Transcription factors		
NFKB1	1679	10528
NFKB2	4463	9040
NFKBIA	5399	20451
NFKBIB	8869	11546
NFKBIE	2379	4421
NFKBIL1	12207	9498
NFKBIL2	788	671
NFRKB	12532	14501
FOS	6821	9042
JUN	2196	1785
IKBKB	1116	1883
IKBKG	1873	2883
REL	393	573
RELA	5387	5659
RELB	5342	11982

Cytokines		
IL10	1031	863
IL12A	1491	1526
IL12B	387	1326
IL1A	478	1200
IL1B	17392	19888
IL2	277	259
IL6	654	1990
IL8	583	6241
IFNA1	2447	1990
IFNB1	984	1053
IFNG	246	240
TNF	643	1561
TNFRSF1A	10990	9038
CXCL10	335	413

Figure 1. PE induces activation of a TLR2 mediated signaling pathway

Conclusions: Toll-like receptors (TLRs) enable antigen presenting cells to recognize different microorganisms and pathological "self" components and then mount the most appropriate immune response. We previously reported that polymers derived from shear PE, upon "in vivo" oxidation" are capable of engaging TLR1/TLR2. This was the first observation of a synthetic polymer engaging a TLR[1,2]. Here we extend our observation by investigating the signal transduction pathway associated with PE -TLR2 engagement in DCs. Upon their activation, DCs contribution to the overall PE-mediated inflammatory response and associated osteolysis is likely multifaceted. In response to TLR2 signaling DCs up-regulate a pro-inflammatory response which includes cytokines, such as IL-1, IL-6, IL-12 and TNF-α. Since these cytokines augment expression and release of TRAP and cathepsin K by resident osteoclasts, DCs have an indirect contribution to the inflammatory process by enhancing the overall rate of osteolysis and extracellular matrix necrosis. DCs can also directly promote de novo osteoclastogenesis by stimulating T cells to express RANK-L, a major differentiation for osteoclast precursors. Interestingly, DCs at osteolytic sites are often multinucleated and present giant cell morphology. Since DCs express cathepsin K, the major enzyme involved in the processing of bone matrix, it is also possible that DC have a more direct role in bone resorption. Taken together these data underline the major role played by DC in PE immune recognition.

Refererences:

1. Maitra R. PLoS One 2008;3(6):e2438.
2. Maitra R Mol Immunol 2009;47(2-3):175-84.

Effect of UHMWPE Particles on Mesenchymal Stem Cell Replication

+Marshall, A D[1,3],Smith, S[1],Stanley, J[1],Lee, R[1],Musib, M K[3],Dean, D D[1,3],Chen, X[2]
+[1]Department of Orthopaedics, The University of Texas Health Science Center at San Antonio, TX; [2]Department of Restorative Dentistry, University of Texas Health Science Center at San Antonio, TX; [3]UTSA/UTHSCSA Joint Graduate Program in Biomedical Engineering, San Antonio, TX
marshalla2@uthscsa.edu

INTRODUCTION:

Ultra-high molecular weight polyethylene (UHMWPE) wear debris particles have been implicated in implant loosening. Implant stability is largely dictated by the osteoblasts' ability to form new bone in the periprosthetic region. As normal bone formation requires an adequate availability of osteoblasts; any negative effect on osteoblast precursors could profoundly impact the body's ability to generate new bone. Since osteoblasts are derived from mesenchymal stem cells (MSCs), the MSCs' replication potential is critical in determining the continued stability of the prosthesis. No study to date has investigated the effect of UHMWPE on human mesenchymal stem cells.

METHODS:

Encouraged by preliminary experiments, we hypothesized that UHMWPE particles will have a dose-dependent effect on human MSCs' ability to replicate.

Preparation of UHMWPE particles: UHMWPE (GUR 1050) particles are suspended in water, pH 5.5, containing 500ppm Pluronic. Earlier studies in our lab have demonstrated that this solvent minimizes particle aggregation and facilitates dispersement in media. The suspension is vortexed for 15mins, sonicated for 2hrs, and then stored at 4 C for 7 days. The suspension is filtered through a 10µm pores size filter to remove large resin particles. Representative images are obtained using a Zeiss EVO50 SEM and analyzed according to ASTM F-1877. Particles are resuspended in media utilizing serial dilution to produce 5 different treatment doses (1×10^4, 1×10^5, 1×10^6, 1×10^7, and 1×10^8 particles).

Effect of particle dose on stem cell self-renewal: Human mesenchymal stem cells (ALLCELLS - Emeryville, CA) from a young bone marrow donor (Passage 1) are expanded in 30 ml of α-MEM 15%FBS media until 70-80% confluent. The cells are lifted, counted, and plated onto 6 well plates. An initial number of MSCs in the bone marrow isolate are determined from a primary CFU-F assay, while other cells in this isolate are expanded with various doses ($1x10^4$ to $1x10^8$) of UHMWPE particles for 7 days. The replication assay cells are lifted for seeding in secondary CFU-F assays with one secondary CFU-F plate per dose of particles. Experiments performed with two different seeding densities (100 cells/well, 300 cells/well) in triplicate. After 14 days of culture, CFU-F colonies are visualized with crystal violet.

Statistical Interpretation of Data: ANOVA utilized to analyze the data; post-hoc testing performed using Student's t-test with Bonferonni correction. P values≤ 0.05 are considered significant.

RESULTS:

The mean UHMWPE particle size was 0.4µm {range:16nm-4µm}. Figure 1 illustrates the size distribution for the particle suspension. Nanoparticles measuring down to 16nm were observed. Figure 2 shows SEM images of the UHMWPE particles. Figure 3 demonstrates cellular uptake of the UHMWPE particles.

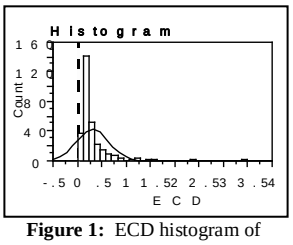

Figure 1: ECD histogram of particle distribution.

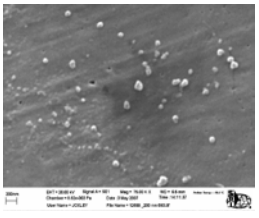

Figure 2: SEM images of UHMWPE particles.

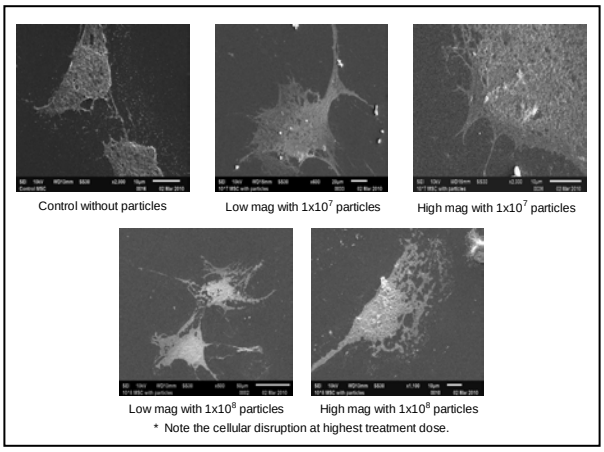

Figure 3: SEM images of stem cell uptake of UHMWPE particles.

Particle treatment had a dose-dependent effect on MSC replication (Figure 4). Control MSCs not subjected to particles demonstrated $2.4x10^6$ CFU-Fs. Increasing concentrations of particles caused a mild elevation ($p>0.5$) in CFU-Fs to $2.8x10^6$. However, particle concentrations of $1x10^7$particles/mL revealed a cytotoxic effect on the MSCs lowering the CFU-F number to $1.8x10^6$ ($p<0.05$). Further increasing the dose of particles inhibited replication to $3x10^5$ CFUs ($p<0.05$). This represents an 8 fold decrease in self renewal capacity for the highest particle load.

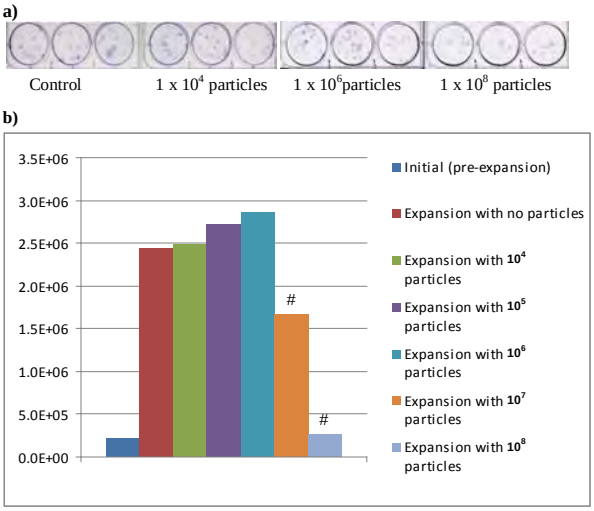

Figure 4. Replication of MSCs subjected UHMWPE particles.
a) Crystal violet staining of secondary CFU-F colonies demonstrating an inhibition of MSC cell number with increasing particle dose.
b) Graph depicting total number of CFU-F colonies after expansion in presence of unfractionated UHMWPE particles.

DISCUSSION:

This study is the first investigation of UHMWPE's effect on mesenchymal stem cell replication. UHMWPE particles have a dose-dependent affect on MSC replication The particles are stimulatory to MSC replication up to a threshold dose. At a dose above $1x10^7$particles/ml, this debris becomes deleterious to the stem cell. Determining the effect of UHMWPE particles on mesenchymal stem cell behavior will enable development of treatment strategies to improve the longevity of existing implants, and possibly allow preoperative risk assessment of an individual's response to the anticipated particle load.

Imaging intra-cellular polyethylene wear debris with coherent anti-Stokes Raman scattering spectroscopy

Martin Lee, Alistair Elfick.
Institute for Materials and Processes, School of Engineering, The University of Edinburgh, Edinburgh, EH9 3JF, UK.

Statement of Purpose: It is currently thought that wear debris generated from the motion of articulating joints enters the periprosthetic space where it is phagocytosed by macrophages. These macrophages then release pro-inflammatory cytokines and other mediators of osteolysis, leading to the eventual loosening of the implant.

Imaging particles in cells can be a key process in understanding the effects of wear debris. Labeling of polyethylene particles themselves are not possible and so either light or electron microscopy have been used as a means of detection their presence in cells. Polyethylene can be identified under polarized light due to a bright birefringence, however, particles less than 1μm in size can be difficult to visualize. Transmission electron microscopy provides much greater magnification but polyethylene shows up poorly, inferred from electron transparent areas. Aggressive sample processing is also required, which may alter the location of the debris and it's also limited to two dimensions.

We investigated the use of coherent anti-Stokes Raman scattering spectroscopy (CARS) as a method of imaging ingested polyethylene particles in macrophages in three dimensions. CARS is used as a label free method of imaging cells and tissues, relying on chemical contrast generated by different vibrational modes in molecules.

Methods: Cell culture: RAW 264.7 (mouse monocyte macrophage) cells between passages 5-15 were seeded on glass bottomed dishes for use in the CARS microscope.

CARS setup: A mode-locked Nd:YVO_4 laser source (PicoTrain, High-Q laser, Hohenems, Austria) produces a Stokes pulse (6 ps, 1064 nm) used in the CARS process. The source also produces a 5 ps, frequency doubled 532 nm beam which was used to pump an optical parametric oscillator (OPO) (APE Levante Emerald, Berlin, Germany). The OPO delivers a signal tunable in the range of 700-1000 nm, which was used as a pump in the CARS process. The two beams are combined using a dichroic mirror (DM) and focused into the input of a laser-scanning confocal inverted optical microscope (Nikon BV C1, Amsterdam, Netherlands). The pulses are synchronized by adjusting a micrometer-driven delay stage. These wavelengths are reflected towards a 60× oil immersion objective (Plan Apo VC, Nikon) with a 1.4 numerical aperture (NA) by a DM. The forward signal is collected by an air condenser (NA 0.72) and directed to two different photomultiplier tubes (Hamamatsu R3896, Shizouka Japan) through a multimode fibre and a DM. A set of appropriately placed filters was to isolate the signal.

Results: Wear particles from a pin-on-plate hip simulator (Kilgour A. Tribol Int. 2009;42:1582-1594) were cleaned using sodium hydroxide and isolated by differential ultracentrifugation in isopropanol. Isolated wear particles were assessed for size by scanning electron microscopy. The average size of polyethylene fragments generated was found to less than 100 nm.

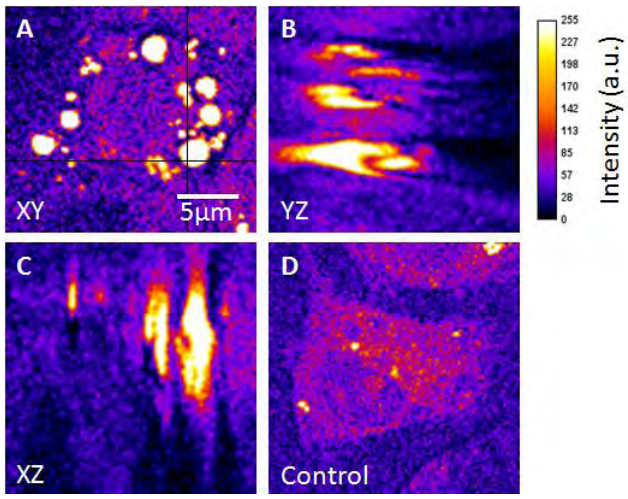

Figure 1. CARS images of a RAW 264.7 cell incubated with UHMWPE. A shows a single slice from a z-stack taken through the XY plane. B and C are slices through the YZ and XZ planes shown in A by the black lines. D shows an image of an untreated cell.

The CARS spectra of polyethylene was examined by adjusting the pump wavelength between 810 and 820 nm (corresponding to wavelengths of 2800 and 2950 cm^{-1}). This was found to be in good agreement with the Raman spectra with peaks visible in the CARS spectra at the corresponding 2850 and 2880 cm^{-1} wavenumber regions. We show that contrast could be enhanced from images by subtracting an off resonance image from an on resonance image a few nanometers apart. This helps to remove non-resonant background signals.

RAW 264.7 cells were incubated with polyethylene particles from both a commercial polyethylene powder, Ceridust 3610 (Clariant, Muttenz, Switzerland) and from a hip simulator for 24 hours, then examined using CARS microscopy. Total laser power falling on the samples was estimated at 65 mW and the pixel dwell was set to 30 μs giving a scan time of just over 7 s per image. CARS images were recorded as stacks with a z-step of 0.25 μm allowing 3D reconstructions. Control cells imaged by CARS showed bright points corresponding to lipid droplets within the cell as shown in Figure 1 D. Cells treated with Ceridust showed large individual particles visible within the cytoplasm, whilst those treated with polyethylene from the simulator contained discrete areas of the cell giving high signal rather than distinct particles (as shown in Figure 1 A-C). 3D reconstruction of the data allowed estimations of the volume of particles within cells to be measured and many cells were found to consist of over 50% ingested wear debris.

Conclusions: We have shown that CARS is a tool used to examine the location and load of wear debris inside of cells in a model environment. We aim to continue the work using post operative tissue to compare results.

Surface Damage, In Vivo Oxidation, and Reasons of Revision for Highly Crosslinked Tibial Inserts for TKA

[1]MacDonald, D; [1]Higgs, G; [1]Hanzlik, J; [3]Parvizi J; [4]Klein, G; [4]Hartzband, M; [4]Levine, H; [5]Kraay, M; [5]Rimnac, C; [1,2]Kurtz, SM

[1]Drexel University, Philadelphia, PA; [2]Exponent, Philadelphia, PA; [3]Rothman Institute, Philadelphia, PA; [4]Hartzband Center for Hip & Knee Replacement, Paramus, NJ; [5]Case Western Reserve University and University Hospitals Case Medical Center, Cleveland, OH

dm68@drexel.edu

Statement of Purpose: Remelted highly crosslinked polyethylenes (HXLPEs) were introduced in total knee replacement (TKR) starting in 2001 to reduce wear and particle-induced lysis [1]. Because elevated radiation crosslinking and remelting reduces the fracture toughness of PE, the use of HXLPE in the knee has been considered controversial [2,3]. Over time, HXLPE has gained acceptance as a candidate biomaterial for TKR [1]. However, few studies have reported on the clinical performance of HXLPE knees [4]. Now one decade following its introduction, knowledge regarding the *in vivo* damage mechanisms and oxidative stability of remelted HXLPEs in the knee remains incomplete.

Until recently, remelted highly crosslinked polyethylene has been considered oxidatively stable, presumably due to the lack of measurable free radicals [1]. Recently, researchers have observed elevated oxidation in retrieved HXLPE hip liners and knee inserts, particularly at the articulating surface [5,6]. The mechanisms of in vivo oxidation of remelted HXLPEs remains poorly understood, but in vivo loading and cyclic stress levels have been suggested as potential factors. Thus, due to different loading paradigms between hip and knee components, it is unclear if remelted highly crosslinked polyethylene will oxidize in total knee replacements to a greater extent than in hips.

The purpose of this study was to investigate the damage mechanisms and oxidative stability of remelted polyethylenes in a consecutive series of retrieved tibial components. We hypothesized that due to the relative lack of free radicals, remelted highly crosslinked polyethylenes would have lower oxidation levels than gamma inert-sterilized controls. Additionally, we hypothesized that the remelted components would remain oxidatively stable over time.

Methods: 186 posteriorly stabilized tibial components were retrieved at consecutive revision surgeries at 7 different surgical centers. 69 components were identified as remelted highly crosslinked polyethylene (Prolong, Zimmer) while the remainder (n=117) were conventional gamma inert sterilized polyethylene. The sterilization method was confirmed by tracing the lot numbers by the manufacturer. The conventional inserts were implanted for 3.4±2.7 years (Range: 0.0 – 10.1 years), while the remelted components were implanted 1.4±1.2 years (Range: 0.0 – 4.2 years). Patient records were reviewed to determine the reason for revision, patient demographics, and activity scores.

Surface damage were assessed using the Hood method [7]. The condyles, post and backside were inspected for 7 damage mechanisms, including scratching, pitting, burnishing, abrasion, delamination, embedded debris, and surface deformation, as previously described [7].

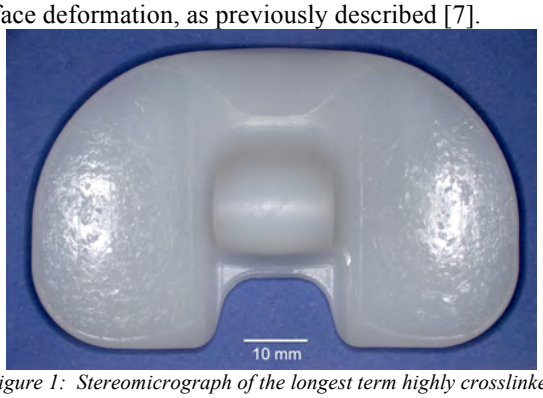

Figure 1: Stereomicrograph of the longest term highly crosslinked insert (4y in vivo). Note the burnishing and extensive pitting on the condyles. This insert was revised for loosening of the tibial component.

For oxidation analysis, a subset of the implants was evaluated in accordance with ASTM 2102. Specifically, remelted components implanted for more than 1 year were analyzed as well as 14 inserts that were implanted for less than 1 year to serve as a baseline. Thus, 41 conventional and 41 remelted inserts were available for oxidation analysis. Thin slices were taken from the medial condyle as well as the central spine and then boiled for 6 hours in heptane to extract any absorbed lipids. Lines scans were then taken at 100 μm increments (32 repeat scans per location) using FTIR spectroscopy. Regions of interest include the bearing surface, the backside surface, the anterior and posterior faces, as well as the post.

Hydroperoxide analysis was performed on 39 conventional inserts and 4 highly crosslinked inserts. Following oxidation analysis, the thin slices were exposed to NO for 16 hours. The NO gas converts hydroperoxides (the precursors to oxidation) to nitrates, which are identified and measured using FTIR spectroscopy. A hydroperoxide index was defined as the ratio of the integral of the curve between 1600-1670 cm^{-1} and the integral of the curve between 1330-1396cm^{-1}.

Results: The predominant reasons for revision were loosening, instability, and infection (Fig. 1). None of the highly crosslinked tibial inserts were revised for osteolysis or component fracture.

Pitting, scratching, and burnishing were the predominant damage mechanisms within both material groups. Delamination was only present on one gamma inert, but was not present within the highly crosslinked group. The prevalence of condylar pitting was similar between the material groups ($p = 0.269$), however, pitting scores were greater at the backside surface in the highly crosslinked retrievals ($p < 0.001$).

Oxidation was lower in the HXLPE group when compared to the gamma inert group at all locations ($p<0.001$; Mann-Whitney U Test; Fig. 3). In the HXLPE

group, the bearing surface had higher oxidation indices than both the backside ($p = 0.012$) and the post ($p = 0.022$). In the gamma inert inserts oxidation indices were positively correlated with implantation at the bearing surface, AP face, and the post (Rho = 0.376-0.475; $p \leq 0.02$; Fig. 4). No positive correlations were detected in the HXLPE group ($p > 0.101$; Fig 4). Oxidation potential was lower in the HXLPE inserts at the backside surface (mean difference = 0.18; $p = 0.006$), the AP face (mean difference = 0.32; $p = 0.003$), and the Post (mean difference = 0.25; $p = 0.042$) when compared to the gamma inert inserts (Fig. 5).

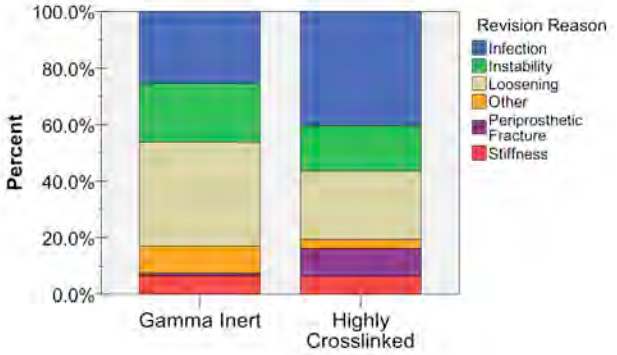

Figure 2: Revision reasons for the conventional and highly crosslinked tibial inserts.

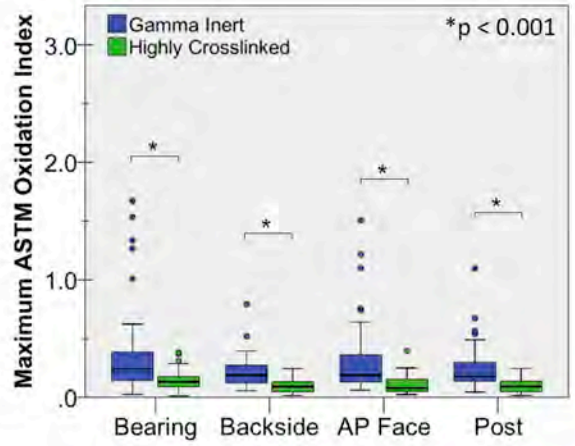

Figure 3: Regional oxidation in gamma inert and highly crosslinked tibial inserts.

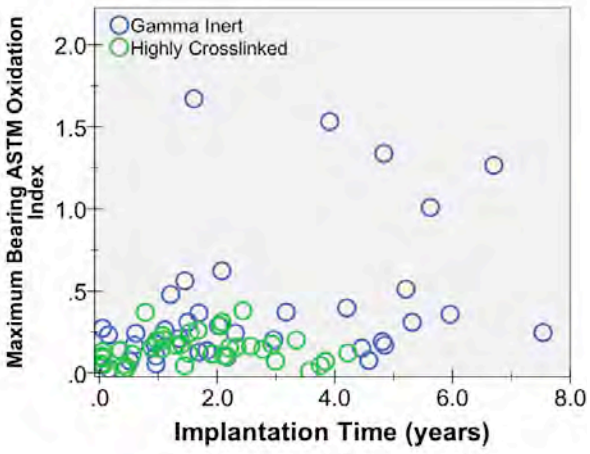

Figure 4: Scatter plot of the bearing surface oxidation index and implantation time.

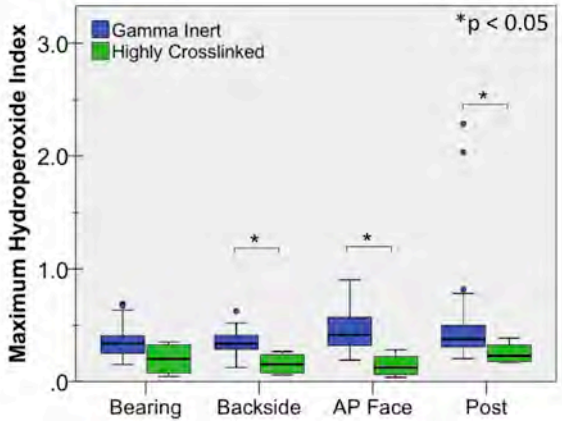

Figure 5: Regional hydroperoxide indices in gamma inert and highly crosslinked tibial inserts.

Conclusions: This study evaluated the surface damage mechanisms, oxidative stability, and reasons of revision for 1st generation highly crosslinked polyethylenes in total knee replacement. Remelted highly crosslinked polyethylenes proved to have reduced oxidation indices as compared with conventional inserts. While we were able to detect oxidation levels (as high as 0.4), we could not detect a correlation with implantation time. Additional long term highly crosslinked retrievals are necessary to ascertain the long term in vivo stability of these materials in total knee replacement.

Acknowledgements: This study was supported by a research grant from Zimmer. Institutional support has been also been received from NIH R01 AR47904, Stryker Orthopedics and Stelkast.

References:

[1] Kurtz SM. The UHMWPE Biomaterials Handbook (2nd Edition). Burlington, MA: Academic Press; 2009.

[2] Baker DA, Bellare A, Pruitt L. The effects of degree of crosslinking on the fatigue crack initiation and propagation resistance of orthopedic-grade polyethylene. J Biomed Mater Res A. 2003;66:146-54.

[3] Huot JC, Van Citters DW, Currier JH, Currier BH, Mayor MB, Collier JP. Evaluating the suitability of highly cross-linked and remelted materials for use in posterior stabilized knees. Journal of biomedical materials research Part B, Applied biomaterials. 2010;95:298-307.

[4] Kurtz SM, Gawel HA, Patel JD. History and systematic review of wear and osteolysis outcomes for first-generation highly crosslinked polyethylene. Clin Orthop Relat Res. 2011.

[5] Currier BH, Van Citters DW, Currier JH, Collier JP. In vivo oxidation in remelted highly cross-linked retrievals. The Journal of bone and joint surgery American volume. 2010;92:2409-18.

[6] Muratoglu OK, Wannomae KK, Rowell SL, et al. Ex vivo stability loss of irradiated and melted ultra-high molecular weight polyethylene. The Journal of bone and joint surgery American volume. 2010;92:2809-16.

[7] Hood RW, Wright TM, Burstein AH. Retrieval analysis of total knee prostheses: a method and its application to 48 total condylar prostheses. J Biomed Mater Res. 1983;17:829-42.

Oxidation of Highly Cross-linked Tibial Inserts

Currier, BH; Currier, JH; Collier, JP; Huot JC; Van Citters, DW
Thayer School of Engineering, Dartmouth College, Hanover, NH
Senior author barbara.h.currier@dartmouth.edu

INTRODUCTION Highly cross-linked (HXL) polyethylene bearings were introduced in the late 1990's to combat unacceptable wear rates in standard polyethylene bearings. These irradiation cross-linked materials have carefully prescribed protocols to stabilize the UHMWPE against oxidative degradation. Gamma sterilization in air was an industry standard until the mid-1990s, when that process was shown to result in oxidative embrittlement. [1] This oxidation was of concern especially in knees, where delamination, bearing wear-through and bearing fracture were documented. [2] Current generation UHMWPE tibial insert materials that are highly cross-linked (HXL) via irradiation are stabilized either by annealing below melt temperature (X3) or remelting above melt temperature (Durasul, Prolong, XLK) to prevent oxidative degradation. The hypotheses examined are (1) highly cross-linked UHMWPE bearings produced by all protocols have the potential to oxidize *in vivo*, and (2) annealed highly cross-linked UHMWPE has a greater potential to oxidize *in vivo* than remelted highly cross-linked UHMWPE.

MATERIALS/METHODS Seventy-three retrieved HXL UHMWPE tibial inerts (21 annealed, 52 remelted) were received at retrieval after *in vivo* time of 0.1 – 6.9 years, Table 1. The retrieved tibial inserts were cut with a band saw to expose a vertical cross-section, and sectioned using a Jung microtome (Jung, Heidelberg, Germany) for FTIR spectroscopy. Sections from selected retrievals were analyzed using EPR spectroscopy to determine free radical concentration (FRC).

RESULTS Below-melt annealed X3 contained free radicals at explantation (Table 2). No remelted HXL retrievals had measureable FRC (Table 2). Seventeen of 21 annealed retrievals (81%) and 22 of 52 remelted retrievals (42%) had subsurface maximum oxidation. Articular oxidation correlated positively with time *in vivo* in X3 retrievals (Spearman's rho=0.767, P<0.0005, Figure 1) and in remelted retrievals (Spearman's rho=0.483, P<0.0005, Figure 1). Independent sample T tests were run to compare oxidation and oxidation rate among tibial polyethylenes: X3, XLK, and Prolong. Comparing the two remelted HXL tibial polyethylenes showed that Prolong retrievals had statistically higher mean articular oxidation rate than XLK retrievals, but statistically equivalent edge oxidation rates. (Table 3a). Comparing remelted HXL (Prolong) and annealed HXL (X3) showed that X3 (annealed) retrievals had statistically higher mean articular oxidation rate and edge oxidation rate than Prolong (remelted) retrievals. (Table 3b). Articular oxidation in all retrieved HXL tibial inserts correlated with nominal cross-linking dose (Spearman's rho=0.538, P<0.0005).

DISCUSSION / CONCLUSIONS Differences in post-irradiation thermal processing of highly cross-linked UHMWPE were shown to lead to differences in oxidation resistance of HXL bearings in vivo. Annealing leaves free radicals in HXL X3 inserts and 81% of retrieved X3 inserts in this study had subsurface oxidation similar to gamma-sterilized retrievals. Because remelted HXL tibial inserts had no measurable FRC either before implantation (as measured in never-implanted shelf-aged HXL bearings) [3] or after retrieval, it was not expected to oxidize *in vivo*. However, 42% of remelted HXL inserts in this study had subsurface oxidation.

In this set of relatively short-term retrievals, the different fabrication methods used for the HXL materials appear to cause differences in oxidation potential. The choice of annealing rather than remelting after cross-linking significantly increases the oxidation potential of HXL materials, as seen in their higher measured oxidation and oxidation rate compared to remelted HXL materials. The different fabrication methods used for remelted HXL materials cause differences in oxidation potential among the remelted HXL materials. If the oxidation measured in HXL UHMWPE is shown to cause a reduction in toughness, the correlation of articular oxidation and nominal cross-linking dose raises questions about the suitability of higher dose HXL materials for application in the knee.

REFERENCES

1. Sutula LC, et al, *Clin Orthop.* Oct 1995(319):28-40
2. Collier JP, et al.. *J Arthroplasty.* 1996;11:377-89.23.
3. Collier JP, *Clin. Orthop.* Sep 2003(414):289-304

Table 1: Retrieved highly cross-linked (HXL) UHMWPE tibial inserts from three manufacturers were analyzed in this study. These materials, varied in cross-linking dose and thermal processing after irradiation.

Retrieved UHMWPE	N=	Thermal process	Nominal cross-linking dose (KGray)	Mean *in vivo* time (years)
X3	21	Annealed	90	1.7 +/- 0.86
Prolong	23	Remelted	64	2.3 +/- 1.29
XLK	24	Remelted	50	2.0 +/- 1.05
Durasul	5	Remelted	95	3.9 +/- 1.89

Table 2: EPR spectroscopy was used to assess the free radical concentration present in retrievals after various *in vivo* time.

Retrieved UHMWPE	N=	Mean *in vivo* time (years)	Average FRC (spins/gram)
X3 (Annealed HXL)	2	1.03 +/- 0.318	2.48E+15
Prolong (Remelted HXL)	3	1.84 +/- 0.386	0.0
XLK (Remelted HXL)	2	1.85 +/- 2.62	0.0

Table 3: Independent sample T-Tests compared groups of retrievals.
(a) Prolong retrievals had higher mean articular oxidation rate than XLK retrievals, but equivalent edge oxidation rates.

Independent T-Test variable	Prolong (n=23)	XLK (n=24)	P value
Mean articular oxidation rate	0.071+/-0.067	0.027+/-0.024	0.006
Mean edge oxidation rate	0.028+/-0.069	0.012+/-0.01	0.282

(b) X3 (annealed) retrievals had higher mean articular oxidation rate and edge oxidation rate than Prolong (remelted) retrievals.

Independent T-Test variable	X3 (n=21)	Prolong (n=23)	P value
Mean articular oxidation rate	0.160+/-0.070	0.071+/-0.067	<0.0005
Mean edge oxidation rate	0.078+/-0.076	0.028+/-0.069	0.025

Figure 1: Maximum ketone oxidation measured in HXL retrievals increases with in vivo time (P<0.0005).

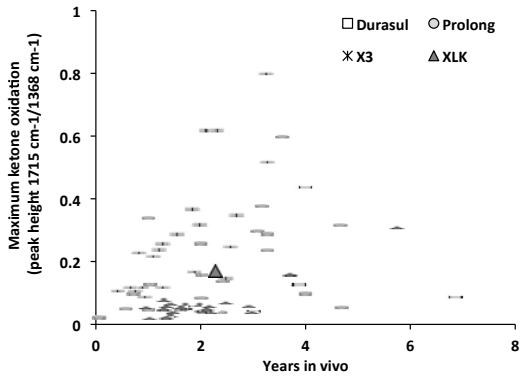

In Vivo Performance of Highly Cross-linked UHMWPE

[1]Rowell SL, [1]Micheli BR, [1]Wannomae KK, [1]Malchau H, +[1]Muratoglu OK
+ [1]Harris Orthopaedic Laboratory, Massachusetts General Hospital, Boston, MA
omuratoglu@partners.org

Introduction

Radiation cross-linking improves the wear resistance of ultra-high molecular weight polyethylene (UHMWPE) used in total hip arthroplasty, shown both *in vitro* [1] and *in vivo* [2], but also generates residual free radicals which are the precursors to oxidative embrittlement. First generation highly cross-linked UHMWPEs used either post-irradiation melting to quench the free radicals, or post-irradiation annealing to reduce free radicals. Each of these methods had their drawbacks: Melt and crystallization of the polymer reduced fatigue strength and lowered mechanical properties, while post-irradiation annealing below the melting point did not eliminate enough free radicals to inhibit *in vivo* oxidation.

The second generation of highly cross-linked UHMWPE introduced two new methods to stabilize free radicals while improving wear resistance and retaining mechanical properties similar to conventional UHMWPE. The first method uses a sequential cross-linking process, where the polymer is cross-linked in three separate cycles consisting of gamma irradiation followed by annealing. The objective of this method is to maximize the reduction of free radicals; however, they are not fully eliminated [3]. Acetabular liners were made available for clinical use in 2005, with the subsequent release of tibial inserts in 2006-2008. The second method infuses vitamin E into irradiated UHMWPE, which acts as an antioxidant to stabilize free radicals. The vitamin E infused implants are terminally sterilized with gamma irradiation to ensure sterility and also to graft the vitamin E to the host polymer backbone for prolonged oxidative stability [3]. This technology was introduced in 2008 for clinical use.

The development of both first and second generation highly cross-linked material focused on stabilizing radiation-induced free radicals as the sole precursor to oxidative degradation; however, secondary oxidation mechanisms have come to light in both conventional and highly cross-linked UHMWPE: absorbed lipids and cyclic load. Recent retrieval studies have reported in vivo oxidation in long-duration highly cross-linked retrievals [4, 5] along with rapid ex vivo oxidation in short-to-mid duration retrievals [6]. Preliminary in vitro accelerated aging tests have shown that both generations of highly cross-linked polyethylene are vulnerable to oxidation in varying degrees after exposure to lipids [7]. These results raise concerns about the long-term in vivo oxidative resistance of highly cross-linked liners, leading us to investigate the effect of lipid absorption in retrievals.

Table 1. 1st and 2nd generation highly cross-linked UHMWPEs

Material	Irradiation + Free radical stabilization	Sterilization
Marathon™ *Acetabular Liner*	50kGy gamma-irradiation at room temperature, followed by melting	Gas plasma
Longevity™ *Acetabular Liner*	100kGy e-beam irradiation at 40C, followed by melting	Gas plasma
Prolong™ *Tibial Inserts*	65kGy e-beam irradiation at 125C, followed by melting	Gas plasma
E1™ *Acetabular and Tibial Inserts*	100kGy gamma-irradiation, followed by vitamin E diffusion and homogenization	25-30kGy gamma
X3™ *Acetabular and Tibial Inserts*	3 cycles of 30kGy gamma irradiation followed by 8 hours of 130C annealing	Gas plasma

Materials and Methods

We collected 32 first generation retrievals including twelve Marathon™ acetabular liners (DePuy, Warsaw, IN), three Prolong™ tibial inserts (Zimmer, Warsaw, IN), and seventeen Longevity™ acetabular liners (Zimmer). Second generation retrievals included ten E1™ (Biomet, Warsaw IN) liners with *in vivo* durations ranging from 3 days to 19.5 months, and fifteen X3™ (Stryker, Mahwah, NJ) with *in vivo* durations ranging from 0.5 months to 45 months. All components were disinfected in ethanol upon receipt; subsequently the components were stored in air in a -20°C environment to minimize *ex vivo* oxidation.

Sections were removed from the rim or non-loaded eminence and the articular surface of each explanted component was microtomed into 150 μm thin films. Thin films (n=3 from each component) were analyzed using Fourier Transform Infrared Spectroscopy (FTIR) as a function of depth from the surface across the thickness of the component. FTIR analyses took place both before and after films were refluxed in boiling hexane for 16 hours to extract absorbed esterified fatty acids. Additional thin sections were also extracted with hexane and reacted with nitric oxide to measure the hydroperoxide content using FTIR [8].

Carbonyl index values both before and after hexane extraction were calculated by normalizing the carbonyl absorbance area over 1680 cm^{-1} - 1780 cm^{-1} to the absorbance area over 1330 cm^{-1} - 1390 cm^{-1}, per ASTM F2102-01^{e1}. Transvinylene index was calculated from post-hexane spectra by normalizing the carbonyl absorbance area over 950 cm^{-1} - 980 cm^{-1} to the absorbance area over 1850 cm^{-1} - 1985 cm^{-1}. Oxidation potential, or hydroperoxide index, was calculated by normalizing the nitrate peak height at 1630 cm^{-1} to the absorbance peak height from the polymer backbone at 1895 cm^{-1}.

Xylene etching was performed on retrievals showing measurable oxidation. 150μm thin films were held in the evaporation fumes of boiling xylene for a 90-second interval in order to visually enhance oxidative embrittlement of the material.

Cross-link density was calculated as per ASTM F2214 through gravimetric swelling analysis using xylene at 130°C for 2 hours on samples from each region of the liners. Crystallinity measurements were performed using differential scanning calorimetry (DSC) by integrating the enthalpy between 20 and 160°C and normalizing that with the heat of fusion of 100% crystalline polyethylene (291 J/g).

Free radical content was measured by electron spin resonance and calculated by double integration of the ESR signal over the magnetic field and normalizing by the sample weight. The data was analyzed by linear or power regression as a function of in vivo duration, and significance assigned using an unpaired, two-tailed student's t-test.

Results and Discussion

Characterizing Lipid Absorption

The absorption of lipids into highly cross-linked polyethylene has been shown to initiate oxidation when exposed to oxygen outside of the body [6]. Lipid absorption rates into the UHMWPE were expected to vary between material types due to differing physical properties affecting diffusion rates, where lower irradiation doses would allow for quicker penetration, if not higher concentrations. All highly cross-linked retrievals showed maximum lipid absorbance at the surface (x = 0), ranging from 0.227 to 1.117 depending on material type (Table 2). Lipid absorption profiles were characterized by decreasing absorption with increasing depth. The depth of lipid absorption increased with respect to time. Maximum lipid absorption was greater than 0.2 in all retrievals, even in those with less than one month of in vivo service. Backside absorption was lower than at the articular surface in tibial inserts. Lipid absorption at non-loaded regions showed an overall lower concentration than the articular surface, most likely due to cyclical loading increasing the lipid uptake at the articular surface.

Table 2. Maximum surface lipid absorbance values in highly cross-linked retrievals

Material	Average Maximum Articular Surface Lipid Absorbance	Average Maximum Rim Surface Lipid Absorbance
Marathon™	0.491 ± 0.062	0.489 ± 0.185
Longevity™	0.482 ± 0.155	0.275 ± 0.184
Prolong™	0.607 ± 0.190	0.148 ± 0.096
E1™	0.525 ± 0.267	0.262 ± 0.233
X3™	0.627 ± 0.215	0.347 ± 0.144

First Generation Highly Cross-linked UHMWPE

Three types of irradiated and melted UHMWPEs were investigated in order to determine the effect of lipid absorption on highly cross-linked polyethylene. Of the three materials, Marathon™ retrievals showed the greatest oxidative stability with up to 84 months *in vivo*. Of the twelve Marathon™ retrievals, oxidation indices averaged 0.002 ± 0.006 with maximum surface oxidation values well below the detection limit in all but one, a 21 month liner (OI=0.160). No other liners showed any trend towards increasing surface oxidation.

Longevity™ retrievals showed detectable oxidation values in 6 out of 20 retrievals. Oxidation profiles of those liners showed increasing oxidation values at the articular surface along with a subsurface increase that was still below detectable limits overall (Figure 1). This subsurface increase was notable in liners from 22 months to 120 months. A correlation curve was fit to the maximum oxidation indices and showed a slow trend towards increasing oxidation with respect to in vivo duration.

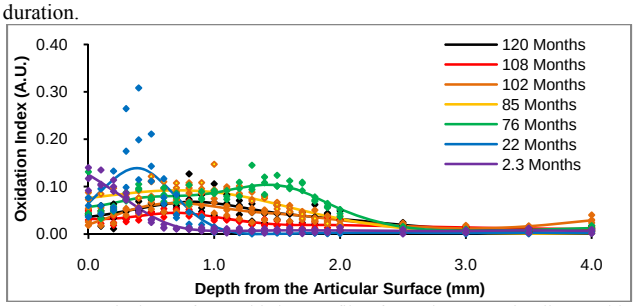

Figure 1. Articular surface oxidation profiles from six Longevity liners with oxidation maximums above 0.1.

While limited sample size prevented any significant conclusions about the oxidative stability of Prolong™ tibial inserts, three of the four tibial inserts had maximum oxidation values above the detection limit. The greatest oxidation was seen in the 47 month liner, where a subsurface oxidation peak reached OI=0.863 at approximately 1 mm below the medial wear scar. Evidence of white-banding was revealed after xylene etching (Figure 2).

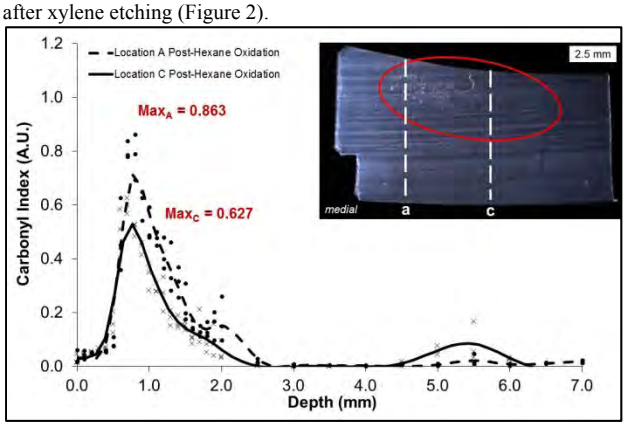

Figure 2. Subsurface oxidation and white banding is found across the articular surface of a four year Prolong™ tibial insert.

Second Generation Highly Cross-linked UHMWPE

X3™ retrieval results showed increasing oxidative instability with respect to in vivo service. In vivo durations from these retrievals ranged from 0.5 to 45 months. All four X3™ tibial inserts showed detectable oxidation levels (OI>0.1) with maximum values ranging from 0.103 to 0.690. Oxidation profiles in these inserts were characterized by subsurface oxidation peaks ranging from 0.1-0.2mm below the loaded region of the articular surface. Likewise, in seven of the eleven acetabular liners, maximum surface oxidation values were also well above detectable limits with values ranging from 0.107 at 1.3 months to 0.943 at 45 months. Oxidation profiles for four of these acetabular liners were characterized by subsurface oxidation peaks approximately 1-2mm below the articular surface. Two of those liners also showed high subsurface oxidation at the rim, including the longest duration acetabular liner revised for infection after four years in vivo (Figure 3). This four year liner had a subsurface peak maximum of OI=1.601 at the rim and revealed distinct white banding approximately 0.1mm below the surface after xylene etching.

Table 3. Average material properties of the second generation UHMWPE retrievals.

	E1™	X3™
***In Vivo* Duration Range (months)**	0.1-19.5	0.5-46
Oxidation Maximum	0.029-0.187	0.023-0.943
Hydroperoxide Index	0.622 ± 0.066	N/A
Crystallinity (%)	58.8 ± 3.2	61.6 ± 1.7
Peak Melt Temp (°C)	142.3 ± 1.4	141.2 ± 0.7
Cross-link Density (mol/dm^3)	0.300 ± 0.014	0.223 ± 0.040

No regional changes were seen in crystallinity, cross-link density, and transvinylene index for any of these liners at current oxidation levels and in vivo durations (Table 3).

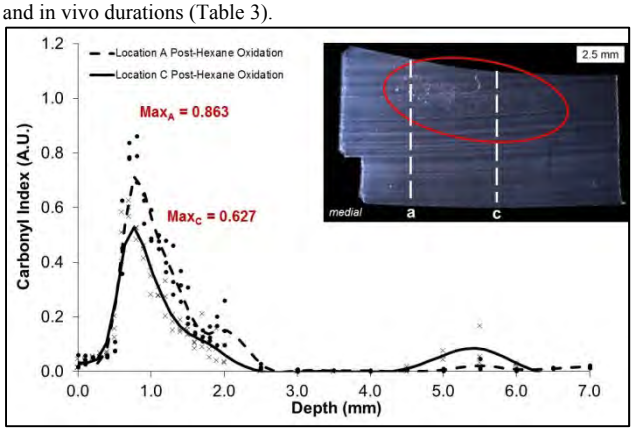

Figure 3. Subsurface oxidation and white banding is found at the rim of a four year X3™ retrieval.

E1™ retrievals showed scratches on the articular surfaces with the machining marks still visible, typical of highly cross-linked UHMWPE retrievals [5]. Seven out of ten retrievals had maximum oxidation values reaching between 0.1-0.2, similar to the other highly cross-link retrievals in the study. There were no correlations between in vivo duration and crosslink density, crystallinity, peak melting point, oxidation, and hydroperoxide index (Table 3), nor were there any regional variations between the non-loaded region and articular surfaces within individual retrievals.

Free radical content in E1™ retrievals decreased significantly with respect to in vivo duration ($p<0.05$), with a reduction of about one order of magnitude (78%) over 20 months. We found an even stronger negative correlation ($R^2=0.74$) between the total age of the liner (pre-implantation shelf duration, in vivo duration, and ex vivo duration) and free radical content (Figure 4). With little to no oxidation present in these retrievals, this decrease in free radical content was likely related to the free radical scavenging activity of vitamin E.

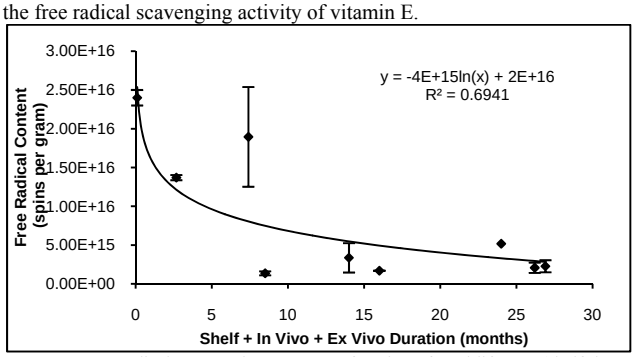

Figure 4. Free radical content decreases as a function of total lifespan (shelf time, in vivo duration and ex vivo duration in air before analysis) in irradiated, vitamin E-stabilized retrievals.

Conclusions

Detectable oxidation has been identified in both generations of highly cross-linked retrievals, including both materials with and without free radicals. No other material properties appear to be affected by the oxidation levels at the short- to mid-duration *in vivo* service times. Investigation of longer duration retrievals will be necessary to determine if this loss of oxidative stability should raise concerns about the long-term clinical performance of these materials.

Acknowledgements

These studies were funded by Zimmer Inc., Biomet Inc. and DePuy Inc.

References

[1] Harris. Clin Orthop, 1995; 311:46-53. [2] Muratoglu, et al. J Arthroplasty, 2001; 16(2):149-160. [3] Kurtz SM. The UHMWPE Handbook. 2nd Ed, 2009; 291-308. [4] Currier, et al., 2010; ORS Annual Meeting, New Orleans, LA. Paper #170. [5] Reinitz, et al. 2011; ORS Annual Meeting, Poster #1188. [6] Muratoglu, et al. JBJS, 2010; 92:2809-2816. [7] Oral, et al. 2011; AAOS Annual Meeting, San Diego, CA. Paper #533. [8] Costa, et al., Biomaterials, 2001; 22(4):307-315.

Autonomous Mathematical Reconstruction of Polyethylene Tibial Inserts to Measure Low Wear Volumes

Knowlton, Christopher B.[1,2], Wimmer, Markus A[1,2].
[1]Rush University Medical Center, Chicago, IL, [2]University of Illinois at Chicago, Chicago, IL.

Statement of Purpose: Wear of the polyethylene tibial component is a major factor limiting the success and longevity of total knee replacements. Although volume loss of knee simulator components can be measured accurately from consecutive coordinate measuring machine (CMM) scans [1], measurement of wear in surgically retrieved components remains challenging because the original surface is not available. The purpose of this study was to validate a method of calculating the volume loss on the articulating surface of a retrieved tibial insert using mathematical reconstruction.

Methods: Three unworn and six worn GUR 1050 ultrahigh molecular weight polyethylene (UHMWPE) NexGen cruciate-retaining tibial inserts (Zimmer, Warsaw, IN) were digitized on a FlashScope coordinate measuring machine (OGP, Inc., Rochester, NY) with a low-incidence laser at 100x100µm in-plane point spacing. To estimate method error, circular regions of points were removed from each tibial plateau of unworn scans and the original surfaces were estimated by a computer-aided design (CAD) model, a size-matched unused insert and autonomous mathematical reconstruction. Reconstruction was performed by least-squares fitting a design-congruent curve to the unworn points of each AP line scan and interpolating the original surface in worn regions. Worn components were worn in three separate level walking gait tests in a four-station knee simulator (Endolab, Rosenheim, Germany) in load-control mode per ISO 14243-1 [2]. After reconstructing these components to estimate volume loss, records of gravimetric mass loss were retrieved and converted to volume loss, assuming ρ=0.931 mg/mm^3.

Results: For a mock wear scar area of 314 mm^2, the mean absolute volume difference (±SD) between the reconstructed surface and the measured unworn surface on each tibial plateau was 4.44±1.75 mm^3. This was significantly less than the volume difference associated with a CAD model (23.81±4.37 mm^3, $p<0.001$) and not significantly different from the volume difference associated with size-matched unused inserts (4.20±1.98 mm^3, p=0.83.) Simulator-tested inserts had wear scars on each tibial plateau with area of 346.94±39.23 mm^2. Autonomous reconstruction accurately ranked volume loss in order of increasing mass loss.

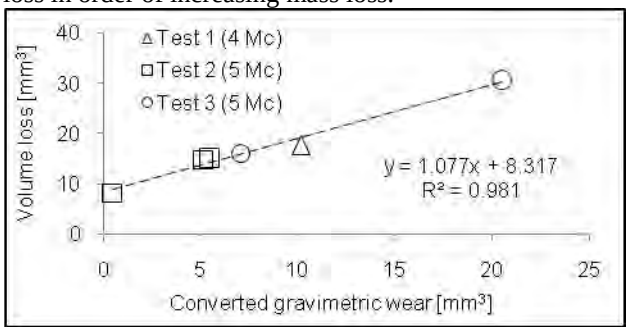

Figure 1. Correlation of volume loss to mass loss

Linear correlation between volume loss and converted mass loss (Fig. 1) resulted in a slope not significantly different from β_0=1(p=0.36). Reconstruction allowed for mapping of volume loss on the articular surface, as exemplified in Fig. 2.

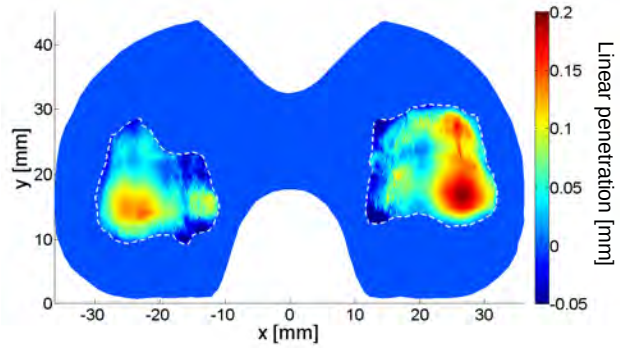

Figure. 2. Wear map of a component worn in Test 3 with total mass loss of 19.09 mg, wear scars outlined (dashed white lines)

Conclusions: Our results indicate that an autonomous mathematical reconstruction of the original surface based on unworn regions can provide accurate measurements of volume loss on the articular surface of tibial inserts. This is useful when the original surface has not been measured, as is the case with retrieved components. The error of this method was lower than estimation by a CAD model, equivalent to estimation by a size-matched unused and less than the 10-20 mm^3 annual wear rate of UHMWPE [3]. However, models and drawings of implants are proprietary, procuring matched inserts is expensive for current designs and impossible for obsolete designs, and neither method can correct for manufacturing variability. Other studies attempting to reconstruct the original surface of tibial inserts have had limited success [4,5]. Our method differs in that a curve congruent to the surface design, instead of a polynomial or non-uniform random b-splines [5], was fit to unworn regions. Though we obtained point cloud representations of the articular surface of one design with a CMM routine, autonomous reconstruction can be applied to articular and backside surfaces of diverse geometries digitized by other methods. Future work will quantify accuracy of our method in the absence of creep, fluid absorption, thermal expansion and backside wear, as well as apply it to other designs, backside surfaces and retrieved components. The many wear metrics that this technique calculates, such as localized penetration (Fig. 2), will provide researchers with a more complete understanding of wear on UHWMPE tibial liners.

References: [1] Muratoglu OK. Clin Orthop Relat Res. 2003;410:155-164. [2] ISO International Standard 14243-1, Part 1, 2002. [3] Kaddick C. Orthopade 2009;38: 690-697. [4] Kop AM. Acta Orthop. 2007;78:364-370. [5] 26. Blunt LA. Proc Inst Mech Eng H. 2008;222:309-318.

Bacterial adherence in infected arthroplasties: material differences.

E. Gómez-Barrena[1], J. Esteban[2], F. Medel[3], L. Gracia[3], A. Ortiz-Pérez[2] , D. Molina-Manso[2], G. del Prado[2], J. Cordero[4], J.A. Puértolas[3].

[1]Hospital La Paz, Autónoma Univ., Madrid, Spain; [2]IIS-Fundacion Jiménez Díaz, Madrid, Spain; [3] Instituto Ciencia de Materiales de Aragón, ICMA, Universidad de Zaragoza-CSIC, Zaragoza, Spain; [4]Hospital La Princesa, Autónoma Univ., Madrid, Spain.

INTRODUCTION: Bacterial adherence and subsequent biofilm formation on total joint replacement implants are at the origin and maintenance of implant-related osteoarticular infection. Different biomaterials in the components are claimed to differently suffer from these processes, justifying clinical decisions such as component exchange. In this study, we aim to verify the adherent microorganisms from different components in retrieved implants from infected joint replacements, particularly the bacterial adherence on UHMWPE components compared with other materials, in hip and knee components retrieved from infected arthroplasties.

MATERIAL AND METHODS: A total of 87 total joint components (51 hip and 36 knee components) from 32 patients (20 hip and 12 knee arthroplasties) with clinical diagnosis of implant-related infection were separately sonicated after surgical retrieval, following a previously published protocol (Esteban et al 2008). Subsequent positive cultures of one or more pathogen microorganisms were obtained and quantified. Material in the component surface was UHMWPE in 31, CrCo in 35, Ti alloys in 16, and hydroxiapatite (HA) in 5. Fixation was cemented in 30 cases, non-cemented in 24, and no fixation (femoral heads and liners) in 33 components. HA was present in 14 components, although only 5 were fully coated. Culture was positive in 67 of the 87 components, and 15 showed more than one microorganism.

The individual components of 6 retrieved joint implants (3 hip replacements and 3 knee replacements) were separately scanned using a Picza 3D Laser Scanner LPX-60 (Roland DG Corporation, Japan). All the components were scanned in the plane mode at 0.6 mm pitch, except for femoral heads, which were scanned in the rotary mode. 3D point cloud data were converted into polygon meshes using Dr. PICZA3 software for further file conversion and analysis. Measurements of the scanned surfaces (in mm^2) were obtained for each individual component with Pixform™ Pro software. A ratio of UFC per mm^2 of implant surface was obtained to compare components. Descriptive and comparative (Kruskal-Wallis, Mann-Whitney, Chi square tests) statistics were used, as UFC/mm^2 variables did not follow a normal distribution in the Kolmogorov-Smirnov test.

RESULTS: The presence of positive culture was different among materials (p=0.025, Chi square). Significant differences were found in the adhered UFC/mm^2 among components (p=0.018) and materials (p=0.005). The second adhered microorganism was higher in the non-cemented components (p=0.023) but not the predominant microorganism, and so happened with the HA-coated components (p=0.019). When comparing adherence to UHMWPE, this was lower than to Ti (p=0.001), but not to CrCo or HA. Also, adherence to CrCo was lower than to Ti (p=0.008). This was not the case for HA.

DISCUSSION: Data from our retrieved components confirm different results as expected from the classical statement about higher polymer infection than metals (Petty et al. 1985). In fact, UHMWPE significantly adhered less microorganisms than other materials in arthroplasty components. This is of particular clinical interest, as the exchange of UHMWPE components is frequent when dealing with early infections, but the effectiveness of this gesture is controversial. We conclude that other components rather than UHWMPE are at similar or greater risk of adhering and maintaining microorganisms in an infected arthroplasty.

REFERENCES:

[1] Esteban et al. *J Clin Microbiol* (2008) 46(2):488-92.
[2] Petty et al. *JBJS-A* (1985) 1985 67(8):1236-44.

ACKNOWLEDGEMENTS: This study was financed by CONSOLIDER FUNCOAT-CSD2008-00023. DMM was granted by Fundación Conchita Rábago. AOP was funded by Comunidad de Madrid.

For submission: Convert to PDF and email abstract with contact information to skurtz@exponent.com

Using Oxidative Induction Time to determine antioxidant concentration in UHMWPE

[1]Heuer, E.G.; [2]Stark, N.; [1]Braithwaite, G.J.C.; [1]McCormack, C.A.; [1]Miller, B.L.; [3]Gsell, R.
[1]Cambridge Polymer Group, 56 Roland Street, Suite 310, Boston, MA, [2]Zimmer GmbH, Sulzer-Allee 8 CH-8404 Winterthur,
[3]Zimmer, Inc., 1800 West Center Street, Warsaw, IN 46580

Statement of Purpose: Vitamin E (VE) is increasingly being used to improve oxidative stability of highly crosslinked ultra-high molecular weight polyethylene (UHMWPE), a prominent orthopaedic implant material. A method for sensitively determining low concentrations of VE becomes crucial for confirming intended material properties including desired loading as a function of position. Here we describe a novel method for quantifying VE concentration using oxidation induction time (OIT) determined by differential scanning calorimetry. Current methods, such as Fourier transform infrared (FTIR) spectroscopy [1], can only quantify with repeatability and reproducibility levels of VE greater than 0.5 wt% (ASTM F2759) which is near the expected loading range for implanted UHWMPE (< 0.5 wt%). OIT is an ASTM method for measurement of oxidative stability and has a broad history of use with polyethylene, chiefly as an indicator of oxidative degradation and/or resistance [2-4]. We conducted OIT measurements on UHMWPE stabilized with varying concentrations of VE at three stages of processing. Comparison with initial VE wt% and processing conditions revealed an exponential relationship that could be used to determine the effective VE concentration of unknown samples using an OIT master curve.

Methods: GUR 1050 powder was blended with VE in the following wt%: 0.01, 0.02, 0.05, 0.10, 0.25, 0.28, and 0.38 with approximately ±0.02% uncertainty. Three sample sets were produced: un-altered powder, direct compression molded pucks, and direct compression molded pucks e-beam irradiated to 200 kGy. OIT analysis was performed on a Q1000 DSC (TA Instruments) according to ASTM D3895-98 [5]. Three specimens per sample from each set were tested. Powder samples were prepared by homogenization at 200 °C under nitrogen in the test pan for 10 minutes. Molded samples were prepared by using a 6 mm punch to cut circles from a microtomed 200 μm thick film. Analysis differed from that outlined in the standard. A method was developed equivalent to the Tangent method that was insensitive to misleading or atypical features present in the oxidative exotherm.

Results: The determined OIT values for the tested samples were compared to the given VE wt% as shown in Figure 1. A strong logarithmic correlation was found for the powder (R^2 = 0.9907). The unirradiated consolidated samples appear to follow a similar trend. These data indicate a logarithmic relationship between OIT and VE concentration dependent upon processing conditions. During processing, some of the VE will presumably be used to protect the UHMWPE reducing the amount of VE available for further protection. OIT measurements should only reflect this reduced amount, termed effective VE concentration (EVC). For instance, since irradiation is known to generate many free-radicals, the EVC of the irradiated samples is considerably lower than the original given concentration.

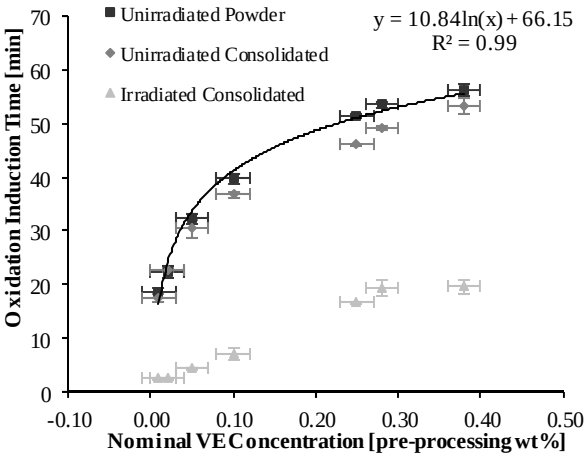

Figure 1: Oxidation induction time as a function of nominal Vitamin E concentration for all samples tested. Error bars are one standard deviation for OIT and ±0.02 for VE concentration.

EVC can be determined by developing a correction for specific processing conditions. Using the minimally processed powder samples as the reference material, an exponential equation was calculated from measured OIT and given VE concentration. A theoretical VE concentration for each sample was then determined using this equation and measured OIT values. Since the theoretical concentration decreased with subsequent processing steps, a scaling factor was determined by dividing the calculated concentration by the given VE wt%. The EVC of each sample was then determined using the average scaling factor for each sample set and given VE concentration. The determined EVC as a function of measured OIT is presented in Figure 2.

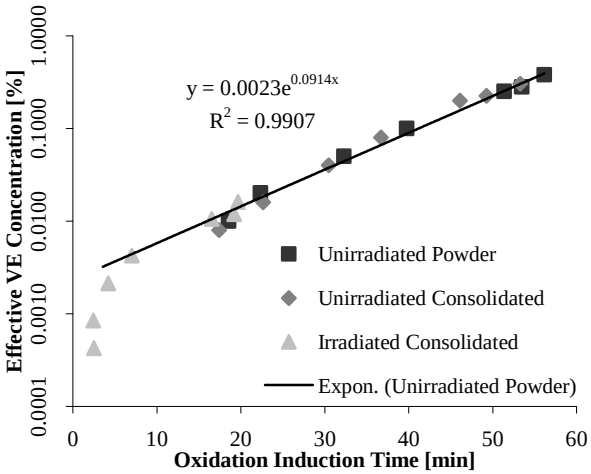

Figure 2: Effective Vitamin E concentration as a function of oxidation induction time. Exponential fit for the unirradiated powder samples used for calculations is shown.

The resulting master curve holds for all samples with OIT values higher than 5 minutes regardless of processing conditions. OIT values of less than 5 minutes are believed to be near the resolution limit of the technique and these rapidly oxidizing samples do not behave in the same manner as the other samples.

Conclusions: The OIT technique presented above provides a novel, sensitive method for determining the VE concentration in UHMWPE components. This method could be used for both QC and R&D purposes to evaluate effective VE levels after different processing conditions. The described master curve implies that, for given processing conditions, OIT can be used to determine the effective VE concentration of a blended and processed UHMWPE component. In addition, this technique is sensitive enough to detect changes in the effective VE concentration after simple compression molding of components. Thus, the technique could be used to investigate the influence of processing on effective VE concentration. We are currently extending this research with a round-robin study to validate intra- and inter-lab repeatability. Suggested future work includes determining the applicability of this method to other antioxidants.

References: [1] E. Oral, et. al., *a-Tocopherol-doped irradiated UHMWPE for high fatigue resistance and low wear*. Biomaterials **25** (2004)

[2] M.L. Morrison. Oxidation Induction Time (OIT) as a Screening Tool for Oxidation Resistance of UHMWPE. 56th Annual Meeting of the Orthopaedic Research Society. 2010.

[3] Y.G. Hsuan, et. al., *Temperature and pressure effects on the oxidation of high-density polyethylene geogrids*. Geotextiles and Geomembranes **23**(1),55-75 (2005)

[4] M. Uhniat, et. al., *Stabilisation of LDPE cross-linked in the presence of peroxides I. Kinetic study of oxidation.* Polymer Degradation and Stability **71**(1),69-74 (2001)

[5] ASTM D 3895-98, "Test Method for Oxidative-Induction Time of Polyolefins by Differential Scanning Calorimetry", ASTM International, West Conshohocken, PA, 1998. DOI: 10.1520/D3895-98, www.astm.org

Acknowledgements: Materials providing by Zimmer, Inc. Funding was provided by Zimmer, Inc.

The influence of antioxidants and crosslinking on the absorption of a model physiological fluid

[1]Berlin, J B; [1]Braithwaite, G J C; [1]Spiegelberg, S; [2]Knight, J; [2]Pletcher, D; [2]Rufner, A.
[1]Cambridge Polymer Group, 56 Roland Street, Suite 310, Boston, MA, [3]Zimmer, Inc., 1800 West Center Street, Warsaw, IN 46580

Statement of Purpose: It is well known that there are a number of chemical species that absorb into UHMWPE implants during in vivo use, such as cholesterol and squalene. It has also been suggested that these absorbable species may play a role in biodegradation of UHMWPE [1-4]. While this has been studied to some extent in first and second generation UHMWPE implants, little is known about the effect of antioxidant stabilizers on the absorption of species into UHMWPE. To further investigate this, we have studied the absorptivity of one representative material, isopropyl myristate (IM), into various UHMWPE formulations. Isopropyl myristate has a similar chemical structure to many biological compounds that might be absorbed into polyethylene, such as triglycerides and fatty acids. Various UHMWPE formulations were soaked at elevated temperatures for up to six weeks in IM and then the bulk concentration of IM determined using FTIR.

Methods: Consolidated GUR 1050 material was gamma sterilized to 25-37 kGy ("UHMWPE"). Highly crosslinked material was e-beam irradiated to 100 kGy and post-melted ("HXPE"). Consolidated GUR 1050 was powder blended with 0.28% vitamin E and gamma sterilized to 28.1-31.4 kGy ("VE-PE"). Consolidated GUR 1050 pucks stabilized with 0.28% Vitamin E by powder blending were e-beam irradiated to 200 kGy ("VE-XLPE"). A portion of the VE-XLPE was reflux extracted for three days in hexanes dried, and reflux extracted for three days in isopropyl alcohol ("Extracted"). Three 3 mm cube samples of each material were analyzed for crosslink density by swell ratio testing according to ASTM F 2214-02 [5]. Additionally, crystallinity was measured in the bulk of the samples prior to aging according to ASTM D 2625 [6]. When possible, samples were packaged in vacuum-sealed bags and stored in the freezer to minimize the possibility of unintended degradation or aging between testing. Five 10-mm cubes of each material were aged in 100% isopropyl myristate solution (Sigma-Aldrich, St. Louis, MO). Care was taken to make sure that all surfaces of the cubes were equally exposed to the aging environment. One cube of each material was removed at 1, 2, 3, 5, and 6 weeks. 200 μm thick slices were microtomed from the center of each cube for FT-IR analysis. The height of the IM peak at 1738 cm^{-1} was ratioed to the polyethylene peak representing C-H overtones at 4322 cm^{-1}. The IM index was reported in the bulk of the material (center 4.8 mm of the cube).

Results: Figure 1 shows the absorption of IM into the bulk of each material at aging time points up to 6 weeks. Figure 2 shows the crosslink density of each material pre-aging. Figure 3 shows the percent crystallinity of each material pre-aging. Absorption over the six week aging period in isopropyl myristate shows some interesting trends. The HXPE materials show a higher initial absorption rate than the PE materials. This trend may be explained by increased free volume in crosslinked and melted materials due to either a greater number of chain ends or a reduced degree of crystallinity. The lower crystallinity of the HXPE supports this theory. Among the HXPE samples, the VE-HXPE has a lower initial absorption rate than either the extracted or the HXPE samples. This may suggest that the presence of Vitamin E reduces the absorption rate of materials from surrounding solutions. The blended materials (VE-PE and extracted) were irradiated at levels intended to yield similar crosslink densities despite the presence of free-radical scavengers, as supported by the SRT swelling data. The extracted sample indicated similar diffusion rates to the HXPE supporting the hypothesis that crosslinking, and its impact on free volume, controls the diffusion rate. However, the VE-HXPE sample, that had a similar crosslink density to the extracted sample, exhibited a markedly reduced diffusion rate, suggesting that the VE actively retards diffusion of species in to the bulk. Although further work is required, this may indicate that the VE acts to physically protect the samples as well as imparting oxidative stability.

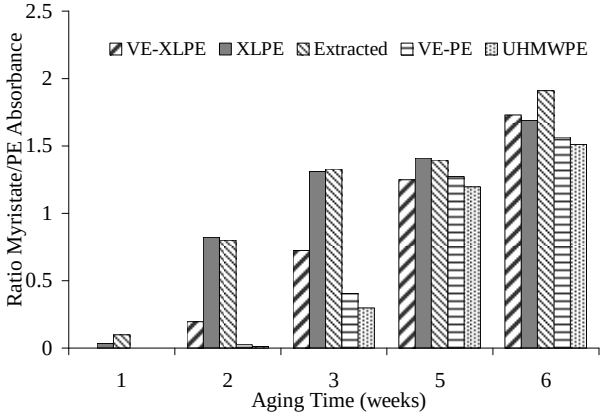

Figure 1. Ratio of IM peak at 1738 cm^{-1} to PE peak at 4322 cm^{-1} as a measure of IM absorption versus aging time.

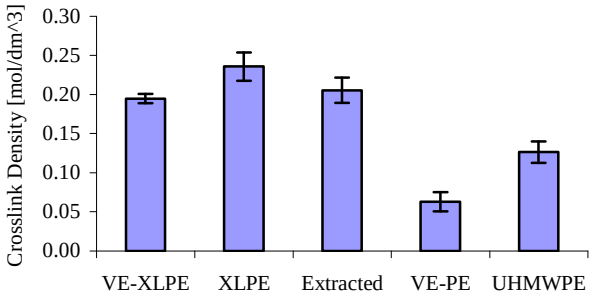

Figure 2. Crosslink densities of the IM aged materials prior to aging.

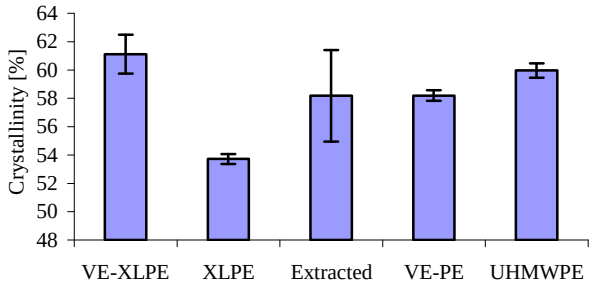

Figure 3. Crystallinity of IM aged materials prior to aging.

Conclusions: In the study presented here, there is evidence that the microstructure of the polyethylene impacts the diffusion rates of a model biological molecule. At short times (over a few weeks), there is a marked difference in diffusion rates with the nominally similar crosslink densities (extracted and HXPE) exhibiting rapid increases. The presence of VE clearly retards diffusion, but equally crosslinking increases diffusion. Although initially counterintuitive, this observation may suggest that antioxidants reduce the available free-volume, thereby influencing the rate of diffusion of biological species. After approximately five weeks the levels of IM appear to be similar, suggesting that it is the initial diffusion of the IM that is impacted, and not the equilibrium concentration at long-times.

References:

[1] L. Costa. Synovial fluid absorption in UHMWPE prosthetic components. 2000. Massachusetts General Hospital. 4-7-2000.
[2] L. Costa, et al. Biomaterials (2001)
[3] J.L. Turner, et al. 49th Annual Meeting of the Orthopaedic Research Society. 2003.
[4] L. Costa, et al. Biomaterials 19,1371-1385 (1998)
[5] ASTM F 2214-02 Standard Test Method for In Situ Determination of Network Parameters of Crosslinked Ultra High Molecular Weight Polyethylene (UHMWPE). 2002.
[6] ASTM F 2625-07 Standard test method for measurement of enthalpy of fusion, percent crystallinity, and melting point of ultra-high-molecular weight polyethylene by means of differential scanning calorimetry. 2007.

Acknowledgements: Materials provided by Zimmer, Inc. Funding was provided by Zimmer, Inc.

Oxidation leads to an increase in wear rate for irradiated/melted UHMWPE

[1]Neils, AL; [1,2]Jun, F; [+,1,2] Oral E; [1,2]Muratoglu OK
[+,1] Harris Orthopaedic Laboratory, Massachusetts General Hospital, Boston, MA; [2]Harvard Medical School 617-726-0657
eoral@partners.org

Introduction

A major problem with UHMWPE implants in total knee and hip replacements is material wear which causes peri-prosthetic osteolysis. Highly crosslinked irradiated and melted (CISM) UHMWPE is used because of its high wear resistance [1, 2]. This material has not shown detectable oxidation in standard accelerated aging tests in contrast to conventional and irradiated/annealed UHMWPEs, which contain detectable residual free radicals [3].

The wear resistance of radiation crosslinked UHMWPE increases with increasing crosslink density, which has been documented [1, 4]. However, the effect of oxidative degradation on the wear rate of highly crosslinked UHMWPE is not known. We created a model where thermal aging caused oxidative degradation in irradiated and melted UHMWPE and measured its wear rate as a function of decreasing crosslink density.

Figure 1. Oxidation profiles of 100 kGy CISM as a function of aging time.

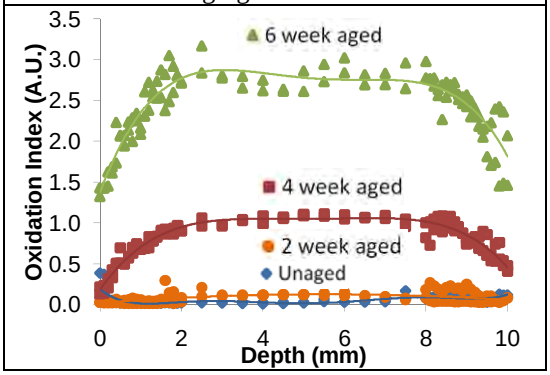

The current clinical outcome of irradiated and melted UHMWPE is excellent [5]. The aging method we are using here may not replicate the oxidation mechanism, if any, that these materials may encounter *in vivo*. The prevalence of any changes in wear and mechanical properties shown here will need to be corroborated by explant analysis in the long-term.

Materials and Methods

Medical grade GUR1050 UHMWPE was e-beam irradiated to 100, 120 and 150 kGy and subsequently melted at 170°C. Cubes (1 × 1 × 1 cm) machined from irradiated and melted UHMWPE blocks were accelerated aged in a pressure vessel in 5 atm O_2 at 70°C for 0, 2, 4,6 or 8 weeks. After aging, 150 µm-thick sections were microtomed from an inner surface of the cubes (n=3 each), boiled in hexane overnight, dried in vacuum for 24 hours and analyzed for carbonyls using Fourier Transform Infrared Spectroscopy (FTIR). Oxidation indices were calculated as a function of depth away from the surface as the ratio of the area under 1715 cm^{-1} normalized by 1895 cm^{-1}. Average surface oxidation indices from the first 1.5 mm and average bulk oxidation indices between 3 and 7 mm are reported.

Surface sections (~2×1×1 mm) and bulk sections (approximately 3x3x3 mm) were swollen in xylene at 130°C for 2 hours. Crosslink density was measured as previously described [6].

Bi-directional pin-on-disc (POD) wear testing [7] of cylindrical pins (9 mm dia., 13 mm length, n=3) were conducted at 2Hz for 1.2 million cycles (MC). Wear rate was measured as the linear regression of gravimetric weight change vs. number of cycles from 0.5 to 1.2 MC.

In accordance with ASTM D638, 3.2 mm thin Type V dog-bone specimens (n=4) were tensile tested at 10 mm/min and elongation at break was measured by laser extensometer. Statistical significance was calculated using a Student t-test to acquire a p-value.

Results and Discussion

Figure 2. Average bulk oxidation levels (3-7 mm) of accelerated aged irradiated and melted UHMWPEs.

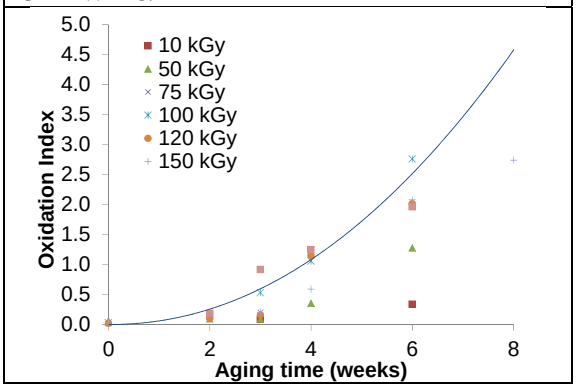

Our goal was to determine the crosslink density dependence of the wear rate of oxidatively degraded highly crosslinked UHMWPE. Standard accelerated aging for 2 weeks (ASTM F2003-02) resulted in very low oxidation in irradiated and melted (CISM) UHMWPE (Figs 1 and 2) but increasing the duration of aging resulted in higher, measureable oxidation (Figs 1 and 2). Therefore, thermal oxidative aging could be used for oxidative degradation of CISM UHMWPE.

While wear rate decreases as a function of increasing crosslink density for unaged UHMWPE (Fig 3), the relationship between crosslink density and wear rate for oxidized highly crosslinked UHMWPE was not known. Wear increased with decreasing crosslink density as a result of oxidation (Fig 3). We showed for the first time that wear behavior of oxidized highly crosslinked UHMWPE is different from its unaged counterpart. On the other hand, the wear rate did not substantially change until the crosslink density fell to about 30% of its original value (~0.1 mol/dm^3), suggesting a large tolerance for oxidation in the wear behavior. Below a crosslink density of 0.1 mol/dm^3, the wear rate increased (p=0.04)

to levels that are higher than those measured for uncrosslinked UHMWPE (Fig 3). These results suggested that the crosslink structure was changed by oxidative degradation. Chain scissioning accompanying the formation of oxidation products may form branched macromolecules and may not cause disintegration of the network at the crosslinks.

Figure 3. Wear rate of oxidized CISM UHMWPE.

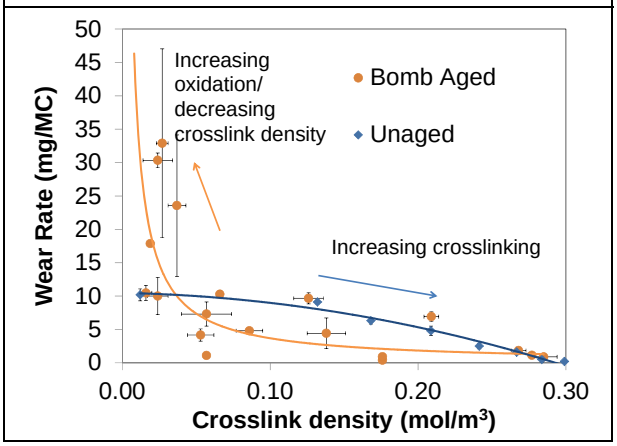

Residual free radicals are reduced to undetectable levels in CISM UHMWPE and hence it is thought to be oxidatively stable *in vivo*. The prevalence of oxidative degradation in CISM UHMWPE *in vivo* is not known; therefore, both the rate of oxidation and changes in wear, if any, will need to be determined by monitoring explanted components. In our study, the increase in wear rate was gradual below an oxidation index of ~0.8, above which the wear rate increased significantly (Fig 4, p=0.005). It is possible that at the lower body temperature and low oxygen concentration, the oxidation level to cause significant changes in wear will not be encountered clinically.

Figure 4. Oxidation of CISM UHMWPE decreases crosslink density and increases wear

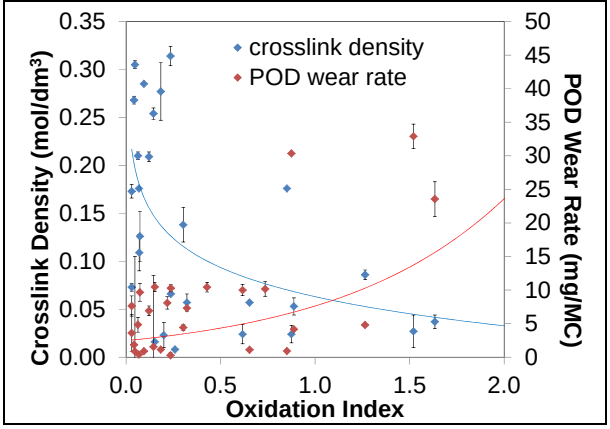

Historically, conventional gamma sterilized UHMWPE showed oxidative degradation and caused osteolysis because of its high wear rate. Highly crosslinked irradiated and melted UHMWPE was designed for increased wear resistance to prevent osteolysis. It is also believed that its mechanical properties will not decrease further due to its oxidative stability. In this study, the ultimate tensile strength of oxidized cross-linked UHMWPE showed an average of 31% loss due to oxidation (Fig 5a). The toughness was more drastically reduced (Fig 5b). These results suggest that oxidation, if present, can have significant effects to the wear and mechanical properties of highly cross-linked UHMWPE.

Conclusions

We showed that oxidative degradation increased the wear rate of irradiated/melted UHMWPE. The wear rate tolerated oxidation well and only increased gradually. In contrast, mechanical strength was more sensitive to oxidation. Currently, the clinical performance of irradiated and melted UHMWPEs is excellent and there are no reports of high in vivo oxidation. The clinical relevance of the results presented here is not known.

Figure 5. Oxidatively degraded CISM UHMWPE has lower tensile mechanical strength (a) and toughness (b).

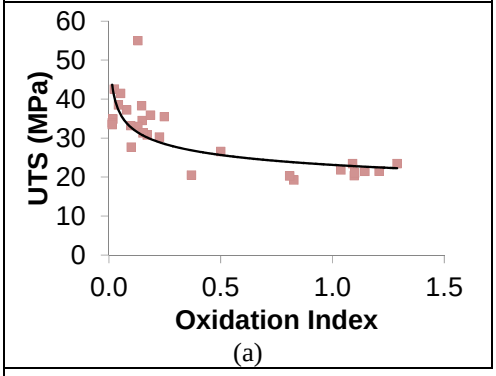

(a)

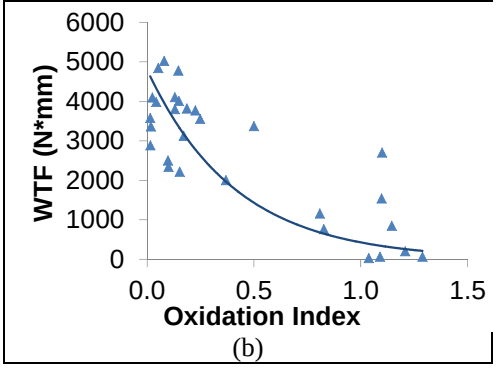

(b)

Acknowledgement

This study was funded by laboratory funds.

References

[1] Muratoglu et al. Biomaterials 20:1463-1470 1999; [2] Digas et al. Acta Orthop 78:746-754 2007; [3]Muratoglu et al. CORR 417:253-262 2003; [4] McKellop JOR 17:157-167 1999 ;[5] Digas et al. Acta Orthop 78:746-754 2007; [6] Oral et al. Biomaterials 31:7051-7060 2010; [7] Bragdon JOA 16:658-665 2001; [8] Oral et al. Biomaterials 27:917-925 2006.

Oxidation of Wear Tested and Shelf-aged UHMWPE Acetabular Liners

Askim F. Senyurt, Stephanie Crews, Venkat Narayan
DePuy Orthopaedics, Warsaw IN

Purpose: Radiation crosslinked and remelted UHMWPE has been shown to be oxidatively stable due to the elimination of the free-radicals during the remelting process. However, recent studies[1,2] suggest that shelf-aged UHMWPE explants and wear tested UHMWPE implants might exhibit low levels of oxidation due to the lipid absorption and cyclic loading conditions. The present study was undertaken to analyze the oxidation levels of wear tested UHMWPE acetabular liners upon shelf-storage for 5 to 7 years. The effect of bovine serum concentration used during wear testing, the cyclic loading conditions, and shelf-storage time after wear testing were studied using FTIR spectroscopy and DSC.

Methods: Loading and soak conditions for the Marathon™ (GUR 1050 crosslinked by gamma irradiation at 50 kGy and subsequently melted) and Enduron™ (GUR 1020, non-crosslinked) acetabular liners are given in Table 1.

				B	C
			A	Soak Cntrl in Serum	
Date	Material	Serum	Wear Tested	Loaded	No Load
11/4/2002	Marathon	0-25-0 %	M23-02		M23-12
	Marathon	90-0-25 %	M23-05		M23-01
2/12/2003	Marathon	90%	M09-07	M09-08	
	Enduron	90%	En9-01	En9-03	
1/9/2004	Marathon	90%	M24-02		M24-04
	Enduron	90%	En24-1		En24-6

Table 1: The acetabular liners (DePuy Orthopaedics, Warsaw, IN), and wear test conditions.

Bovine serum concentration of M23 liners was changed between intervals. The serum concentration of M23-05/01 was 90% between 0 to 3.5 M cycles, saline solution (0% serum) between 3.5 to 5 M cycles, and then 25% from 5 M to 6 M cycles. Once the wear test was completed, all of the liners were cleaned and stored in deionized water until being analyzed in this study. The % crystallinity of the liners was determined using a TA Instruments DSC Q1000 per ASTM F2625-07. 400 µm films were microtomed and three 5 mm diameter samples were punched out. DSC was run at a scan rate of 10° C/min from 30 to 180° C under a nitrogen environment. Percent crystallinity measurements were taken from the load bearing-articulating and rim sections of the acetabular liners and reported with ± 1 % standard deviation. The FTIR evaluation was performed on samples in accordance with ASTM F2102-06 by using a Thermo Fisher Scientific spectrometer with a Nicolet iN10 MX microscope. 200 µm cross-sections were taken from the articulation/load bearing and rim regions of each liner and placed on the motorized stage of the FTIR. The stage was then advanced in increments of 0.5 mm starting at the ID surface. Spectra were obtained at each depth. The ASTM oxidation index (OI) was determined at each depth and maximum OI measured for each samples is reported here.

Results: The lipid-induced oxidation of acetabular liners was investigated by analyzing the liners (Column **C**, Table 1) that were only soaked in serum. The results are summarized in Table 2.

Sample	M23-12	M23-01	M24-04	En24-6
% Cryst.	45	47	58	61
ASTM OI (max)	0.063	0.047	> 2	> 2

Table 2. Percent crystallinity and ASTM OI (max) results.

Marathon (M24-04) and Enduron (En24-6) liners that were soaked in 90 % bovine serum exhibited delamination upon microtoming and high OI with increased crystallinity after 5 years of shelf-storage. M23-12 and M23-01did not show any sign of oxidation even though they were stored for 7 years. In order to determine the effect of the cyclic loading conditions on the oxidative stability of the liners, the crystallinity and ASTM OI (max) of M09-08/En9-03(Column **B**, Table 1) were compared to M24-04/En24-6 (Table 2) and results are given in Table 3.

Sample	M09-08		En9-03	
Location	Articulating	Rim	Articulating	Rim
% Cryst.	57	57	53	53
ASTM OI (max)	> 2	> 2	0.159	0.144

Table 3. Percent crystallinity and ASTM OI (max) results.

Each of these liners exhibited white banding upon microtoming along with increased crystallinity and OI. M09-08 and En9-03 liners (6 yrs) had subsurface oxidation peaks on both the articulating and rim regions. The wear tested liners (Column **A**, Table 1) were studied for the cumulative effect of lipids exposure and cyclic loading conditions. The results (Table 4) show that M23 liners maintained their oxidative stability after wear testing in varying concentration of bovine serum and following 7 years of shelf-storage.

Sample	M23-02		M23-05	
Location	Articulating	Rim	Articulating	Rim
% Cryst.	48	48	51	49
ASTM OI (max)	0.055	0.023	0.238*	0.066

Table 4. Crystallinity and ASTM OI (max) results of liners.*Surface peak reduced to 0.031 after hexane extraction.

However, M09-07/En9-01 and M24-02/En24-1 liners that were wear-tested only in 90 % bovine serum and shelf-aged 6 and 5 years after testing exhibited high oxidation (% crystallinity: 57; ASTM OI: >2).

Conclusions: This study demonstrates that exposure to only 90% bovine serum followed by multiple years of shelf ageing has a deleterious effect on the oxidative stability of UHMWPE hip bearings regardless of cross-linking and loading conditions. The difference in shelf-storage time (5 to 7 years) did not show any effect on the oxidative stability of these liners. Conventional (non-crosslinked) UHMWPE liners, that are oxidatively stable during long-term in-vivo use also show comparable oxidation upon shelf storage to irradiated, remelted UHMWPE. Therefore this study shows the bovine serum induced oxidation of UHMWPE has no clinical relevance.

References:

1) Muratoglu et al., ORS 2011, Paper #374
2) Rowell, et al., ORS 2010, Paper # 358

Structural differences of UHMWPE induced by high dose gamma irradiation

Kerstin von der Ehe, Daniela Robertson, Dietmar Wolff, Martin Böhning
BAM Federal Institute for Materials Research and Testing, Unter den Eichen 87, 12205 Berlin, Germany

Introduction

UHMWPE is a well-known and often used material in the field of medical technology for joint replacements. Furthermore it is a good choice as material for neutron shielding in casks for storage and transport of radioactive materials. This suitability can be traced back to the fact that UHMWPE possesses an extreme high hydrogen content. In the medical field as well as during neutron radiation shielding application, UHMWPE is exposed to gamma irradiation: in the first case requested as sterilization process and for surface-crosslinking and in the second case existing as a side effect of inserting the radioactive material in the cask. For sterilization of UHMWPE the dose normally not exceeds 25 kGy, whereas for shielding application in the cask the material is exposed for instance to doses up to 600 kGy. Given that UHMWPE has to withstand any type of degradation affecting safety relevant aspects to be applicable for long term radiation shielding purposes for instance over a period of 40 years, the durability of the material is of special interest. The scope of our investigation comprises an estimation of the radiation and thermal impact on the molecular and supra molecular structure of UHMWPE used for neutron shielding cask components. A further point which is worth to explore is to what extent these changes are detectable by conventional analysis methods.

Materials and Methods

The UHMWPE (GUR 4120; Ticona) used in this study was provided by Quadrant, Vreden, Germany. The samples were irradiated with gamma up to a dose of about 600 kGy at RT under inert conditions. Afterwards the samples were prepared for every measurements and a comparison of the obtained results of the untreated and the irradiated samples was carried out. For analysis of the samples conventional methods were applied. Thermo-analytical measurements were performed like for example Differential Scanning Calorimetry (DSC), Oxidation Induction Time (OIT), Thermomechanical Analysis (TMA), and Thermo Gravimetry (TG) in order to obtain information about melting temperature, degree of crystallinity, thermal expansion coefficient, and thermal degradation processes. Furthermore FT-IR spectra were taken to investigate changes of the chemical structure and gas sorption measurements were made for determining the diffusion coefficient, and the solubility coefficient of carbon dioxide, oxygen, and nitrogen addressing properties of the amorphous regions of the material. The density of all samples was determined via Density Gradient Column (DGC) containing a solvent mixture of diethylenglycol and isopropanol.

Results and Discussion

The irradiated samples were characterized and compared to the untreated material. The Differential Scanning Calorimetry was performed with a heating rate of 10K/min in a temperature region from -50 up to +160 °C. The melting temperature is shifted to higher values induced by irradiation, subsequent recrystallization led to a shift to lower values (figure 1). Likewise the degree of crystallinity shows the same dependence on the irradiation: it increased by irradiation and through thermal treatment (recrystallization) it shows lower values. A suggested reason for the increase of the crystallinity is that the radiation induced chain scission, followed by increased crystallization due to higher molecular mobility of the released new free chain segments, is the predominant effect. The decrease after recrystallization and remelting could be explained by constrained chain mobility through the existence of radiation induced crosslinks.

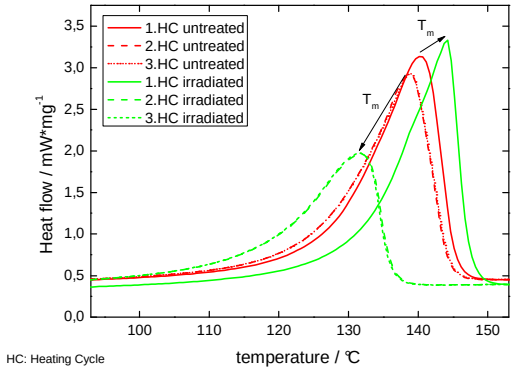

Figure 1. DSC curves of untreated/irradiated UHMWPE

One possibility to determine the existence of crosslinks and insertion of oxygen in the structure of UHMWPE is the use of FT-IR spectroscopy. The spectra were measured in transmission mode. In case of the irradiation impact on the chemical structure the absorption bands at 965 cm^{-1} (trans-vinylene group) and at 1700 cm^{-1} (carbonyl group) are of special interest. The former might be correlated to crosslinking and the latter is an indication for sample oxidation.

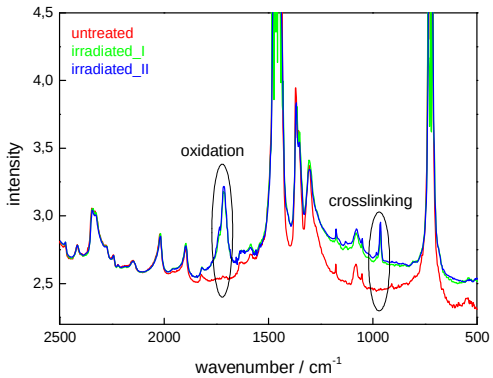

Figure 2. FT-IR spectra of untreated/irradiated UHMWPE

The obtained spectra (figure 2) of the untreated and irradiated material show large similarities except for the formation of two new absorption bands in the spectra of the irradiated material. They indicate that oxidation as well as crosslinking of the samples occurred in consequence of irradiation.
In order to detect changes in the amorphous regions of the semicrystalline polymer gas sorption measurements were performed at 35 °C using oxygen, nitrogen, and carbon dioxide respectively. The concentration of every particular gas in relation to the amorphous phase in both, untreated and irradiated material, is shown in figure 3. The gas uptake decreases for the irradiated material and for the solubility of the different gases the following order is found: nitrogen<oxygen<carbon dioxide. Also diffusion coefficients can be determined and reflect changes in structure and mobility of the amorphous phase similar to those observed for the gas uptake, i.e. the respective solubility coefficients.

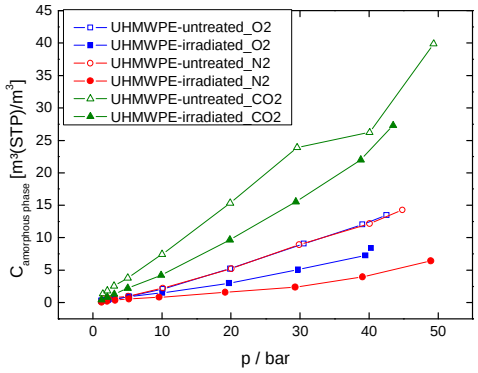

Figure 3. Gas concentration in untreated/irradiated UHMWPE

For an analytical determination of the thermal expansion behavior of the irradiated UHMWPE compared to that of the untreated material, TMA measurements were performed. The linear expansion coefficient was graphically determined and the obtained values for the coefficient were in the expected range of 10^{-4}. However irradiation caused lower values compared to that of the untreated sample. In addition the degradation behavior was determined by TG under inert atmosphere and synthetic air. In an inert atmosphere, UHMWPE showed a single-step degradation. Compared to that, the measurements under synthetic air showed that an insertion of oxygen took place first, afterwards the degradation started. This time a two-step process was observed: first the oxygenated structures degraded and one fourth of the original mass was lost. However the main loss of weight could be observed at the second step of degradation at slightly lower peak temperatures as for the inert atmosphere.

Conclusions

With the applied conventional analytical techniques it is possible to detect structural changes of UHMWPE induced by γ-irradiation. With regard to the special application as shielding material in casks for storage and transport of radioactive materials the impact of irradiation lead to changes of material properties. A consolidated view indicates that the detected changes of the irradiated UHMWPE are not safety relevant for long term radiation shielding purposes over a period of 40 years.

Anisotropy of Ram Extruded NIST 1050 Reference UHMWPE

Kluk HL, Reinitz SR, Gray LT, Van Citters DW
Thayer School of Engineering at Dartmouth College, Hanover, N.H.

INTRODUCTION:

UHMWPE reference material, NIST RM 8456 (GUR 1050), is produced through the process of ram extrusion. Previous research has suggested that the mechanical properties of ram extruded polyethylene vary as a function of the distance from the center axis of the extruded bar [1]. However, these previous experiments have relied on traditional dog-bone tensile tests to quantify various mechanical parameters in a uniaxial state of stress. Due to size limitations, these specimens are generally limited to a plane oriented parallel to the centerline of the extruded rod. As such, material properties can only be measured in two directions.

The small punch test has allowed for greater precision and flexibility in characterizing material properties of the polyethylene in an equibiaxial state of stress [2]. The objectives of the current study are to investigate the anisotropy of ram extruded 1050 UHMWPE and characterize any differences between samples oriented parallel and perpendicular to the centerline of the extruded rod.

Methods: Small punch tests were performed according to ASTM F2183 on NIST RM 8456 ram extruded bar stock (Gaithersburg, MD). Samples were processed by producing thin (0.5mm thick) sections on a microtome and using a punch to produce disks 6.4 mm in diameter. *Parallel Edge* samples were taken within 1cm of the circumferential surface with the sample face normal to the radius of the rod. *Parallel Bulk* samples have similar orientation but are greater than 2cm from the surface. *Perpendicular Edge* samples are taken near the circumference with the sample face normal to the rod axis and *Perpendicular Bulk* samples have the same orientation but are taken from the bulk material. Data for an initial peak load, ultimate load, and ultimate displacement were also recorded.

Results: The results of the small punch tests indicate a statistically significant difference between samples parallel to the axis of extrusion and samples perpendicular to the axis of extrusion in work to failure, ultimate load, and peak load. Table 1 shows the values for toughness and the standard deviations.

The full factorial design of the study allows comparison of the toughness (J), peak load (N), ultimate load (N), and ultimate extension (mm). The results show a significant difference ($p<0.05$) in the toughness, peak load, and ultimate load of samples oriented perpendicular to the direction of extrusion as compared to samples oriented parallel to the direction of extrusion. The parallel samples exhibit a greater toughness and a higher ultimate load and peak load than the perpendicular samples. The location of the sample (edge vs. bulk) showed no statistical difference ($p>>0.05$). Figure 1 displays a main effects plot for mean work to failure (toughness).

The difference in means of work to failure between parallel and perpendicular samples is 0.024 J. Thus, the material in a perpendicular orientation exhibits a 7.82% +/- 0.082 lower toughness value than that in the parallel orientation.

NIST RM 8456: GUR 1050 UHMWPE			
Sample direction/location	**n**	**Toughness (J)**	
		Mean	**St. Dev**
Perpendicular / Bulk	10	0.285	0.019
Parallel / Bulk	10	0.304	0.021
Parallel / Edge	10	0.307	0.015
Perpendicular / Edge	10	0.278	0.017

Table 1. Properties for different locations and directions

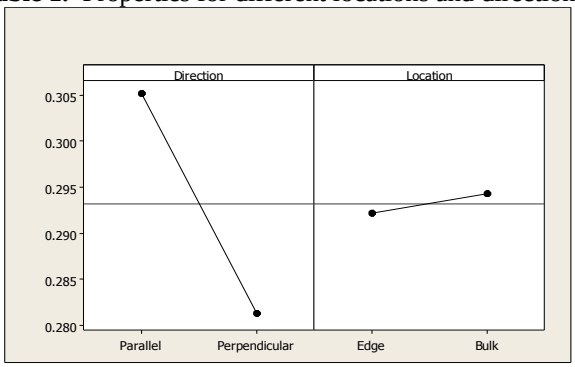

Figure 1. Main Effects Plot for Work to Failure

Discussion and Conclusions: **T**he mechanical behavior of polyethylene is not commonly characterized in the orientation normal to the axis of extrusion. However, the small punch test allows for a more detailed and acute description of the anisotropy of the material. During ram extrusion, mechanical deformation can induce molecular alignment. This molecular alignment is hypothesized to contribute to the anisotropy of the material.

The observed variation in mechanical properties of ram extruded UHMWPE could directly affect the in-vivo performance of polyethylene. For instance, locking mechanisms and contact regions are at greater risk of failure due to stress concentrations and non-conformities. Given the variation in material properties identified in the present work, components should be designed with consideration for the lowest ductility, strength or toughness values in the bulk material.

References: [1] Kurtz, Steven M. (2009). UHMWPE Biomaterials Handbook - Ultra-High Molecular Weight Polyethylene in Total Joint Replacement and Medical Devices (2nd Edition). Elsevier.

[2] Kurtz, Steven M. Radiation and chemical crosslinking promote strain hardening behavior and molecular alignment in ultra-high molecular weight polyethylene during multi-axial loading conditions. Biomaterials 20 (1999) 1449-1462.

In Vivo Crosslink Density Changes in Highly Crosslinked UHMWPE Bearings

Reinitz, S D; Currier, B H; Van Citters, D W
Dartmouth College, Hanover, NH

INTRODUCTION

Highly crosslinked and remelted ultra high molecular weight polyethylene bearings have been shown to significantly reduce wear rates while also demonstrating oxidative stability during shelf aging. However, measurable subsurface oxidation has been reported in a number of highly crosslinked polyethylene bearings.[1]

Since the accepted oxidation mechanism depends upon the presence of free radicals, it was expected that remelting would result in oxidative stability *in vivo* as it did in shelf aging. The presence of oxidation in these materials in the absence of free radicals suggests an alternative mechanism of oxidation taking place *in vivo*.

Because the purpose of irradiating and remelting the polyethylene is to increase crosslinking, thereby increasing wear performance, it is of interest to know how *in vivo* oxidation is impacting the crosslink density. Based on previous oxidation models one would expect a decrease in crosslink density. The purpose of the present study is to investigate whether *in vivo* oxidation is accompanied by decreased crosslink density. We hypothesize that *in vivo* oxidation will not be accompanied by a decrease in crosslink density.

MATERIALS AND METHODS

An IRB approved retrieval database was queried for highly crosslinked UHMWPE samples showing measurable ketone oxidation and having been on the shelf less than three months post explantation (Table 1). A set of never implanted control specimens was selected. Oxidation analysis was performed using Fourier transform infrared spectroscopy following hexane extraction. From each specimen, five cubes were cut approximately 1.5-2.5 mm per side (5-15 mg) using a razor blade and massed to 10 µg precision using an analytical balance (Mettler-Toledo Inc., Columbus, OH). All cubes were immersed in graduated cylinders containing 20 mL of mixed xylenes and placed in a silicone oil bath heated to 130ºC for 2 hours (Haake, now Thermo Scientific, Waltham, MA). Samples were removed to tared vials and massed while wet. Using the dry and wet masses the crosslink density for each sample was calculated according to ASTM F 2214. Retrieved specimens were tested against their matched controls using a Student's t-Test

RESULTS

Peak ketone oxidation levels are found in the last column of Table 1. Results from gel swell measurements are presented in Table 2. None of the tibial insert materials showed significant ($p<0.05$) differences from their never implanted controls. Unlike the tibial inserts, all acetabular components showed significant increases in crosslink density compared to their controls.

DISCUSSION

All of the materials evaluated in this study are highly crosslinked UHMWPE materials which have been shown to be oxidatively stable during shelf aging. However, there were measurable subsurface peaks found in most of the materials even after hexane extraction. Oxidation was present in both tibial inserts and acetabular components independent of the initial radiation dose received. Since most of these specimens are remelted materials which contain no measurable free radicals, an alternative mechanism of oxidation must be taking place independent of free radical concentration.

Component	Manufacturer	Material	Duration (months)	Max Ketone Oxidation
Knee	Zimmer (Warsaw, IN)	Prolong	42.7	0.682
Knee	DePuy (Warsaw, IN)	XLK	25.9	0.020
Knee	Stryker (Mahwah, NJ)	X3	30.7	0.297
Hip	Zimmer (Warsaw, IN)	Longevity	29.8	0.247
Hip	Zimmer (Warsaw, IN)	Longevity	112.3	0.177
Hip	Zimmer (Warsaw, IN)	Longevity	117	0.228
Hip	Smith and Nephew (Memphis, TN)	XLPE	3.7	0.003
Hip	DePuy (Warsaw, IN)	Marathon	64.2	0.112

Table 1: Summary of the eight samples used in the study, along with measured peak ketone oxidation following extraction. The samples include six different materials from four manufacturers with a range of *in vivo* durations.

Sample	Sample Crosslink Density (mol/dm^3)	Control Crosslink Density (mol/dm^3)	Percent Change
Prolong	0.1940 ± 0.0131	0.1832 ± 0.0030	5.9
XLK	0.1830 ± 0.0080	0.1896 ± 0.0037	-3.5
X3	0.2260 ± 0.0241	0.2601 ± 0.0141	-13.1
Longevity 1	0.3455 ± 0.0049	0.2780 ± 0.0141	24.3 *
Longevity 2	0.3680 ± 0.0269	0.2780 ± 0.0141	32.4 *
Longevity 3	0.3830 ± 0.0071	0.2780 ± 0.0141	37.8 *
XLPE	0.3861 ± 0.0511	0.2780 ± 0.0141	38.9 *
Marathon	0.2939 ± 0.0348	0.1257 ± 0.0642	133.7 *

Table 2: Crosslink density measurements for retrieved devices and their control materials, and percent change. * *Denotes significance ($p<0.05$).*

No samples showed statistically significant ($p<0.05$) decreases in crosslink density after time *in vivo* despite measurable oxidation in most of these samples.

Unexpectedly, all of the acetabular components showed statistically significant increases in crosslink density versus their paired never implanted control specimens. This does not appear to be related to *in vivo* oxidation, since even sample A4, which showed near zero oxidation, showed a nearly forty percent increase in crosslink density while sample T1, which had the highest oxidation value of any sample, did not show any significant change. This indicates a second *in vivo* chemical change taking place specific to acetabular components.

Further research into the mechanism of oxidation is merited.

[1] Currier BH, et al. "In Vivo Oxidation in Remelted Highly Cross-linked Retrievals", J Bone Joint Surg Am. 2010;92:2409-18.

Resistance of Crosslinked, Vitamin E Blended UHMWPE to Oxidation

J Knight, A Rufner, D Pletcher
Zimmer Inc., 1800 W Center St, Warsaw, IN, USA
john.knight@zimmer.com

Introduction

Crosslinking of ultra-high molecular weight polyethylene (UHMWPE) improves the wear resistance of the UHMWPE, but the post-irradiation melt annealing typically employed for oxidative stability can cause a reduction in crystallinity, fatigue resistance, and mechanical properties of the finished material. The addition of Vitamin E to a crosslinked UHMWPE prior to irradiation provides oxidative stability in the material without the need for melt annealing, therefore preserving these properties. The oxidative resistance of Vitamin E stabilized UHMWPE under a cyclic load is of interest due to the cyclic loads that are applied to bearing materials in orthopaedic applications. The goal of this study was to investigate a new method of accelerated aging UHMWPE under a cyclic load, and to compare the relative oxidation resistances of Vitamin E blended UHMWPE and non-Vitamin E blended UHMWPE.

Methods & Materials

Vitamin E (alpha-tocopherol, DSM, Geleen, Netherlands) was blended with GUR 1050 UHMWPE resin flake (Ticona, Oberhausen, Germany) to a Vitamin E concentration of 0.20% (w/w). The blended resin was then compression molded into 6.4cm diameter x 3.8cm thick disk forms. The forms were then preheated for 12 hours at temperatures below the melt, and subjected to a 10 MeV electron beam irradiation cross-linking process (Iotron Industries, Port Coquitlam, Canada) at 104 – 110 kGy. The irradiated pucks were then machined into modified constant stress specimens (Figure 1) for testing. The specimens had a thickness of 6.5mm, and were designed such that the edges of the puck formed the edges of the specimen as it was being machined. Surface sterilization methods (e.g. gas plasma, ethylene oxide) are typically used on highly crosslinked materials; since surface sterilization would not affect fatigue properties, the Vitamin E containing molded forms in this study were not sterilized prior to testing.

Figure 1. Constant stress specimen

For comparison, virgin GUR1050 UHMWPE flake was also molded into 6.4cm diameter x 3.8cm thick disks. The 1050 disks were machined into CSS specimens without further processing, but were then sealed inside a foil pouch in a nitrogen atmosphere and sterilized with a 37 kGy gamma dose (Sterigenics, Westerville, OH). The CSS specimens were then fixtured into a custom-built test apparatus based on the apparatus description in reference [1], in which the large end of the specimen shown in Figure 1 was held stationary, and the small end of the specimen was flexed upwards and downwards, 3mm from the neutral position in each direction, at a frequency of 0.5 cycles per second while enclosed in a chamber maintaining a constant air temperature of 80°C. In addition, two sterilized GUR1050 specimens were placed inside the oven during testing, but were not flexed. These two specimens served as controls. Each specimen was cycled for five weeks, or until visual inspection of the specimens revealed cracks present in the neck region. If cracks were observed, the test was stopped at that point. Following testing, each specimen was removed from the test apparatus, sectioned in the neck region, and a film was cut from the neck region using a microtome. If present, the Vitamin E was extracted from the films by immersion in boiling hexane prior to analysis. The film was then analyzed using FTIR to determine oxidation index (OI), found by determining the ratio of the area under the FTIR peak from 1765 – 1680 cm^{-1} to the area under the peak from 1392 – 1330 cm^{-1}.

Results

Cracks were noted in the sterilized GUR1050 specimens on day 35 of testing when the test was stopped. Neither of the control specimens had any cracks visible. The Vitamin E UHMWPE specimens did not have any visible cracks present on day 35 of their testing. Results of the OI testing are shown in Figure 2.

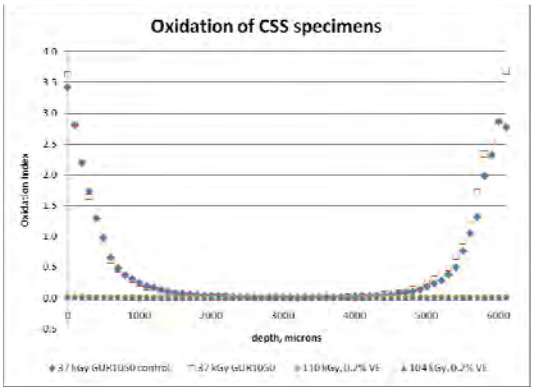

Figure 2. OI results of CSS specimens

Discussion

The results shown in Figure 2 demonstrate that the 37 kGy sterilized GUR1050 UHMWPE had high levels of oxidation, even to depths exceeding 1mm from the surface of the specimens. However, no difference was found between the test specimens and the unloaded controls with the sterilized GUR1050. In comparison, the Vitamin E blended crosslinked UHMWPE has high oxidation resistance, showing no significant oxidation after 5 weeks of aging under a cyclic load. These results indicate that Vitamin E UHMWPE maintains its oxidation resistance even when the Vitamin E is present during irradiation. Further testing will be required to determine the proper balance of wear resistance, fatigue resistance, and mechanical properties in a commercialized product, but this work demonstrates that Vitamin E blended crosslinked UHMWPE material can be obtained with great improvements in oxidative resistance over currently successfully used materials, which may allow for additional design freedom in new devices.

References

[1] Oral, E., and Muratoglu, O. The UHMWPE Handbook, 2009, chapter 15.

Resistance of Crosslinked, Vitamin E Blended UHMWPE to Fatigue Crack Propagation

J Knight, A Rufner, D Pletcher, H Brinkerhuff
Zimmer Inc., 1800 W Center St, Warsaw, IN, USA
john.knight@zimmer.com

Introduction

Crosslinking of ultra-high molecular weight polyethylene (UHMWPE) improves the wear resistance of the UHMWPE, but the post-irradiation melt annealing typically employed to quench residual free radicals can cause a reduction in crystallinity of the UHMWPE with a subsequent reduction in fatigue crack propagation (FCP) resistance. The FCP resistance of UHMWPE materials is of interest due to the cyclic loads that are applied to bearing materials in orthopaedic applications. A crack initiated in the material, for example by manufacturing process, damage, or fatigue, will tend to propagate until reaching a critical length at which point fracture of the component will rapidly occur. The addition of Vitamin E to a crosslinked UHMWPE prior to irradiation provides oxidative stability without the need for melt annealing, therefore preserving the crystallinity and FCP resistance of the material. The goal of this study was to evaluate the fatigue crakc propagation resistance of highly crosslinked Vitamin E-containing UHMWPE that has been specifically formulated for hip bearing applications.

Methods & Materials

Vitamin E (alpha-tocopherol, DSM, Geleen, Netherlands) was blended with GUR 1020 UHMWPE resin flake (Ticona, Oberhausen, Germany) to a Vitamin E concentration of 0.14% (w/w). The blended resin was then compression molded into 6.4cm diameter x 3.8cm thick disk forms. The forms were then preheated for 12 hours at a temperature below the melt, and subjected to a 10 MeV electron beam irradiation cross-linking process (Iotron Industries, Port Coquitlam, Canada) at 185 kGy. The irradiated forms were then machined into ASTM E647-08 compact tension (CT) specimens (Figure 1) for testing. The CT specimens had a width of 32mm, a thickness of 8mm, and a_n of 6.4mm. The forms were also machined into pin-on-disk wear pins. Surface sterilization methods (e.g. gas plasma, ethylene oxide) are typically used on highly crosslinked materials; since surface sterilization would not affect fatigue properties, the molded forms in this study were not sterilized prior to testing.

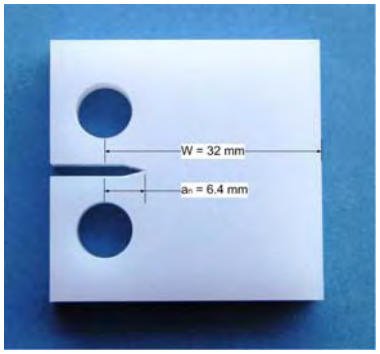

Figure 1. ASTM E647-08 fatigue crack specimen

The CT specimens were sent to Exova OCM Test Laboratories (Anaheim, CA) for testing per ASTM E647-08. A starter crack of length 3mm was machined into the notch prior to testing. Specimens were tested with an R-ratio of 0.1, a sinusoidal waveform, and a frequency of 3Hz. All testing was performed at room temperature. Fatigue crack growth was measured periodically during the testing with an optical microscope. The number of cycles (n) for each growth period was recorded, and specimens were cycled until failure occurred. The cyclic stress intensity (ΔK) and the average crack growth rate (da/dn) for each specimen were plotted. Linear regression analysis was performed on each curve and used to determine the exponent (m) and coefficient (C) of the Paris equation, $da/dn = C(\Delta K)^m$, for each specimen. Wear pins were tested on an OrthoPOD pin-on-disk wear test machine (AMTI, Watertown, MA) for 1 million cycles at 3.5 MPa contact stress in undiluted bovine calf serum at 37°C.

Results

Fatigue crack propagation and pin-on-disk wear properties of the crosslinked, Vitamin E blended UHMWPE are summarized in Table 1. For comparison, the results for 100 kGy electron beam irradiated, remelted UHMWPE (Zimmer Inc., Warsaw, IN) are also provided.

Table 1. Fatigue Properties of Vitamin E UHMWPE

	185 kGy, 0.14% VE	100 kGy remelted
Exponent (m)	7.42 ± 0.39	6.89 ± 0.48
Coefficient (C) [$x10^{-7}$]	0.17 ± 0.03	1.35 ± 0.42
$\Delta K_{inception}$, Mpa-$m^{0.5}$	1.73 ± 0.03	1.29 ± 0.01
OrthoPOD wear, mg/MC	0.16 ± 0.06	0.33 ± 0.31

Discussion

The results shown in Table 1 demonstrate that the Vitamin E blended, crosslinked UHMWPE had higher FCP resistance than the 100 kGy remelted UHMWPE, showing a 33% improvement in FCP resistance, as measured by the cyclic stress intensity required for crack inception ($\Delta K_{inception}$). Table 1 also shows that the Vitamin E UHMWPE had a higher exponent for the Paris equation, which may indicate a faster propagation of the crack once initiated. However, as noted by Gencur [1], the number of cycles endured by a material after crack inception is a small percentage of component lifetime, so the better indication of fatigue performance may be the increased resistance to crack initiation, for which the Vitamin E UHMWPE was superior. Note that although the Vitamin E UHMWPE had higher crack propagation resistance than the 100 kGy remelted UHMWPE, the presence of Vitamin E in the UHMWPE during irradiation may inhibit the crosslinking reaction [2]; the resulting lower crosslink density would then result in an apparent improvement in fatigue crack propagation resistance but a reduction in wear resistance. A higher dose was used in the Vitamin E UHMWPE to counter this inhibiting effect, resulting in a material that had improved fatigue resistance without a reduction in wear. Further testing will be required to determine the proper balance of wear resistance, fatigue resistance, and mechanical properties in a commercialized product, but this work demonstrates that Vitamin E blended crosslinked UHMWPE material can be obtained with fatigue improvement over currently successful materials, which may allow for additional design freedom in new devices.

References

[1] Gencur et al, Biomaterials 27 (2006) 1550-1557
[2] Furmanski et al ORS paper #0329, 2007

Chronic Impingement of Lumbar Disc Arthroplasty Increases the Functional Biologic Activity of Polyethylene Wear Debris

Ryan M. Baxter, MS†, Daniel W. MacDonald, MS†, Steven M. Kurtz, PhD†, Marla J. Steinbeck PhD†
† Drexel University, Philadelphia, PA

Statement of Purpose:

Wear, oxidation and particularly rim impingement damage have been observed following revision surgery of ultra-high molecular weight polyethylene (polyethylene) total disc replacement (TDR) components [**1**]. However, neither *in vitro* testing nor retrieval-based evidence has shown the effect(s) of impingement on the characteristics of polyethylene wear debris.

Thus, we sought to determine (1) differences in polyethylene particle size, shape, number or biological activity that correspond to intermittent (mild) or chronic (severe) rim impingement and (2) for all TDRs regardless of impingement classification, whether correlations exist between the extent of regional damage and the characteristics of polyethylene wear debris.

Methods: The extent of dome and rim damage was characterized for 11 retrieved polyethylene cores obtained at revision surgery: chronic impingement (n=6), intermittent impingement (n=4) and one TDR with osteolysis. TDRs were revised after an average of 9.7 years (range: 4.6-16.1 years) due to persistent back and leg pain and one case of osteolysis. Polyethylene wear debris were isolated from corresponding periprosthetic tissues using nitric acid and imaged using ESEM. Subsequently, particle size, shape, number were determined. Particle characteristics were used to calculate the biological activity of wear debris from both impingement groups [**2**]. Statistical analysis (Wilcoxon and Spearmans Rho) was performed using JMP 8.0.

Results: Separation of particles by size ranges that represent high (<0.1-1 μm), intermediate (1-10 μm) and low (>10 μm) biological relevance revealed an increased number of particles in the 1-10 μm size range (p=0.03) and larger particles in the >10 μm size range for the chronic impingement group (p=0.03).

For TDRs with intermittent impingement, the specific biological activity per unit particle volume (SBA) was increased (**Fig. 1**). Specifically, for the intermittent impingement group, SBA was increased in the <0.1-1 and 1-10 μm size ranges (p=0.04 and p=0.01, respectively). In contrast, when SBA was normalized by particle volume (mm^3)/gram, functional biological activity (FBA) of the chronic impingement group was increased in the >10 μm range (p=0.01) and for the cumulative value of all three size ranges (p=0.01) (**Fig. 1**).

Previous findings showing increased rim penetration of chronic TDRs were observed in the current subset (p=0.03) [**1**]. In addition, for all TDRs, the extent of rim penetration positively correlated with increasing particle size (ρ=0.68) and number (ρ=0.72) (**Fig. 2**).

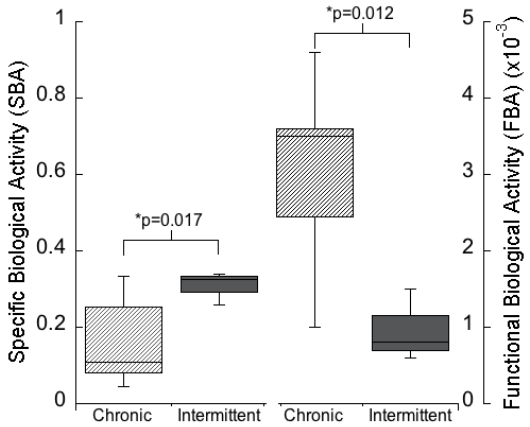

Figure 1. Specific biological activity/unit volume (SBA) was increased for particles from TDRs with intermittent impingement. After normalizing SBA by the total particle volume (mm^3), functional biological activity (FBA) was increased for TDRs with chronic impingement.

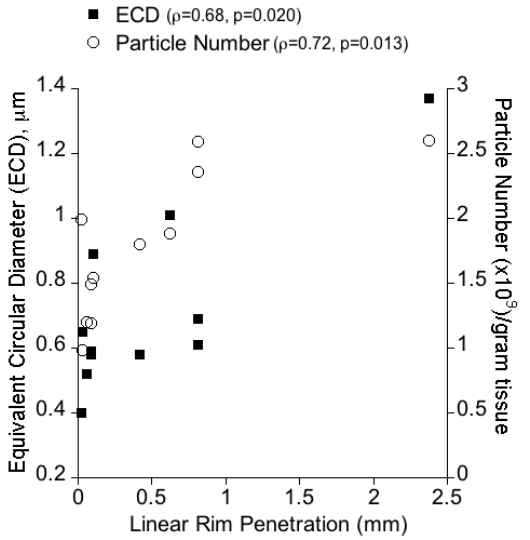

Figure 2. For all TDRs, the extent of linear rim penetration positively correlated with increasing particle size and number.

Conclusions: The results of this study show that chronic rim impingement increases the production of biologically relevant particles from mobile-bearing lumbar TDR components. *In vitro* test methods to simulate this unintended wear mode are warranted.

References: [**1**] Kurtz, S.M. Spine J, 2007;7:12-21.[**2**] Fisher J. Proc Inst Mech Eng H, 2001;215:127-32.

Acknowledgements: NIH (R01AR056264) and FDA (HHSF223200930112G)

The Novel Use of UHMWPE as a Spinal Implant

Oded Loebl, Didier Toubia, Dr. Tzony Siegal.
NonLinear Technologies Ltd

The patented Prow™ Spacer is the first spinal device to be made solely out of UHMWPE, and the only UHMWPE implant with direct contact with the bone. The Prow™ Spacer is a motion preservation interspinous device, implanted between the spinous processes of the lumbar vertebrae, addressing the very common problem of degenerative lumbar spinal canal stenosis. The design is based on the patented NonLinear core technology, allowing minimally invasive surgical procedures which are simple and relatively quick.

The implant body is made by forming an UHMWPE rod with wedged, incomplete cuts transversely at set distances and at 90 degrees to the rod`s long axis. See figure 1. When compressed along its long axis, the segmented rod rolls up to become a rigid, circular structure. See figure 2. The incomplete cuts leave a 'backbone' of UHMWPE that acts as intrinsic hinges. This enables deployment of these segmented structures into the body through a straight conduit and allows accurate positioning of large implants and tools through a minimal incision. The Prow™ Spacer consists of 2 components: the leader assembly and the puller assembly. The leader separates from the puller at the end of the implantation procedure, leaving only the leader assembly implanted in the body. The implant body is manufactured from medical grade GUR 1050 UHMWPE by machining, and the additional components are made from medical grade stainless steel. During sterilization process, the complete assembly is radiated with 6 Mrad dose of gamma radiation in a vacuum. GUR 1050 UHMWPE has been shown to have lower wear volumes when cross linked with the gamma in an inert atmosphere, and has an additional improvement in reducing osteolytic potential or functional biological activity than other UHMWPE grades used for hip and knee implants.

Mechanical tests were performed to evaluate the fatigue and wear performance of the Prow interspinous Spacer (according to ASTM F 2624). Fatigue evaluation included axial compression test and extension test. The two tested specimens completed 1M cycles of max 300N load in the axial compression test and 10M cycles of max 600N load in the extension test without failure. In addition, the mechanical characteristics of elasticity and creep of the device design proved to be highly beneficial for the clinical functionality of an interspinous spacer motion preserving implant, providing improved load distribution as well as a cushioning effect that reduces impact loads on the bone. Two implants underwent 10 million cycles of wear test regime (constant 300N z-axis compression load and ±7.5° rotation around the y-axis). Results show that wear volume and rate are lower than other orthopedic implants that utilize cross-linked UHMWPE. Particle size distribution shows that over 63% of the particles are greater than 0.1 µm.

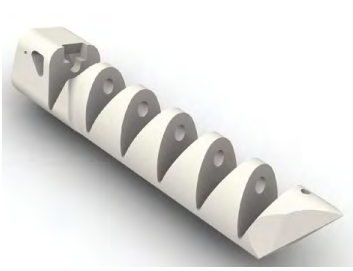

Figure 1: The Prow ™ Spacer as supplied

Figure 2: The Prow ™ Spacer in its closed configuration post implantation

Recent studies show that debris of micro particles (or larger) do not raise a detrimental reaction. The particle shape factor was determined to be 0.69 ± 0.27 µm at 1 M cycles and 0.75 ± 0.22 µm at 5 M cycles (0 = needle shaped, 1 = perfectly round). Elongated particles (fibers) are generally more proinflammatory than round particles.

The Prow™ Spacer is implanted in an average 30-minute procedure requiring a short learning curve. It was successfully implanted in a cohort of six patients with a diagnosis of lumbar spinal canal stenosis in a study performed at the Czech Republic. All six completed six months follow up, and one completed 12 months of follow up. The evidence presented of improved pain parameters, expedient treatment and high surgeon and patient satisfaction at follow-up visits are a proof of the efficacy of the Prow™ Spacer and its "NonLinear" MIS approach to implantation.

Figure 4: Lateral radiograph showing the Prow™ Spacer 2 weeks following implantation

Figure 4: Lateral radiograph showing the Prow™ Spacer 2 weeks following implantation

UHMWPE holds substantial benefits using as a spinal implant material. Its attributes derived from elasticity modulus close to that of bone will grant support to adjacent bone with a lessened chance of subsidence. With the introduction of the Prow™ Spacer, the current interspinous spacers shortcomings in terms of product materials and soft tissue damage are overcome.

Introduction of a Novel Modified UHMWPE Prosthetic Material; Test Results

ZSOLDOS, Gabriella, SZABO, Tamas
University of Miskolc, Department of Polymers Engineering

Ultra High Molecular Weight PolyEthylene (UHMWPE) is the material of choice for Hip-Joint prosthetic implants. In most cases reoperations for replacing the prostheses are necessary because the wear of the acetabular component. UHMWPE is composed from ethylene monomers forming –CH2-CH2– units. The backbone of the polymer is formed by C-C covalent bonds. The average molecular weight of UHMWPE used for manufacturing acetabular components of prostheses is 5-8 MDa (Daltons), which results in chain lengths on a millimeter scale. To improve resistance against wear and increase effective lifetime of the prosthetics significant research is carried out worldwide. Crosslinking is a chemical process during which shorter chains are used to form bridges between the very long polymer chains, thus creating a 3 dimensional structure and forming a much stronger molecular composition. This way the excellent mechanical properties of UHMWPE can be further enhanced. There are many different methods used to crosslink UHMWPE for biomedical use [1-4]. In our research we have not only altered the molecular structure of PE, but also introduced a co-monomer to produce a crosslinked polymeric material with improved mechanical properties and biocompatibility.

Methods: The surface of UHMWPE was treated with selected monomers, some of them multifunctional like ethylene glycol dimethacrylate, in order to form graft-cross linked copolymers with UHMWPE in a reaction initiated by high energy radiation. UHMWPE samples were in the selected monomers until saturation and graft polymerized/crosslinked using high energy radiation during the sterilization step.

The resulting copolymers were examined using spectroscopic (IR and RAMAN) and mechanical testing (hardness, tribology) methods to determine the structure and behavior. Infrared measurements were carried out on a TENSOR 27 FTIR spectrometer from BRUKER with a reflection type sample holder. Depth analyses on sample crosssections were carried out using WiTec CRM 200 confocal RAMAN microscope with a (red) laser of a wavelength of 632 nm. The wear resistance of the samples was determined dry, on a Tribotester constructed at the Univ. of Godollo, and also on a CSM pin-on-disk tribometer [5].

Results: Investigation of the graft co-polymeric material obtained, shows that we have succeeded in creating a gradient material where the concentration of the copolymer in the UHMWPE matrix changes with depth.

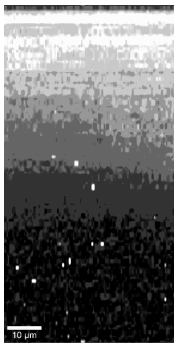

Figure 1. Confocal RAMAN imaging of a cross section of the obtained material (white – co-monomer; black – UHMWPE)

The results of tribological measurements on these functionally gradient materials indicate wear resistance enhancement about 35% compared to the original pure UHMWPE materials. The two tribometers measured the wear differently. For the Tribotester of UG a sample rod was pushed against the spinning disk with no lubrication at a force of 120N, and the equipment measured the reduction of the length of the rod.

Table 1. Results on the Tribotester (arranged by co-monomers)

10000 sec	Chirulen + (mm)			
	UHMWPE	DEGBA	EGDMA	MMA
Wear	0,103	0,105	0,084	0,088

In case of the CSM POD tribometer a steel ball was dragged on the surface of the plastic disc and it measured the volume removed through wear.

Table 2. Results on the CSM tribometer (arranged by co-monomers)

1000 m	Chirulen + (mm^3)			
	UHMWPE	MMA	EGDMA	DEGBA
Wear	0,51	0,32	0,33	0,31

Conclusions: In cooperation with MetriMed Medical Equipment Manufacturing Ltd we have managed to prepare graft co-polymeric materials in UHMWPE matrix using incompatible starting materials. We have determined the amount of monomers the PE absorbs until saturation and formed the co-polymeric crosslinked material with high energy radiation in the same step as the material was sterilized. The obtained material shows improvement in the wear resistance. We have also found that the introduction of acrylate type polymers in the system improves the adhesion to bone cement and probably also the biocompatibility. This research also resulted in a new technology and knowhow being patented both in Hungary and in Europe.

Acknowledgement:
This research work is supported by:
TÁMOP-4.2.1.B-10/2/KONV-2010-0001

References:

[1] Benson RS Nucl Ins and Meth In Phys Res B 2002;191:752-757.
[2] Muratoglu O Biomat 2002;23:717-724.
[3] Gencur SJ Biomat 2003;24:3947-54.
[4] Kurtz SM Biomat 2002;23:3681-97.
[5] Pauwels F Biomechanics of the locomotor apparatus. Springer, New York, 1980.

Effects of Resin Type and Remelting on Crack Propagation in Crosslinked UHMWPE

Nathan D Webb, MS; Jon P. Moseley, PhD
Wright Medical Technology, Arlington, TN

Statement of Purpose: The fatigue properties of UHMWPE are important in the design of total joint devices. The purpose of this study was to measure differences in fatigue crack growth rate and initiation between different post-crosslinking thermal treatments and resin types. Specifically, the change in UHMWPE fatigue properties from crosslinking, and subsequent remelting on Ticona (Oberhausen, Germany) GUR1020® and GUR1050® resins. Compact specimens were made according to ASTM E647 and stress intensity factor of inception (ΔK_{incep}) and a plot of various ΔK values and their corresponding crack growth rates were measured.

Methods: The following groups of material were tested (N=3):

1. Compression molded (CM) GUR1020
2. Ram-Extruded (RE) GUR1050
3. CM GUR1020, 100 kGy crosslinked, remelt annealed
4. CM GUR1020, 100 kGy crosslinked, stabilized with Chimassorb 944 (1000ppm) (antioxidant)
5. RE GUR1050, 100 kGy crosslinked, remelt annealed
6. RE GUR1050, 100 kGy crosslinked, tested within 1 week of crosslinking
7. CM GUR1020, 100 kGy crosslinked, tested shortly after crosslinking (ongoing)

Samples were machined according to ASTM E647-08, Appendix A1, Compact Specimen, with W=25mm and B=11mm. Side grooves with a root radius of 0.25mm were cut into the side to a depth of 1.5mm. In the case of the ram-extruded materials, samples were machined so that crack propagation direction was perpendicular to the extrusion direction. Crosslink density was measured per ASTM F2214 for crosslinked samples. Crystallinity was measured per ASTM F2625 for all samples.

Samples were pre-notched with a razor and tested on a load controlled servohydraulc load frame. Load ratio ($R = P_{min}/P_{max}$) was set to 0.1, with a sinusoidal load at 1Hz. After cracks propagated to failure the initial crack length was measured. Stress intensity factor was calculated per the ASTM standard. Since ΔK continuously increases with the growth of the crack tip, ΔK was calculated at the midpoint between measurements, so for each plotted crack growth velocity, the average ΔK is assumed. To estimate ΔK_{incep}, Paris regime coefficients were calculated, and the equation was used to extrapolate the ΔK that would result in a da/dN of $1*10^{-5}$ mm/cycle.

Results: Figure 1 shows propagation rates for the crosslinked materials. For a given stress intensity factor, K, the crosslinked, stabilized GUR1020 showed the slowest crack propagation, followed by crosslinked GUR1050 and crosslinked, remelted GUR1020. The crosslinked, remelted GUR1050 gave the fastest crack growth. Table 1 lists the calculated values of ΔK_{incep}. The trends are the same as in the propagation rate. The ΔK_{incep} measured for crosslinked, remelted GUR1050 fall between previous published values[1,2].

Discussion: Samples machined from stabilized GUR1020 had the lowest crack propagation velocity for a given ΔK. Samples machined from GUR1020 and remelted preformed better than samples machined from remelted GUR1050. Differences between resins were not found in the non-crosslinked materials. The crystallinity was not significantly different between the remelted GUR1020 and 1050. Testing is currently being performed on crosslink density to determine if differences in the crosslinking could explain the difference in the resins. While crack propagation is an important parameter to understand and characterize a material, the ΔK_{incep} is a more useful design parameter, allowing careful design of fatigued components to avoid exceeding the crack inception K, reducing risk of mechanical failure. This test increased load at shorter intervals than some published tests. Allowing longer time intervals between measurements could more accurately measure ΔK_{incep}, at the expense of additional creep during the duration of the test. The comparisons between resin type are potentially affected by consolidation method. However, a study comparing crack propagation of compression molded versus ram extruded GUR 1050 showed negligible differences so long as the crack orientation for extruded material was perpendicular to the extrusion axis.[1]

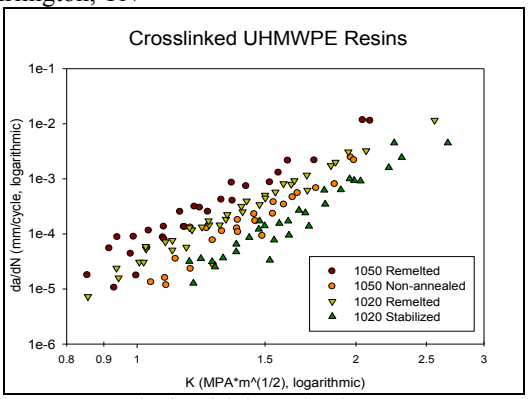

Figure 1: Plot of crosslinked material crack propagation rates

Resin	Dose	Anneal	ΔK_{incep}
GUR1050	100	Remelt	0.77 (0.23)
GUR1020	100	Remelt	0.83 (0.05)
GUR1020+C944	100	none	1.17 (0.03)
GUR1050	100	none	1.04 (0.02)
GUR1020	0	none	1.36 (0.10)
GUR1050	0	none	1.39 (0.16)

Table 1: ΔK_{incep} ($MPA*m^{1/2}$) extrapolated values (standard deviations in parentheses)

Conclusions: Crosslinking had a large negative impact on crack inception and growth, and remelting caused additional changes, both in agreement with previous studies. Although resin type was not a factor for conventional UHMWPE, crosslinked GUR1020 exhibited improved properties compared to crosslniked GUR 1050, especially for non-remelted specimens.

References: [1] Gencur S.J., et al; *Fatigue crack propagation resistance of virgin and highly crosslinked, thermally treated ultra-high molecular weight polyethylene*, Biomaterials 27 (2006) 1550–1557.

[2] Baker D.A., et al; *The Effects of degree of crosslinking on the fatigue crack initiation and propagation of orthopedic-grade polyethylene*, JBMR 66A (2003) 146-154

DIAMOND-LIKE-CARBON COATINGS FOR UHMWPE: A WAY TO MINIMIZE WEAR AND BACTERIAL ADHERENCE

G. del Prado[1], A. Terriza[2], A. Ortiz-Pérez[1], D. Molina-Manso[1], I. Mahillo[1], F. Yubero[2], J.E. Puértolas[3], E. Gómez-Barrena[4], and J. Esteban[1].

[1]IIS-Fundacion Jiménez Díaz, Madrid, Spain, [2]Instituto de Ciencia y Materiales CSIC, Sevilla, Spain [3]ICMA (CSIC-Univ. Zaragoza), [4]Hospital La Paz and Autónoma University, Madrid, Spain

INTRODUCTION: Bacterial adherence and subsequent biofilm development are a matter of concern because of their importance in implant- related infections [1]. Diamond like carbon (DLC) coating has been proposed to improve the antibacterial performance of biomaterials in addition a reduction of the wear [2-3]. This study was performed with the aim of testing the anti-adhesive effect of DLC and other C-F functionalities.

MATERIAL AND METHODS: Adherence of 11 clinical staphylococci strains (6 *S. aureus*, 5 *S. epidermidis*) as well as 2 reference strains of *S. aureus* ATCC 15981[4], and *S. epidermidis* ATCC 35984, was evaluated with raw ultra high molecular weight polyethylene (UHMWPE) and three UHMWPEs coated with 1) DLC (DLC), 2) fluorine doped DLC (F-DLC), and 3) high fluorine content carbon-fluor (CFx).

The three coated surfaces were obtained by enhanced chemical plasma deposition using acetylene and octo-fluoro-cyclobutene (C_4F_8) gases as precursors of C and F incorporated in the coatings. Superficial functional groups were identified by X-ray photoemission spectroscopy (XPS) and water contact angle (WCA) measurement was performed.

For adherence studies, the 4 sterilized surfaces were exposed to $\approx 10^8$ colony former units (CFU)/mL [5] during 90 minutes at 35º C. Surfaces were washed with PBS (X 3) and incubated 24 hours at 4ºC. Finally, surfaces were stained with Acridine Orange for 2 min. 10-20 fields/ surface were photographed at 40x magnification. Assays were made in triplicates.

The percentage of covered surface was determined using *Image J* software. Differences between surfaces were individually analysed by *t* tests. Lineal regression models were performed for multiple comparisons.

RESULTS: Data from XPS analysis revealed that the superficial structures of raw UHMWPE and DLC were totally based in C-C bonds (100%). Fluorine addition to DLC coating took place randomly, diminishing C-C bonds formation (73 %), and incorporating F atoms to the DLC structure ([F]/[C]=0.32) mainly in the form of -C-CF (21 %), and also -C-F (5 %) and $-CF_2$ (1%) bond types. On the other hand, the direct decomposition of C_4F_8 precursor in an Ar plasma induced a high F incorporation ([F]/[C]=1.25) in the CF_x coating, with significant formation of $-CF_2$ (26%) and $-CF_3$ (15%) bond types. The WCAs were of 100 ± 5º (UHMWPE), 79 ± 3 º (DLC) , 98 ± 4º (F-DLC) , and > 170 º (CF_X). Figure shows the percentage of bacterial coverage per surface type (mean ± S.D). Significant reduction was observed in 9 staphylococci strains (5 *S. aureus*, 4 *S. epidermidis*) when compared UHMWPE to DLC and in 6 strains (4 *S. aureus*, 2 *S. epidermidis*) comparing UHMWPE to F-DLC and CFx.

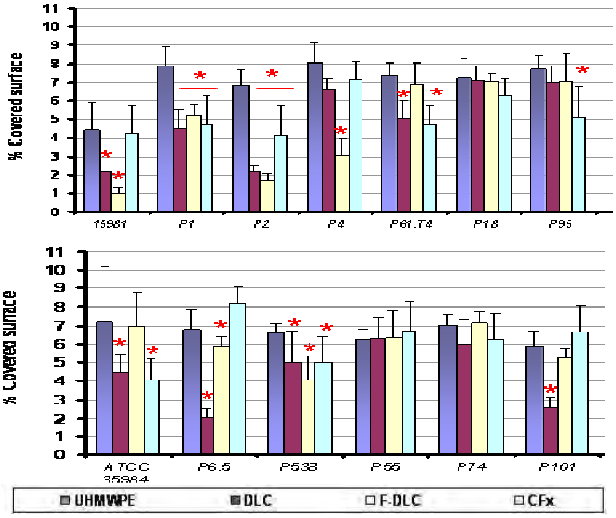

* Statistically significant reductions $p \leq 0.001$

Figure. *Percentage of bacterial coverage in raw and modified UHMWPE surfaces (mean ± +S.D).*

In a global analysis, all the coated surfaces diminished bacterial adherence, and DLC was found as the least adherent. Besides, the significant reduction in bacterial adherence observed with DLC was independent of the bacterial species, while the observed reduction with F-DLC and CF_X was species – dependent.

DISCUSSION & CONCLUSIONS: The capability of DLC in diminishing bacterial adherence could be species-independent. Although F-DLC coating could be interesting by the antimicrobial properties of fluorine, some increase in bacterial adherence was observed versus DLC alone and this effect could be due to the higher hydrophobic behaviour of F-DLC coating. This increase of WCA correlates to incorporation of F atoms in the C matrix.

REFERENCES:

[1] Kurtz *et al. J Arthroplasty* (2008) **23**: 984-91

[2] Katsikogianni M and Missirlis Y F. *Eur Cells Mat* (2010) **8**: 37

[3] Puértolas J A *et al. Wear* (2010) **269**: 458.

[4] Valle *et al. Mol Microbiol* (2003) **48**: 1075-87

[5] Kinnari *et al. J Biomed Mat Res* Part A (2008) **86**: 760-8

ACKNOWLEDGEMENTS: This study was financed by CONSOLIDER FUNCOAT-CSD2008-00023. AT was granted by JAE-CSIC. DMM was granted by Fundación Conchita Rábago. AOP and GDP were funded by the Comunidad de Madrid.

HALS (Hindered Amine Light Stabilizers) as alternative stabilizer for medical implants

Leon Stijkel*, Pieter Gijsman*, Detlef Schuman*, Harold Smelt*, Ryan Siskey◆
.* DSM Geleen, the Netherlands, ◆Exponent®, Bellevue (WA), United States
leon.stijkel@dsm.com

Statement of Purpose: Cross-linking UHMWPE implants using Gamma or Electron Beam (EB) radiation leads to a significant decrease of wear rates. Radicals formed during irradiation are 'trapped' in the crystalline phase and could be present for years. These remaining alkyl radicals will, in contact with air, initiate oxidation of the polymer, leading to a reduction in properties and possible premature failure of the implant.
Radical scavengers, like Vitamin E, are blended into the UHMWPE to reduce the amount of residual radicals. The main disadvantage of Vitamin E is that it instantly reacts with radicals during the cross-linking process leading to a reduced radiation efficiency (cross-link density) and partly consumption of the dosed amount of stabilizer. Hindered Amine Light Stabilizers (HALS) can be blended in before irradiation, without showing any negative aspects as described for Vitamin E [1].

The aim of this study was to compare the mechanical properties (tensile) and wear resistance as a function of the oxidative stability of Chimassorb 944 or Vitamin E blended UHMWPE, under accelerated aging conditions.

Methods:
Conventional medical grade UHMWPE (GUR1020) was blended with 0.10 wt.% Vitamin E or Chimassorb® 944; by solution blending of the stabilizers in iso-propanol. Quantification of the homogeneity of stabilizer in the blended powder was done by FT-IR, using absorbance at 1530 cm^{-1} (peak height) for Chimassorb 944 and 1210 cm^{-1} for Vitamin E. For normalization the absorbance at 2018 cm^{-1} was used.
Subsequently the powder was compression molded into 80 mm thick sheets at Quadrant MediTECH. Material was machined into bars (1 m length) and than gamma irradiated with 100 kGy (at Beta-Gamma-Services GmbH). After annealing the sample dimensions needed for analyses were machined from the corresponding molded sample bars.
Non-aged analysis (t=o); ASTM F2214 swell ratio testing, ASTM D3895 oxidation induction time, ASTM F2102 Oxidation index (OI) and ASTM D638 tensile testing.
For a maximum time interval of 24 weeks microtomed films have been aged according to ASTM F2003 and in parallel in an air oven at 100 °C.
OI (F2102) measurements started after 4 weeks, in case OI > 0.5 tensile testing according to ASTM D638 was performed. 2 Sets of wear pins of each material aged 8 and 16 weeks have been tested in a 100 station multiaxial POD wear tester [2].

Results:

Study starts March 2011.

- oxidation index vs. time (F2003 and oven)
- tensile vs. time (F2003 and oven)
- POD data vs. aging/time (F2003 / oven)
- Overall stabilizer performance under different conditions

To be determined by Exponent study!

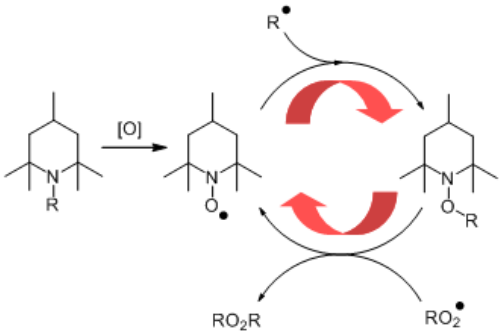

Figure 1. Hindered Amine Light Stabilizers (HALS)

Figure 2. result from Exponent study

Conclusions:

To be determined by Exponent study!

References:
1. P. Gijsman et al. / Biomaterials 31 (2010) 6685-6691
2 Saikko, V. Proc. IMechE 2005, 219 Part H:J. Engineering in Medicine, 309.

Wear of Vitamin E UHMWPEs Under Ideal and Adverse Conditions

Joanne L Tipper, Andrew Beadling, Haleema Hussain, Serena Russell, John Fisher
Institute of Medical & Biological Engineering, University of Leeds, Leeds, LS2 9JT, UK

Statement of Purpose: UHMWPE containing 1000 ppm Vitamin E (VE) is now offered as a bearing material by orthopaedic device manufacturers. Limited information is available regarding the wear of 1000 ppm VEE UHMWPE under the range of tribological conditions likely to be encountered *in vivo*. Under ideal conditions i.e. knee simulator studies, 3000 ppm VEE UHMWPE exhibited a 45% reduction in wear volume compared to UHMWPE without VE [1] and in hip simulator studies VE doped highly crosslinked UHMWPE exhibited a 4 fold lower wear rate compared to UHMWPE without VE [2]. However, to date the wear resistance of 1000 ppm VEE UHMWPE has not been investigated under adverse conditions i.e. against scratched counterfaces. The aim of this study was to investigate the wear of a variety of different GUR1050 UHMWPE materials containing Vitamin E with and without crosslinking against smooth and scratched cobalt chromium counterfaces in simple configuration wear tests.

Methods: Five different GUR1050 UHMWPE materials were tested, Virgin, 300 ppm Vitamin E, 1000 ppm Vitamin E, 1000 ppm Vitamin E plus 5 MRad gamma irradiated and 1000 ppm Vitamin E plus 10 MRad gamma irradiated (Figure 1; kindly donated by Meditech Medical Polymers, USA). Pins were machined from the different materials to have a 12 mm diameter with a 10 mm contact face. Plates were made from high carbon cobalt chromium and were either smooth (Ra 0.01 – 0.02 µm) or scratched with a 100 µm diameter diamond stylus (scratch lip height 1.0 µm). Wear tests were carried out in 25% (v/v) bovine serum using simple configuration multidirectional wear test rigs. Four pins of each material were tested for a minimum of 2 weeks. Pins were weighed before and after testing to calculate wear factors. Results were compared using one-way ANOVA.

Figure 1. UHMWPE Pins (left to right) Virgin, 300 ppm VE, 1000 ppm VE, 1000 ppm 5 MRad and 1000 ppm 10 MRad.

Results:
The mean wear factors for each material against smooth and scratched counterfaces are shown in Figure 2. The data indicated that when Vitamin E concentrations of 300 ppm and 1000 ppm were included wear was not significantly affected compared to the virgin control samples. However, as the level of crosslinking increased, from 5 to 10 MRad, wear resistance of the 1000 ppm Vitamin E material also increased. The wear rate of the 1000 ppm 10 MRad UHMWPE was statistically significantly lower ($p<0.05$) than the wear rate of the 1000 ppm Vitamin E UHMWPE, indicating that the introduction of high levels of crosslinking (10 MRad) caused a significant improvement in the wear resistance. Against scratched counterfaces the 1000 ppm Vitamin E UHMWPE material exhibited a significant ($p<0.05$) increase in wear compared to the virgin material. When moderate (5 MRad) and high (10 MRad) levels of crosslinking were introduced into the 1000 ppm Vitamin E UHMWPE the wear factors were statistically significantly lower ($p<0.05$), indicating that the introduction of crosslinking into the VEE material improved wear resistance.

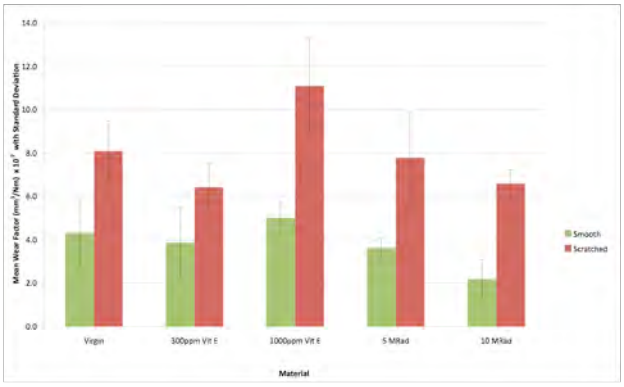

Figure 2. Wear Factors for UHMWPEs with different levels of Crosslinking and Vitamin E against Smooth and Scratched Counterfaces.

Conclusions: The addition of 1000 ppm Vitamin E caused wear rate to increase against both scratched and smooth counterfaces compared to the virgin material. Gamma radiation crosslinking (10 MRad) combined with Vitamin E caused a significant reduction in wear against smooth counterfaces and the addition of moderate or high levels of crosslinking (5 & 10 MRad) improved wear resistance against scratched counterfaces. These results indicate that the addition of Vitamin E alone is not beneficial to wear performance of the UHMWPE material, however, when Vitamin E is combined with high levels of crosslinking wear performance improved. These results are in contrast to those described by Termura *et al.* [1], where the wear rate of vitamin E enhanced UHMWPE was lower than virgin UHMWPE, however these authors used approximately three-fold higher concentrations of Vitamin E. When the same materials were tested in simple configuration wear tests these advantages were not demonstrated [3].

References [1] Teramura *et al* 2008. J Orthop Res 26, 460-464. [2] Oral *et al* 2006 J Arthroplasty 21, 580-591. [3] Teramura *et al* 2009 Trans ORS, Las Vegas 2277.

Cytotoxic Effects of Anti-Oxidant Compounds on Primary Human Peripheral Blood Mononuclear Cells

Joanne L Tipper, Julie Liu, Catherine L Bladen.
Institute of Medical & Biological Engineering, University of Leeds, Leeds, LS2 9JT, UK.

Statement of Purpose: Sterilisation of UHMWPE joint replacement components by gamma irradiation causes the release of free radicals, which if not dealt with by post irradiation processing, can lead to oxidative damage within the polymer [1]. Oxidation of the UHMWPE components has been shown to lead to altered mechanical properties and increased wear [2]. The addition of anti-oxidant compounds, in particular Vitamin E, has been gaining popularity over recent years and UHMWPE containing 1000 ppm Vitamin E (VE) is now now offered as an alternative bearing material in the clinic. A number of other anti-oxidant compounds are being added to UHMWPE such as hindered phenols [3], anthocyanins, lanthanides and nitroxides. The emphasis in these studies has been on studying the effects of these compounds on the mechanical properties of the polymer and/or on wear resistance, with little regard for the biological consequences. The aim of this study was to investigate the effects of these anti-oxidant compounds on the cell viability of a human histiocytic cell line and peripheral blood mononuclear cells (PBMNCs) *in vitro*.

Methods: The cytotoxicity of several anti-oxidant compounds was investigated and compared to vitamin E. These included HPA01, a hindered phenol; TEMPO, a nitroxide; and the lanthanides Europium (II) and Europium (III). U937 human histiocytes or PBMNCs from healthy volunteers (ethical approval granted by University of Leeds ethics committee) were seeded at 2 x 10^4 per well and incubated in RPMI 1640 medium with antioxidant compounds at concentrations between 1µm and 5 mM in an atmosphere of 5% (v/v) CO_2 in air (n = 4). Glutathione (100 µm), a naturally occurring anti-oxidant, and cells only were included as negative controls and 75 µm Menadione, a known inducer of oxidative stress, was included as positive control. Cell viability was measured using the ATP-Lite assay after 24h. Data was fitted to a sigmoidal dose response curve by log transforming the X column values then normalizing the Y column values. A non-linear regression was then performed.

Results The dose response curve for vitamin E in PBMNCs is shown in Figure 1. Vitamin E was well tolerated by the cells, only becoming toxic at high concentrations (≥4 mM). All other anti-oxidant compounds were toxic to the cells at micro molar concentrations. The dose response curve for the hindered phenol HPA01 in PBMNCs is shown in Figure 2, which is representative of the response to both nitroxide and lanthanide anti-oxidants. In general the primary cells were less sensitive to the anti-oxidant compounds, indicated by the higher concentrations required to exert an adverse effect on cell viability. Interestingly, the HPA01 and TEMPO antioxidants conferred protection against the toxic effects of solvents (DMSO and ethanol) in both the cell line U937 and in primary cells, suggesting that these compounds are functioning as antioxidants.

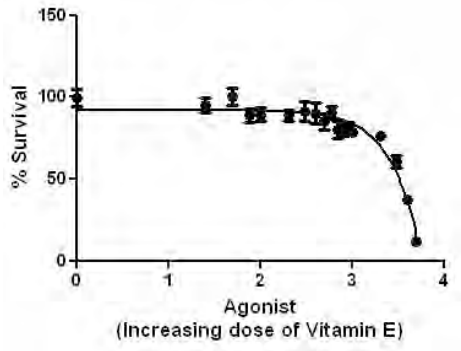

Figure 1. Dose response curve for vitamin E in PBMNCs

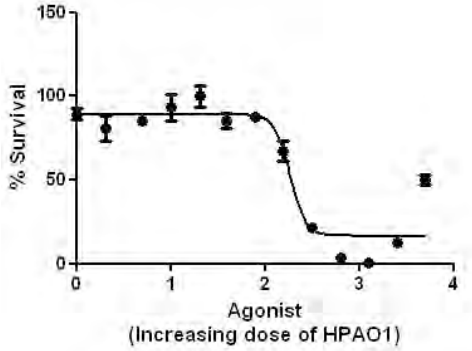

Figure 2. Dose response curve for HPAO1 in PBMNCs

Conclusions: Concerns about residual free radicals in UHMWPE and the resultant oxidative damage to the polymer has lead to the inclusion of a number of different anti-oxidant compounds in UHMWPE, however the biological consequences of these compounds have not been considered. This study has revealed that the majority of these compounds are toxic to human monocytic cells at relatively low doses, however, it is not known whether these compounds will leach from the polymer *in vivo* and therefore pose a cytotoxic risk. Previous studies on HPA01 have indicated that the compound is not lost from the bulk material [4], however it is not known whether the compounds will be lost from particulate wear debris, which has a comparatively large surface area. In addition, at low concentrations the HPA01 and TEMPO antioxidants had a protective effect against the solvents, and this requires further investigation. The concentration of antioxidants included in TJR components has been determined based on oxidative index, however, important the biological effects of these compounds should also be considered, in terms of cytotoxicity, resistance to oxidative stress and osteolytic cytokine release from macrophages.

References

[1] Oral et al 2004 Biomaterials 25, 5515-22. [2] Muratoglu et al 1999 Biomaterials 20, 1463-70. [3] Narayan et al 2010 Trans 56th ORS p2317. [4] King & Sharp 2010 Trans 56th ORS p2286.

The mechanical wear properties and surface characteristics of the UHMWPE material used on wear couple systems

Geriel A. Ettienne-Modeste[1], L.D. Timmie Toploeski [2]
[1,2] Department of Mechanical Engineering, University of Maryland Baltimore County, Baltimore, Maryland, USA

Statement of Purpose: There are over 500,000 total joint replacements (TJR) performed in the U.S. every year and TJR remains one of the most successful treatments for arthritis [1]. Currently, the most commonly used materials for artificial joints are metals such as cobalt-chrome alloys or titanium alloys, which articulate against ultra-high molecular weight polyethylene (UHMWPE) [1-3]. However, there has been ongoing concern about the use of UHMWPE because wear of this material often leads to the generation of numerous submicron sized particles [4-6]. The submicron UHMWPE particles cause a cascade of biological responses which can ultimately lead to osteolysis and loosening of the artificial joint [2,5]. Wear-particle-induced osteolysis is one of the leading problems associated with TJR [4,6]. Despite these complications, there continues an on-going research effort to improve the metal-on-UHMWPE couple. Simultaneously, alternative bearing surface materials are also under investigation; this research represents such an effort.

Alternative bearing surfaces are attractive materials for studying the micro-structural behavior of the UHMWPE material because the harder, more wear resistant material has the potential to reduce UHMWPE wear, improve mechanical and surface properties [6,7]. A micro-textured carbide-CoCrMo alloy surface can be used as an alternative bearing material in artificial joints. Quantifying the mechanical and material properties and surface morphology of the UHMWPE surface on the conventional CoCrMo alloy and our new novel micro-textured carbide-CoCrMo alloy surfaces are important to control the rate of wear for artificial joints. In this study, the ability to understand the micro-structural properties of the UHMWPE surfaces, shown by the optical microscope and properly characterize the wear properties for the CoCrMo-on-UHMWPE and carbide-on-UHMWPE wear couple systems was achieved. Surface profile parameters (Ra, rms, and PV) were measured using white light interference surface profilometer (WLISP). We reported that the formation and characterization of the carbide surface layers created by the microwave plasma chemical vapor deposition (MPCVD) [7-8]. This paper reports on our recent progress in the wear studies on the average surface, Ra for two wear couple systems CoCrMo-on-UHMWPE and carbide-on-UHMWPE.

Materials and Methods: The specimen preparation for the CoCrMo and UHMWPE involved a wrought CoCrMo alloy rod (ASTM F1537, Teledyne Allvac) and UHMWPE GUR 415 medical grade round rod (E.I. Dupont de Nemours and Company, Inc. DE) machined to 16 mm diameter, 7 mm thick disk specimens and 44 mm diameter, 7 mm thick plate specimens, respectively. Fifty of the CoCrMo alloy disks were created, polished and prepared for film deposition in the MPCVD system. Fifty of the UHMWPE plates were created, ultrasonically cleaned in a solution of 1% detergent in D.I. water for 15 minutes, rinsed and dried according to a standard test method [8]. Prior to plasma processing, the top and bottom of all the fifty CoCrMo alloy disks were polished to a mirror finish with #P500, #P800, #P1200, #P2400, #P4000 SiC abrasive paper and 3µm diamond suspension, sequentially using a (Buehler LTD-Ecomet III, Model 850) grinder/polisher and ultrasonically cleaned with D.I. water and acetone for 15 minutes using a (Cole-Parmer, Model 8849-00). The weight, thickness and diameter were measured for all disks and plates using a digital balance (Mettler Toledo, Model AX205) with a precision of 0.0001 grams. The carbide coated CoCrMo alloy disk surfaces were created using the MPCVD system at 2.45-GHz in a mixture of methane (99.97% pure) and hydrogen (zerograde 99.99% pure) with a total gas pressure of 70 Torr and a total gas flow rate of 100 sccm (1 sccm CH4, 99 sccm H2) for 0.5-6 hours, depending on film thickness (Mitutoyo). After deposition, the carbide specimens were polished with a SiC abrasive paper #P2400 and #P4000 for 60-second each then followed by mirror finishing with a 3-µm diamond suspension for two 45-second sessions to create a smooth carbide surface with reduced peak-valley roughness effects. Thirty measurements for each of the surface profile parameters (Ra, rms, and PV) were made along the diameter of the fifty specimens to compare the changes in surface profile roughness of the UHWMPE material on the carbide-CoCrMo and CoCrMo alloy surfaces. Wear tests were conducted using the standard CoCrMo-on-UHMWPE, and a novel micro-textured carbide surface [8] (carbide-on-UHMWPE). Data were analyzed by ANOVA with post-hoc Tukey tests for multiple comparisons and linear regression. The wear factor was determined from the wear rate and the applied load during wear testing using the following equation [8]:

$$\textbf{Wear factor}(\mathrm{mm^3\,N^{-1}\,m^{-1}}) = \frac{Wear\ rate(\mathrm{mm^3 m^{-1}})}{Load(N)}$$

Visible impurities due to wear properties for the CoCrMo-on-UHMWPE and carbide-on-UHMWPE wear couple systems were observed using the DCM200 (Scopetek) optical microscope and camera.

Results: The profilometer (WLISP) results indicated that the coating thickness of 3µm improves the average surface roughness, initial Ra values agree with previous studies [7-8], which also agreed with an improved average surface roughness for the UHWMPE material (Figure 1). The profilometer and optical microscope results also suggested that the brain coral morphology or coated CoCrMo alloy specimen shows more evidence from the remaining crystal nuceelation on the UHMWPE material images than when the CoCrMo alloy specimens was used as the counterbody material (Figures 1 and 2(b)). In addition, the surface roughness profile (the average surface, Ra) for (n=50) specimens of the UHMWPE plate, the mirror polished non-coated CoCrMo alloy disk and the micro-textured coated

CoCrMo alloy disk was 0.070 µm, 0.037 µm, and 0.310 µm, respectively. Therefore, (the average surface, Ra) is greater for the micro-textured coated CoCrMo alloy disk than the non-coated CoCrMo alloy disk. The values of average surface (Ra) for the UHMWPE material lubricated in (BCS 100, 50, 25, and 0%) at 1,000,000 cycles for the two wear couples systems are: 0.72µm, 0.81µm, 0.92µm and 0.83µm, respectively for the carbide-on-UHMWPE wear couple system and 0.81µm, 0.57µm, 0.72µm and 0.59µm, respectively for the CoCrMo-on-UHMWPE wear couple system, ($p<0.001$), ANOVA. Lastly, the UHMWPE plate material wear results (Figure 3), showed that the CoCrMo-on-UHMWPE and carbide-on-UHMWPE wear couple systems produced the greatest total volumetric wear for BCS 100, 25 and 0% and BCS 50% lubricants, respectively after 1,000K cycles. The UHMWPE wear properties (factor and rate) as well as R^2 value were generally lower in the micro-textured CoCrMo alloy than the CoCrMo alloy surfaces (Table 1) for the two wear couple system after wear at 1,000,000 cycles for each lubricant type, expect BCS 0% (DDW).

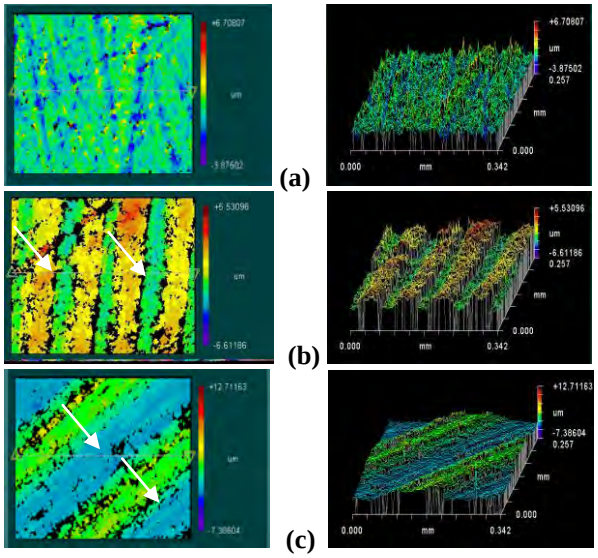

Figure 1. The UHMWPE specimen (a) prior to wear testing with R_a= 0.58 µm, (b) and (c) after wear at 1,000,000 cycles lubricated in BCS 100% showing the wear tracks (white arrows) for the (b) carbide-on-UHMWPE and (c) CoCrMo-on-UHMWPE wear couple systems with R_a= 0.72 µm and R_a= 0.81 µm, respectively

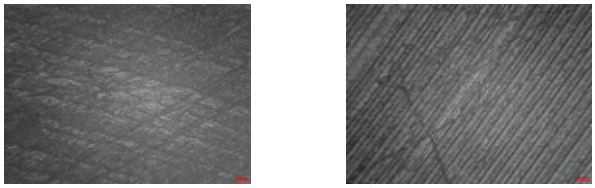

Figure 2. Optical microscope image analysis after wear at 1,000,000 cycles lubricated in BCS 100% for the UHMWPE material for both the carbide-on-UHMWPE (left) and CoCrMo-on-UHMWPE (right) wear couple systems

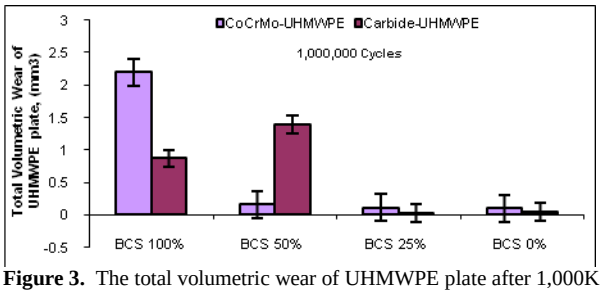

Figure 3. The total volumetric wear of UHMWPE plate after 1,000K cycles lubricated in (BCS 100- 0%) has no significant difference

Wear Couple	Lubricant Concentration	UHMWPE Wear Factor (mm^3/Nm /million cycles	UHMWPE Wear Rate (mg /million	R^2 values of linear regression
CoCrMo-on-UHMWPE	BCS 100	2.08E-04	9.90E-03	0.9591
	BCS 50	1.53E-05	7.28E-04	0.8432
	BCS 25	1.05E-05	4.98E-04	0.6177
	BCS 0	9.11E-07	4.33E-05	0.313
Carbide-on-UHMWPE	BCS 100	8.23E-05	3.91E-03	0.8361
	BCS 50	1.32E-04	6.25E-03	0.485
	BCS 25	1.16E-05	5.52E-04	0.232
	BCS 0	4.30E-05	2.04E-03	0.6805

Table 1. The UHMWPE wear behavior derived from the calculated volume loss of the UHMWPE weight loss at 1,000,000 wear cycles

Conclusions: The results showed that UHMWPE material produced a lower wear rate and greater average surface roughness (R_a) for the micro-textured carbide-CoCrMo alloy than of CoCrMo base metal. The fact that UHMWPE plastically deforms and the measured CoCrMo alloy-on-UHMWPE wear couple has a higher wear rate is consistent with published studies. The surface roughness parameters produced a statistical significant for both wear couple systems. The micro-textured carbide-CoCrMo alloy specimens also may have the potential to retain lubricating fluid and reduce UHMWPE wear because of the textured morphology created during the coating process. In addition, the micro-textured carbide-CoCrMo alloy may have the potential to provide high wear resistance in a severe wear environment. Recommendations for future study include optimizing the wear parameters for the carbide-on-UHMWPE wear couple by using other grades of UHMWPE as well as crosslinked UHMWPE to reduce wear particle generation. Conducting wear studies to compare the properties of crosslinked UHMWPE and medical grade GUR UHMWPE on other surfaces such as Ti alloys as a function of lubricant concentration and mechanical properties may potentially increase wear performance.

References:

[1] McKellop H, et al. *J Biomed Mater Res* 1978;12(6):895-927.
[2] Clarke IC, et al. *American Society for Testing and Materials* 1983:p.136-147.
[3] Rostoker W, and J.O. Galante. *J Biomed Mater Res* 1976;10(2):303-310.
[4] Howie DW. *J Arthropl* 1990;5(4):337-348.
[5] Doorn PF, P.A. Campbell, and H.C. Amstutz. *Clin Orthop* 1996;329 Suppl(S206-S216).
[6] G. Ettienne-Modeste, *56th Ann Meeting of the Orthopaedic Research Society*, 2010.
[7] Vandamme, N.S.; Que, L.; Topoleski, L.D.T. *J of Materials Science*, v 34, n 14, Jul, 1999, p. 3525-353.
[8] Vandamme,N.S.; Topoleski, L.D.T. *J of Materials Science: Materials in Medicine*, v 16, n 7, July, 2005, p. 647-654.

Effect of Thermal Treatment on the Wear of Radiation-Crosslinked UHMWPE with and without Vitamin-E

Aiguo Wang, Lizeth Herrera, Kim Phuong Le, Lin Song, Twana Davisson
Stryker Orthopaedics, Mahwah, NJ

Statement of Purpose: Contemporary highly crosslinked UHMWPEs that have been developed for orthopaedic bearing applications are based on two key principles: ionizing radiation to generate free radicals and thermal treatment to crosslink residual free radicals for improving oxidation resistance [1]. The level of crosslinking, which is essential for wear resistance, is determined by both the dose of irradiation and the method of thermal treatment. Recent studies on UHMWPE that contains Vitamin-E indicate that post-irradiation thermal treatment, either in the form of remelting or annealing, may not be necessary for improving the oxidation resistance since residual free radicals are effectively neutralized by Vitamin-E [2]. However, it is unclear how the wear resistance of Vitamin-E containing UHMWPE would be affected by post-radiation thermal treatment. The objective of the present study is to determine the effect of thermal treatment on the wear resistance of radiation-crosslinked UHMWPE with and without Vitamin-E stabilization.

Methods: Two materials with three treatment conditions were evaluated in this study, as shown in table 1:

Material	Irradiation dosage	Thermal treatment
GUR 1020	90 kGy	no heat treatment
GUR 1020 with Vitamin E	90 kGy	no heat treatment
GUR 1020	90 kGy	single annealing
GUR 1020 with Vitamin E	90 kGy	single annealing
GUR 1020	90 kGy	Sequential annealing
GUR 1020 with Vitamin E	90 kGy	Sequential annealing

Table 1: Material and treatment conditions

The vitamin E material contains 1000 ppm of vitamin E; which was blended into the GUR 1020 UHMWPE resin before consolidation. Wear testing was conducted with 32 mm acetabular cups on a multi-station hip stimulator (MTS, Eden Prairie, MN). Appropriate diameter CoCr femoral heads were mated against the inserts. Testing was run at 1 Hz with cyclic Paul curve physiologic loading applied axially and a lubricant of 50% alpha calf serum [3,4]. Inserts were cleaned and weighed according to standard protocols every 0.5 million cycles and serum was also changed at that interval [5]. Statistical analysis was performed using the Student's t-test ($p<0.05$). The test was conducted for a total of 2 million cycles.

Results: Wear rate results are shown in figure 1. Results show no statistical difference ($p>0.05$) in wear rate for any of the materials containing vitamin E regardless of thermal treatment. While, polyethylene without vitamin E shows a significant reduction in wear rate as a function of thermal treatment as shown in figure 2. All of the materials without vitamin E had better wear characteristics than vitamin E containing polyethylene.

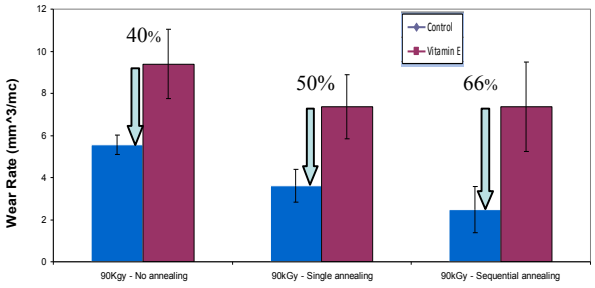

Figure 1: Wear Rate at 2 million cycles showing improved wear characteristics for material without vitamin E

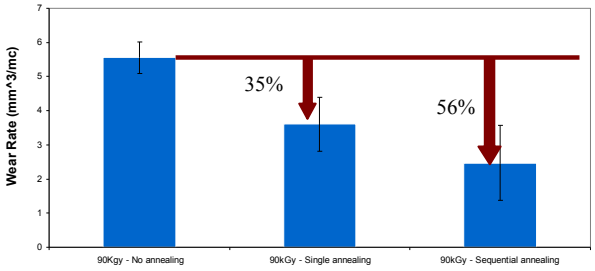

Figure 2: Wear rate of GUR 1020 without vitamin E showing improved wear characteristics as a function of thermal treatment

Conclusions: The effect of vitamin E on the wear characteristics of UHMWPE were investigated in this study. This study shows that regardless of thermal treatment, the addition of vitamin E negatively affects the wear characteristics of polyethylene by at least 40%. These results suggest that the addition of vitamin E significantly decreases the ability to create crosslinks during both irradiation and post-irradiation thermal treatment and consequently increasing wear rate.

References:[1] Polineni, VK; et al. ASTM STP 1307: American Society for Testing and Materials; 1998 p. 95-108 [2] Rowell, SL; et al. J. Orthop Res 29:773-780; 2011[3] Paul JP. Proc Inst Mech Engrs, 1966, 181, 8. [4] Wang A. et al J Biomed Mater Res B, Appl Biomater 2004, 68B, 45. [5] ASTM F2025 – standard Practice for gravimetric Measurement of polymeric Components for Wear Assessment.

Systematic Review of Highly Crosslinked Polyethylene Wear Rates and Patient Factors

[1, 2]Patel JD; [1]Gawel, HA; [1]Hanzlik, JA; [1,2]Kurtz, SM
[1]Drexel University, Philadelphia, PA; [2]Exponent Inc., Philadelphia, PA

Statement of Purpose: Ultrahigh-molecular-weight polyethylene (UHMWPE) has been an orthopaedic bearing material for total joint arthroplasties for almost 50 years. Highly crosslinked polyethylene (HXLPE) was introduced in the late 1990's to reduce wear and revision rates due to osteolysis. While many studies report wear and osteolysis associated with HXLPE, patient populations and device fixation modes can differ substantially among clinical investigations [1]. Our present study addressed 2 questions: (1) How do patient factors (eg, age, weight, body mass index (BMI)) influence radiographic wear outcomes for the hip? (2) How do cemented and uncemented implants influence radiographic wear outcomes in the hip?

Methods: A systematic review was conducted based on a PubMed search of the hip and knee arthroplasty literature. PubMed identified 391 studies of which 28 met the inclusion criteria for a weighted-averages analysis of two-dimensional femoral head penetration rates.

Two reviewers (JDP, HAG) extracted information from 44 hip studies independently using a standardized extraction form. Information extracted included number of patients, patient demographic information (age, gender, weight, body mass index), follow up time, fixation modes (uncemented/cemented), and radiographic wear outcome measures (polyethylene two-dimensional total linear penetration rates). Extracted data were compared, and in the case of disagreements, original data were rechecked by both investigators and resolved by discussion and consensus with the last author (SMK). Studies with duplicate trial data or lack of relevant clinical data were excluded, as well as studies with less than 2 years of radiographic follow up for wear. Only 2 studies for HXLPE in knee arthroplasty were identified which was insufficient for a detailed evaluation for systematic review and weighted-averages analysis.

By inspecting the extracted data, we determined sufficient information was available to compare 2-D femoral head penetration outcomes among a subset of the reported THA studies. Specifically, 2D linear penetration rates were pooled from randomized controlled trials (RCTs) and prospective and retrospective cohort studies with comparable outcome measures to conduct a weighted averages analysis using a random-effects model using the Comprehensive Meta-analysis™ Version 2.2 software (Biostat, Englewood, NJ). The 28 studies included in the weighted averages are comprised of nine RCTs and 19 observational cohort studies. To determine whether patient factors or fixation modes influenced reported radiographic penetration rates, the continuous data for each of the factors listed in Table 1 were converted to dichotomous categorical data.

Results: Our results showed that the weighted average linear penetration rate for conventional UHMWPE liners in patients above the age of 60 was lower than that of younger patients (≤ 60yo) (Fig 1), possibly due to lower levels of activity. However, no difference in the linear penetration rates for the HXLPE liners was found between the 2 age groups and was significantly lower when compared to conventional liners (Fig 1).

Factor	Categories
Age	≤ 60 years or > 60 years
BMI	≤ 25 kg/m^2 or >25 kg/m^2
Weight	>150 lbs
Fixation	Uncemented or Cemented

Table 1. Factors considered in the systematic review of 2D linear penetration rates

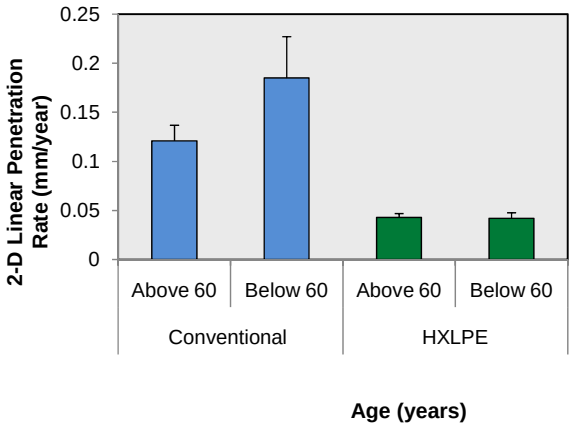

Figure 1. Pooled 2-D linear penetration rates of conventional and HXLPE liners in hips

When comparing the pooled linear penetration rates of obese patients (BMI >25 kg/m^2) with conventional UHMWPE liners to those with HXLPE liners, we found that the rates were markedly lower in patients with HXLPE liners (0.045 mm/year; SE=0.007 vs. conventional 0.141mm/year; SE=0.012). The pooled HXLPE linear penetration rates were similar in patients with and without obesity. Similarly, in patients with an average weight of >150 pounds, the 2-D penetration rates were higher in patients with conventional liners (0.138mm/year; SE=0.02) versus those with HXLPE liners (0.059 mm/year; SE=0.01).

The mode of fixation did not have considerable influence on the wear of HXLEP and conventional PE liners. However, the overall pooled penetration rates for uncemented (0.041 mm/year; SE=0.004) and cemented (0.061 mm/year; SE=0.02) HXLPE liners was markedly lower in comparison to uncemented (0.156 mm/year; SE=0.02) and cemented (0.125 mm/year; SE= 0.043) conventional PE liners.

Conclusions: Our results showed reduced wear in patients with HXLPE liners, regardless of patient or fixation factors, which supports the use of HXLPE liners over conventional polyethylene liners.

References: [1] Kurtz SM, Gawel HA, Patel JD. Clin Orthop Relat Res 2011 Mar 23 Epub

Wear Evaluation of Simpirica's LimiFlex™ Flexion-Limiting Device Containing UHWMPE Straps

Ryan Siskey, M.S.[1,2], Louie Fielding[3], Anand Parikh[3], Steven Kurtz, Ph.D.[1,2]
[1]Exponent, Philadelphia PA; [2]Drexel University, Philadelphia PA, [3]Simpirica Spine, Inc., San Carlos, Ca
rsiskey@exponent.com

Statement of Purpose:
The LimiFlex™ Spinal Stabilization System is a new, minimally-invasive flexion-restricting device that stabilizes a spinal segment by limiting the spreading of the spinous processes in flexion. The LimiFlex Device includes a pair of titanium couplers secured to medical-grade ultra-high molecular weight polyethylene (UHMWPE) straps that pass around adjacent spinous processes. The system is illustrated below as Figure 1. The purpose of this experiment was to assess wear of the LimiFlex device per *ASTM F2624 Standard Test Method for Static, Dynamic and Wear Assessment of Extra-Discal Spinal Motion Preserving Implants*.

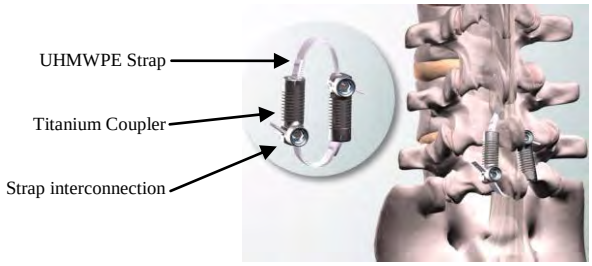

Figure 1. LimiFlex™ Spinal Stabilization System

Methods:
Eight devices were used for wear assessment: six were assigned as wear samples and two used for load soak control samples. All devices were packaged, sterilized commercial units. Devices were provided assembled and sized by Simpirica Spine. A six degree of freedom spine wear simulator (MTS, Eden Prarie, MN) and custom stainless steel spinous process fixtures were used for testing (Figure 2). *Ex vivo* biomechanical validation found the average moment-arm for the LimiFlex Device to be R=47.2±2.0mm (range: 44.0 – 49.1mm) from the center of rotation of the motion segment. Therefore a moment-arm R from the device to the center of the test fixtures was chosen to be R=50mm. The selected moment arm was chosen as a worst-case scenario in which the device would experience maximum elongation and load, for this study.

The entire test (including presoak) was conducted using environmental chambers holding fluid at 37±3°C, to simulate the *in vivo* environment and its effect on the UHMWPE straps. Devices were pre-soaked for 155 days in distilled water to stabilize the samples. Wear testing was conducted in phosphate buffered saline to simulate body fluid, as allowed by ASTM F2624. The two soak control samples were installed and loaded in axial tension at static tensile load of approximately 16N. The six wear samples were installed with a preload of 2-5N to settle the device into the fixtures and ensure consistent installation. The axial displacement of each wear station was locked so that the coupled motion would load the devices. A sinusoidal, coupled cyclic loading was applied to the six wear test samples at a rate of 2Hz per ASTM F2624. Specifically, ±7.5° flexion/extension, ±3° right/left axial rotation, and ±6° right/left lateral bending were applied to each sample. The profile resulted in the maximum elongation of the device and required that the axial rotation and lateral bending motions be in-phase; and that the flexion/extension motion be 180° from the other two motions.

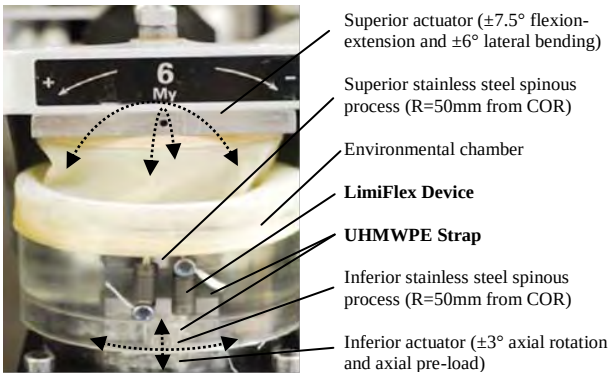

Figure 2. Wear Station Setup

The test was conducted to 10-million cycles and interval analysis performed every 250,000 cycles from 0-1M cycles, every 0.5M cycles until 2M cycles; and every 1M thereafter. During each interval analysis, the testing medium was replaced, and the fluid from each chamber was frozen for subsequent analysis. All devices were cleaned, dried and weighed per Annex A4 of ASTM guide F1714. Devices were rinsed with deionized water and acetone and then dried with compressed air and desiccated for 18-24 hours. Control and test articles were weighed in rotation three times each, using a Sartorius balance (Bohemia, NY). The mass of each device (including controls) was recorded at all pre-soak and test intervals. Wear results were calculated and interpreted per ASTM F2624. Volumetric wear was not calculated due to heterogeneous materials (titanium and polyethylene) and the complex geometry of the strap weave.

The size distribution and morphology of any particle debris generated during the test was determined per *ASTM F1877 Standard Practice for Characterization of Particles*. Fluid samples from 1.5MC and 10MC were selected for particle analysis representing run-in and steady-state wear rates respectively. From each of these intervals, three fluid samples were analyzed, representing the lowest, average and highest gravimetric changes from the respective analysis intervals. From each 400mL sample, 150mL was enzymatically digested (TergAZyme®, Alconox, White Plains, NY) at 50°C for 24 hours to remove bacterial contamination. Digested samples were filtered using first 1.0µm and then 0.1µm filters to isolate particles >1.0µm and 0.1-1.0µm. Filtered samples were platinum sputter coated and imaged with scanning electron microscopy (SEM) using an analytical scanning electron microscope (FEI/Phillips XL30 SEM). Per ASTM F1877, five fields of view were SEM imaged from each filtered specimen at 1,000x magnification for the 1.0µm filters and 10,000x magnification for the 0.1µm filters. Energy dispersive x-ray (EDS) analysis was conducted to capture elemental composition of the filtered particles using an EDS detector (EDAX, Mahwah, NJ) equipped with the SEM. SEM micrographs were processed with Adobe Photoshop (San Jose, CA) and a custom script in NIH ImageJ (National Institutes of Health, USA) to obtain particle counts and parameters described by ASTM F1877.

Results:

All test articles endured 10 million cycles of the prescribed coupled cyclic loading without failure. Minimal changes in dynamic stiffness and device length were observed throughout the test. Gravimetric results are summarized in Figure 3.

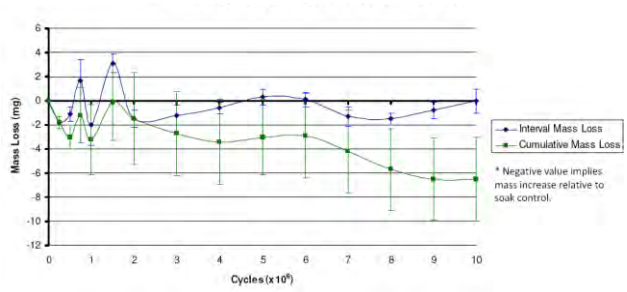

Figure 3. Load-soak-adjusted interval and cumulative mass loss for the six wear samples.

After completion of 10 million cycles, the samples were washed using an enzymatic cleaner (TergAZyme®, Alconox, White Plains, NY) at 50° C for 24 hours to minimize the gravimetric effects of any confounding bacterial contamination. Following cleaning the samples were again allowed to dry for 24 hours and then re-weighed. This process reduced the average mass gain from 6.5 ± 3.5 mg to 3.8 ± 2.7 mg (Δ = 2.7 mg). Consistent with the gravimetric results, the test articles displayed a slight discoloration of the straps consistent with bacterial contamination typical of such a long-duration test. The straps did exhibit some polishing of the strap surfaces where they contact the simulated stainless steel spinous process fixture.

The results of the particle analysis, including size and shape parameters per ASTM F1877, are summarized below as Table 1. The particle size distribution for all samples was a bimodal distribution centered at 0.1-0.2µm and 1-2µm (Figure 4). A representative particle size distribution is provided below. SEM images and EDS elemental analysis were also consistent across all samples. Elemental analysis revealed carbon and oxygen consistent with polymeric debris; sodium consistent with salt residue from the saline solution; platinum consistent with the coating applied to the particles; and finally silicon indicating that the polymeric particles are likely from the rubber gasket used to seal the environmental chamber to the test machine. A representative SEM micrograph and EDS spectra are provided as Figure 5.

Table 1. Summary of ASTM F1877 particle parameters.

Cycle [MC]	Wear Station	Particles [N]	Equivalent Diameter [µm]	Aspect Ratio	Roundness	Elongation	Form Factor
1.5	1	836	0.79±0.92	2.25±1.24	0.53±1.19	1.53±0.57	0.42±0.23
1.5	3	712	0.75±0.82	2.03±1.00	0.57±0.94	1.44±0.51	0.43±0.25
1.5	5	814	1.14±0.94	2.06±0.92	0.56±0.97	1.47±0.51	0.39±0.25
10	4	825	1.09±1.05	2.14±1.13	0.55±0.97	1.45±0.45	0.36±0.24
10	6	1563	1.05±0.98	1.94±0.82	0.58±0.97	1.40±0.41	0.51±0.23
10	5	1129	1.10±1.06	2.01±0.98	0.57±0.98	1.41±0.46	0.38±0.26

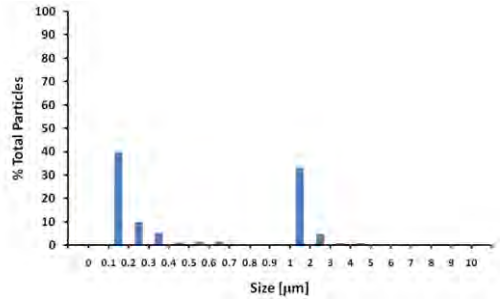

Figure 4. Representative particle size distribution.

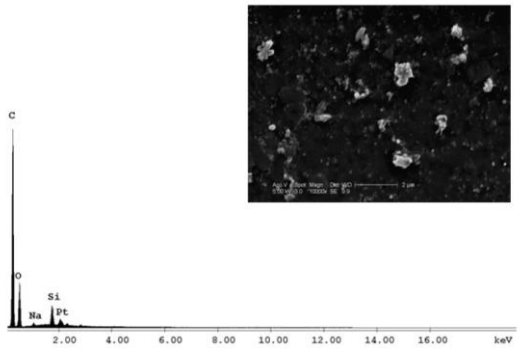

Figure 5. Representative SEM micrograph and EDS spectra at 1.5MC.

Conclusions:

A 10.0 million cycle wear test of the LimiFlex Device was conducted to evaluate the LimiFlex Device using ASTM F2624 as a guide. All samples were found to increase in mass over the duration of the test; enzymatic digestion reduced, but did not eliminate the mass increase. However, changes were extremely small (< 0.1% of the average initial mass of all eight devices) and bordered on the detectable limits of wear. No functional failures of the couplers or UHMWPE straps were observed during the test. As described above, wear was undetectable using gravimetric techniques. The articulating surfaces of the UHMWPE strap demonstrated an extremely mild burnished appearance consistent with very mild abrasive wear against the stainless steel spinous process fixtures. No evidence of wear of the titanium couplers was observed. Particle analysis of the test medium revealed a small amount of particulate debris, most likely from the rubber gaskets sealing the environmental chambers. In this cyclic multi-axial *in vitro* wear test, the LimiFlex Device showed almost no wear and did not generate any biologically relevant wear debris from the UHMWPE straps or titanium coupler components.

References:

1.) ASTM F2624-07 Standard Test Method for Static, Dynamic, and Wear Assessment of Extra-Discal Spinal Motion Preserving Implants
2.) ASTM F1714-98(2003) Standard Guide for Gravimetric Wear Assessment of Prosthetic Hip Designs in Simulator Devices
3.) ASTM F1877-05 Standard Practice Characterization of Particles

Wear Analysis of Fixed and Mobile Bearing Knee Systems

Korduba, LA; Loving, L; Herrera, L; Essner, A.
Stryker Orthopaedics, Mahwah, NJ

Statement of Purpose: The debate between fixed-bearing and mobile-bearing systems continues due to the lack of clinical evidence showing survivorship of one to be superior to the other [1,2]. Literature states theoretical benefits to mobile-bearing systems in terms of wear because of the decoupling of motion onto two articulating surfaces [3]. However, literature also indicates there is a higher occurrence of osteolysis in mobile bearing knees compared to fixed bearing knees [4]. Therefore, the purpose of this study was to compare the wear properties and characterize the polyethylene debris of commercially available fixed-bearing and mobile-bearing knee systems.

Methods: The fixed-bearing system (Triathlon®, Stryker Orthopaedics, Mahwah, NJ) consisted of cobalt chrome femoral components and tibial trays, and polyethylene inserts that were manufactured from GUR 1020 UHMWPE that was sequentially irradiated to 30 kGy and annealed three times and then gas plasma sterilized (X3®, Stryker Orthopaedics, Mahwah, NJ).

Both mobile-bearing systems consisted of cobalt chrome femoral components and tibial trays (Mobile1-LCS, Mobile2-Sigma, DePuy, Warsaw, IN). The polyethylene inserts were manufactured from GUR 1020 that was sterilized using gamma irradiation in a near vacuum environment (GVF, DePuy, Warsaw, IN).

A 6-station knee simulator was utilized for testing (MTS, Eden Prairie, MN). All motion and loading was computer controlled and followed ISO 14243-3 [5]. The lubricant used was Alpha Calf Fraction (Hyclone Labs, Logan, UT) diluted to 50% with a pH-balanced 20-mMole solution of deionized water and EDTA [6]. Standard test protocols were used for cleaning, weighing and assessing the wear loss of the inserts [7]. Statistical analysis was performed using the Student's t-test.

A serum sample from each testing group was collected after testing. Samples were protein digested following the published process by Scott et al [8]. The digested serum was then filtered through a series of polycarbonate filter papers (pore size = 0.05 µm) and analyzed using scanning electron microscopy. Image fields were randomized and wear debris was compared in terms of its aspect ratio and equivalent circular diameter (ECD).

Results: The results of wear testing are shown in Figure1. There is a significant decrease of 95% and 93% for the fixed-bearing system compared to the two mobile-bearing systems ($p < 0.05$). The size and distribution of particles are displayed in Table 1 and Figure 2.

Conclusions: Wear testing shows that the fixed-bearing system produced significantly less wear than the mobile-bearing systems. The increase in contact area due to two articulating surfaces may predominately affect wear [9].

The debris analysis and wear rates correlate to one another. The fixed-bearing design has the lowest wear rate and produces smaller and fewer particles than the mobile-bearing designs. Only 6 and 2 images, respectively, were needed to reach a minimum of 100 particles for Mobile1 and Mobile2, while the fixed-bearing system required 16 images. The average aspect ratio of the mobile-bearing designs indicates an increased generation of fibrillar and larger elongated particles than the fixed-bearing design. The increased contact area of the mobile-bearing knee combined with the difference in polyethylene, leads to an increase in wear and number of wear particles. [9] This increase in wear rate and number of particles which could ultimately lead to osteolysis and failure of the implant.

It is important to note that all three knee systems are commercially available; however, the mobile-bearing systems are not available with a highly crosslinked polyethylene, like the fixed-bearing system is. This difference in polyethylene material may play a large role in the differences seen in wear properties. However, the contribution of material difference cannot be determined from this study.

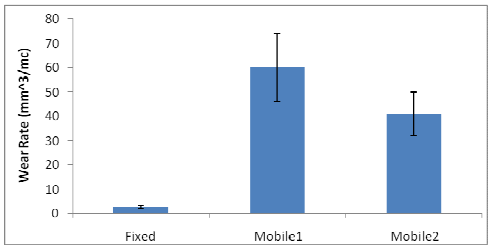

Figure 1: The wear rate after 1 million cycles of testing.

	Mobile 1	Mobile 2	Fixed
Aspect Ratio	2.41 ± 1.69	1.98 ± 1.04	1.58 ± 0.92
ECD	0.29 ± 0.16	0.28 ± 0.16	0.19 ± 0.07

Table 1: Average values for the debris of the three systems.

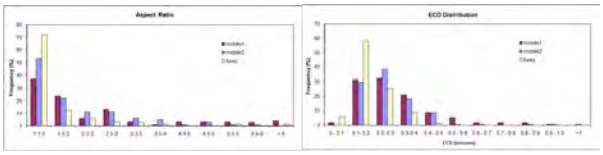

Figure 2: Wear debris distribution plots

References: [1] Bhan S, et al. J Bone Joint Surg, 87-A(10): 2290, 2005. [2] Aglietti P, et al. J Arthroplasty, 20(2): 145, 2005. [3] Haider H, et al Clin Orthop Relat Res, 466: 2677, 2008. [4] Huang CH, et al. J Bone Joint Surg, 84: 2224, 2002. [5] ISO/DIS 14243-3. [6] Wang, A., et al., J. Biomed. Mater. Res. Part B: Appl Biomater 68B: 45, 2004 [7] ASTM F2025 [8] Scott M, et al, Trans 6th WBC, 2000:177. [9] Mazzucco D, et al.. Wear, 254: 514, 2003.

For submission: Convert to PDF and email abstract with contact information to skurtz@exponent.com

High Oxidation- and Wear-resistances of Polyethylene Arisen by Vitamin E-blending and Poly(MPC) Grafting

Masayuki Kyomoto[1, 2, 3], Toru Moro[2], Kenichi Saiga[1, 2, 3], Yoshio Takatori[2], Kazuhiko Ishihara[1].
[1]Department of Materials Engineering, [2]Division for Joint Reconstruction, The University of Tokyo,
[3]Research Department, Japan Medical Materials Corporation

Statement of Purpose: We have recently developed a novel surface modification technology (Aquala® technology) with poly(2-methacryloyloxyethyl phosphorylcholine) (PMPC)-grafting for an acetabular cup in an artificial hip joint system, aiming to reduce wear and avoid bone resorption [1]. The oxidation- and wear-resistances determined *in vitro* and *in vivo* are important indicators of the clinical performance of acetabular cups. For improvement of these indicators, it is a technological factor to consider not only the bearing surface of implant, but also the substrate material. The purpose of this study is to investigate the effects of substrate materials, such as vitamin E-blended cross-linked polyethylene (CLPE), on the oxidative and tribological stabilities of PMPC-grafted CLPE and to examine the possibility of controlling the longevity of artificial hip joints by utilizing this material.

Methods: Compression-molded sheet stock of 0.1 mass% vitamin E-blended polyethylene (GUR1020 resin; Quadrant PHS Deutschland GmbH) was gamma-irradiated with a highly dose of 100-150 kGy and annealed at 120°C for 7.5 hours for cross-linking (HD-CLPE+E). The HD-CLPE+E specimens were machined from this sheet stock. The HD-CLPE+E specimens coated with benzophenone were immersed in the 0.5 mol/L aqueous MPC solution. The photo-induced graft polymerization on the HD-CLPE+E surface was carried out with ultraviolet irradiation of 5 mW/cm^2 at 60°C for 90 min [2]. Then, the PMPC-grafted HD-CLPE+E was sterilized by gamma-ray with a dose of 25 kGy under N_2 gas. A CLPE with 50 kGy gamma-ray irradiation and 25 kGy gamma-ray sterilization was used as control.

The surface properties of the PMPC-grafted HD-CLPE+E were examined by Fourier-transform infrared (FT-IR) spectroscopy, X-ray photoelectron spectroscopy (XPS), and the static water-contact angle measurement. The oxidative property of accelerative aged PMPC-grafted HD-CLPE+E (ASTM F2003) was evaluated by FT-IR according to ASTM F2102. The wear test was performed using a 12-stations hip joint simulator (MTS System Corp.). A mixture of 25% bovine serum, 20 mM/L of ethylene diamine tetraacetic acid, and 0.1% sodium azide was used as lubricant. Loads simulating a physiologic loading curve with double peaks of 1793 and 2744 N loads were applied with a frequency of 1 Hz.

Results: After PMPC-grafting, the peaks ascribed to MPC unit were clearly observed in both FT-IR and XPS spectra. The static water-contact angle of both the PMPC-grafted CLPE and HD-CLPE+E was approximately 15°. Oxidation index of CLPE and PMPC-grafted CLPE increased gradually and reached approximately 2.0 (Fig. 1). In contrast, the oxidative degradation of the PMPC-grafted HD-CLPE+E was hardly observed.

After 5.0 × 10^6 cycles of the simulator test, both the PMPC-grafted CLPE and HD-CLPE+E were found to show extremely low and stable wear (Fig. 2).

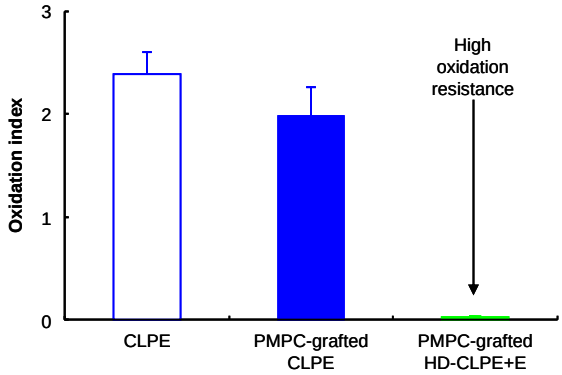

Fig. 1. Oxidation index of PMPC-grafted HD-CLPE+E after accelerative aging.

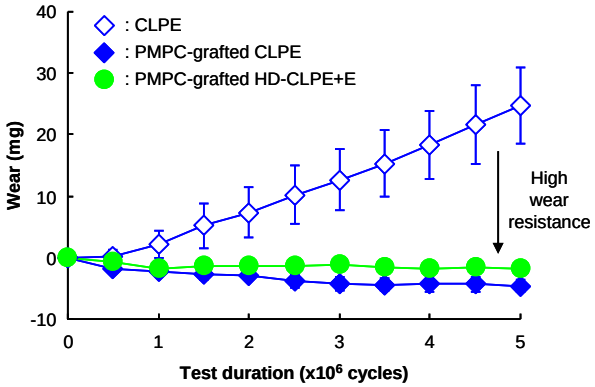

Fig. 2. Volumetric wear of PMPC-grafted HD-CLPE+E in the hip joint simulation test.

In this study, we confirmed that the PMPC-grafted layer was successfully fabricated on the HD-CLPE+E surface, and the PMPC-grafted HD-CLPE+E brought high oxidation- and wear-resistances. When the surface is modified by PMPC grafting, the PMPC-grafted layer leads to a significant reduction in the sliding friction between the surfaces which are grafted because water thin films formed can act as extremely efficient lubricants. In addition, the large-scale clinical trials of total hip arthroplasty with PMPC-grafted CLPE acetabular cups are currently underway to evaluate clinical efficiency.

And, in spite of high-dose gamma-ray irradiation for cross-linking, the substrate modified by vitamin E-blending maintains high oxidation-resistance, because vitamin E can act as extremely efficient radical scavenger.

Conclusions: In conclusion, the novel concept Aquala® technology is applicable for several type of CLPE. The HD-CLPE+E makes not only high wear resistance but also high oxidation-resistance, and can pioneer the "next generation" artificial joint.

References: [1] Moro T. Nature Mater. 2004;3:829-837, [2] Kyomoto M. Clin Orthop Relat Res 2011;469:2327-2336.

For submission: Convert to PDF and email abstract with contact information to skurtz@exponent.com

High Oxidation- and Wear-resistances of Polyethylene Arisen by Vitamin E-blending and Poly(MPC) Grafting

Masayuki Kyomoto[1, 2, 3], Toru Moro[2], Kenichi Saiga[1, 2, 3], Yoshio Takatori[2], Kazuhiko Ishihara[1].
[1]Department of Materials Engineering, [2]Division for Joint Reconstruction, The University of Tokyo,
[3]Research Department, Japan Medical Materials Corporation

Statement of Purpose: We have recently developed a novel surface modification technology (Aquala® technology) with poly(2-methacryloyloxyethyl phosphorylcholine) (PMPC)-grafting for an acetabular cup in an artificial hip joint system, aiming to reduce wear and avoid bone resorption [1]. The oxidation- and wear-resistances determined *in vitro* and *in vivo* are important indicators of the clinical performance of acetabular cups. For improvement of these indicators, it is a technological factor to consider not only the bearing surface of implant, but also the substrate material. The purpose of this study is to investigate the effects of substrate materials, such as vitamin E-blended cross-linked polyethylene (CLPE), on the oxidative and tribological stabilities of PMPC-grafted CLPE and to examine the possibility of controlling the longevity of artificial hip joints by utilizing this material.

Methods: Compression-molded sheet stock of 0.1 mass% vitamin E-blended polyethylene (GUR1020 resin; Quadrant PHS Deutschland GmbH) was gamma-irradiated with a highly dose of 100-150 kGy and annealed at 120°C for 7.5 hours for cross-linking (HD-CLPE+E). The HD-CLPE+E specimens were machined from this sheet stock. The HD-CLPE+E specimens coated with benzophenone were immersed in the 0.5 mol/L aqueous MPC solution. The photo-induced graft polymerization on the HD-CLPE+E surface was carried out with ultraviolet irradiation of 5 mW/cm^2 at 60°C for 90 min [2]. Then, the PMPC-grafted HD-CLPE+E was sterilized by gamma-ray with a dose of 25 kGy under N_2 gas. A CLPE with 50 kGy gamma-ray irradiation and 25 kGy gamma-ray sterilization was used as control.

The surface properties of the PMPC-grafted HD-CLPE+E were examined by Fourier-transform infrared (FT-IR) spectroscopy, X-ray photoelectron spectroscopy (XPS), and the static water-contact angle measurement. The oxidative property of accelerative aged PMPC-grafted HD-CLPE+E (ASTM F2003) was evaluated by FT-IR according to ASTM F2102. The wear test was performed using a 12-stations hip joint simulator (MTS System Corp.). A mixture of 25% bovine serum, 20 mM/L of ethylene diamine tetraacetic acid, and 0.1% sodium azide was used as lubricant. Loads simulating a physiologic loading curve with double peaks of 1793 and 2744 N loads were applied with a frequency of 1 Hz.

Results: After PMPC-grafting, the peaks ascribed to MPC unit were clearly observed in both FT-IR and XPS spectra. The static water-contact angle of both the PMPC-grafted CLPE and HD-CLPE+E was approximately 15°. Oxidation index of CLPE and PMPC-grafted CLPE increased gradually and reached approximately 2.0 (Fig. 1). In contrast, the oxidative degradation of the PMPC-grafted HD-CLPE+E was hardly observed.

After 5.0 × 10^6 cycles of the simulator test, both the PMPC-grafted CLPE and HD-CLPE+E were found to show extremely low and stable wear (Fig. 2).

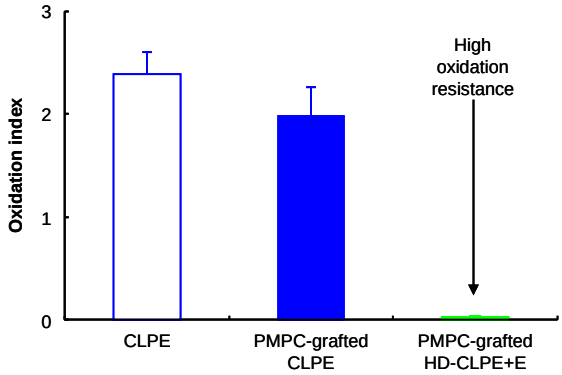

Fig. 1. Oxidation index of PMPC-grafted HD-CLPE+E after accelerative aging.

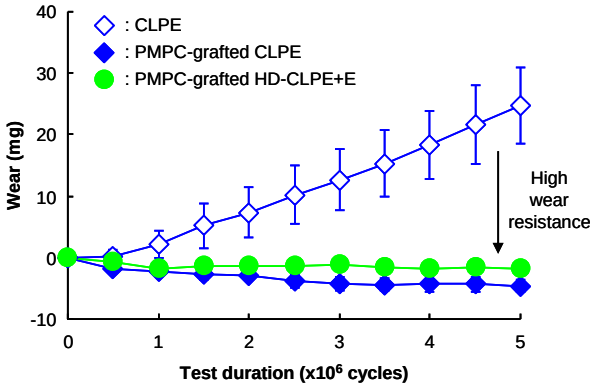

Fig. 2. Volumetric wear of PMPC-grafted HD-CLPE+E in the hip joint simulation test.

In this study, we confirmed that the PMPC-grafted layer was successfully fabricated on the HD-CLPE+E surface, and the PMPC-grafted HD-CLPE+E brought high oxidation- and wear-resistances. When the surface is modified by PMPC grafting, the PMPC-grafted layer leads to a significant reduction in the sliding friction between the surfaces which are grafted because water thin films formed can act as extremely efficient lubricants. In addition, the large-scale clinical trials of total hip arthroplasty with PMPC-grafted CLPE acetabular cups are currently underway to evaluate clinical efficiency.

And, in spite of high-dose gamma-ray irradiation for cross-linking, the substrate modified by vitamin E-blending maintains high oxidation-resistance, because vitamin E can act as extremely efficient radical scavenger.

Conclusions: In conclusion, the novel concept Aquala® technology is applicable for several type of CLPE. The HD-CLPE+E makes not only high wear resistance but also high oxidation-resistance, and can pioneer the "next generation" artificial joint.

References: [1] Moro T. Nature Mater. 2004;3:829-837, [2] Kyomoto M. Clin Orthop Relat Res 2011;469:2327-2336.

Oxidation in UHMWPE Powder Containing Vitamin E: Combined TSL, ESR, and FTIR Analyses

Dereje Abdi, Benjamin Walters, M Shah Jahan
The University of Memphis, Memphis, TN

Statement of Purpose: Oxidation in UHMWPE with and without vitamin E has been studied quite extensively in literature.[1] Most show limited or no oxidation in vitamin-E-containing UHMWPE, depending on concentration. While existing literature contains information comparing consolidated UHMWPE, we have studied the UHMWPE powder in an attempt to obtain a more basic understanding of the activity in the unconsolidated material. GUR1050 powder, and the same powder containing 1000ppm vitamin E (provided by Ticona, Florence, KY), were irradiated (Steris, Libertyville, IL) to 30-kGy-gamma in both air and in nitrogen. We have then used electron spin resonance (ESR) to observe free radical behavior at multiple time periods in air, and compared with similarly-timed thermally stimulated luminescence (TSL) measurements, in an attempt to correlate the two sets of observations. Finally, FTIR testing was performed at the conclusion of the measurements (after 90 days in air) to obtain oxidation data, relative amongst the samples. Hopefully these results with provide an additional information point to include among the existing literature concerning vitamin E in UHMWPE, enabling a more thorough understanding of its interactions.

Methods:

- Two types of UHMWPE resin powders were used:
  1. GUR 1050-E (containing 1000 ppm vitamin E)
  2. GUR 1050 (without vitamin E)
- There were three conditions for both 1050 and 1050-E:
  1. Gamma-irradiated in air at RT (30kGy).
  2. Gamma-irradiated in nitrogen at RT (30-kGy).
  3. No irradiation (virgin material), stored in air.

Irradiated samples remained in their environments (air or nitrogen) for 10 days, at which time they were all opened to air and "initial" or "0 minute" testing was performed.

- Three types of post-irradiation testing performed:
  1. ESR: Bruker EMX X-band; microwave power ranging from 0.01mW to 40mW. Testing at room temperature in air. Equal mass tested for each sample. Two samples for each condition were tested initially and at each subsequent time period: 1, 13, 43, 69, and 90 days.
  2. TSL: Harshaw-Bicron 3500, powders heated in DSC pans, from room temp. to 299^{o}C in a dry nitrogen environment. Three samples for each condition were tested initially and at each subsequent time period: 1, 13, 69, and 90 days.
  3. FTIR: Thermo Scientific Nicolet iN10. Three samples for each condition were tested at the conclusion of the ESR and FTIR measurements (after 90 days in air). The ratio of the areas of carbonyl absorption near 1720 cm^{-1} to the areas of the absorption peak centered near 1370 cm^{-1} were used as comparative, arbitrary values of oxidation, relative amongst the samples.

Results and Conclusions:

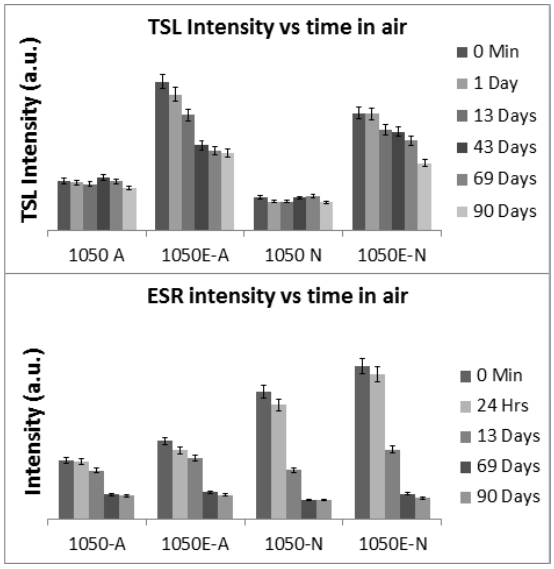

Figure 1: (Top) TSL intensity vs. time in air, and (bottom) ESR intensity vs. time in air, up to 90 days.

Powder	Irradiated	Stored	Oxidation	Stdev.
1050	Air	Air	0.84	0.06
1050-E	Air	Air	0.50	0.03
1050	Nitrogen	Air	0.65	0.03
1050-E	Nitrogen	Air	0.55	0.02

Table 1: FTIR after 90 days in air (relative values).

TSL results suggest that (Fig. 1) 1050-E shows a weak luminescence peak without gamma-irradiation and this peak (which is at peak shoulder near 185^{o}C) has a much higher intensity in the irradiated samples. This peak is unaffected by the presence of air and may be attributed to thermally stimulated recombination of the vitamin E radicals. The ESR data (Fig. 1) suggest that, irrespective of the initial irradiation environment, there is a significant decay of free radicals in all of the samples; at the end of the 69 days all the samples shows a similar structure of ESR spectra. The sample containing vitamin E that was irradiated in nitrogen shows a higher decay rate; the non-vitamin E sample, irradiated in air, shows the least decay rate. From FTIR data (Table 1), GUR1050 irradiated in air shows higher oxidation which is due to the reaction of free radicals with oxygen. Still, some significant amount of oxidation is observed in GUR1050E powder sample.

References:

[1] e.g., see Kurtz UHMWPE Handbook 2nd ed. ch. 15, 16, 21, 29, and references therein.

Acknowledgements: Thanks to Wright Medical Technology (Arlington, TN) for use of their FTIR facilities.

Detection of Oriented Allyl Radicals at Room Temperature in Gamma-Irradiated UHMWPE

Jahan M. Shah[1], M.S. Mehmood[1, 2] and Benjamin M. Walters[1]
[1]*Biomaterial Research Lab, Physics Department, University of Memphis, Memphis TN 38152, USA*
[2]*Pakistan Institute of Engineering and Applied Sciences, Nilore, Islamabad 45650, Pakistan*
Corresponding author email: mjahan@memphis.edu

Statement of Purpose: The well-studied six-line pattern due to an alkyl radical and the seven-line pattern due to an allyl radical in the respective ESR spectrum of gamma-irradiated UHMWPE are produced by an average coupling/splitting from the nearby protons.[1] Because the PE molecules are randomly oriented in the semi-crystalline UHMWPE matrix, the protons (hydrogen atoms) at nearest (α protons) and next nearest (β protons) positions from the unpaired electron site (radical site, Fig. 1) are indistinguishable. The effects of the α- and β-protons on the ESR spectrum were demonstrated by Ohnishi et al. in an oriented or stretched PE at low temperatures.[2] In this study, we detected oriented allyl radicals at room temperature in gamma irradiated UHMWPE. The effects of vitamin E and storage at room temperature were also investigated during the study.

Fig.1. Molecular structure of an allyl radical.

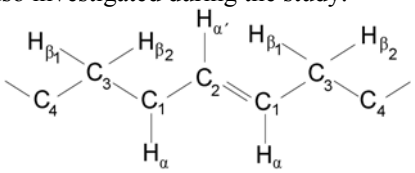

Methods: All samples were prepared from GUR 1020 (Ticona) powder containing 0.1% by wt. vitamin E (α tocopherol). Samples without vitamin E were also used in this study. Compression-molded bar stocks were prepared using a customized Wabash vantage series 50 ton heating press. These samples were irradiated with gamma rays using ^{60}Co source for a total dose of 100-kGy (Steris-Isomedix). Following irradiation, the powder samples were stored at -78.5 ^{o}C (dry ice temperature) and consolidated samples were stored at -196^{o}C (liquid nitrogen temperature) for approximately one year to minimize the radical reaction.

Free radicals were detected at room temperature using an X-band ESR spectrometer (EMX 300 by Bruker), operating near 9.8 GHz microwave frequency and 100 kHz modulation and detection frequencies. All ESR spectra (first derivative of absorption) were recorded using microwave power ranging from 0.01-1mW at 2G modulation amplitude.

Results: While we tested powder as well as compression-molded solids, with or without vitamin E, we present ESR spectrum of powder samples only. Figure 2 (a) shows a typical ESR spectrum recorded at room temperature following 100-kGy gamma dose and subsequent storage at -78.5 ^{o}C for one year. The simulated component spectra are: 5% alkyl (Fig. 2(c)), 65% allyl (Fig. 2 (d)) and 30% polyenyl (Fig. 2 (e)) produced a 98.7%-best fit spectrum Fig. 2 (b). Furthermore, the allyl radical signal gives approximately 20 % of random orientations and 80 % of oriented molecules. In oriented PE, measured at -196^{o}C, Ohnishi observed 25 lines within a total magnetic field width of approximately 133 G. Our spectra also show 25 lines spread over 136 G.

According to the published reports, the theoretical values of hyperfine (hf) coupling constant α_1 and α_2 proton in the "allyl –type" radical are 6.9 G and 18.7 G, respectively.[2] The corresponding values in our study are approximately 6 G and 18 G, respectively. However, our observations of the ESR spectra due to allyl radical are different from recently published report of Zhao et al.[3] in which they observed 11 lines for allyl radical because of small hf value of α_1 proton. The allyl radical is distributed over three carbon atoms as shown in Fig.1. It interacts with three hydrogen atoms at α positions (one at α_1 and two at α_2 position) and four β hydrogen (two β_1 and two β_2) with different hf constants.[2,3] The hyper fine values for six hydrogen atoms (two at α position and four at β position) give the seven-line ESR spectrum, and the contribution from α_1 hydrogen atom results in a doublet structure. The best fit (with fitting correlation of 0.94) of the experimental spectrum (Fig. 2) using WinSim program[4] gives the hf constant values of α_1, α_2, β_1 and β_2 5.9, 17.2, 23.6 and 12.7, respectively. The values of hf constants reported earlier for allyl radicals in highly oriented polyethylene fibers at +11 °C are 5.51, 21.3, 24.4 and 17.4, respectively. These additional lines, also known as superhyperfine lines, disappear or decay in 24 hours in air.

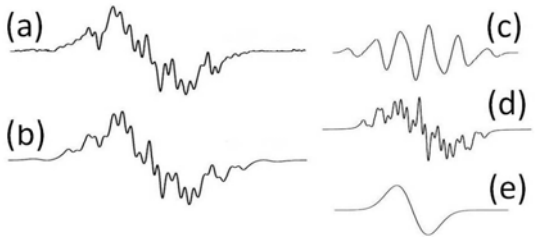

Fig. 2. Experimental (a) and simulated (b) ESR spectra of 100-kGy powder sample. The simulated component spectra are: alkyl (c) allyl (d) and polyenyle (e).

Conclusions: Production of superhyperfine lines ESR spectra of 100-kGy UHMWPE at room temperature, due to separate couplings of α- and β-protons with the unpaired electron at the free radical site, is reported for the first time, to our knowledge. The results further suggest that allyl radicals are ~ 80% oriented. While similar spectra are produced by vitamin E-containing powder and consolidated solids, the superhyperfine pattern disappears in all samples in 24 hours in air.

References

1. Jahan, 2009, UHMWPE Biomaterials Handbook 2nd ed., Ch. 29, 433-449.
2. Ohnishi, et. al. 1962. J. Chem. Phys. 37, 1283–1288.
3. Zhao et. al. 2010. Radiat. Phys. Chem. 79, 429-433.
4. Duling, et. al. 2004 J Mag Reso. B. 104, 105-110.

Acknowledgments

Higher Education Commission (HEC), Pakistan.
NSF IUCB at the Univ. of Memphis.

Comparison of Damage in Design Matched Mobile and Fixed Bearing Total Knee Arthroplasty Prostheses

Kirsten E. Stoner[1], Seth Jerabek[1], Stephanie Tow[1], Natalie Kelly[2], Timothy Wright[1], Douglas Padgett[1].
[1]Hospital for Special Surgery, New York, NY.
[2]Cornell University, Ithaca, NY

Statement of Purpose:

One of the most challenging issues in total knee arthroplasty design is creating an implant that is highly resistant to wear damage. Implants with greater surface congruity allow polyethylene contact stresses to decrease; however, this also causes larger stresses at the fixation interface that can lead to implant loosening. The mobile bearing implant was designed to balance these two competing objectives: allow a high surface congruity to decrease polyethylene contact stresses and rotational mobility to decrease fixation interface stresses.

A previous damage study by Kelly et. al. showed that mobile bearing implants have higher damage scores when compared to published fixed bearing damage scores.[1] The documented fixed bearing scores were taken from sample sizes of different designs than that of the mobile bearing. To have a more accurate comparison between fixed and mobile implants, the design must be similar. Therefore we assessed the wear damage of DePuy Sigma Fixed implants and compared the damage characteristics to those of the previously reported DePuy Sigma Mobile.[1] We examined the differences in damage between the insert tray and the tibiofemoral surfaces on the fixed and mobile bearing versions.

Methods:

We analyzed 33 fixed bearing implants (Sigma Fixed Press Fit Condylar, DePuy, Warsaw, IN) from our IRB approved retrieval database. Twenty nine included the metal femoral component, and 28 included the insert tray. The 33 polyethylene tibial inserts were divided into 20 regions (Fig. 1) and wear was graded using a previously reported subjective grading system.[1,2] The tibiofemoral and insert tray surfaces of the implants were digitally photographed. The surface damage was outlined using Adobe Photoshop (Adobe Systems Inc. San Jose, CA). The percentage area covered by each damage mode was then determined using ImageJ (NIH Bethesda, MD). Clinical data including length of implantation (LOI), reason for revision, and body mass index (BMI) were collected for all patients.

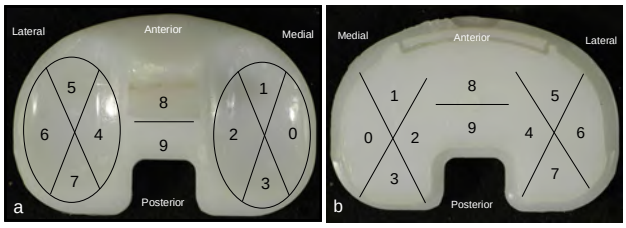

Figure 1: The 10 tibiofemoral (a) and 10 insert tray (b) bearing surface regions.

We used a Kruskall-Wallis ANOVA on ranks followed by a Dunn's post hoc test to determine differences among sectioned regions on the same insert. A Mann-Whitney Rank Sum test was used when the data were not normally distributed to determine the differences in sectioned regions between mobile and fixed bearing implants. Linear regression analysis was used to examine the effects of LOI and BMI on wear damage scores.

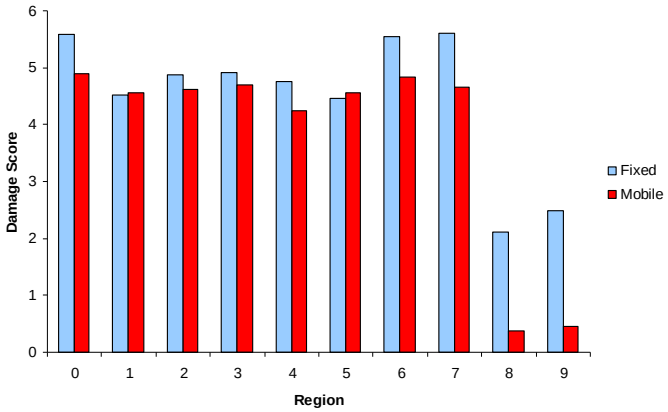

Figure 2: Graph of damage scores on regions of the tibiofemoral surfaces

Results:

The mean damage score (45±16, range: 19 to 85) for the tibiofemoral surface was significantly less ($p<0.001$) than that of the insert tray surface (mean 13±8, range: 0 to 33). Primary damage modes on both tibiofemoral and insert tray surfaces included burnishing, pitting, and scratching. On the tibiofemoral surface, burnishing covered 69.1±18.3%, pitting: 7.5±7.0% , and scratching: 7.0±4.5% of the available area. On the insert tray surface burnishing covered 15.8±17.6%, pitting: 3.1±5.3%, and scratching: 2.0±3.5% of the area.

Individual damage scores of regions 0 to 9 were not different on the insert tray surface on the fixed implant. For example, no difference was found in damage scores between region 0 and 7 of fixed bearing implants. There was also no difference in individual damage scores of regions 0 to 9 for insert tray of mobile bearing either. On the tibiofemoral surface, regions 8 and 9, which are located at the post, were significantly different from the rest of the regions on both mobile and fixed bearing implants ($p\leq0.001$) (Fig 2). The mobile bearing had significantly lower damage to the post area that that of the fixed bearing ($p\leq0.001$).

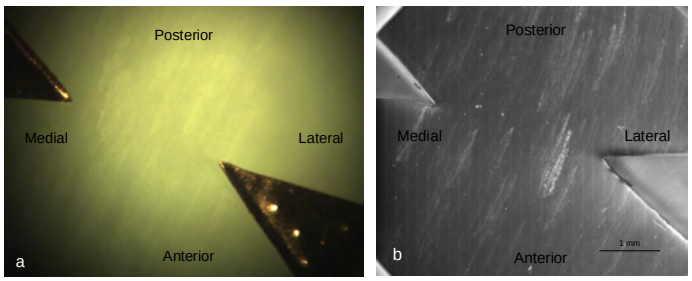

Figure 3: Scuffing wear pattern imaged under 20x (a) and SEM (b).

A distinct damage pattern was noted on the insert tray surface of the fixed implants. Small "scuffs" were noted across the surface in a concentric semi-circular arc about the center of the implant (Fig 3a). These were graded as burnishing. The marks were imaged using SEM, which revealed a slightly tufted surface (Fig 3b). EDAX revealed no foreign 3rd body debris within the "scuffs".

Clinical data were obtained for all 33 patients. The mean LOI was 7.7 ±5.2 years, ranging from 0.2 to 19.9 years. The mean BMI for the patients was 28.7 ± 5.5, ranging from 17.7 to 40.2 years. The majority of the implants (19/33 or 58%) were revised for osteolysis/loosening. The second most prevalent cause for revision was infection/inflammation (in 8 or 24%) followed by stiffness (4, 12%). One implant was removed for instability and one for periprosthetic fracture. Damage in neither implant type showed a significant correlation with LOI or BMI.

Conclusions:

Our study supports the previous findings that the average total damage score for the fixed implants was significantly less that than of the mobile bearing. While the average total tibiofemoral damage scores of the fixed and mobile implants were not different, the fixed bearing design had lower average insert tray scores ($p \leq 0.001$). This supports the hypothesis that the mobile bearing may not be decreasing contact stresses as much as originally intended and may instead be simply introducing a second bearing surface for damage to occur.

The uniformity in wear across the insert tray surface for both the fixed and mobile implants indicates that both designs allow for uniform stress distribution across the insert tray. Had there been non-uniformity, areas with higher wear scores would indicate areas of higher stress. The similarities in condylar damage scores between fixed and mobile tibiofemoral surfaces suggest that the polyethylene contact stresses were not greatly reduced in the mobile bearing design. However the lower post damage scores in mobile designs indicates that the additional allowed rotational motion may reduce post impingement and subsequent damage.

Evaluating implants for damage is limited by the fact that it is not a direct measure of implant wear. Damage grades can only give us ideas as to the where material removal occurred and in what areas it was most severe. However, it does not provide a quantitative measure of the amount of material removed due to wear. To better understand the wear of these implants, we are currently using imaging techniques to gather pristine and worn implant dimensions that can then be compared to as an estimate of material loss.

In conclusion mobile and fixed bearing implants of similar designs have similar wear patterns and major modes of damage. The extra rotational motion in the mobile bearing implants allows for less post damage. However this additional motion and bearing surface allows for more polyethylene damage making it no more advantageous than the fixed bearing design.

References:

[1] Kelly N. CORR. 201; 469:123-130. [2]Hood RW. J Biom Mater Res. 1983; 17:829-42. [3]Fu R. ORS. 2010.

Retreival Analysis of Tibial Post Wear Damage and Implant Design in Four Contemporary Designs of Constrained Condylar Knee

Xiaonan Wang, Yanguo Qin, Vishal Hegde, Douglas E Padgett, Timothy M Wright
Hospital for Special Surgery, 510 East 70th Street, New York, NY, 10021
WrightT@HSS.EDU

Statement of Purpose: Constrained Condylar Knee (CCK)'s liners used for soft tissue imbalance in revision total knee arthroplasty or in severe deformities with collateral ligament insufficiency [1, 2] gives large stress to the post. There is little information on the characteristics of polyethylene damage the enlarged posts goes through in vivo. We used observations made on retrieved implant components from four contemporary constraint condylar knee designs to examine how differences in tibial post location affected wear damage pattern on the post.

Methods: We identified 35 Zimmer NexGen®, 34 Smith and Nephew Genesis® II, 35 Zimmer Insall-Burstein® II, and 82 Exactech Optetrak® CCK (54 Non-modular and 28 modular designs) inserts that were explanted at our hospital and registered in our implant retrieval archive since Feb 2000 to Feb. 2010. Clinical and radiographic reviews were done for all cases, and polyethylene wear mode and subjective severity scores on all the five surfaces of the tibial posts were graded according to Hood's method [3]. To obtain objective measurements of the tibial post design for comparisons, the post size and location of a similar size for each design were measured by a caliper. The anterior and posterior location of the tibial post was measured as distance the anterior and posterior aspects of the tibial post to the edge of the anterior edge of the tibial insert [4]. The measurement was represented as the percentile of the distance over the overall anterior-posterior width of the insert.

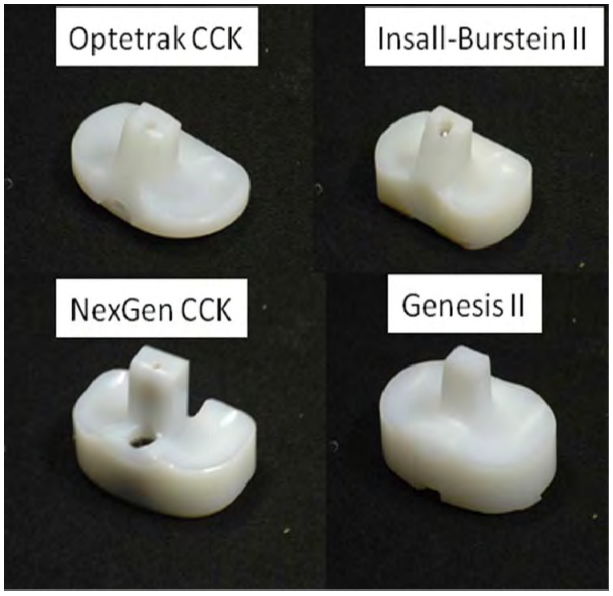

Figure 1: Images of polyethylene inserts of four CCK designs.

Results: For all CCK designs the amount of damage correlated with the length of implantation (Figure 2).

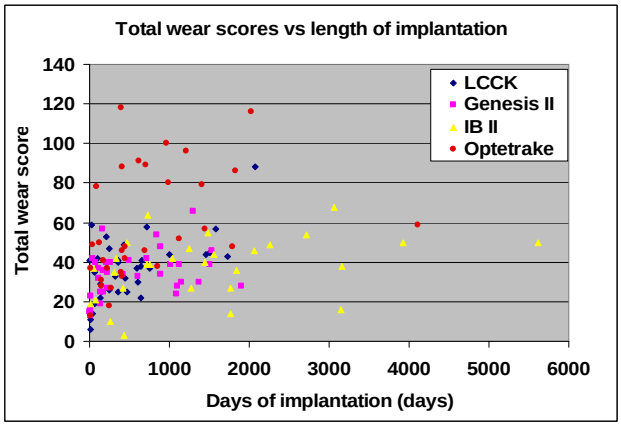

Figure 2: Dependency of total wear scores on the tibial post vs the length of implantations of all the four CCK designs.

All CCK designs showed significantly greater wear in the medial and lateral posts, but total wear scores and scores for wear damage on the anterior post differed among designs (Figure 3). Non-modular Optetrack® had global high wear damage than modular Optetrack® and all the other four designs (Table 1), so modular Optetrack® was used to do comparison with the other CCK designs.

Table 1: Total wear score and standard deviations for the four contemporary CCK knee designs

Implant	Total Wear Score	SD
Non-modular Optetrak®	61.4	25.9
Modular Optetrak®	33.2	14.2
Insall-Burstein® II	38.8	18.4
NexGen®	37.3	15.5
Genesis® II	34.6	11.7

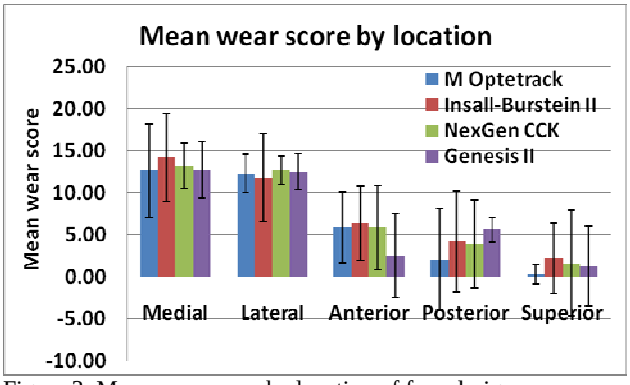

Figure 3: Mean wear score by location of four designs.

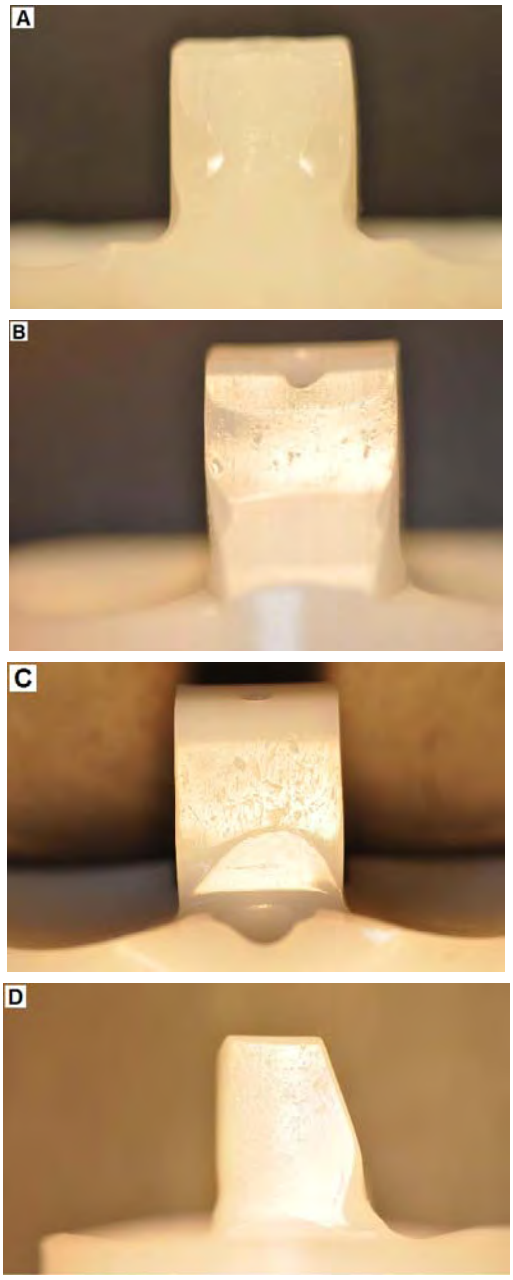

Figure 4: Photographs of representative post wear of the four designs. (A) Characteristic surface deformation on the anterior tibial post of the Optetrak® is shown. (B) Characteristic burnishing and surface deformation on the anterior tibial post of the Insall-Burstein® II is shown. (C) Surface deformation and pitting on the anterior tibial post of the NexGen® is shown. (D) Surface burnishing and pitting on the medial tibial post and surface deformation on the posterior post of the Genesis® II is shown

Genesis® II had less anterior wear damage than the other three designs ($P<0.01$) due to the posterior location of post (Table 2), while it had predominantly posterior wear damage than all the other three designs ($P=0.02$). Burnishing was the predominant mode of wear in all knee designs. Anterior surface deformation occurred on 80% of Optetrack®, Insall-Burstein® II and NexGen® CCKs, but the location of the deformation depended on designs (Figure 4). Burnishing was the predominant mode of wear on the top part of anterior surface of the Insall-Burstein® II CCK. Genesis® II showed a tendency towards more deformation damage but did not show statistical significance ($p=0.28$), while all the other three CCK designs showed greater damage by scratching ($p=0.025$).

Table 2: Relative post location for the four contemporary CCK knee designs

Implant	Implant Measurement (mm)		
	A	B	C
Optetrak®	68	8.2	44.2
Insall-Burstein® II	65	5.2	39.0
NexGen®	66	20.5	43.6
Genesis® II	68	28.6	49.7

CCK = posterior stabilized; A = overall width of the tibial insert; B = distance of the anterior surface of the tibial post relative to the anterior edge of the insert; C = distance of the posterior surface of the tibial post relative to the anterior edge of the insert.

Conclusions: Although tibial post wear damage is multi-factorial, the primary determinant of wear damage, and specifically anterior wear damage, is implant design. The constraint provided by the constraint condylar knee post-cam contact in modern knee arthroplasties is reflected in the wear damage patterns that occur during in vivo use. Unintended constraint such as anterior impingement should be addressed through design modifications for future constraint condylar knee arthroplasties.

References: [1] Scuderi GR. *Clin Orthop Relat Res.* 2001;392:300-5. [2] Lachiewicz PF, Soileau ES, *et al. J Arthroplasty*. 2006;21:803-8. [3] Hood RW, Wright TM, Burstein AH. *J Biomed Mater Res*.1983;5:829–842. [4] Dolan MM, Kelly NH, Nguyen JT, Wright TM, Hass SB. *Clin Orthop Relat Res*.2011;469(1):160-7.

Effect of Non-uniform De-cohesion on Crack Initiation from Notches in Crosslinked UHMWPE

P. Abhiram Sirimamilla[1], Jevan Furmanski[2], Clare Rimnac[1]
1. Case Western Reserve University, Cleveland, Ohio, 2. Los Alamos National Laboratory, Los Alamos, New Mexico.

Introduction: In ultra high molecular weight polyethylene (UHMWPE) joint replacement components, crack initiation from a stress-concentration design feature has been observed to lead to catastrophic failure in-vivo [1]. Thus, it is important to understand crack initiation from clinically relevant notches to mitigate the risk of component fracture.

The objective of this study was to investigate the time-evolving process of crack initiation in UHMWPE occurring at a clinically relevant notch and to quantify the crack initiation time and propagation velocity under constant load for two crosslinked UHMWPEs.

Methods: Round compact tension specimens of remelted 65 kGy and 100 kGy material were machined according to ASTM 1820-01 with: notch depth, a=17mm; specimen length, w=40mm; thickness, b=20mm; and side groove depth of 2 mm on each side [Fig 1a]. A notch radius of 0.25mm was chosen to imitate the geometry of actual orthopedic components with an acute notch design feature. At least two specimens of each material were tested at three constant loads (Table 1) using an Instron 8511 servohydraulic load frame. Two independent crack initiation times were recorded, from a Sony video microscope focused on the face of the crack (ti-video) and from data obtained from a travelling microscope measuring the ligament reduction (ti-tm) which was also used in a previous study [2]. Ligament reduction, Δ (W-a) is due to a combination of specimen deformation and crack extension. The elapsed time at catastrophic fracture was also recorded (t-fail). It was noted whether de-cohesion occurred at the notch root or away from the notch root (Init. pos.). A de-cohesion separation distance (δ), which is the vertical distance between multiple de-cohesion planes (if present), was also measured.

Results: Surface de-cohesion occurred and led to crack initiation and propagation to failure in all specimens. From video observation of the notch surface, it was found that non-uniform de-cohesion occurred in some specimens, e.g., it was found that the crack initiated either on a single plane at the notch root or on multiple planes away from the root of the notch (Fig 1b, Fig 1c). Failure time varied substantially between specimens for the same applied load. In all cases, cracks that initiated away from the notch root had a longer de-cohesion time compared to cracks that initiated at the root of the notch (Table 1). The crack initiation time obtained from the video and the travelling microscope were in agreement when δ was negligible but the two initiation times differed when was δ large (Table 1).

Discussion: The local deformation and failure processes that lead to crack initiation in clinically relevant notches in crosslinked UHMWPE were directly observed, and the effective material resistance to crack initiation at a notch was quantified for two crosslinked formulations.

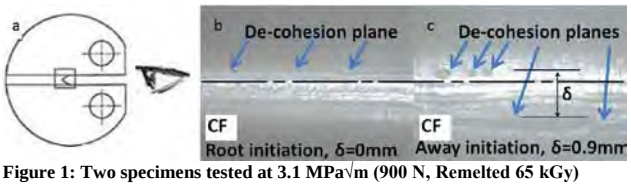

Figure 1: Two specimens tested at 3.1 MPa$\sqrt{m}$ (900 N, Remelted 65 kGy) showed different de-cohesion phenomenon. CF-Crack Front. Dotted line indicates the notch root (notch plane of symmetry) and δ is the vertical distance between crack initiation sites. Arrows indicate the crack initiation planes. (a) Direction of view for (b) and (c) ;(b) De-cohesion occurring on a single layer at the root of notch for specimen 1 ;(c) De-cohesion occurring on multiple layers and at the edge of the notch for specimen 2.

Table 1: Initiation and failure times, and de-cohesion separation distances.

Material	Load	Specimen	ti-video, ksec	ti-tm, ksec	t-fail, ksec	δ(avg) mm	Init. Pos
Remelted 65 kGy	950N	1	15.7	15	37.1	0.27	root
		2	24.6	16.5	47.4	0.31	away
	900N	1	10.7	12.5	33.6	0.06	root
		2	47.3	30.5	114	0.95	away
	800N	1	1225	735	1728	0.77	away
		2	200.1	160	432	0.075	root
		3	457.5	241	648	0.11	away
Remelted 100 kGy	900N	1	25.9	15.1	33.0	0.59	away
		2	N/A	6.7	10.0	N/A	N/A
		3	N/A	6.2	16.9	N/A	N/A
	800N	1	42.6	7.5	51.7	0.38	away
		2	95.6	15	125	0.45	away

Crack initiation was preceded by a time-evolving process of distributed material de-cohesion on the notch surface; a phenomenon typically neglected in modeling of crack initiation phenomena. De-cohesion in some cases occurred away from the notch root, and in these cases initiation time was substantially greater than when initiation occurred at the notch root (root vs away, Table 1). Therefore, de-cohesion away from the notch root may lead to longer crack initiation times at notches of finite radius, which is relevant for actual component failure. Obtaining the crack initiation time without notch surface observation could lead to an erroneous value in the case of non-uniform de-cohesion. The study suggests that there is a direct positive relationship between the de-cohesion separation distance (δ) and the crack initiation time (ti-video) observed from the videos. Non-uniform de-cohesion at the initiation site may make predicting catastrophic component failure more challenging, though assuming initiation at the notch root and a continuous de-cohesion front may be a conservative approach. Although the fatigue crack propagation resistance of crosslinked material has been qualitative established, this study suggests that resistance to crack initiation is an independent relationship that can provide better information to grade the crosslinked material.

Further work is needed to quantify the effect of multiple layer de-cohesion and the effect of notch radius on component performance in vivo.

REFERENCES: [1] Furmanski et al, Biomat 2009; 30 5572-5582; [2] Trans. 56th ORS 35:271, 2010.

ACKNOWLEDGEMENTS: NIH/NIAMS T32 AR00750, NIH/NIAMS R01AR047192, Orthoplastics, Wilbert J Austin Chair

For submission: Convert to PDF and email abstract with contact information to skurtz@exponent.com

A new highly crystalline UHMWPE: a comparative study against conventional resins

F.J. Medel [1,2], M.J. Martínez-Morlanes[3], F.J. Pascual[3], P.J. Alonso[2], M.D. Mariscal[3], R. Ríos[3], J.A. Puértolas[2,3]
[1]Centro Universitario de la Defensa, Zaragoza, Spain
[2]Instituto de Ciencia de Materiales de Aragón, Universidad de Zaragoza-CSIC, Zaragoza, Spain
[3]Instituto de Investigaciones en Ingeniería de Aragón, Universidad de Zaragoza, Spain

Introduction: A new medical UHMWPE resin (Homopolymer MG003; DSM Biomedical; The Netherlands) has been very recently introduced for total joint arthroplasty components. MG003 resins feature higher crystallinity than conventional GUR resins due to a high degree of linearity. To make this material resistant to oxidation and suitable for radiation-crosslinking, MG003 resins stabilized by trace concentrations of vitamin E have been also developed. The aim of this study was to characterize the chemical, physical and mechanical properties of this material and compare them to those of conventional, commercially available, resins. In addition, we explored the changes experienced by this new resin upon radiation crosslinking.

Methods: 0.1% vitE-MG003 material was kindly supplied by DSM Biomedical in both powder and consolidated form. Neat and vitamin E stabilized GUR 1020 and GUR 1050 materials were also available. In addition to control samples, specimens were prepared for further gamma-irradiation (90 kGy) in air. After irradiation, electron spin resonance (ESR) and FTIR experiments were performed to detect residual free radicals, and changes in the trans-vinylene absorption band (TVI), respectively. Thermogravimetric and calorimetric analyses were also conducted to assess the oxidation resistance and microstructure, respectively. Thus, the crystallinity content (%), melting transition temperature (T_m), the onset of oxidation (T_B) and the beginning of thermal degradation (T_1) could be obtained [1]. Crystal morphology and thickness (L_c) were characterized based on Transmission Electron Microscopy (TEM) images. Finally, uniaxial tensile tests per ASTM D638M and dynamic mechanical thermal analyses (DMTA) were carried out to evaluate the mechanical behavior.

Results and Discussion. MG003 materials exhibited the highest crystallinity (62%) and crystal thickness (36 nm) among samples produced from commercially available UHMWPE resins (Table 1). Upon gamma-irradiation in air, all the UHMWPE materials experienced crystallinity, melting temperature, and lamellar thickness increases, which were associated to radiation-induced molecular rearrangements. Free radicals were detected in all the gamma irradiated materials, although vitamin E stabilized specimens showed weaker ESR signals than unstabilized samples (Figure 1). Coherently, thermogravimetric experiments suggested an augmented oxidation resistance of vitamin E stabilized specimens based on the shift towards higher temperatures of the onset of mass increase (T_B). Despite gamma irradiation in air provoked a decrease in T_B even in vitamin E stabilized materials, oxidation-induced mass increases started at higher temperatures than in virgin specimens (Table 3). Irradiation was also responsible of increased trans-vinylene indices (0.04-0.05) in all the UHMWPE materials. On the other hand, the beginning of thermal degradation (T_1) was delayed upon irradiation for unstabilized specimens. In contrast, stabilized materials exhibited a comparatively decreased T_1 upon irradiation, phenomenon which might be related to the radiation grafting of vitamin E to polyethylene molecules [2-4]. Finally, the present mechanical data confirmed the elevated yield stress of MG003 resins, in agreement with their high crystallinity contents. As expected, irradiation caused elastic moduli and yield stresses to increase, and fracture strain reductions in all the UHMWPEs (Table 3). DMTA experiments confirmed the gamma relaxation occurred at lower temperatures for MG003 samples. In general, irradiated UHMWPE samples exhibited an increase in storage modulus and more intense alpha relaxations.
This study confirms vitamin stabilized MG003 resins exhibit a comparable oxidative behavior than GUR conventional resins upon irradiation. The superior microstructure and mechanical properties conferred by the highly linear character warrants enhanced performance.

Figure 1. ESR signals corresponding to unstabilized GUR 1050, a), vitamin E stabilized GUR 1050, b), and MG003, c), materials after gamma irradiation to 90 kGy.

References.

[1] Martínez-Morlanes MJ. Polym Testing 2010; 29:425-432.
[2] Wolf C. ORS Transactions 2011; Poster n. 1178.
[3] Catarí E. Nucl Instrm Meth in Phys Res B 2005; 236: 338-342.
[4] Westerhout RWJ. Ind Eng Chem Res 1997; 36: 1955-1964.

Acknowledgements.

Research funded by MAT 2010-16175.

Table 1. Typical thermal and microstructure parameters of control and irradiated UHMWPEs. (* In-house consolidated specimens)

Material	T_m(ºC)	% Crystallinity	L_c (nm)
GUR 1050	136.2 ± 0.5	55.0 ± 0.3	27 ± 4
GUR 1020	135.9 ± 1.4	56.4 ± 2.1	31 ± 3
GUR 1050-0.1%VE*	134.9 ± 0.5	49.8 ± 0.8	-
GUR 1020-0.1%VE	137.3 ± 0.2	60.3 ± 0.4	-
MG003-0.1%VE	139.7 ± 1.0	61.6 ± 1.1	36 ± 3
GUR 1050-I	140.4 ± 0.3	59.9 ± 0.7	-
GUR 1020-I	-	-	-
GUR 1050-0.1%VE-I*	138.8 ± 0.5	58.6 ± 0.2	-
GUR 1020-0.1%VE-I	-	-	-
MG003-0.1% vitE-I	143.3 ± 1.8	63.3 ± 1.7	39 ± 6

For submission: Convert to PDF and email abstract with contact information to skurtz@exponent.com

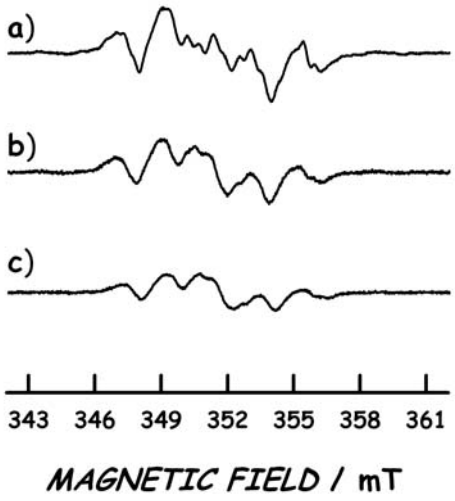

Table 2. Thermogravimetric parameters obtained for virgin and vitamin E stabilized UHMWPEs before and after gamma irradiation. (* In-house consolidated specimens)

Material	T_B(°C)	T_0(°C)	T_1(°C)
GUR 1050	185.0 ± 3.3	227.6 ± 3.5	411.1 ± 12.6
GUR 1020	170.9 ± 6.2	226.8 ± 4.0	415.4 ± 18.7
GUR 1050-0,1%VE*	240.3 ± 2.2	252.5 ± 1.1	414.5 ± 11.5
GUR 1020-0.1%VE	240.5 ± 1.9	252.1 ± 0.5	439.6 ± 10.7
MG003-0.1% VE	254.3 ± 2.2	260.9 ± 0.4	447.0 ± 5.2
GUR 1050-I	157.2 ± 2.5	221.7 0.4	433.3 ± 9.4
GUR 1020-I			
GUR 1050-0,1%VE-I*	174.7 ± 2.3	236.6 ± 0.4	404.0 ± 2.0
GUR 1020-0.1%VE-I			
MG003-0.1% VE-I	204.4 ± 1.62	234.4 ± 1.2	410.2 ± 16.3

Table 3. Mechanical properties obtained from uniaxial tensile data. (* In-house consolidated specimens)

Material	Yield Stress(MPa)	Fracture Stress (MPa)	Fracture Strain (%)
GUR 1050*	18.6 ± 0.9	30.7 ± 2.0	505 ± 22
GUR 1020	-	-	-
GUR 1050-0.1%VE*	19.4 ± 0.6	31.5 ± 0.8	480 ± 15
GUR 1020-0.1%VE	-	-	-
MG003-0.1%VE	25.0 ± 0.4	48.0 ± 2.0	650 ± 32
GUR 1050-I*	21.1 ± 0.5	27.6 ± 2.1	304 ± 45
GUR 1020-I	-	-	-
GUR 1050-0.1%VE-I*	21.2 ± 0.3	29.0 ± 1.1	365 ± 18
GUR 1020-0.1%VE-I	-	-	-
MG003-0.1% vitE-I	26.6 ± 0.1	45.3 ± 2.5	479 ± 27

TOUGHNESS IN HIGHLY CROSSLINKED UHMWPEs BY ESSENTIAL WORK OF FRACTURE

F. J. Pascual [1], R. Ríos [1], L. Gracia-Villa [1], F.J. Medel [2,3], V. Martínez-Nogués[1], J.A. Puértolas[1,3]
[1]Instituto de Investigación en Ingeniería de Aragón, Universidad de Zaragoza, Spain
[2]Centro Universitario de la Defensa, Zaragoza, Spain
[3]Instituto de Ciencia de Materiales de Aragón, ICMA, Universidad de Zaragoza-CSIC, Zaragoza, Spain

INTRODUCTION:

Up to date, the investigation on UHMWPE has aimed at resolving this paradigm: to avoid or delay particle-induced osteolysis by achieving wear resistance, concurrently ensuring oxidative stability and minimal reduction in mechanical properties, in particular toughness and fatigue resistance [1,2]. Highly crosslinked UHMWPE obtained by gamma or electron beam irradiation stabilized by thermal treatments or antioxidant addition have given substantial breakthroughs in the first two concerns, while the improvement in fracture resistance remains open. Different approaches have been used to determine the toughness of UHMWPE, such as the work of fracture obtained from uniaxial tensile test-curves, impact toughness and J-integral experiments. In this work, we introduce the essential work of fracture (EWF) to assess the fracture resistance of ductile highly crosslinked polyethylenes [3,4]. This technique allows discrimination between the essential work required to fracture the polymer in its process zone, w_e, and the non-essential or plastic work consumed by various deformation mechanisms in the plastic zone, w_p. Besides, a comparison of the different toughness techniques, as well as an attempt to correlate these data to the microstructure of the material, have been carried out.

MATERIAL AND METHODS:

The UHMWPE grade GUR1050 used in this work was manufactured by Tycona and supplied by Orthoplastics (Todmorden Road, Bacup, Lancashire, UK) in the form of a molded block. On the other hand, the UHMWPE grade MG003+0.1%vitE (MG003-VE) was kindly supplied by DSM Biomedical (Geleen, The Netherlands) in the same form. Both materials were gamma irradiated in air to a dose of 90 kGy (Aragogamma S.A., Barcelona, Spain). The most relevant difference between both materials in pristine condition is their degrees of crystallinity, which are typically 50-55%, and close to 60%, for GUR 1050 and MG003-VE, respectively.

Work to fracture values were calculated from the area below the engineering stress-strain curves of uniaxial tensile tests per ASTM D638M (n=3).
J-integral versus crack growth resistance, J–R, curves were obtained following ASTM D6068-02 for all material groups (n=7 per group).
Impact Izod tests were carried out at room temperature on double-notched specimens (n=5) following ASTM F648 guidelines.

For the EWF study, double deeply edge-notched tensile (DDEN-T) specimens with different free ligament length, l_o, were tested to fracture. Free ligament lengths were selected in the range l_o = 4 to 12 mm by sharpening the machined edge with a fresh razor blade. Specific essential work of fracture (w_e) results were determined from linear regression of specific total fracture energy versus ligament length plots. Finally, fracture surfaces of EWF specimens were observed by SEM.

RESULTS:

Figure 1 depicts the load-displacement (F −x) curves of DDENT-T specimens at various ligaments for γ-irradiated in air GUR 1050 EWF specimens. Similar curves were obtained for the remaining materials.

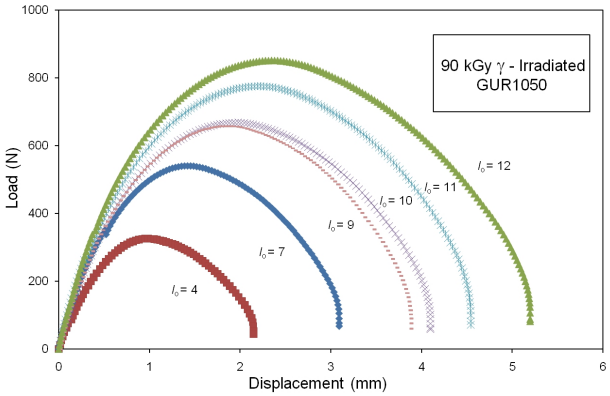

Figure 1 Load-displacement curves for γ-irradiated GUR 1050 EWF specimens.

Material	w_e (KJ/m^2)	Impact Toughness (KJ/m^2)	Work to Fracture (MJ/m^3)	J-integral a=0.5mm (kJ/m^2)
GUR 1050 Virgin	54.6 R^2 = 0.95	106.2 ± 2.7	234.0 ± 33.3	35
GUR 1050 90 kGy	19.7 R^2 = 0.93	62.6 ± 4.7	145.3 ± 18.3	-
MG003-VE Virgin	21.7 R^2 = 0.97	50.1 ± 6.1	219 ± 16	25
MG003-VE 90 kGy	17.3 R^2 = 0.98	50.9 ± 1.5	150 ± 13	-

Table 1 Toughness metrics for all the materials studied.

Table 1 shows a comparison between the toughness values obtained for virgin and irradiated polyethylenes by the different techniques used in this work.

The analysis of fracture surfaces after EWF tests revealed morphological differences between pristine and irradiated polyethylenes.

DISCUSSION AND CONCLUSIONS:

The current results confirm the loss of toughness experienced by GUR 1050 upon irradiation. This effect is well known and is attributed to the elevated radiation-induced crosslink density, which, in turn, reduces the amorphous deformation modes of the polymer and, therefore, its ductility. Nevertheless, the reduction in fracture resistance varies depending on the technique employed to assess this property. On the contrary, and according to the impact toughness and essential work of fracture results obtained for MG003-VE, it is not possible to confirm whether this microstructural feature governs the toughness behaviour, since the effect of irradiation was practically negligible. A more detailed analysis of the w_e values and the plastic areas, w_p, deduced from EWF tests, along with the fractographic study of the DDEN-T specimen surfaces may help to ascertain the mechanism responsible for the changes in fracture resistance in the different highly crosslinked polyethylenes.

REFERENCES:

[1] Kurtz S.M. The UHMWPE handbook: ultra-high molecular weight polyethylene in total joint replacement, Academic Press, New York (2009) 2nd edition.

[2] Gomez-Barrena E. et al. Acta Orthopaedica (2008) 79: 832

[3] Martínez A.B. et al. Engineering Failure Analysis 16 (2009) 2604–2617

[4] Naz S. et al. J Mater Sci (2010) 45:448-459

ACKNOWLEDGEMENTS:

Research funded by the Comisión Interministerial de Ciencia y Tecnología (CICYT), Spain. Project: MAT 2010-16175.

Detection of vitamin E in ultra high molecular weight polyethylene by colorimetry and water contact angle techniques

A. Terriza[1], M.J. Martínez-Morlanes[2], F. Yubero[1], J.A. Puértolas[2,3]
[1]Instituto de Ciencias de Materiales de Sevilla, (CSIC-U. Sevilla), Spain
[2]Instituto de Ciencia de Materiales de Aragón, Universidad de Zaragoza-CSIC, Spain
[3]Instituto de Investigaciones en Ingeniería de Aragón, Universidad de Zaragoza, Zaragoza, Spain

INTRODUCTION:

The incorporation of vitamin E in medical grade polyethylenes intended for surgical implant has well recognize benefits due to its anti-oxidant effect keeping the wear performance of highly crosslinked ultra high molecular weight polyethylene (UHMWPE) [1]. Vitamin E is usually quantified by FTIR using a vitamin E index defined as the area ratio between the absorption peak at 1262 cm^{-1}, which correspond to the C-O stretching of the phenol group, and a reference absorption peak at 1895 cm^{-1} corresponding to the polyethylene skeleton. However, this method has a 0.2 wt% detection limit. UV absorbance is also used to detect vitamin E, by means of the absorption at 290 nm corresponding to the aromatic chromophone in vitamin E [2]. In this case, the detection limit is about 0.01 wt%. However, these two methods are destructive and not free of some controversial. So there is still a challenge to identify more robust non destructive methods to quantify more reliable vitamin E index in medical grade polyethylenes. In this work we assess the influence of the vitamin E, introduced by diffusion in the UHMWPE, on the color and the water contact angle.

METHODS:

The raw materials used in this study were GUR 1050 UHMWPE. Vitamin E was incorporated into the foregoing materials by diffusion. The discs were soak in a bath of vitamin E at 120ºC in a N_2 atmosphere during different periods. At the end of the diffusion process, the discs were taken out of the bath, cleaned and homogenized at 120ºC during 24 hours in N_2. Thus, specimens with concentrations of α-tocopherol of 0.3-3.0 % were prepared. The vitamin E concentration was also evaluated by UV spectroscopy. Water contact angle (WCA) measurements were performed with deionized water. Colorimetric analysis of the samples was also evaluated.

RESULTS:

Figure 1 shows the correlation between WCA and percentage of vitamin E in the discs. It is observed a smooth increase of WCA from 102º to 117º as the amount of vitamin E incorporated in the polyethylene increases from 0.0 % to 3.0 %. Unfortunately the R-squared of the linear regression is very low (0.26) due to the high uncertainty in the determination of WCA (in general about a 4% of the actual measured value) compared with the small increase of WCA with vitamin E doping. Therefore, this characterization cannot be used alone to quantify the amount of vitamin E incorporated in the polyethylenes.

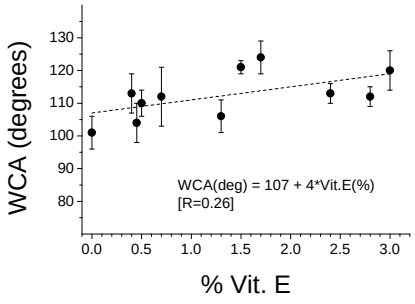

Figure 1. Correlation between WCA and percentage of vitamin E in UHMWPE discs.

Figure 2 shows the variation in color difference ΔE (in CIELAB color space) between vitamin E doped and undoped UHMWPE. It is observed a linear increase of ΔE between 6 to 20 as the amount of vitamin E incorporated in the polyethylene increases between 0.3 and 3.0 %. Other set of vitamin E doped UHMWPE samples, previously irradiated with 90 kGy, show color differences 3 units larger than the non-irradiated for the same level of vitamin E doping. In both cases, the R-squared of the linear regressions is about 0.95, suggesting that this procedure might be used for quantification purposes.

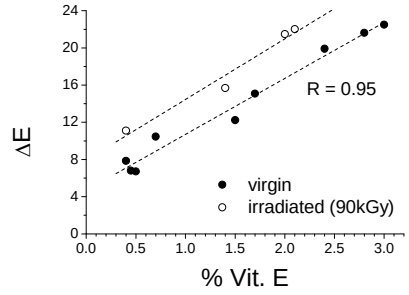

Figure 2. Correlation between color difference ΔE and vitamin E content in UHMWPE disks

CONCLUSIONS:

It is observed an increase of WCA as the vitamin E doping in UHMWPE increases. However, only a very rough estimation of vitamin E content of polyethylene sample with an unknown vitamin E doping level could be assessed by this procedure. On the other hand, a linear correlation between the color difference and percentage of vitamin E incorporated in UHMWPE has been found. In this former case, the statistics of the analysis was more favorable, suggesting that this procedure might be used for quantification purposes.

REFERENCES
[1] Puértolas JA et al. J. Appl. Polym. Sci. 2011; 120: 2282.
[2] Bracco P et al. Clin Orthop Relat Res 2010

ACKNOWLEDGEMENTS:
This study was financed by Consolider FUNCOAT-CSD2008-00023, which is a project of the Spanish Ministerio de Ciencia y Tecnología.